RETINAL ANATOMY OF AUSTRALIAN MARSUPIALS

by

Janet Megan Fuss, B. Sc. Dent. (Hons).

Submitted in fulfilment of
the requirements for the
Degree of Master of Science.

Department of Anatomy and Histology,
The University of Adelaide.

AWARDED 12th AUGUST, 1986

March, 1986.

TABLE OF CONTENTS

SUMMARY

The retinal anatomy of the Brush-tailed possum, Kowari and Kangaroo Island kangaroo was studied by both light and electron microscopy. These species were chosen as representative of the families Phalangeridae, Dasyuridae and Macropodidae.

The duplex retinae of these marsupials conform to the general vertebrate pattern with the neuronal cell bodies being confined to 3 nuclear layers separated by 2 layers of interneuronal synapses. In each of these species the cones show reptilian features, particularly with respect to the presence of oil droplets sclerad to the ellipsoids, while the rods resemble those of placental mammals. The interneuronal synapses of the outer and inner plexiform layers are similar to those of placental mammals.

The rod to cone ratio, however, varies from 130:1 in the Brush-tailed possum to 40:1 in the Kangaroo Island kangaroo and 25:1 in the Kowari. This variation may be related to lifestyle and behaviour.

SIGNED STATEMENT

This report contains no material which has been accepted for the award of any other degree or diploma in any university.

To the best of my knowledge and belief, it contains no material previously published or written by another person except when due reference is made in the text.

The author consents to this thesis being made available for photocopying and loan if accepted for the award of the degree.

JANET MEGAN FUSS

ACKNOWLEDGEMENTS

I wish to thank Dr. Adam Locket for his kind advice and guidance in the laboratory and for his patience during the preparation of this manuscript. My sincere appreciation is also extended to Chris Leigh for his technical assistance, and to the other members of the Department of Anatomy and Histology for their kind support.

I also wish to thank Dr. Wayne Sampson, Dr. Milton Sims, Dr. Helen McLean and Lorraine McMahon for their support during the past year and last, but not least, my family for simply being there.

1 INTRODUCTION

1.1 Aims and Objectives

Only a small proportion of the literature available on the vertebrate visual system is devoted to marsupials, and the majority of this deals with the retinal ganglion cells (RGCs) and retinal projections. Few reports have been published on the retinal anatomy of marsupials leaving enormous scope for further research. A comparative study of the retinae of 3 diverse marsupials appeared therefore to be an appropriate way in which to extend what is known about the group.

One species from each of 3 marsupial families was chosen; the Brush-tailed possum from the Phalangeridae, the Kowari from the Dasyuridae and a macropod, the Kangaroo Island kangaroo. Each was selected for its differing habitat and lifestyle in an effort to represent the likely variation of retinal anatomy seen within the order Marsupialia.

The light and electron microscopic retinal structure of each species will be compared and then considered with respect to the general vertebrate pattern.

A Golgi-staining investigation proved disappointing. The incomplete results obtained are however presented to provide a more coherent picture of the gross morphology of the retinal cell types.

2 LITERATURE REVIEW

The Marsupial Visual System

Forenote: Species names used in the text are those used by the original authors. An asterisk (*) indicates the latin binomials not in current use. Where possible an attempt has been made to correlate these names with those in current use [See Appendix I].

2.1 Ophthalmoscopic Appearance

The eyes of a variety of marsupials were examined ophthalmoscopically by JOHNSON (1901) who described them as having a circular disc frequently covered by a fine network of blood vessels or capillaries projecting vitreally like a dome. In most cases he noted that opaque nerve fibres radiate from the optic disc.

Initially JOHNSON (1901) reported that all the marsupials he examined show a complete lack of retinal vessels "with the exception of the carnivorous and nocturnal Tasmanian Devil (Dasyurus ursinus*) and the Virginian Opossum (Didelphis virginiana)". The retinal vessels in these 2 species form a complete network arising mostly from the centre of the disc, "there being, besides smaller more peripheral vessels, one or more typical arteriae and venae centrales".

However, he also describes the circular disc as being covered by a network in the Short-tailed wallaby (Halmaturus brachyurus*), Bennett's tree wallaby (Dendrolagus inustus*), Black-faced kangaroo (Macropus melanops) and Red kangaroo (Macropus rufus). The Brush-tailed wallaby (Petrogale penicullata) and the Rufous rat kangaroo (Hypsiprymnus rufescens*) were also described by JOHNSON (1901) as having fine capillaries covering the disc and arising from the centre.

Later in the same publication JOHNSON (1901) also reported that a few small vessels arise from the optic disc and extend to the edge of the disc or a short distance beyond in the phalangers Belideus*, Petaurus, Hypsiprymnus*, Dendrolagus* and the bandicoot Perameles obesula*.

Specifically JOHNSON (1901) reported that ophthalmoscopic examination did not reveal the presence of retinal vessels in the Rabbit-eared perameles, Perameles lagotis*.

The presence of prominent choroidal vessels was reported by JOHNSON (1901) for all the marsupials he examined, with the exception of the Black phalanger (Phalangista vulgaris*), in which "they can be distinctly seen", and the Squirrel-like phalanger (Belideus sciureus*), in which they were not seen.

The fundus of the wombat was described by JOHNSON (1901) as characteristic of that of the diprotodonts, while that of the kangaroos resembles closely that of the Agoutis being devoid of retinal vessels, grey-brown in colour and possessing many prominent choroidal vessels. JOHNSON (1901) also described B. sciureus as having a pink-brown fundus covered with large black dots and P. vulgaris as possessing a creamy-white fundus with vermillion dots.

A number of marsupial species were reported by JOHNSON (1901) to possess a vestigial pecten extending into the vitreous. The pecten, a structure characteristically found in birds, is a vascular "ectodermal papilla" (WALLS, 1942) which projects into the eye from the optic disc and provides nutrients which diffuse through the vitreous to the retina. A less well developed papilla, called a conus papillaris, is found in reptiles and a few mammals (RODIECK, 1973). It may be that JOHNSON'S vestigial pecten is in fact a conus papillaris. No further reports of any pecten-like structures in the eyes of marsupials have appeared in the literature.

2.2 Retinal Pigmented Epithelium and Bruch's Membrane

The structure and function of the marsupial retinal pigmented epithelium (RPE) have been investigated by several authors. BRAEKEVELT (1973) described the ultrastucture of the RPE in the Quokka (Setonix brachyurus), an Australian macropod of nocturnal habit. He found the RPE to consist of a single layer of cuboidal cells separated from the choriocapillaris by Bruch's membrane (BM). The epithelial cells were reported to be rich in cytoplasmic organelles; abundant smooth endoplasmic reticulum (SER), mitochondria, Golgi complexes, pigment granules and phagosomes. The basal (sclerad) portion of the cell membrane shows numerous infoldings typical of mammalian RPE cells. Whereas the apical (vitread) surface exhibits numerous microvillous processes that surround the tips ofthe photoreceptor outer segments.

The RPE of D. virginiana was described by BRAEKEVELT (1976) as being typical of that found in other vertebrates and consists of a single layer of heavily pigmented cells exhibiting intercellular junctions. These epithelial cells were found to contain basal nuclei, abundant SER and mitochondria, but little rough endoplasmic reticulum (RER). As in the Quokka, the RPE cells exhibit extensive basal infoldings and numerous apical processes that enclose photoreceptor outer segments.

HAZLETT (1976) also described the ultrastructure of the RPE in the North American opossum (D.virginiana). He observed the epithelial cells to contain large oval nuclei with vesicular chromatin and a prominent eccentric nucleolus. The basal cytoplasm was reported to contain numerous coated

vesicles, a small Golgi complex, tubular profiles of SER and scattered cisternae of RER. Polyribosomes and numerous rod-shaped mitochondria were also evident in the basalcytoplasm while the apical cytoplasm was found to contain large, elongate pigment granules. HAZLETT (1976) also reported modifications of the cell membranes such as numerous basal infoldings and short, irregular apical processes projecting vitreally to incompletely surround the photoreceptor outer segments.

Both BRAEKEVELT (1976) and HAZLETT (1976) have reported the presence of reflective lipoidal spheres scattered throughout the tapetal RPE. This will later be discussed in greater detail.

GOLDMAN and STEINBERG (1977) have also studied the RPE of D.virginiana. They found few cytoplasmic organelles present and noted that they mostly occupied the basal regions of these large cells which are up to 90.0 µm high. Short apical processes were observed but no evidence of phagocytosis was found. In all animals used in GOLDMAN and STEINBERG's study a small population of leucocytes was found against the apical surface of the RPE cells in close association with the photoreceptor outer segments. Leucocytes were also observed between the RPE cells and adherent to the vascular endothelium adjacent BM. The authors found no sign of disease or infection and suggested that these leucocytes migrate vitreally through the intercellular junctions of the choroidal endothelium and RPE.

GOLDMAN and STEINBERG (1977) found few phagosomes within the RPE cells of Didelphis, and those in the later stages of digestion were found basally suggesting that

digestion occurs in an apical-basal direction.

HERMAN and STEINBERG (1982a and 1982b) have made extensive studies of the phagocytic function of the marsupial RPE. Phagocytosis of the rod outer segment (ROS) membranes conforms to a diurnal pattern reported for other vertebrates such as the rat (LA VAIL, 1976), and frog (BASINGER, HOFFMAN, and MATTHES, 1976). At the onset of the light period the apical processes of the RPE phagocytose portions of photoreceptor outer segments. The phagosomes apparently remainin the apical cytoplasm for a short period; 1 to 2 hours following light onset HERMAN and STEINBERG (1982a) found large numbers of phagosomes in the basal region of the RPE cells. Colchicine was found to block basal migration of phagosomes suggesting a microtubule-mediated movement of phagosomesfrom the apical region of the cells (HERMAN and STEINBERG, 1982a). In a subsequent paper HERMAN and STEINBERG (1982b) examined the ultrastructural and cytochemical features of phagosome breakdown in the RPE of the North American opossum. They found the phagosomes to be degraded by lysosomes in the basal region of the cytoplasm. Acid phosphatase, the enzyme involved in phagosome degeneration, activity was only detected in the basal cytoplasm; this is consistent with lysosomal breakdown of phagosomes. In the apical and middle regions of the cytoplasm no enzyme activity was evident and here the phagosomes still possessed a double membrane.

HERMAN and STEINBERG (1982c) have also reported on the formation and degeneration of melanosomes in the RPE of the adult North American opossum. They were able to demonstrate the formation of melanosomes ultrastructurally by the

presence of stage II and III premelanosomes. This was confirmed by an autoradiographic study of the incorporation of dihydroxyphenylalanine, a melanin precursor.

In D.virginiana BM displays the pentalaminate structure, typical of vertebrates, throughout the retina (BRAEKEVELT, 1976; HAZLETT, 1976). Nor does the choriocapillaris show any regional variation in structure. In both the tapetal and non-tapetal areas the vascular endothelium adjacent BM, but not that lining the sclerad portion of the vessel, is very thin (HAZLETT, 1976) and characterised by pores and numerous pinocytotic vesicles (HAZLETT, 1976).

More recently HAZLETT, HAZLETT, IRELAND and BRADLEY (1978) described the presence of microperoxisomes in the RPE and tapetum lucidum of the North American opossum. These structures, which are often found in cells with a high lipid content (NOVIKOFF and NOVIKOFF, 1973), were found to contain a granular matrix and to be similar in size, shape, location and number in both the RPE and tapetum lucidum. The limiting membranes of these round to ovoid organelles were found to be associated with SER. After incubation of the retina in diaminobenzidine and hydrogen peroxide HAZLETT et al. (1978) found that the microperoxisomes exhibited an electron dense reaction product indicating the site of peroxidatic activity of the enzyme catalase. ROBISON and KUWABARA (1975) have published evidence which implicates microperoxisomes in the transport, storage and turnover of lipid which has lead HAZLETT et al. (1978) to suggest a similar functional relationship between the microperoxisomes and lipid droplets in the RPE of D. virginiana. Large numbers of these

organelles have been found in the RPE of a variety of animals which suggests they may play a role in photoreceptor outer segment membrane renewal (ROBINSON and KUWABARA, 1975).

2.3 Neuroretina

As early as 1876 the literature contained reports on the marsupial retina. HOFFMANN (1876) described oil droplets in the cone cells of two Australian macropods; Bennett's wallaby (Wallabia bennetti*) and the Eastern grey or Grey forester kangaroo (Macropus giganteus).

Marsupial retina does not seem to have been examined histologically again until 1936 when O'DAY described, in some detail, the retina of the Australian native cat (Dasyurus viverrinus) in which the presence of double cones with oil droplets is of particular interest. D. viverrinus is a small, carnivorous marsupial inhabiting the arid regions of southern Queensland and South Australia. It is predominanatly nocturnal and was described as possessing a well marked tapetum in the superior fundus with the optic disc lying in the superior temporal quadrant. Following ophthalmoscopic examination O'DAY reported a well developed retinal vascular system but saw no fovea. He suggested however, that the arrangement of blood vessels may define "a central strip".

O'DAY (1936) described the appearance of the fundus of D. viverrinus as being "not unlike that of the Virginian opossum (Didelphis)" as reported by JOHNSON (1901).

O'DAY's description of the outer nuclear layer (ONL) in D. viverrinus conforms to that generally reported for mammals. The central region of the ONL is 8 to 10 nuclei thick and the chromatin of the rod nuclei is arranged in 2 or

3 densely stained masses. The cone nuclei, scattered along the outer limiting membrane (OLM), possess diffuse chromatin.

In Mallory's stained retina O'DAY reported the cone myoids stain less deeply than the bulbous ellipsoids. The cone outer segments (COS) are conical and stain a deeper blue than the inner segments. The ROS on the other hand stain bright orange.

O'DAY also described the ellipsoids as containing a non-staining globular mass, surrounded by a lightly stained rim. These masses blackened when treated with osmic acid and O'DAY reported it as "reasonable to assume" that they are of lipid composition thus confirming HOFFMANN's (1876) report of oil droplets.

O'DAY noted that many of the cones occur in pairs, both members being equal in size and containing the same globular mass in the ellipsoids. This indicates the presence of twin cones but O'DAY's drawing shows the members as unequal in size, with the oil droplets lying at different distances from the OLM suggesting double cones. This discrepancy has been previously noted by WALLS (1938).

O'DAY (1936) also reported the presence of double cones and oil droplets in the retina of the Ring-tailed possum (Pseudocheirus laniginosus) but did not provide a detailed histological description of his specimens.

Shortly after O'DAY's publication WALLS (1938) described the retina of D. virginiana as having abundant rods and few cones. He also noted the presence of paired cone nuclei and classified the cones as single cones with or without oil droplets and double cones with one oil droplet located in the principal member, not two, one in each member,

as reported earlier by O'DAY (1936) for other marsupials. The oil droplets were reported to be colourless in fresh retina. WALLS went on to describe the retina of Marmosa mexicana, an American opossum, as having abundant rods and few cones. The cones are of the 3 types described for D. virginiana. In both species the members of the paired cones were dissimilar in size and form so were correctly referred to as double cones.

The literature also contains some more recent reports on the retina of Australian marsupials. In 1973 BRAEKEVELT reported 3 photoreceptor types in the Quokka; single rods which he described as being smaller and more electron dense than cones, which they outnumber 50 to 1, and 2 types of cones. The single cones possess a large oil droplet in their inner segments, as do both members of the so called "twin" cones. BRAEKEVELT described the "twin" cones as being formed by 2 cones lying in close apposition, with each member being morphologically "quite similar" to the other and to the single cones. BRAEKEVELT's light micrograph, however, clearly shows that the oil droplets lie at different distances from the OLM suggesting that the members of the "twin" cones are of different size and form. It may therefore be more accurate to describe these "twin" cones as double cones with an oil droplet in each member. The 2 members of a twin cone are identical and only occur in teleosts (WALLS, 1942).

The ultrastructural details of the photoreceptors of the Quokka as described by BRAEKEVELT (1973) fit the general vertebrate pattern. The CIS have a diameter of 10.0 µm and broaden to 15.0 µm at the sclerad end. The short COS taper

to a blunt end and contain double membrane discs that are not generally enclosed in the cell membrane. He reported the presence of a round to ovoid oil droplet lying sclerad to the ellipsoid. The nuclei, larger and less electron dense than the rod nuclei, lie immediately vitread to the OLM. The elongate ROS contain double membrane discs with deep incisures which break the periphery into lobules. BRAEKEVELT found that calycal processes extend from the sclerad end of the RIS to surround the ROS to which it is connected by a ciliary stalk. Elongate mitochondria are arranged longitudinally in the Quokka RIS to form a diffuse ellipsoid and the elongate nuclei contain several clumps of chromatin.

In the Quokka the photoreceptor synapses of both rods and cones appear to be formed by superficial and invaginated contacts with processes of bipolar and horizontal cells (BRAEKEVELT, 1973).

2.4 The Retinal Ganglion Cell Layer

The RGC layer has proven to be an area of considerable interest in retinal research and much of the literature available on the marsupial visual system deals with the RGC population. Mammalian RGCs have generally been studied using Nissl-stained retinal wholemounts. A number of authors, however, have taken advantage of the retrograde axonal transport of horseradish peroxidase (HRP) in their studies of RGCs. To date it appears that only Nissl-stained retinal wholemounts have been employed in the preparation of cell counts and isodensity maps of the RGC populations in marsupial retinae.

The topography of the RGC layer has been studied in several Australian marsupials (HUGHES, 1975b; FREEMAN and

TANCRED, 1978; TANCRED, 1981; BEAZLEY and DUNLOP, 1983) and in two species of American opossum (HOKOC and OSWALDO-CRUZ, 1978 and 1979; RAPAPORT, WILSON and ROWE, 1981). The distribution of RGCs has also been reported for Doria's tree-kangaroo (Dendrolagus doriana) (HUGHES, 1975b), an arboreal marsupial native to the Western Highlands of New Guinea.

The RGC layer of many vertebrates exhibits a regional specialisation called a visual streak. This streak may be described as a band of increased RGC density that extends across the retina in a position corresponding to the retinal image of the animal's horizon. The increased density of RGCs provides the potential for greater visual acuity as it decreases the convergence ratio of photoreceptors to RGCs. In the marsupial retina RGC counts for the visual streak generally exceed 2,000 cells/mm^2 compared with approximately 250 - 500 cells/mm^2 in the peripheral retina.

The presence of a well developed visual streak has been reported by HUGHES (1975b) in the Red kangaroo and the Grey forester kangaroo and in the Brush-tailed possum by FREEMAN and TANCRED (1978). Following a comparative study of the RGC populations in 5 Australian marsupials, TANCRED (1981) reported the presence of well developed visual streaks in two macropods, the Pademelon wallaby (Thylogale billiardieri), and Scrub wallaby or Tammar (Macropus eugenii). The Tasmanian devil (Sarcophilus harissi) and the Southern hairy-nosed wombat (Lasiorhinus latifrons) were also reported by TANCRED (1981) to have well developed visual streaks. While a less well developed streak was found in the retina of the Brown bandicoot (Isodon obesulus). Most recently BEAZLEY and

DUNLOP (1983) reported a well developed streak in the Quokka similar to that reported for the Tammar, Pademelon wallaby, Tasmanian devil and Brush-tailed possum.

In certain nocturnal tree-dwelling marsupials no visual streak has been found. In these cases the isodensity lines on the RGC maps are roughly concentric. Lack of a visual streak (or any horizontal band of increased sensitivity) has been reported for Doria's tree-kangaroo (HUGHES, 1975b), the South American opossum (Didelphis marsupialis aurita) (HOKOC and OSWALDO-CRUZ, 1978 and 1979) and the North American opossum (RAPAPORT et al., 1981).

In general it appears that terrestrial marsupials possess a visual streak while those species occupying an arboreal niche do not. The only notable exception being the Brush-tailed possum which has a prominent streak despite being mainly arboreal (FREEMAN and TANCRED, 1978). It was suggested by GIBSON (1950) that the presence of a visual streak is associated with species that live or graze on open plains and therefore need to survey the horizon for predators. There are however mammalian species, such as the Grey forester kangaroo, that do not normally enter open country yet possess a visual streak. Hence HUGHES (1977) considers that the streak is not exclusive to open country species but rather correlates with the terrestrial as opposed to the arboreal life-style. According to GIBSON (1950) the gradation of the "visual texture perceived" is the same whether or not the field of vision includes an overt or less well defined horizon. Furthermore, the relative position of the horizon in the retinal image remains invariant for open country species (HUGHES, 1975b). Therefore, as stated by

HUGHES (1975b), species from either open or forested country needing to survey their horizon might match the highest RGC densities with that portion of the retinal image corresponding to "the overt, or implicit, horizon".

If the field of vision of a grazing animal be compared with that of a tree-dwelling species it becomes apparent that the latter visual field lacks a fixed horizon. Therefore no features of the arboreal species' visual field occupy an invariant position in the retinal image and their retinae generally exhibit a high degree of radial symmetry (with respect to the isodensity lines drawn from RGC counts) about the point of fixation (HUGHES, 1975b). This is true of the North and South American opossums (RAPAPORT et al., 1981; HOKOC and OSWALDO-CRUZ, 1978 and 1979), and of Doria's tree-kangaroo (HUGHES, 1975b). As stated previously, this is not the case in the retina of the Brush-tailed possum which has a well developed visual streak (FREEMAN and TANCRED, 1978) and is reported to have a highly developed system of central visual projections (GOLDBY, 1941).

A second regional specialisation, the area centralis, is known to occur in the retina of some placental mammals. The area centralis generally lies along the retinal horizon temporal to the optic disc and may be incorporated within the visual streak. Its increased concentration of RGCs and reduced convergence ratio provide the potential for greater visual acuity than exhibited by the visual streak. A well defined area centralis has been reported in several terrestrial species of marsupials: M. rufus (HUGHES, 1975b), T. billiardieri, M. eugenii and S. harissi (TANCRED, 1981), and S. brachyurus (BEAZLEY and DUNLOP, 1983). The Brown

bandicoot possesses a less well defined area centralis (TANCRED, 1981), and despite the occurence of a well developed visual streak no area centralis was evident in the Southern hairy-nosed wombat (TANCRED, 1981). The presence or absence of an area centralis does not appear to be correlated with either the terrestrial or arboreal habitats, and its presence has also been reported in the retina of the following arboreal marsupials; D. doriana (HUGHES, 1975b), T. vulpecula (FREEMAN and TANCRED, 1977), D. marsupialis aurita (HOKOC and OSWALDO-CRUZ, 1978 and 1979) and D. virginiana (RAPAPORT et al., 1981).

In his study of the cat RGC population HUGHES (1975a) reported that the presence of cytoplasmic Nissl substance allows the differentiation of neurons from glia. Using cell soma diameter and Nissl-staining properties HUGHES described a method, now widely used, for classifying RGCs. Large- and medium-sized neurons typically contain a large nucleus with prominent nucleolus. The cell bodies are generally irregular in outline and the cytoplasm contains Nissl granules. Small neurons also possess a large, but often eccentric, nucleus with prominent nucleolus but have relatively less cytoplasm and little Nissl substance. Most glia are smaller than the smallest neurons of the RGC layer, have small nucleoli and lack Nissl substance.

Several authors have employed Nissl-stained wholemounts of adult marsupial retinae to determine the density of cells whose bodies lie within the RGC layer. The total number of RGCs has been calculated for both the North and South American opossums (RAPAPORT et al., 1981; HOKOC and OSWALDO-CRUZ, 1978 and 1979), and for the Brush-tailed possum

(FREEMAN and TANCRED, 1978). For the opossums the total RGCs numbers are 77,000 and 101,000 cells respectively; while the total number of RGCs is much higher for the Brush-tailed possum (approximately 280,000). The only other marsupial for which this type of data is available is the Quokka (BEAZLEY and DUNLOP, 1983) (see Table 2.4.1) in which the total number of RGCs ranges from 336,000 to 393,000.

From the published data it appears that an increase in the total RGC population is usually accompanied by an increase in the retinal area, although these increases are not directly proportional.

FREEMAN and TANCRED (1978) reported that the soma diameter of the RGCs in the Brush-tailed possum ranges from 5.0 to 26.0 µm. The mean soma diameter is 12.8 µm and roughly two thirds of the total RGC population has a diameter between 7.0 and 13.0 µm. No attempt appears to have been made to classify the RGCs according to either size or staining properties.

In 1978 HOKOC and OSWALDO-CRUZ reported similar data for the South American opossum. Cell soma diameter ranges from 6.0 to 21.0 µm with the larger RGCs being present at the periphery. Using the same criteria of HUGHES (1975a) HOKOC and OSWALDO-CRUZ (1979) divided the RGCs into 3 groups. The largest cells have a soma diameter between 13.0 and 19.0 µm, large coarse Nissl-granules and a large nucleus with prominent nucleolus. The small RGCs have a thin rim of cytoplasm with few Nissl granules and a soma diameter between 6.0 and 12.0 µm. While the medium cells have a soma diameter between 9.0 and 15.0 µm, smaller nuclei than the large cells and finer Nissl granules. Once again it was found that the

larger RGCs are more numerous at the periphery, and there is a gradual reduction in cell size as the area centralis is approached.

According to the data supplied by RAPAPORT et al. (1981) the North American opossum exhibits a broader range of RGC soma diameter (7.0 to 32.0 µm) than its South American counterpart. These authors were also able to distinguish 3 different classes of RGCs on the basis of soma size and retinal topography. The large RGCs measure 24.0 and 32.0 µm in diameter and were found to be evenly distributed across the retina. Medium-size RGCs measure from 12.0 to 23.0 µm in diameter and were found to be most numerous in the superior temporal quadrant. While small RGCs are prominent in all regions of the opossum retina, particularly in nasal and inferior retina, and soma diameter ranges from 7.0 to 11.0 µm. Upon further analysis of soma size distribution RAPAPORT et al. (1981) suggested that the medium-size RGCs be further divided into small-medium and large-medium groups.

Work by TANCRED (1981) has shown that the ranges of RGC soma diameter in the retinae of five Australian marsupials are similar to those reported for the two Didelphis species and the Brush-tailed possum (see Fig. 2.4.1).

TANCRED has also reported some interesting trends relating to the distribution of these RGCs. Supportive of HOKOC and OSWALDO-CRUZ (1979) is her statement that there is a decrease in mean cell size from the periphery to the visual streak and area centralis. Further, she found that the distribution of small and medium RGCs shows regional variation. The percentage of small RGCs increases from a minimum level nasally to a maximum temporally. Small, medium

and large RGC soma diameters were given for the Tasmanian devil, Tammar and Pademelon wallaby.

The most recent study of RGCs to have appeared in the literature is that of BEAZLEY and DUNLOP (1983) which deals with the development of the area centralis and visual streak in the Quokka (see Section 2.6).

Species	Total number of Retinal Ganglion Cells
D. virginiana	n = 77,4000
D. marsupialis	n = 101,000
T. vulpecula	n = 280,000
S. brachyurus	336,000 - 393,000

Table 2.4.1 Total number of ganglion cells in the retinae of four species of marsupials showing considerable variation possibly due to the variation in retinal area (see text Section 2.4).

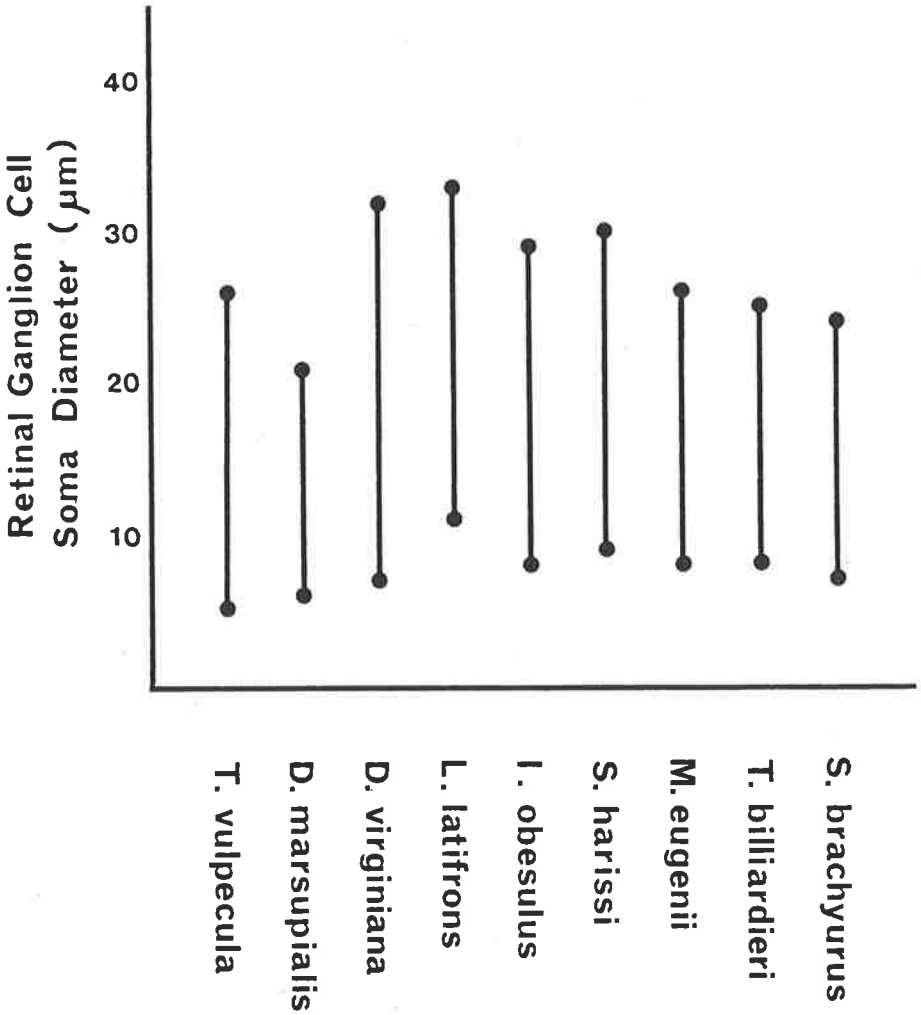

Figure 2.4.1 Range of retinal ganglion cell soma diameter in nine species of marsupials as determined from retinal wholemounts: T. vulpecula 5-26 µm (FREEMAN and TANCRED, 1978); D. marsupialis 6-21 µm (HOKOC and OSWALDO-CRUZ, 1978); D. virginiana 7-32 µm (RAPAPORT et al., 1981); L. latifrons 11-33 µm, S. harissi 9-30 µm, M. eugenii 8-26 µm and T. billiardieri 8-25 µm (TANCRED, 1981); S. brachyurus 7-24 µm (BEAZLEY and DUNLOP, 1983).

2.5 Tapetum

Many animals show eyeshine when light is shone into their eyes. This phenomenon is usually due to the presence of a reflecting layer called a tapetum lucidum in either the RPE or the choroid. When a tapetum is present light not absorbed by the photoreceptors is reflected or scattered back through the retina where the photoreceptors are thus exposed a second time. Any reflected light not absorbed by the photoreceptors passes out of the eye and results in eyeshine. Tapeta function to enhance the sensitivity of the eye; important in an environment where there is a limited amount of light. Where there is no tapetum most of the light is absorbed by the pigment in the RPE or the choroid.

Tapeta lucida have been classified according to location (choroidal or retinal), to whether the reflecting material is extra- or intra-cellular (tapetum fibrosum or tapetum cellulosum), or their optical properties (specular, diffuse reflecting or scattering).

The extracellular tapetum fibrosum, exemplified by that of ungulates, lies in the choroid immediately sclerad to the choriocapillaris. Light is reflected by a dense, regular array of collagen fibres that glistens like a tendon and is perforated by a minimum number of blood vessels supplying the choriocapillaris.

In most tapeta the reflecting material is intracellular. These tapeta cellulosa may be choroidal, as in elasmobranchs, or retinal, as in most of those teleosts that have tapeta. In the choroidal tapeta of this type in the cat and the bush-baby (Galago crassicaudatus) the specialised cells are stacked so that their boundaries are

aligned, and the cytoplasmic optical elements occur in very regular arrays. In the retinal tapeta cellulosa of teleosts the reflecting material occurs within the cells of the RPE.

The most highly reflecting tapeta are those containing guanine, which has a refractive index of 1.8. A stack of flat crystals of quarter wave thickness separated by quarter wave spaces gives a very high reflectance due to constructive interference (see LAND (1972) for discussion). Specular tapeta depending on orientated guanine crystals occur in fishes and some invertebrates, but not in mammals. The tapeta of carnivores also depend on constructive interference for their reflectance. The reflecting elements, however, are not flat crystals but rodlets; of a zinc-containing protein in the cat, and of riboflavin in the bush-baby (PIRIE, 1959).

The reflection from a specular tapetum may be directional so that reflected light will pass out of the eye and not degrade the image. Some teleosts possess this type of tapetum with regular arrays of crystals in the RPE cells. In other cases the tapetal material occurs as randomly arranged particles or droplets of irregular size that scatter light and give a diffuse rather than specular reflection. The scattering particles may be lipid, complex substances such as pteridine or crystals, including guanine. Diffuse tapeta occur in many fishes (NICOL, ARNOTT and BEST, 1973). As will be discussed later, the Virginian opossum is unusual among marsupials since it has a diffuse retinal tapetum in which the reflecting material is lipid.

BRÜCKE (1845) reported the presence of a fibrous tapetum in the Native cat. According to WALLS (1938), however, the structure of the tapetum in this nocturnal

marsupial resembles that of a tapetum cellulosum. O,DAY (1936) confirmed the presence of a tapetum in the superior fundus of Dasyurus by ophthalmoscopic examination.

BRÜCKE (1845) also reported that the Tasmanian wolf (Thylacinus cynocephalus) possesses a fibrous choroidal tapetum. This marsupial is considered to be extinct and no further reports have appeared in the literature so BRÜCKE's report is likely to remain unconfirmed.

Sometime later JOHNSON (1901) reported the presence of a tapetum in the superior fundus of the North American opossum's eye. WALLS (1938) has since confirmed JOHNSON's report and described the tapetum of D. virginiana as being "quite unlike that of any other known marsupial": consisting of large RPE cells devoid of pigment but full of reflective particles. PIRIE (1961) was able to determine that the reflective material in the tapetal cells of Didelphis is cholesterol or cholesterol esters, and went on to describe the reflective particles as crystalline. RODIECK (1973) however, reported that these reflective particles are in fact lipoidal spheres. BRAEKEVELT (1976) stated that in species where lipoidal spheres are present as the reflective particles the tapetum is invariably located within the RPE. Furthermore, HAZLETT (1976) found that the tapetal retina of D. virginiana is characterised by the presence of many closely-packed rounded, membrane-bound droplets in the cells of the RPE. He also noted that the tapetal retina blackened when placed in a mixture of chloroform and methanol suggesting the presence of a lipid tapetum. BRAEKEVELT (1976) confirmed the presence of numerous lipoidal spheres, that function as the reflecting material, in the RPE of

D. virginiana. He also reported that few or no melanosomes are present in the RPE indicating that the tapetum is of the non-occlusible type. Both melanosomes and lipoidal spheres are present in the peripheral cells of the RPE of the tapetal area.

WALLS (1938) considered the presence of a tapetum in the superior fundus of Didelphis has a marked effect upon the distribution of the retinal photoreceptors. There is reportedly a high concentration of rods with exclusion of cones with out oil-droplets associated with the tapetum. In comparison, M. mexicana lacks a tapetum lucidum (WALLS, 1938) and rods are uniformly distributed throughout the retina. Cones are more numerous centrally and scattered toward the periphery.

JOHNSON (1901) reported that the tapeta of all the marsupials examined produce eyeshine. He also suspected the presence of a tapetum in the "marsupial flying squirrel", an unspecified member of the Petaurus genus. The Tasmanian devil was reported by FRANZ (1934: cited by WALLS, 1938) to possess a tapetum in which the reflective particles may be occluded by the migration of melanin granules in the choroidal cells.

More recently FREEMAN and TANCRED (1978) noted the presence of a "weak" tapetum, apparently seen during dissection under saline, in the superior fundus of the eye of the Brush-tailed possum. They further noted that the lower border of the tapetum appears to coincide with the animal's horizon, assumedly the horizon of the retinal image, when the eyes are in their presumed primary position.

The South American opossum (D. marsupialis aurita) is

described as having a retinal tapetum in the superior fundus which is yellowish in colour and charcterised by a large number of granules within the RPE (HOKOC and OSWALDO-CRUZ, 1979). As with the Brush-tailed possum HOKOC and OSWALDO-CRUZ (1979) suggested that the line separating tapetal from non-tapetal retina corresponds to the projection of the horizon onto the retina.

2.6 Development of the Marsupial Retina

The literature on the marsupial visual system contains only limited information on the development of the retina. LEURE-DU-PREE (1975) briefly described the retinal ultrastructure of 7 day old pouch young of the North American opossum, observing the maturation of the retina to occur in a centrifugal manner, and reported that the retinal layers are recognisable. Development of the photoreceptors is incomplete at this age; nucleus, basal body and cilium are reportedly present, and synaptic terminals moderately differentiated. The inner plexiform layer (IPL)is clearly delineated but contains rather few conventional synapses, and no dyads, serial or reciprocal synapses were found.

Using Nissl-stained wholemounts BEAZLEY and DUNLOP (1983) examined the developing RGC population of the Quokka in specimens from 25 days postnatal to adulthood. Prior to 50 days postnatal the RGC population was found to be evenly distributed, and after this age increased RGC densities were observed in those areas corresponding to an horizontal visual streak and area centralis.

At 33 days postnatal BEAZLEY and DUNLOP (1983) observed all the cells in the RGC layer to be differentiated. RGCs were discernible at 87 days postnatal and noted to have

diameters of 7.0 to 18.0 μm. At 143 days the soma diameter ranged from 7.0 to 23.0 μm and in adult retinae a range of 7.0 to 24.0 μm was noted.

Between 25 and 250 days postnatal the total number of RGCs remained similar to the adult range of 336,000 to 393,000. Counts of optic nerve axons ranged from 75,000 at 25 days to 224,000 in adults. The authors have also proposed and discussed mechanisms to account for the development of a visual streak and area centralis.

2.7 Optic Nerve

Following electrical stimulation of the optic chiasma of the Brush-tailed possum FREEMAN and WATSON (1978) were able to record a compound action potential from the optic nerve. The trace showed 4 negative peaks each of which corresponded to a conduction velocity group of optic nerve fibres. They were unable to find any direct correlation between the frequency distributon of optic nerve fibre diameters and the conduction velocity groups. Similarly, FREEMAN (1978) was unable to find any correlation between size distribution of RGC axons at the nasal and superior temporal margins of the optic disc and the action potential recorded at these sites. However, by considering the frequency distribution differences between these sites FREEMAN(1978) was able to infer that the second conduction velocity group is represented by a population of medium sized axons and that the fourth (slowest) conduction velocity group may be represented on the nasal side of the optic disc by a population of small axons.

Using electrophysiological stimulation and recording techniques ROWE, WILSON and RAPAPORT (1981) were able to

demonstrate the presence of 3 conduction velocity groups among the axons in the optic nerve of D virginiana. They were also able to determine the probable RGC types from which the axon groups arise by injecting HRP into one optic tract and tracing the axons to the RGC layer. The fastest velocity group of axons (d1) appear to originate from the large RGCs which project both ipsilaterally and contralaterally from the temporal retina. Most of the fibres belonging to the middle velocity group (d2) arise from the large-medium RGCs which project mainly from temporal retina to the ipsilateral side. While the majority of the slowest conducting axons (d3) probably arise from the small RGCs, most of which projectcontralaterally from the temporal retina. The RGC soma size groups used in this paper were those previously determined by the authors (RAPAPORT et al., 1981). This type of velocity grouping of optic nerve fibres is common among mammals of varying habitat and visual needs, and therefore ROWE et al. (1981) suggested that it may have been characteristic of early mammals.

2.8 Visual Field

By standardising the posture SOUSA, GATTASS, HOKOC and OSWALDO-CRUZ (1978) were able to investigate the optical and retinal visual fields of the South American opossum. They found that the monocular visual field of this tree-dwelling marsupial corresponds to the "optical field of an eye" as defined by HUGHES (1977). The binocular retinal cyclopic field is that portion of space accessible to both eyes and extends over 125^{o} in the opossum.

The effective visual field is that region of space which forms a retinal image and is smaller than that

determined for optical or retinal visual fields due to the presence of cranial structures that block the light rays. SOUSA et al. (1978) determined that this restricted field of vision extends over 100° at the level of the horizontal plane.

The visual fields of this opossum are similar to those found in other predatory animals (SOUSA et al., 1978) and are comparable to the cat (HUGHES, 1977). No other reports on the visual fields of marsupials have been found in the literature.

2.9 Marsupial Retinal Projections

The literature on the marsupial visual system includes reports on the retinal projections of several Australian and American species. As a general rule the primary optic centres in the mammalian brain include both dorsal and ventral lateral geniculate nuclei (LGNd and LGNv), lateral posterior nucleus (LPN), pretectal nuclei, superior colliculus (SC) and suprachiasmatic nucleus of the hypothalamus (SCN). These nuclei represent the terminations of optic nerve fibres that have arisen directly from the RGCs. The accessory optic system includes secondary neurons that radiate from the LGNd and LGNv to the visual (striate) cortex.

As will be seen, the marsupial visual system conforms to this general mammalian arrangement. It is interesting to note that while the retinal projections in each marsupial species so far studied are very similar, the internal arrangement of the LGNd shows considerable variation.

In the following paragraphs the general arrangement of the retinal projections of marsupials will be considered.

With the exception of the LGNd no attention will be given to the details of the terminations of the retinal projections as this is beyond the scope of this review.

At least 2 studies of the visual system of D. virginiana have appeared in the literature. GIOLLI (1965) investigated the fibre organisation of the accessory optic system of this opossum. Using silver staining and axon degeneration techniques GIOLLI demonstrated that all the accessory fibres cross at the optic chiasma and leave the primary optic tract to travel caudally on the surface of the cerebral peduncle and terminate in the nucleus of the transpeduncular tract.

GIOLLI reported that organisation of the accessory optic system in D. virginiana is similar to that of birds and reptiles, and that comparison with "more advanced" mammals indicates that this system has undergone organisational changes in the latter.

More recently ROYCE, WARD and HARTING (1976) published a report on the visual centres of D. virginiana. They were able to demonstrate that the arrangement of the visual nuclei is typical of that described for other marsupials. According to these authors the direct ipsilateral input to the LGNd is overlapped completely by the more extensive contralateral retinal projections. They were unable to demonstrate the presence of any obvious cell layers within the LGNd while OSWALDO-CRUZ and ROCHA-MIRANDA (1967) reported that α and β divisions are apparent.

ROYCE and his co-workers also described the retinal projections of Marmosa mitis and found them to be similar to those in Didelphis. However, the internal

arrangement of the LGNd differs considerably. They described the LGNd of this species as showing considerable separation and overlap of ocular inputs. Several laminae of retinal fibre terminations were identified; 2 with ipsilateral input, 3 with contralateral input and 2 that receive bilateral retinal projections.

There have also been several reports dealing with the projections to and the organisation of the visual cortex of the North American opossum (BENEVENTO, 1968; BENEVENTO and EBNER, 1969 and 1971).

Using a combined autoradiographic and degenerative study LENT, CAVALCANTE and ROCHA-MIRANDA (1976) were able to describe the retinofugal projections in the South American opossum. Their autoradiographic material demonstrated that the accessory optic system of this opossum is similar to that found in the Australian Brush-tailed possum by HAYHOW (1966 and 1967). This study also confirmed the presence of retinal projections ending in the hypothalamic SCN, and demonstrated that the terminals of the retinal projections to the LGNd have a laminar pattern. Projections to the pretectum and LGNv were observed using both techniques, and the authors concluded that the general pattern of retinal projections in D. marsupialis aurita is similar to that for eutherian mammals.

Several reports of the visual pathways of T. vulpecula have also appeared in the literature. PACKER (1941) reported all fibres of the optic nerve to be myelinated and that all degenerate following section of the nerve. This however was a light microscopic study and small unmyelinated fibres may not have been resolved. He found that 75% of these fibres

cross at the chiasma and end in the LGNd, LGNv, SC, and nucleus opticus tegmenti via the accessory optic system. The remaining uncrossed fibres were observed to terminate in the LGNd. No evidence was found for retinal connections to the LPN or pretectum. Uncrossed and crossed fibres ending in the LGNd mostly lie in alternate laminae.

HAYHOW (1966) studied the accessory optic system of the Brush-tailed possum by removal of one eye and subsequent staining of degenerating fibres. He also found that 25% of the degenerating optic nerve fibres remained uncrossed, and observed them to occupy a superficial venterolateral position within the optic chiasma the uncrossed fibres remain separate from those fibres that project contralaterally, but they mix in more posterior chiasmatic regions. The crossed accessory fibres form a diffuse fasciculus superficial to the contralateral supraoptica hypothalami where they follow the primary optic fibres. Posterior to the pars tuberalis these fascicular fibres were found to pass the basis pedunculi and subthalamic nucleus of Luys to terminate in the medial terminal nucleus of the accessory optic system.

HAYHOW (1967) confirmed that the LGNv and pretectum are primary centres in the Brush-tailed possum. He also reported the presence of 4 obvious cell layers within the LGNd, and 6 bands formed by optic nerve fibre terminations. Of these bands number 1, 2b, 4 and 5 receive bilateral retinal input and laminae 2a, 3 and 6 receive contralateral projections with bilateral overlap in 1, 2a and 2b.

Shortly after the publication of data for the retinal projections of the Brush-tailed possum, JOHNSON and MARSH (1969) described the arrangement of laminae within the LGNd

of the Sugar glider (Petaurus breviceps). They reported the presence of a central core and 4 laminae which thay designated outer and inner layers of large cells (OL and IL) and outer and inner layers of small cells (OS and IS). JOHNSON and MARSH indicated that the core of the LGNd of P. breviceps is the equivalent of the β-division of D. virginiana and lamina 6 in T. vulpecula (OL=1,IL=2a+2b, OS=3 and IS=4+5). These authors also reported a less well developed arrangement of laminae within the LGNd of M. rufogriseus and M. rufus.

All the primary visual centres except the SCN of the hypothalamus have been demonstrated to be present in Pseudochierus peregrinus, the Ring-tailed possum (PEARSON, SANDERSON and WELLS, 1976). No obvious cell layers were found in the LGNd while several laminae resulting from optic nerve fibre terminations were found. Laminae 1 and 3 receive contralateral input and laminae 2 and 4 receive ipsilateral input; these 4 laminae constitute the α-division of the LGNd. The fifth internal lamina of the LGNd of P. peregrinus forms the β-division.

In their study of the retinal projections of the Native cat (D. viverrinus) SANDERSON and PEARSON (1977) were able to demonstrate that the majority of the primary optic centres receive bilateral retinal input. While the LPN and accessory optic system receive only contralateral projections. The hypothalamic region was not investigated in this study. SANDERSON and PEARSON were able to identify 5 internal laminae in the LGNd of this Dasyurid. Layers number 1 and 2 receive contralateral and ipsilateral input respectively. The contralateral input is confined to the ventral quarter of

the LGNd and represents the monocular visual field. While layers 3,4 and 5 receive retinal projections from both eyes. The extensive overlap in the LGNd of D. viverrinus was reported to be similar to that found in D. virginiana by ROYCE et al. (1976) and LENT et al. (1976).

More recently SANDERSON and PEARSON (1981) have reported on the retinal projections of the Southern hairy-nosed wombat. The general arrangement of optic nerve fibre terminations is similar to that reported for other marsupial species. The pretectal nuclei, LGNv and SCN receive bilateral input similar to that reported by CAVALCANTE et al. (1975), LENT et al.(1976), PEARSON et al. (1976), ROYCE et al. (1976), SANDERSON and PEARSON (1977), LENT and ROCHA-MIRANDA (1978), SANDERSON, PEARSON and DIXON (1978) and SANDERSON, PEARSON and HAIGHT (1979). The SC and accessory optic system also receive bilateral input while the LPN receives mostly contralateral retinal projections.

SANDERSON and PEARSON (1981) were able to identify 3 obvious cell layers (A,B and C) within the LGNd and 8 cytoarchitectural laminae of retinal input. Laminae 1, 3, 5, 6 and 8 receive projections from the ipsilateral eye, and laminae 2, 4 and 7 receive only contralateral input. No overlap of optic nerve fibre terminals was found in the LGNd. The ventral portion of the LGNd which represents the monocular segment is large and receives only contralateral input. The monocular segment is obviously larger than the binocular segment. As indicated by the authors this is not unexpected since the wombat has a rather large head with laterally positioned eyes and therefore most of its visual field is monocular.

GAWRYSLEWSKI and HOKOC (1981) studied the retinal projections of D. marsupialis aurita with respect to the position of the RGC soma within the RGC layer. Following HRP filling of cut axons in the optic tract, and surgical section of the optic tract, they were able to determine from retinal wholemounts that most ipsilaterally projecting RGC lie in the temporal retina. They also showed that contralaterally projecting RGCs lie in both nasal and temporal retina. The density of RGCs with uncrossed projections is low at the area centralis and gradually increases toward the periphery. While the reverse was reported for contralaterally projecting RGCs.

2.10 Concluding Remarks

Literature dating from the 19th. and early 20th. centuries contains few reports on the eyes of marsupials. Two of these dealt with the ophthalmoscopic appearance of the fundus of a variety of marsupials. More important, however, was HOFFMANN'S report of the presence of oil droplets in the retinae of two Australian marsupials. This was the first time oil droplets had been reported in mammalian photoreceptors.

This work was not followed up until the 1930's when O'DAY and WALLS separately confirmed HOFFMANN'S report of oil droplets following their own histological examinations. Their concurrent ophthalmoscopic examinations also extended the earlier work.

Nearly forty years elapsed before any further work on the structure of the marsupial retina when several papers became available; most of them concentrated on the ultrastructure of the RPE rather than the neuroretina. At

the same time a limited number of publications appeared on the development of the marsupial retina and only one dealing with the visual field.

Within the last decade, however, a considerable volume of work has been carried out on the RGC population of a variety of marsupials native to Australia and America. This, in combination with the extensive work conducted since 1939 on the retinal projections of the marsupial visual system, forms the majority of the recent work.

Little modern work has been done on the retinal structure as such and it is intended that the following comparative study will enlarge the scope of knowledge of the marsupial visual system.

3 MATERIALS AND METHODS

3.1 Animals

Specimens were collected from adult Brush-tailed possums (Trichosurus vulpecula) obtained from the Central Animal House of the University of Adelaide.

Material from adult Kowaris (Dasyuroides byrnei) was kindly provided by Dr. W.G. Breed of the Department of Anatomy and Histology, University of Adelaide and Dr. K. Sanderson of the School of Biological Sciences, Flinders University of South Australia.

Specimens from adult Kangaroo Island kangaroos (Macropus fuliginosus fuliginosus) were initially collected by Mr. John Watkins of the National Parks and Wildlife Service and Dr. P. Phillips of the Institute of Medical and Veterinary Science, Adelaide. Subsequently a field trip was made to Kangaroo Island, South Australia where I collected eyes from adult kangaroos made available by Mr. John Watkins the Ranger at Murray's Lagoon National Park.

Possums and Kowaris were killed using an overdose of Nembutal (pentobarbitone sodium, Ceva Chemicals Australia) administered intraperitoneally. Kangaroos were shot by Mr. John Watkins as part of the normal control of the size of the herd (under a National Parks and Wildlife Service destruction permit).

3.2 Removal of Eyes and Dissection

Subsequent to performing a canthotomy the eye was removed by carefully snipping through the conjunctiva and then severing the extra-ocular muscles and optic nerve. Orientation was maintained by placing a 6/0 silk suture in the vertical midline of the eye just superior to the cornea.

The eye was immediately punctured using a sliver of razor blade and a small triangular window cut just posterior to the limbus to allow fixative to enter the vitreous chamber.

Following approximately 15 minutes fixation (see Section 3.4) the anterior segment of the eye was removed under fixative (see Fig.3.2.1) and the vitreous carefully cleaned away from the retina. At this time the eyecup was dissected into triangular segments using a razor blade and the sclera removed from the choroid and retina by blunt dissection.

3.3 Technical Considerations

During the initial phase of this study the retinal tissue from adult Kowaris and Brush-tailed possums was fixed using the 2.5% glutaraldehyde - 1.0% paraformaldehyde fixative routinely used in this laboratory (GLAUERT, 1975) [see Appendix II]. Despite the good results previously obtained by others using this fixative, the fixation of both the inner and outer plexiform layers was poor and ultrastructural details not readily resolved. Therefore the aldehyde fixative was modified over a period of time by the addition of sucrose and/or polyvinylpyrrolidone (MW=40,000). Satisfactory results were finally obtained using the aldehyde fixative of FORSSMANN (1981) [see Appendix III].

Since good fixation was achieved with FORSSMAN's fixative it was used on the field trip. Upon removal a triangular window was cut in each of the kangaroo eyes which were then immersed in fresh fixative. It was not possible to remove the anterior segment until reaching the field station laboratory some two hours later. This considerable delay in dissection probably resulted in the relatively poor fixation

achieved.

It should also be mentioned that the herd from which the adult kangaroos were obtained was affected by a neurotoxin present in the Phillaris grass upon which they grazed. Brain tissue from kangaroos in this population was being examined by Dr. P. Phillips who reports the presence of toxin-related pigment granules in the neurons (personal communication). Therefore it is possible that the retinal neurons may also contain such pigment.

During the period in which the Golgi study was conducted no camera lucida attachment was available for the Olympus BH transillumination light microscope used. Therefore serial sections showing retinal cells with adequate filling were photographed using a Wild MP551 camera and tracings were made from micrographs. Measurements were made from these scale tracings which were subsequently reproduced in ink (see Sections 7.1, 7.2 and 7.3). Care was taken during this process to minimise the margin of error in the measurements.

3.4 Microscopy

Following removal eyes were fixed in phosphate-buffered glutaraldehyde - paraformaldehyde fixative (FORSSMAN, 1981) for 2 to 8 hours at 4°C. The retina, with choroid intact, was then washed 3 times at 15 minute intervals in 0.1M phosphate buffer, pH 7.4, and post-fixed in 1.0% osmium tetroxide in 0.1M phosphate buffer, pH 7.4 for 1 hour at room temperature.

Specimens were again washed in phosphate buffer before being dehydrated through a graded series of ethanol which was removed by 3 15 minute washes in propylene oxide [see

Appendix IV]. Tissue was infiltrated with and embedded in Araldite resin (Polaron Equipment Ltd., England) [see Appendix V] and polymerised for 24 to 48 hours at 70°C.

a) Light microscopy

1.0 µm sections were cut, using glass knives, on a Cambridge Huxley Mk II ultramicrotome and stained with a polychrome stain [see appendix VI]. All slides prepared in this manner were examined using an Olympus BH transillumination light micrscope.

b) Transmission electron microscopy

Thin sections with silver-gold interference colours (60 - 90 nm thickness) were cut on a Cambridge Huxley Mk II ultramicrotome using glass knives. Sections were collected from the distilled water bath using 200 or 300 mesh copper - rhodium grids (Graticules Ltd., England) and stained with uranyl nitrate and Reynold's lead citrate [see Appendix VII]. Sections were examined in a JEM-100S transmission electron microscope (Jeol Ltd., Japan) at 60kV.

c) Histochemistry

Retinal tissue for histochemistry was obtained and dissected as previously described (see Section 3.2), but the sclera was not removed. Fixation was by immersion in cold 10% neutral-buffered formalin; dehydration through ethanol and infiltration of paraffin were done in a Duplex Processor (Shandon Elliot) and the tissue embedded in paraffin.

Serial 7.0 µm thick sections were cut on a Leitz microtome using a metal knife, floated on a water bath and collected on albuminised slides. Following drying

in a 30°C oven serial sections were alternately stained using the Periodic Acid-Schiff's reaction, Gomori's reticulin method and orcein [see Appendix VIII].

3.5 Golgi silver-staining

Initially retina from the Kowari was processed for silver-staining using a modified form of NASSEL and SEYAN's (1979) Golgi-Colonnier method (cited by STRAUSFELD, 1980) [see Appendix IX]. While this method proved moderately successful with Kowari retina adequate results were not obtained with similarly processed retina from the Brush-tailed possum. Subsequently a number of other Golgi silver-staining techniques were employed. The rapid Golgi-aldehyde method of MOREST (1981) was tried both with and without recycling [see Appendix IX] but did not provide adequate filling of cells. Nor were modifications of KEMALI's (1976) rapid Golgi method and COLONNIER's (1964) modified Golgi Kopsch method [see Appendix IX] successful when used for possum retina.

Kangaroo retinal tissue collected during the field trip was subsequently processed for both the Golgi-Colonnier and rapid Golgi-aldehyde methods described in Appendix IX and previously used with retinal tissue from the Kowari and Brush-tailed possum. Neither of these methods provided good silver-impregnation of the Kangaroo retinal cells and very few impregnated cells were identified.

There is an apparent species difference with respect to the Golgi impregnation of retinal cells between the marsupials studied. Further sampling and modification of the techniques may or may not result in more success given the unpredictable nature of the Golgi methods.

3.6 Photography

All light micrographs were taken on Ilford PanF ASA50 black and white film using a Wild MP551 camera and Photoautomat MPS45 on an Olympus BH microscope.

Macrophotography of the eyecups was done using an Olympus OM-2 camera on OM autobellows and stand, and an 80 mm Olympus macro lens. Ilford FP4 ASA125 black and white film was used for this purpose.

Ilford PanF and FP4 films were developed using Patterson's Aculux developer diluted 1:9 for 5 1/2 and 6 1/2 minutes at 20°C, respectively, with agitation, and fixed in Ilford Hypam Rapid Fixer diluted 1:4.

Electron micrographs were taken using a JEM-100S transmission electron microscope (Jeol Pty. Ltd., Japan) and recorded on 3 1/2 x 4 inch Ilford Technical film. This was processed using Kodak D19 developer diluted 1:2 for 4 1/2 minutes at 20°C and subsequently fixed in Ilford Hypam Rapid Fixer diluted 1:9.

35 mm negatives and plates were enlarged using Leitz Focomat IIa and Durst Laborator 1000 enlargers respectively, and printed on Ilford paper subsequently developed with Ilford Ilfospeed paper developer and fixer.

3.7 Retinal Wholemount Preparation (after STONE, 1981)

Eyes were fixed by immersion in 10% formal-saline for 1 week following removal of the anterior segment.

Working under saline the eyecup was orientated and a small cut made superiorly to allow orientation of the free retina.

The retina was freed along its edge using a blunt probe and the sclera progressively cut away. A scalpel was then

used to free the retina (with choroid) from the optic nerve.

A tear was then made in the choroid near the optic disc and the choroid (with pigmented epithelium attached) pulled away piecemeal using fine-tipped forceps.

The free retina was orientated, floated onto a clean glass slide and removed from the saline. Several cuts were then made peripherally and the retina flattened with its vitread surface uppermost and the vitreous carefully blotted to leave the retinal surface clean.

Once clean, the retina was refloated on saline, floated onto a gelatine-coated slide and reflattened.

The retina was then fixed to the slide by exposure to formalin vapour for 48 hours at room temperature and subsequently stained with cresyl violet [see Appendix X].

Cell soma diameter of the cells within the RGC layer of wholemounted retinae was determined by measuring their maximum diameter. When determining both the RGC counts and the cell types, as described by HUGHES, 1975a), cells were examined from an area of retina measuring 100 μm x 100 μm.

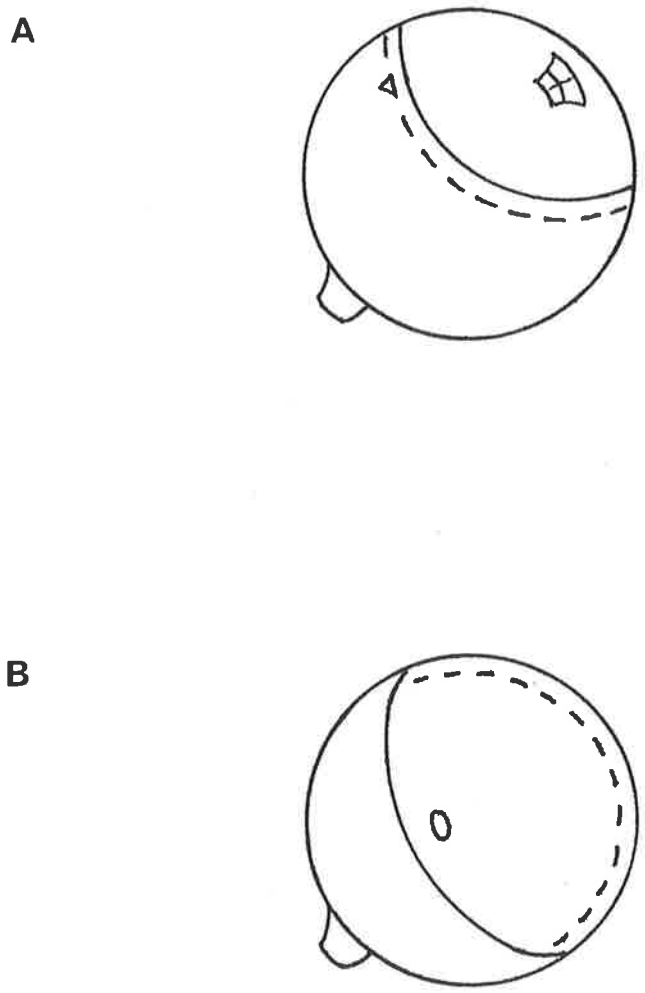

Figure 3.2.1 Disection of eyes.
A. Using scissors and forceps the cut is continued from the triangular window just posterior to the limbus as indicated by the dotted line (----).
B. The eyecup after the anterior segment has been removed.

4 RETINAL ANATOMY OF THE BRUSH-TAILED POSSUM

4.1 Fundus

The fresh eyecup of the Brush-tailed possum is divided into roughly equal superior and inferior portions. The superior fundus appears orange while the inferior fundus exhibits the transluscent grey colour typical of retinae that lack tapeta (see Figure 4.1.1). Across a sigmoidal horizon (see Figure 4.1.1) there is a narrow band where the orange and grey appear to be mixed. The orange colour of the superior fundus is due to the presence of a tapetum, which in this marsupial appears to be choroidal as there is no evidence to suggest that it lies within the retinal pigmented epithelium (RPE). The presence of a choroidal tapetum is also indicated by the absence of pigment in the RPE in the superior fundus. Whereas abundant pigment is present in the RPE adjacent the non-tapetal retina in the inferior fundus.

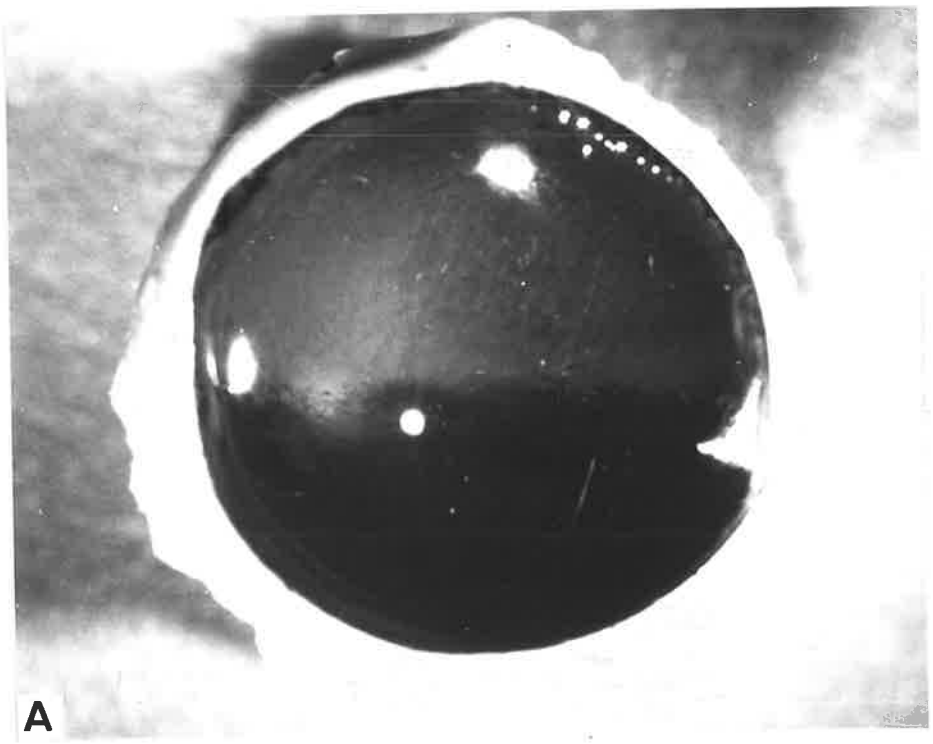

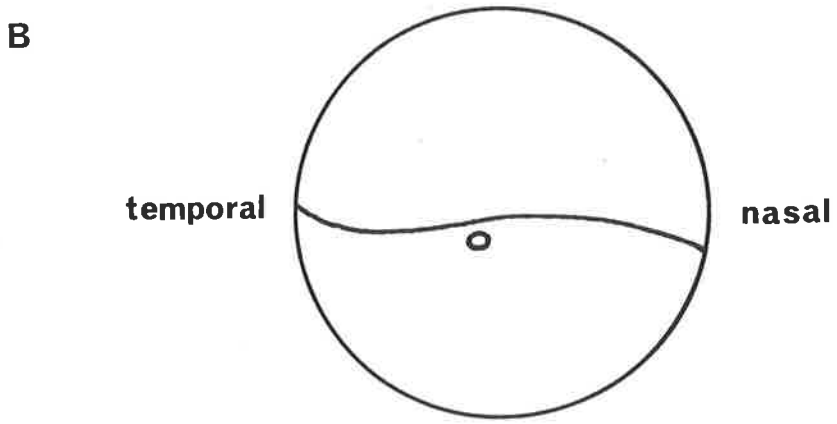

Figure 4.1.1 Eyecup, possum.
A. Macrophotograph of a fresh right eyecup showing the division into superior and inferior halves and the sigmoidal horizon.
B. A schematic diagram showing the eyecup of the possum. The horizon is represented by the solid line (——) and the optic disc (od) is seen to lie inferior to the horizon.

4.2 Choroid

In the Brush-tailed possum the choroid consists of tightly packed layers of large flattened cells separated by extracellular fibres as seen in Figure 4.2.1.

Melanocytes constitute the largest group of choroidal cells. The cell body of these cells, which are elongate in radial section and rounded in tangential section, is packed with spindle-shaped melanin granules that appear brown in unstained 1 µm sections. These membrane-bound granules exhibit high electron density, lack any internal ultrastructure, and measure between 1.0 and 2.5 µm long and 0.2 µm across. Other cytoplasmic structures include a moderate amount of perinuclear Golgi apparatus, polyribosomes and a few membrane-bound inclusions. These inclusions, which are of unknown significance, are larger than the melanin granules but less electron dense.

The nuclei of these cells are disc-shaped; elongate in radial section and circular when cut tangentially. They possess a prominent nucleolus and rather patchy chromatin. A narrow rim of dense chromatin lies beneath the nuclear envelope.

Fibroblasts are easily recognised among the heavily pigmented melanocytes despite their similar nuclear morphology. Their most distinctive feature is the large number of fine cytoplasmic processes that arise from the cell body and extend between the other choroidal elements. Unlike melanocytes the cytoplasm of these cells is free of pigment granules. However, small inclusions of moderate electron density are occasionally seen. The cytoplasm also contains small, rounded mitochondria, a small amount of rough

endoplasmic reticulum (RER) and free ribosomes.

Occasionally a macrophage was found among the cells of the choroid. The nuclear material is finely granular with dispersed patches of low electron density. Abundant polyribosomes and moderate numbers of elongate mitochondria with transverse cristae occur in the cytoplasm. A small amount of RER and Golgi, and numerous irregularly-shaped lysosomes are also present. The lysosomes are large in relation to other cytoplasmic structures, measuring 1.0 to 3.0 µm in diameter, and contain numerous engulfed melanin granules as seen in Figure 4.2.2. Membrane-bound inclusions of moderate electron density, and measuring between 0.25 and 0.75 µm in diameter, are also present in the cytoplasm of these cells.

An extensive capillary network lies within the choroid immediately sclerad to Bruch's membrane (BM). Fenestrations measuring approximately 50 nm in diameter with a single central density, are evident in those capillary endothelial cells adjacent BM (see Figure 4.2.3). The elongated nuclei of these endothelial cells are densely staining and therefore prominent. The cytoplasm of these cells contain scattered polyribosomes and small electron dense inclusions measuring approximately 0.2 µm in diameter.

Abundant extracellular fibres occur between the tightly packed cell layers of the choroid. These randomly orientated fibres stain intensely with the polychrome stain used [see Appendix VI]. Electron microscopy shows them to have the 64 nm periodicity typical of collagen.

Occasionally large nerve bundles are seen between the choroidal cells. Typically they posses an external covering

of dense connective tissue, epineurium, giving rise to septa which penetrate the bundles of nerve fibres. Both myelinated and non-myelinated fibres are present in these bundles and Schwann cell nuclei are prominent.

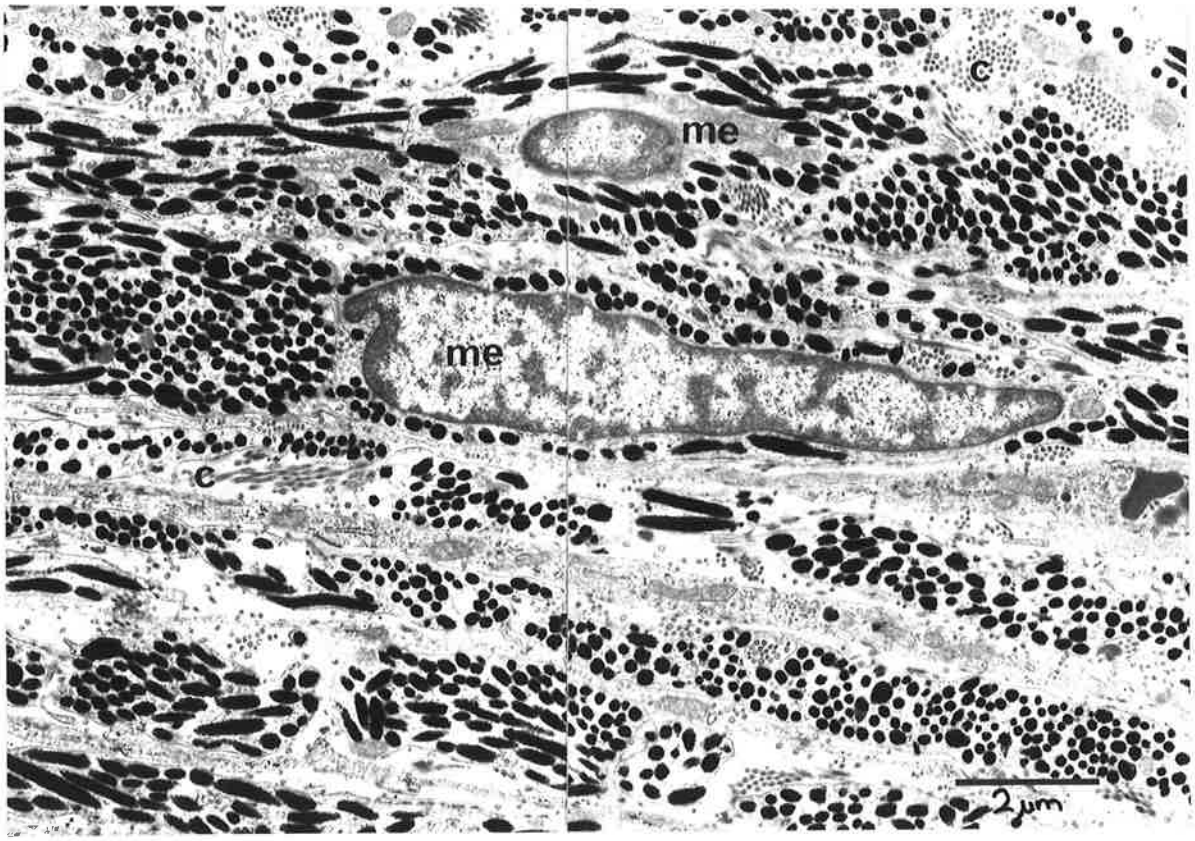

Figure 4.2.1 Choroid, possum.
Electron micrograph of radially sectioned choroid showing the layered arrangement of the melanocytes (me) and extracellular collagen fibres (c).

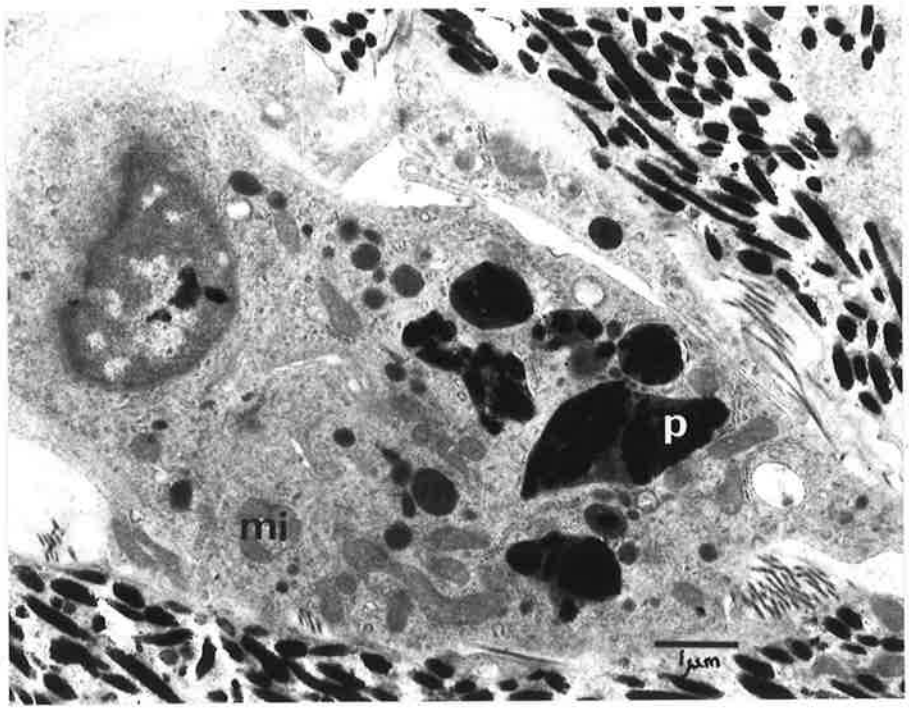

Figure 4.2.2 Choroid, possum.
Electron micrograph of a choroidal macrophage containing engulfed pigment granules (p), membrane-bound inclusions (in) and elongate mitochondria (mi).

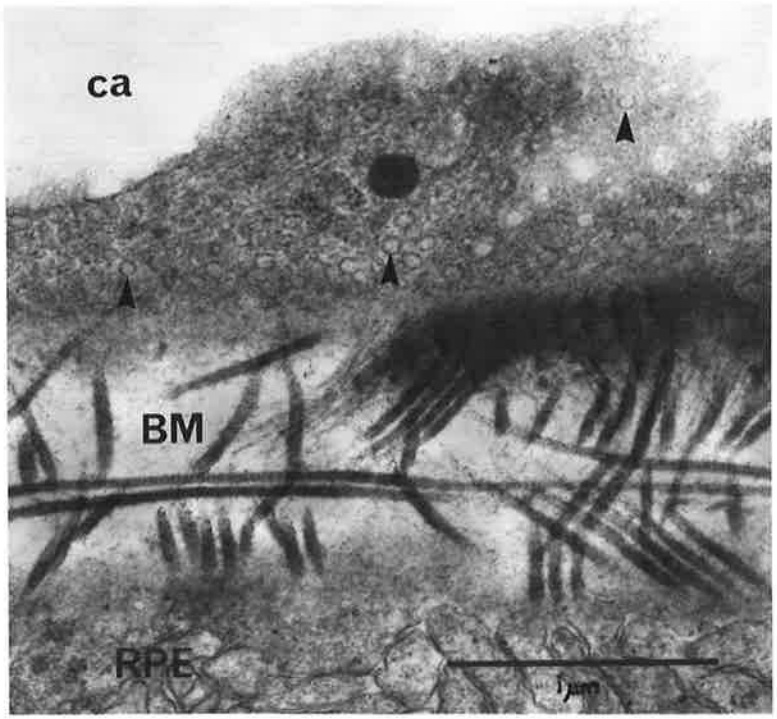

Figure 4.2.3 Choriocapillaris, possum.
Electron micrograph showing fenestrations (arrows) present in the capillary endothelium of the choriocapillaris adjacent Bruch's membrane (BM). Capillary (ca); retinal pigmented epithelium (RPE).

4.3 Bruch's Memrbrane

BM separates the choroid from the retina and measures approximately 0.5 μm across in the Brush-tailed possum (see Figure 4.3.1).

The most vitread layer of this pentalaminate structure is the basement membrane of the RPE. This apparently granular layer measures 50 nm across, contains embedded fibrils and is separated from the basal portions of the RPE cells by about 25 nm. This moderately electron dense membrane runs parallel to the vitread surface of the retina but does not follow the contours of the basal infoldings of the RPE cells (see Figure 4.3.1).

The second layer is roughly 0.15 μm thick and consists of a rather open meshwork of randomly arranged fibres which are acidophilic and exhibit the 64 nm periodicity typical of collagen.

The middle layer is also approximately 0.15 μm thick, slightly basophilic and stains with orcein, a stain specific for elastin, in paraffin sections. Electron microscopy shows this layer to be moderately electron dense and to have a fine fibrillar appearance. An interesting feature of this layer is that it is interrupted by irregularly spaced pores through which fibres of the 2 adjacent layers pass.

Immediately sclerad to the middle elastic layer is a layer with the same structural features as the second layer but measuring only 75 nm in thickness.

The fifth and most sclerad layer of BM is the basement membrane of the choroid. This layer is similar to the basement membrane of the RPE and is separated from the choroidal and endothelial cells by approximately 50 nm.

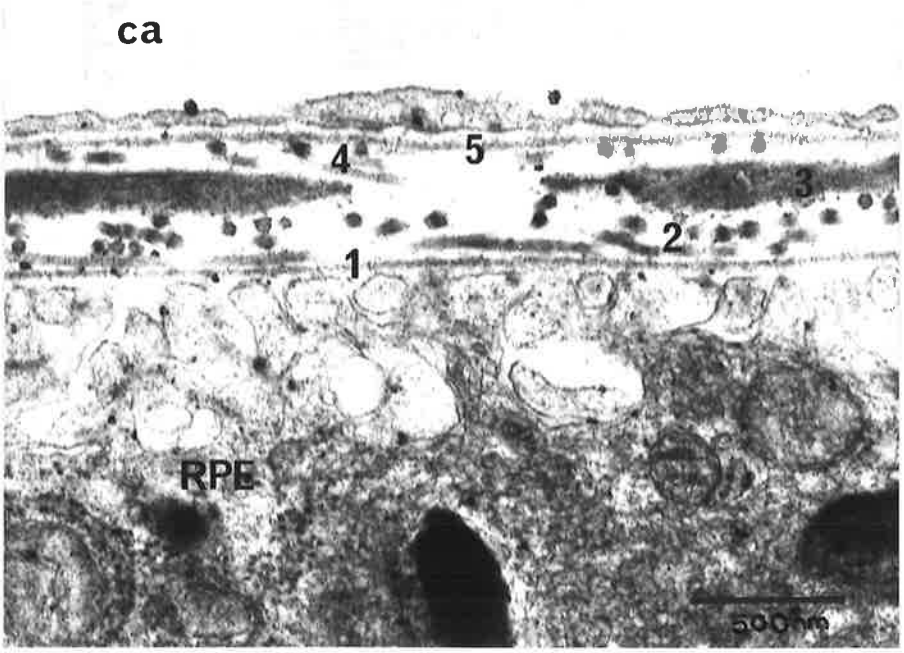

Figure 4.3.1 Bruch's membrane, possum.
Electron micrograph showing the pentalaminate structure of Bruch's membrane: basement membrane of the retinal pigmented epithelium (1), inner collagen layer (2), middle elastic layer (3), outer collagen layer (4) and basement of the choriocapillaris (5). Retinal pigmented epithelium (RPE); capillary (ca).

4.4 Retinal Pigmented Epithelium

Lying vitread to BM is the RPE; the outermost and only non-neuronal layer of the retina. The RPE comprises a single layer of low oblong cells (5.0 µm high), most of which are hexagonal in tangential section (see Figure 4.4.1). Extensive folding of the basal portion of the cell membrane is characteristic of these cells. Their membranous folds extend approximately 0.5 µm into the cytoplasm while numerous microvilli project from the apical regions of these cells into the ventricular space (see Figure 4.4.2).

A disc-shaped nucleus, elongate in radial section and rounded in tangential section, with a single nucleolus lies in the basal region of each RPE cell. Small clumps of chromatin are scattered throughout the nucleoplasm and beneath the nuclear envelope.

Oil droplets measuring 2.0 to 3.0 µm in diameter and numerous small round mitochondria occupy the basal cytoplasm, while numerous clusters of free polyribosomes are present in both the apical and perinuclear regions. The apical microvillous processes and the apical cytoplasm contain large numbers of elliptical membrane-bound melanin granules which range in size from 0.4 to 0.6 µm in diameter and can reach up to 1.0 µm in length. These granules show no internal ultrastructure and exhibit a high degree of electron density. Phagosomes were commonly found in the basal cytoplasm of the RPE cells. They measure approximately 1.0 µm in diameter and contain whorls of membranes resembling the photoreceptor outer segment discs.

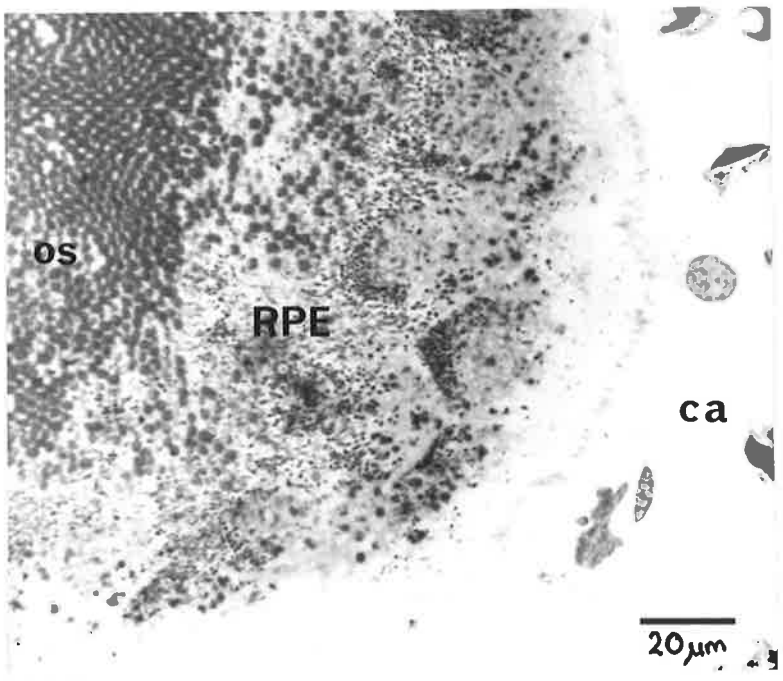

Figure 4.4.1 Retinal pigmented epithelium possum.
Light micrograph showing the polygonal profiles of the cells of the retinal pigmented epithelium (RPE). Capillary of the choriocapillaris (ca); photoreceptor outer segments (os).

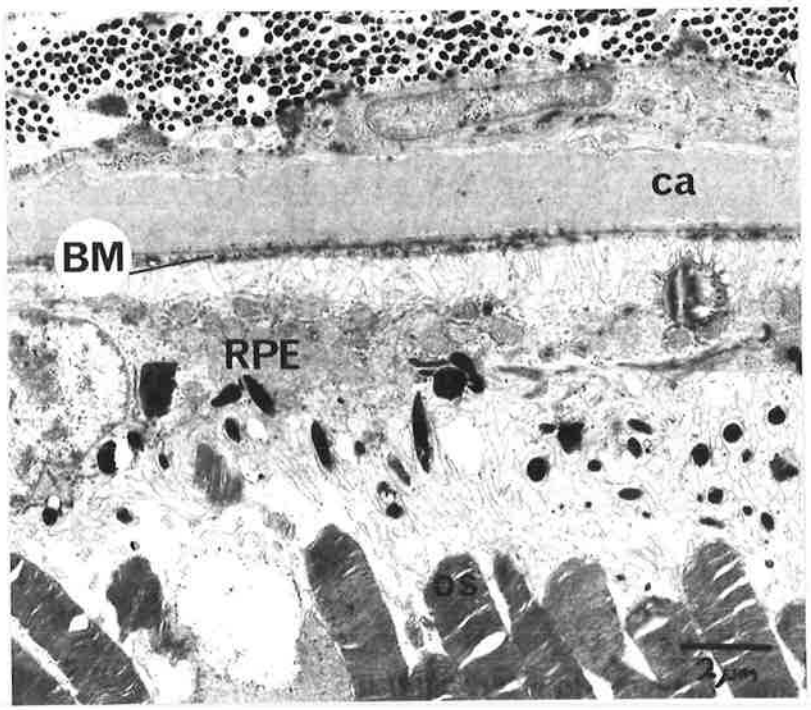

Figure 4.4.2 Retinal pigmented epithelium, possum.
Electron micrograph showing the retinal pigmented epithelium (RPE) lying between the photoreceptor outer segments (os) and Bruch's membrane (BM) adjacent a capillary (ca) of the choriocapillaris.

4.5 Rod Outer Segments

The thin cylindrical outer segments of the rods extend from their connection with the inner segments to the RPE where they are surrounded and contacted by numerous apical processes of the RPE as seen in Figure 4.4.2. They measure approximately 16.0 μm in length and 1.5 μm in diameter.

In polychrome-stained 1 μm orientation sections these closely packed rod outer segments (ROS) stain light blue and show fine cross-striations. The membranous discs responsible for this striated appearance are resolved with the electron microscope and lie within the cell membrane at right angles to the long axis of the ROS. Structurally each disc is a flattened sac consisting of 2 parallel membranes separated by a narrow intradisc space and continuous with each other at a cicumferential dilatation. The interdisc space separating each disc from the next is wider than the more dense intradisc space. Examination of tangentially cut thin sections (see Figure 4.5.1) has shown that the discs usually have a circular outline interrupted only by a single incisure which is aligned with the connective stalk. Occasionally 2 incisures positioned opposite each other were found while some sections did not clearly show any incisures. No evidence has been found to suggest that the discs make contact with the cell membrane. In the incisures of the discs near the base of the outer segments cross-sections of single microtubules were sometimes seen and appeared to be aligned with the connective stalk.

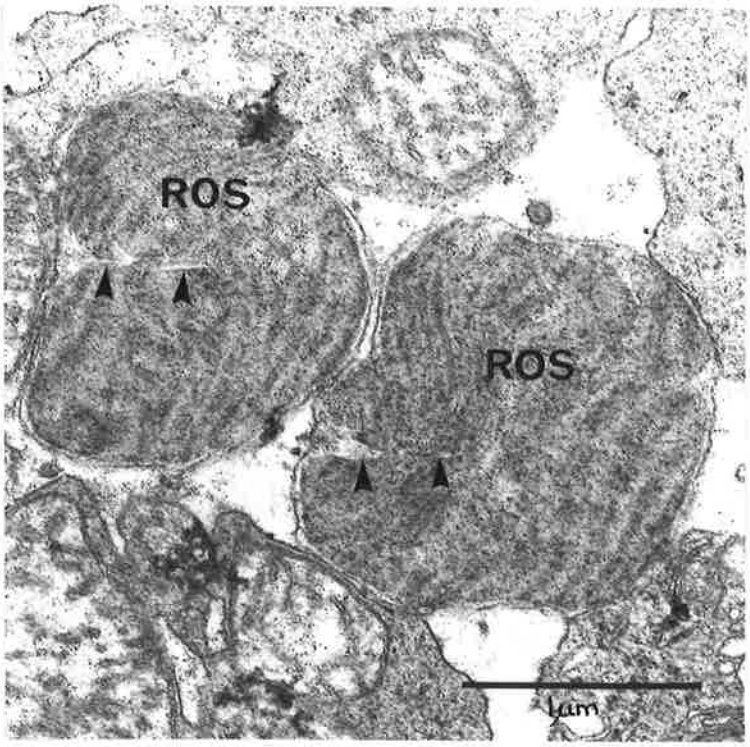

Figure 4.5.1 Rod outer segment, possum.
Electron micrograph of a tangentially cut section of the photoreceptor layer. Discs are evident in 2 rod outer segments (ROS) and an incisure (arrow) is seen in 1 disc.

4.6 Rod Ciliary Region

A modified ciliary stalk measuring 1.0 to 1.5 μm in length and 0.3 μm in diameter connects the apical region of each rod inner segment (RIS) to the base of its outer segment (see Figure 4.6.1).

As seen in Figures 4.6.2 and 4.6.3 there are 2 centrioles in the apical region of the RIS. The primary centriole is positioned at the base of the ciliary stalk with which it is aligned. At right angles and in close proximity to the primary centriole lies the secondary centriole to which it oftens appears to be connected by moderately dense filaments. Each centriole is a short hollow cylinder consisting of 9 peripheral microtubular triplets. As is usual in the basal bodies of cilia 1 complete and 2 incomplete microtubules make up each triplet.

Examination of tangential sections of this region has shown that a variable number of tufts radiate from the primary centriole but do not appear to make contact with the cell membrane. At the point where the ciliary stalk leaves the inner segment the triplets become doublets, each consisting of 1 complete and 1 incomplete microtubule. Nine doublets arranged in a cylindrical manner form the internal framework of the ciliary stalk. No central doublets are present, so the stalk has the '9+0' structure typical of sensory cilia. The cytoplasmic matrix within the ring of doublets is less electron dense than the peripheral matrix in which the doublets are embedded.

Most of the circumference of the stalk lies within a niche in the apical portion of the inner segment. However, a small portion of the stalk is exposed to the extracellular

space and it is here that 2 calycal processes (see Figure 4.6.4), measuring 50 to 75 nm in diameter, are seen to extend sclerally from the inner segment for approximately the length of the cilium. Occasionally a single calycal process is seen adjacent the cilium of its inner segment.

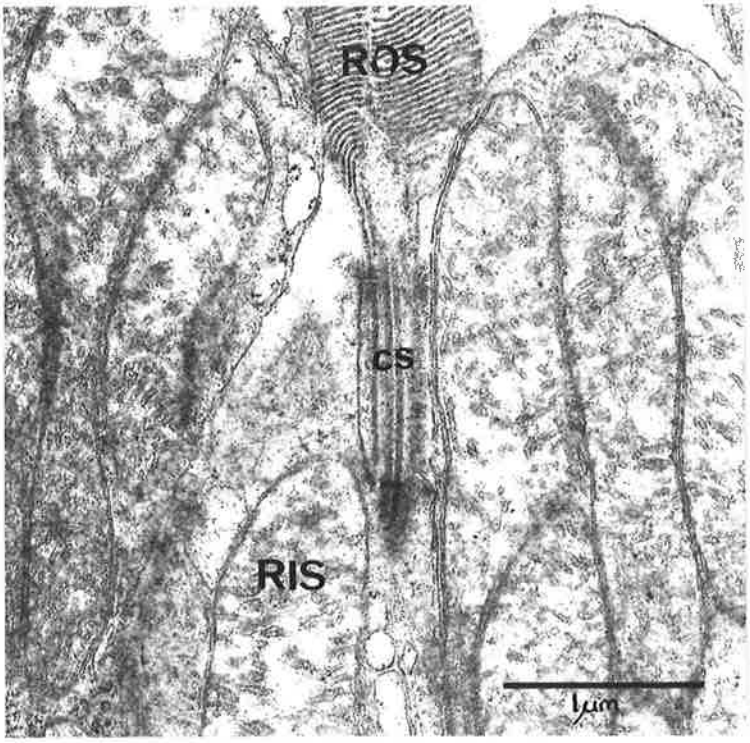

Figure 4.6.1 Rod ciliary region, possum.
Electron micrograph of a radial section showing a ciliary stalk (cs) connecting a rod inner segment (RIS) to its outer segment (ROS).

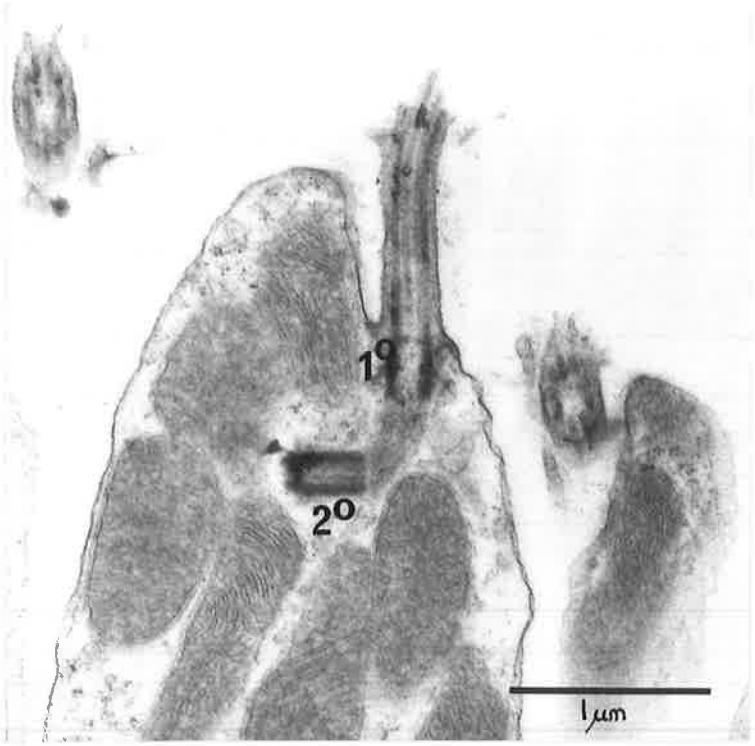

Figure 4.6.2 Rod ciliary region, possum.
Radial electron micrograph showing both the primary (1^{o}) and secondary (2^{o}) centriole evident in a rod inner segment.

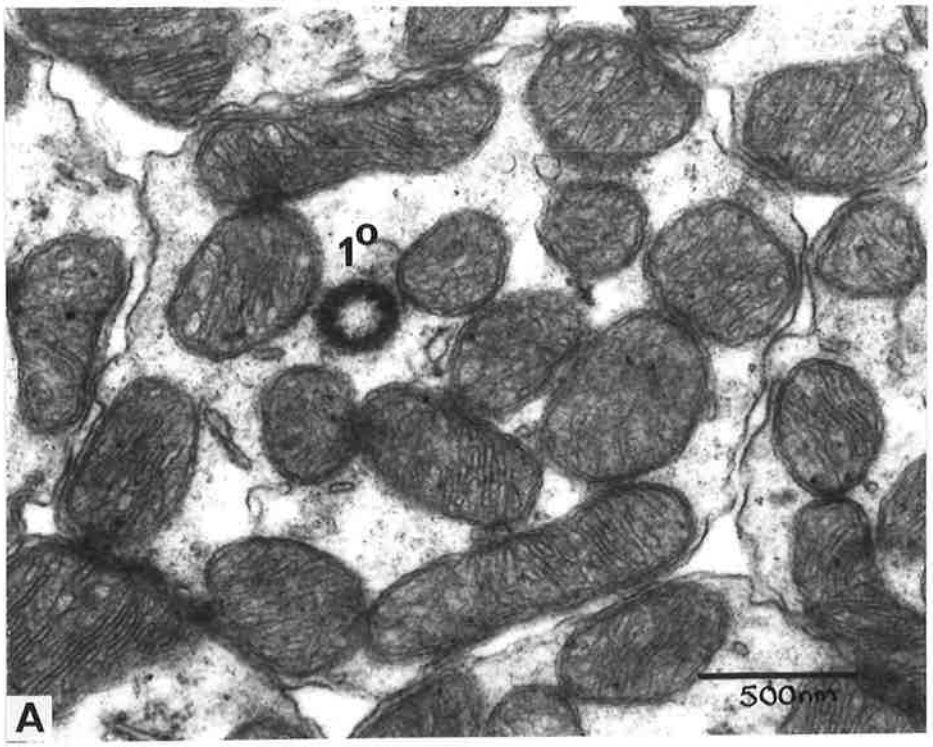

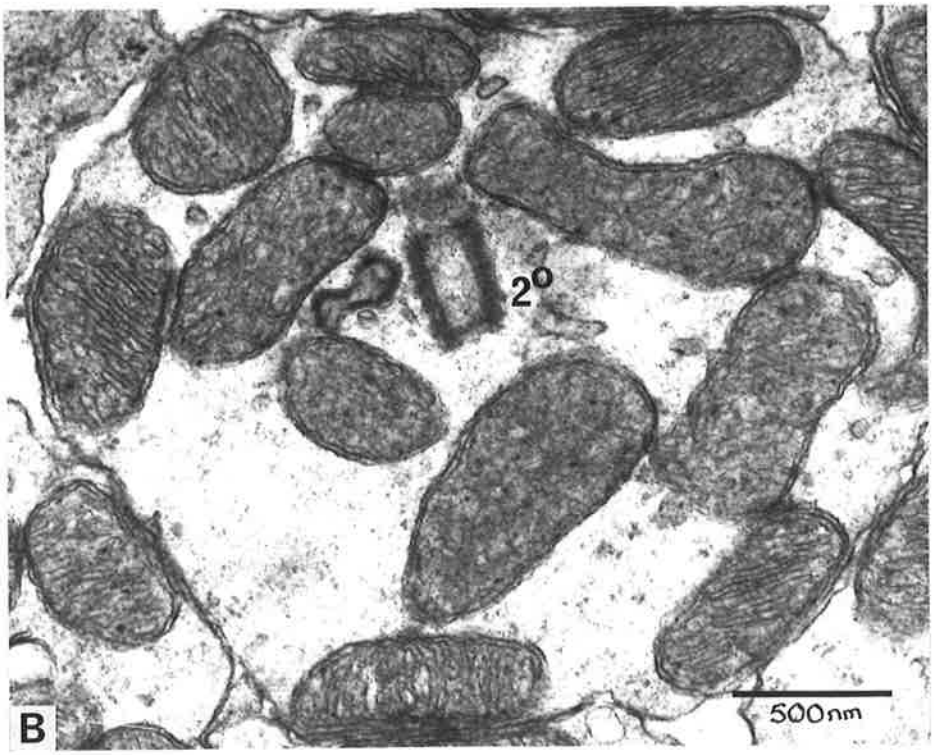

Figure 4.6.3 Rod ciliary region, possum. Electron micrographs of tangentially sectioned rod inner segments showing A. a primary centriole (1^{o}) and B. a secondary centriole (2^{o}) lying at right angles.

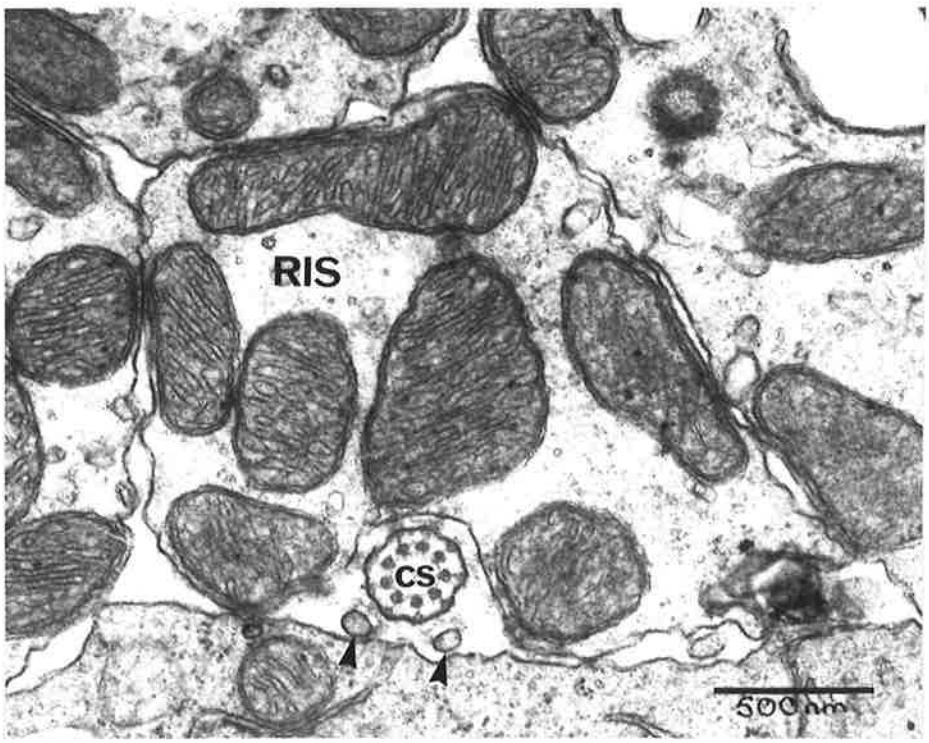

Figure 4.6.4 Rod ciliary region, possum.
Apical region of a rod inner segment (RIS) in cross-section showing the ciliary stalk (cs) and associated calycal processes (arrows). The microtubule doublets of the ciliary stalk appear to have a filamentous attachment to the cell membrane.

4.7 Rod Inner Segments

The inner segments of rods are cylindrical structures measuring approximately 18.0 µm in length and 2.0 to 3.0 µm in diameter. They stain lightly with the polychrome stain and appear amorphous at the light microscopic level. However, electron microscopy has shown that each RIS has 2 regions of differing cytoplasmic organisation.

The more sclerad ellipsoid contains numerous elongated mitochondria that measure several µm in length and have transverse cristae. Examination of tangential sections, such as those seen in Figure 4.6.3, has shown that these mitochondria are not closely packed but separated by cytoplasmic matrix of low electron density and devoid of organelles. Polyribosomes and small vacuoles are commonly seen near the centrioles in the apical region of the ellipsoids.

The myoids occupy the more vitread position of the RIS. The cytoplasmic matrix exhibits very little electron density and contains abundant polyribosomes, the occasional mitochondrion, and small amounts of smooth endoplasmic reticulum (SER) (see Figure 4.7.1). Small vacuoles are seen in close relation to the Golgi complexes. Numerous microvilli from the Müller cells (MC) separate the myoids from each other and extend for several µm into the ventricular space (see Figures 4.7.1 and 4.7.2).

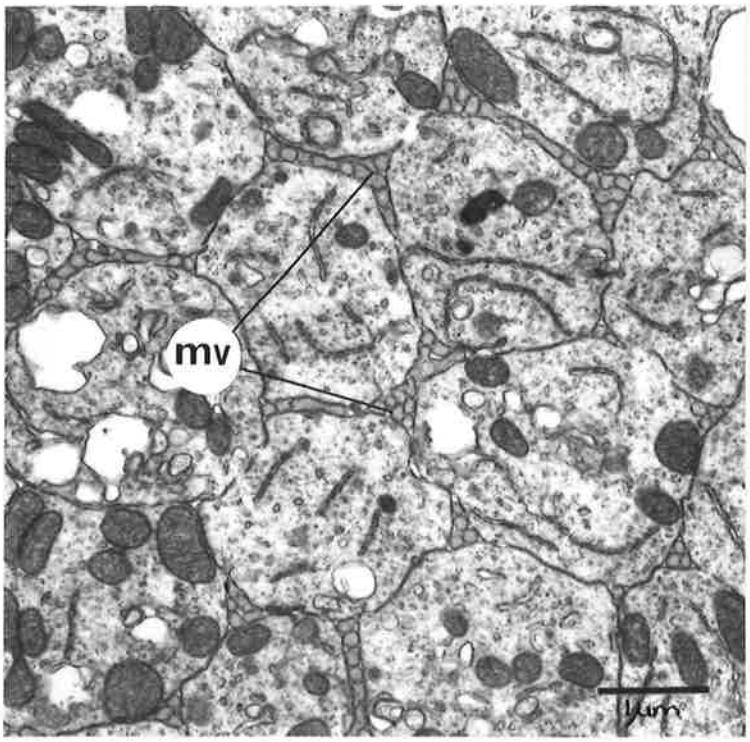

Figure 4.7.1 Rod inner segments, possum. Tangential electron micrograph showing the rod inner segment myoids in cross-section. Microvilli (mv) of the Müller cells are seen between the myoids.

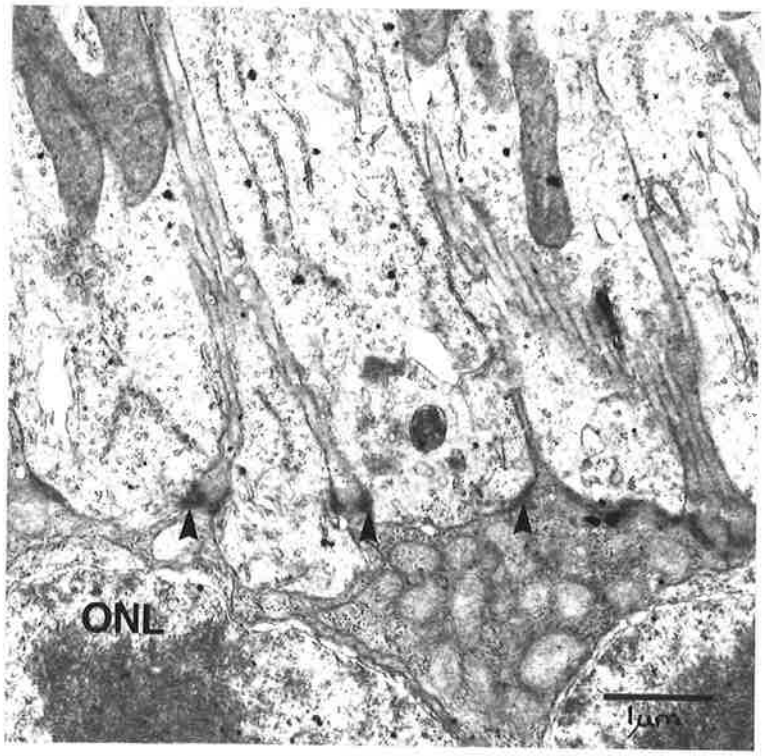

Figure 4.7.2 Rod inner segments, possum. Radial electron micrograph showing the myoids of the rod inner segments sclerad to the outer nuclear layer (ONL). Note also the intercellular junctions (arrows) of the outer limiting membrane.

4.8 Cone Outer Segments

The cone outer segments (COS) in the possum retina have proven difficult to find in both the thick and thin sections examined which has made it difficult to collect clear structural details.

These small structures, which are triangular in radial section, lie between the sclerad tips of the more numerous ROS in close association with the RPE. They stain lightly blue with the polychrome stain thus having similar staining porperties to the ROS.

4.9 Cone Inner Segments

The inner segments of the cone cells extend from the connection with their small outer segments to the cell body just vitread to the outer limiting membrane (OLM) and measure approximately 30.0 µm in length. They are also divided into myoid and ellipsoid, and have a teardrop shape. The myoid is narrow (2.0 to 3.0 µm in diameter) at the level of the OLM but gradually increases in diameter to approximately 7.0 µm at the widest point of the ellipsoid; both myoid and ellipsoid are rounded in tangential sections.

These structures are large in comparison to the more numerous RIS, and can be readily identified at the light microscopic level. They exhibit pale staining similar to that shown by rod myoids but less intense than that of the rod ellipsoids and outer segments. Those cones possesing oil droplets are more noticable in 1 µm sections than those without.

The myoids characteristically contain abundant free polyribosomes, moderate amounts of RER and Golgi complexes, and a small number of moderately dense membrane-bound inclusions. Small, rounded mitochondria with transverse cristae are occasionally present near the OLM and increase in number sclerally.

The ellipsoids contain numerous long thin mitochondria with transverse cristae. They appear to be present in greater numbers than in the rod ellipsoids and extend into the cytoplasm peripheral to the oil droplet, if present. Abundant polyribosomes occur in the apical cytoplasm where small vacuoles and electron dense inclusions lie in the vicinity of the centrioles.

Large spherical droplets,measuring from 2.0 to 5.0 µm in diameter, are present sclerad to the ellipsoids of some cone inner segments (CIS) in the retina of the possum. These droplets are refractile in fresh tissue, blackened by osmium tetroxide and extracted by chloroform, and are therefore assumed to be lipid in nature. They do not stain with the polychrome stain used for routine 1 µm sections and electron microscopic examination has shown that they are membrane-bound, moderately electron dense and lack any internal ultrastructure.

From examination of radial and tangential sections it appears that most of the cone cell population is made up of sinlge cones, most of which contain a single oil droplet. Single cones without oil droplets were only seen occasionally. The remainder of the population consists of double cones containing 1 oil droplet in each member. The accessory cone lies alongside its principal cone and its oil droplet lies further sclerad.

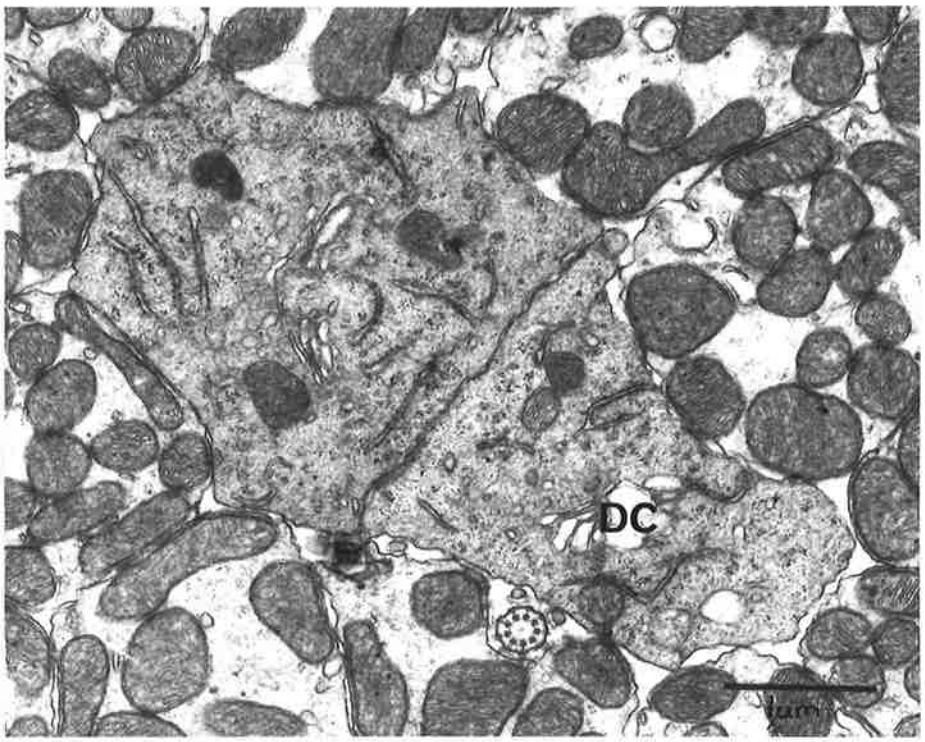

Figure 4.9.1 Cone inner segments, possum. Electron micrograph of a tangential section showing the myoids of a double cone (DC) surrounded by ellipsoids of rod inner segments.

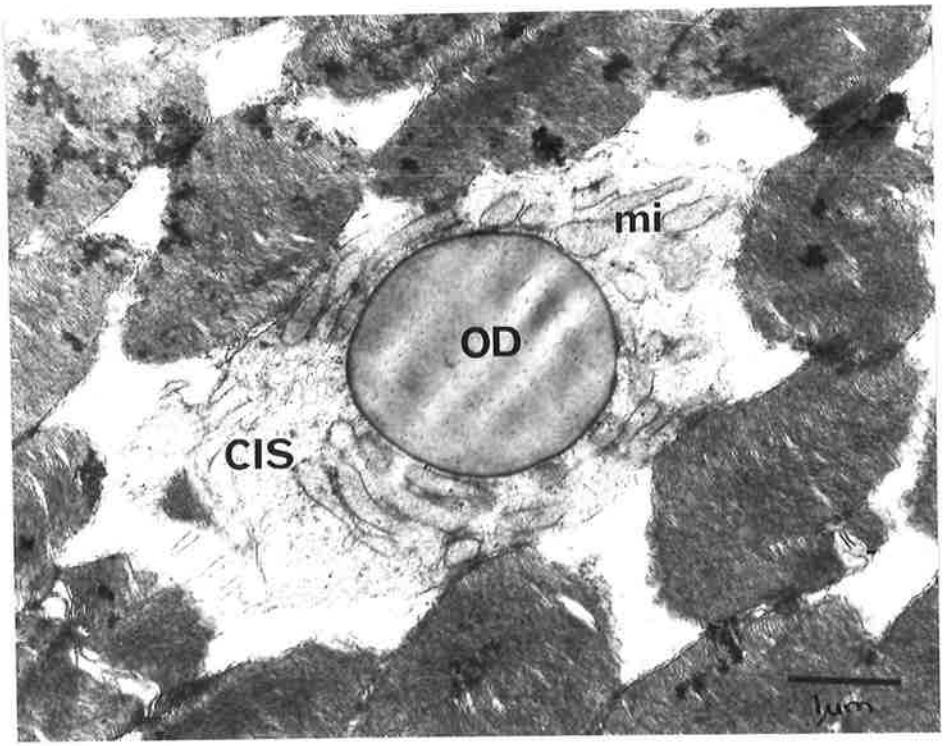

Figure 4.9.2 Cone inner segment, possum.
Electron micrograph of an obliquely sectioned cone inner segment (CIS) containing an oil droplet (OD) surrounded by mitochondria (mi).

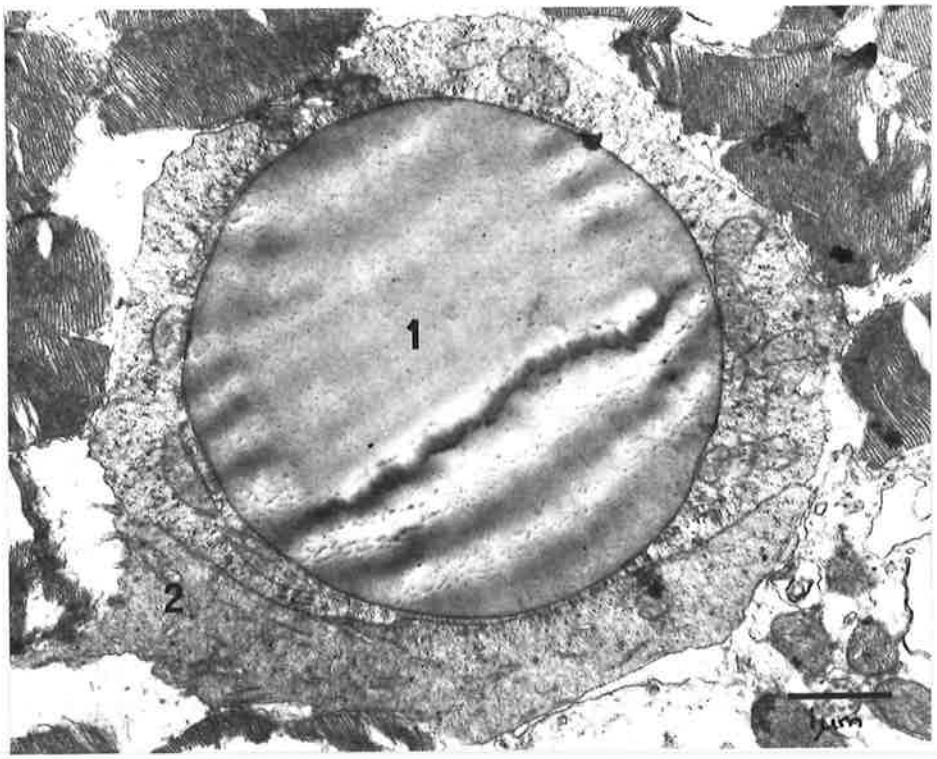

Figure 4.9.3 Cone inner segments, possum.
Electron micrograph of a double cone seen in cross-section. The principal member (1) is seen as a large droplet-bearing structure and the accessory member (2) forms an apposing crescent.

4.10 Outer Limiting Membrane

Upon light microscopic examination the OLM of the possum appears as a densely staining discontinuous line along the sclerad edge of the outer nuclear layer (ONL). However, electron microscopy shows that this structure is not a membrane but is an extensive network of intercellular junctional complexes (see Figures 4.7.1 and 4.10.1).

At the level of the OLM the myoids of the photoreceptor cells are widely separated by short thick MC processes. As seen in Figure 4.10.1 these processes make extensive contacts with each other and with the photoreceptors. Despite the presence of double cones in the retina of the possum no photoreceptor-to-photoreceptor contacts were seen at this level. The increased density of the cytoplasm adjacent the intercellular contact and the wider intercellular space indicates that the OLM is made of zonulae adherentes junctions.

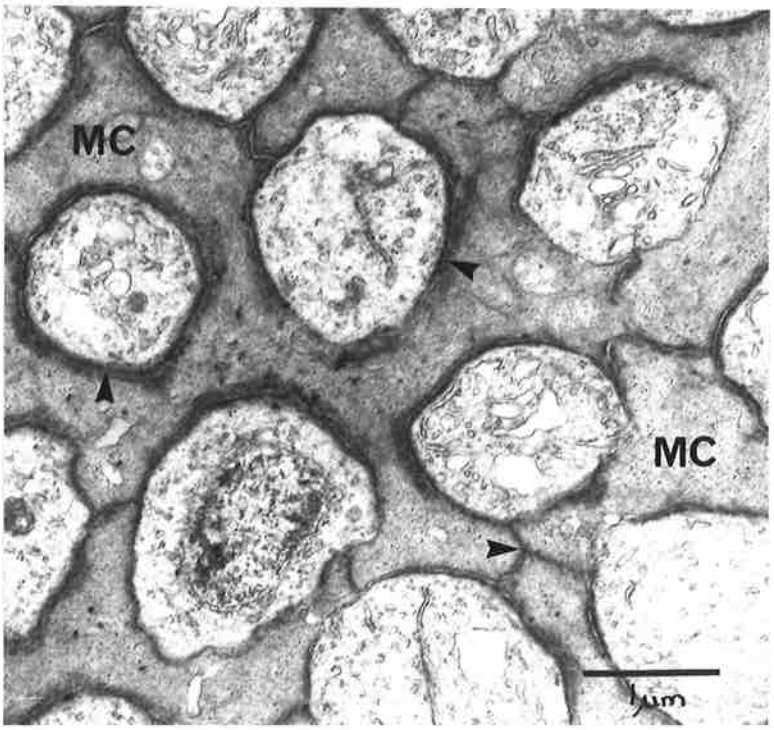

Figure 4.10.1 Outer limiting membrane, possum.
An electron micrograph showing a tangential section cut from the level of the outer limiting membrane. The intercellular junctions (arrows) comprising this structure occur between the photoreceptors (ph) and Müller cell processes (MC), and between the Müller cells themselves.

4.11 Outer Nuclear Layer

The cell bodies of both the rods and cones lie in radially orientated columns in the ONL. In the central retina there are 9 or 10 cell bodies in each column, as seen in Figure 4.11.1, while in the periphery there are fewer cell bodies in each of the less orderly columns.

Examination of both radially and tangentially sectioned material has shown that the rod nuclei far outnumber the cone nuclei. Counts made from tangential sections have shown the rod to cone ratio to be 130:1 in both the central and peripheral retina.

The intensely staining nuclei of the rod cells are elliptical and measure approximately 6.0 µm in length and 4.0 µm in diameter. The majority of these nuclei have 2 prominent densely staining patches of chromatin while few show 1 or 3 (see Figures 4.11.1 and 4.11.2). A narrow rim of cytoplasm of low electron density, containing polyribosomes and neurotubules surrounds each nucleus.

The less common cone nuclei are rounded, measure 8.0 to 10.0 µm in diameter and have pale-staining chromatin. Surrounding each cone nucleus is a very narrow rim of cytoplasm of low electron density.

Each photoreceptor has 2 radially directed processes that arise from opposite poles of the cell body. The length of each process is determined by the position of the cell body within the ONL. Extending between the sclerad aspect of the cell bodies and the OLM are the outer conducting fibres. The inner conducting fibres extend toward the outer plexiform layer (OPL) where they terminate as synaptic swellings (see Section 4.12). Numerous neurofilaments occur within the

cytoplasmic matrix that fills these neuronal processes.

The outer processes of MC fill the vertical spaces between the columns of photoreceptor cell bodies and conducting fibres (see Figure 4.11.2). From these processes fine processes extend laterally and appear to fill most of the remaining extracellular space. The cytoplasmic matrix of these non-neuronal MC processes is more electron dense than the conducting fibres or the perinuclear cytoplasm of the photoreceptors.

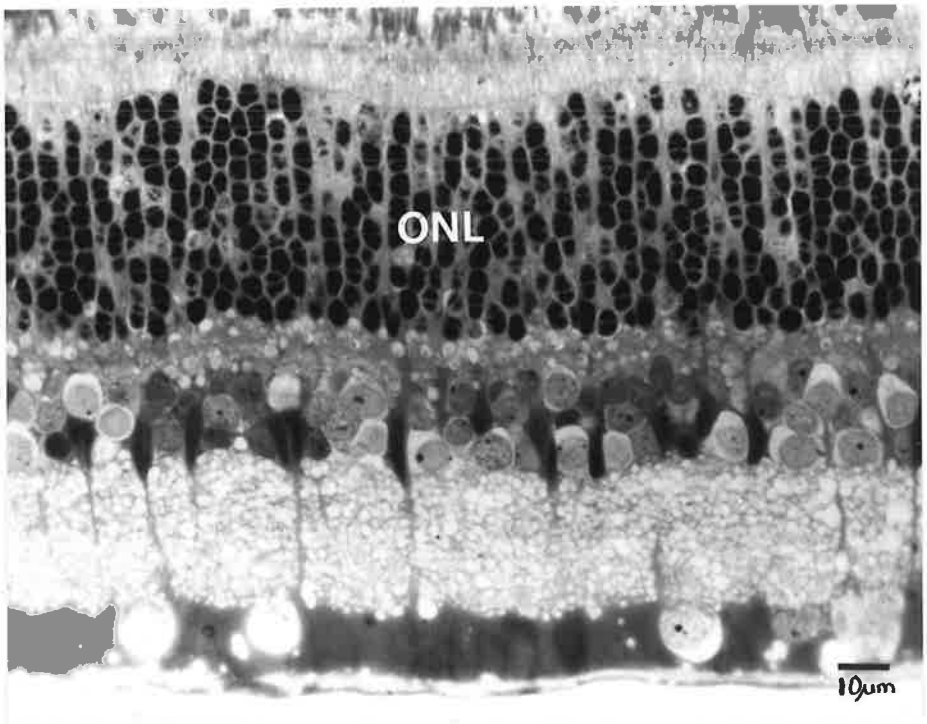

Figure 4.11.1 Outer nuclear layer, possum. Light micrograph of a polychrome-stained radial section showing the columnar packing of photoreceptor cell bodies in the outer nuclear layer (ONL) in the central retina.

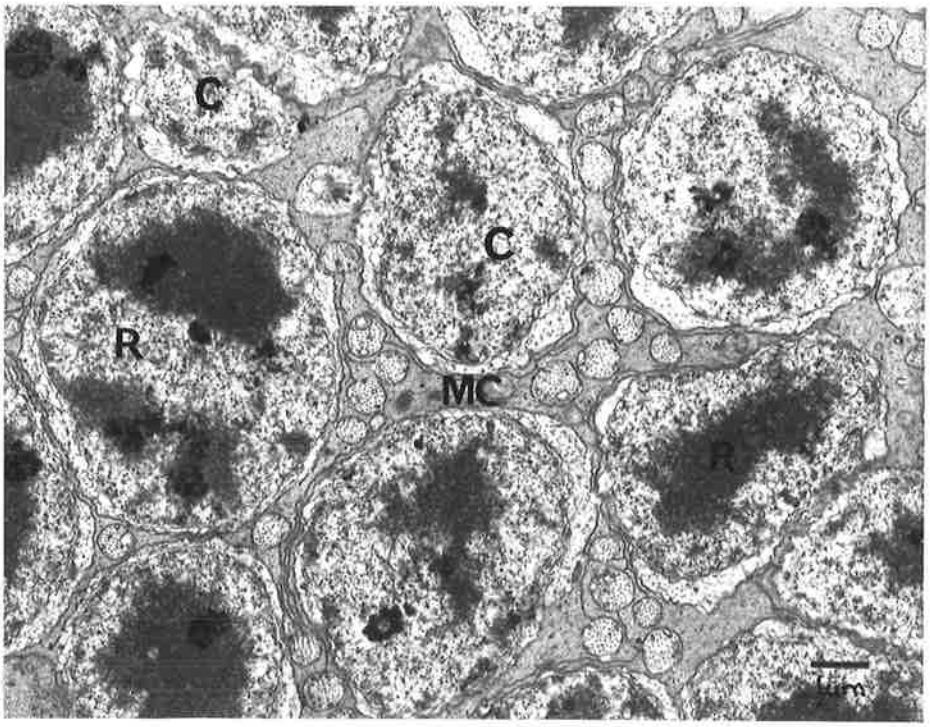

Figure 4.11.2 Outer nuclear layer, possum. Tangential electron micrograph of the outer nuclear layer showing both rod (R) and cone (C) nuclei, Müller cell processes (MC) and conducting fibres (arrows).

4.12 Outer Plexiform Layer

The OPL appears by light microscopy as a narrow pale-staining layer; electron microscopy shows that it consists of photoreceptor synapses and processes from the cells of the inner nuclear layer (INL). In the Brush-tailed possum this complex layer is divided into 2 layers the first of which lies adjacent the ONL and contains the photoreceptor synapses. The second, more vitread layer, lies between the synaptic layer and the INL and contains processes which arise from cells within the INL.

In the possum the most common type of synaptic complex in the OPL is the rod spherule which is usually a spherical dilatation of the inner conducting fibre. However, in the less numerous sessile synapses there are no intervening conducting fibres and the spherules are directly attached to the cell bodies.

These small bulbous structures measure 2.0 to 3.0 µm in diameter, exhibit low electron density and contain numerous 40 nm diameter synaptic vesicles. As seen in Figure 4.12.1 they are characterised by the presence of a single electron dense synaptic ribbon. This small pentalaminate structure lies close to and at right angles with the thickened presynaptic membranes, and is concave toward the presynaptic membrane (see Figure 4.12.2). Lying between this ribbon and the cell membrane is a small semitubular structure of high electron density called the arciform density. This structure, often seen in mammalian visual cell synapses, has its convex surface facing and following the curve of the synaptic ribbon as illustrated in Figure 4.12.2. The ribbon is usually surrounded by an array of synaptic vesicles but is

separated from them by a narrow space of organelle-free cytoplasm.

Thickening of the post-synaptic membrane is less marked than that of the pre-synaptic membrane from which it is separated by a 20 nm wide synaptic cleft.

Despite having only one synaptic complex each rod spherule makes contact with multiple post-synaptic processes. Firstly, there is a single centrally positioned process that is aligned with the synaptic ribbon and terminates bluntly some distance from it. Positioned on opposite sides of this central process there are usually 2 and occasionally 3 lateral processes that extend further into the spherule than the central invaginating process and appear to end as branched swellings.

The cone synaptic pedicles are considerably less numerous than the rod spherules and consequently are difficult to find in thin sections. However, several pedicles were found just vitread to the rod spherules in the central retina.

The pedicles are conical dilatations of the vitread end of the inner conducting fibres of cones. They are larger than the rod spherules, measuring approximately 5.0 μm in diameter, and their cytoplasm has a higher density of 40nm synaptic vesicles than the spherules.

Each pedicle contains several synaptic ribbons exhibiting the same structure and relations as described for the larger, single ribbons found in the rod spherules. These ribbons appear to be randomly arranged in a plane parallel to the base of the cone.

Several basal filaments radiate laterally from each

pedicle at (or slightly sclerad to) the level of the synaptic ribbons and run through the OPL. Some of these basal filaments have been seen to make contact with rod spherules.

Besides the numerous invaginating post-synaptic processes that contribute to the pedicle there are other processes that make superficial contacts along the base of the conical pedicle. These post-synaptic processes appear to run toward the cells of the INL in random fashion.

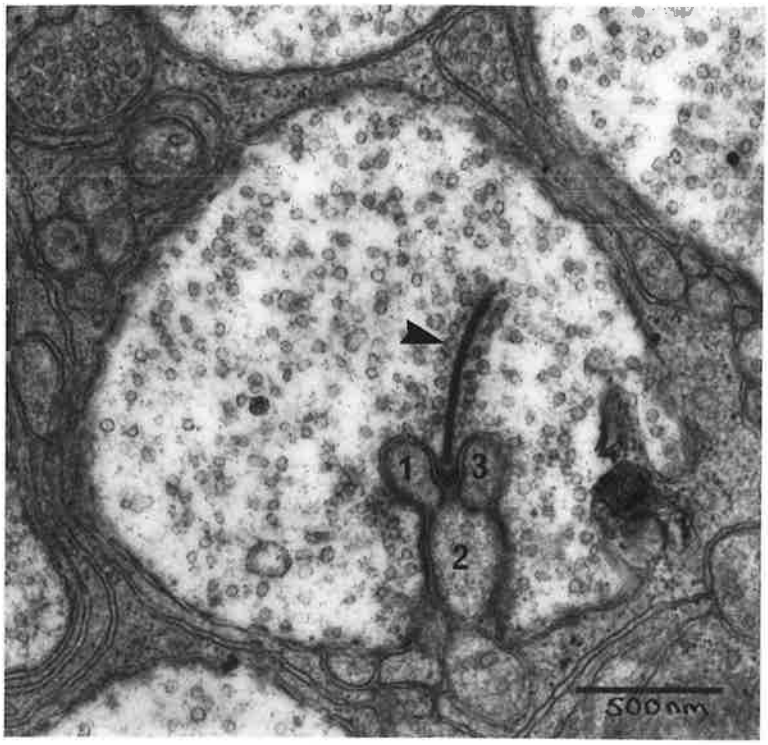

Figure 4.12.1 Outer plexiform layer, possum. Electron micrograph of a rod spherule showing the synaptic ribbon and its halo of vesicles (arrow) and the 3 post-synaptic processes (1-3).

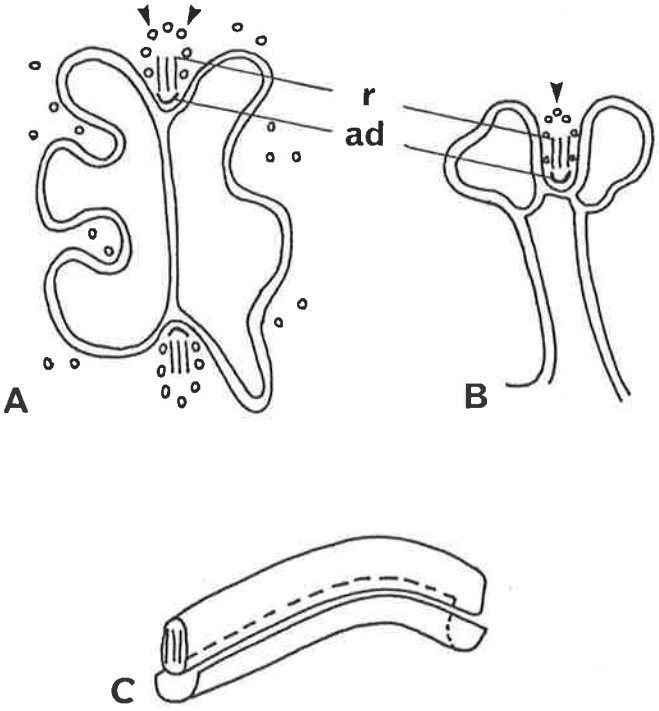

Figure 4.12.2 A and B Schematic diagrams showing the arrangement of the synaptic ribbon (r) and its associated synaptic vesicles (arrows) and arciform density (ad) as seen in the rod spherules of the Brush-tailed possum. C A 3 dimensional representation of a synaptic ribbon and its associated arciform density.

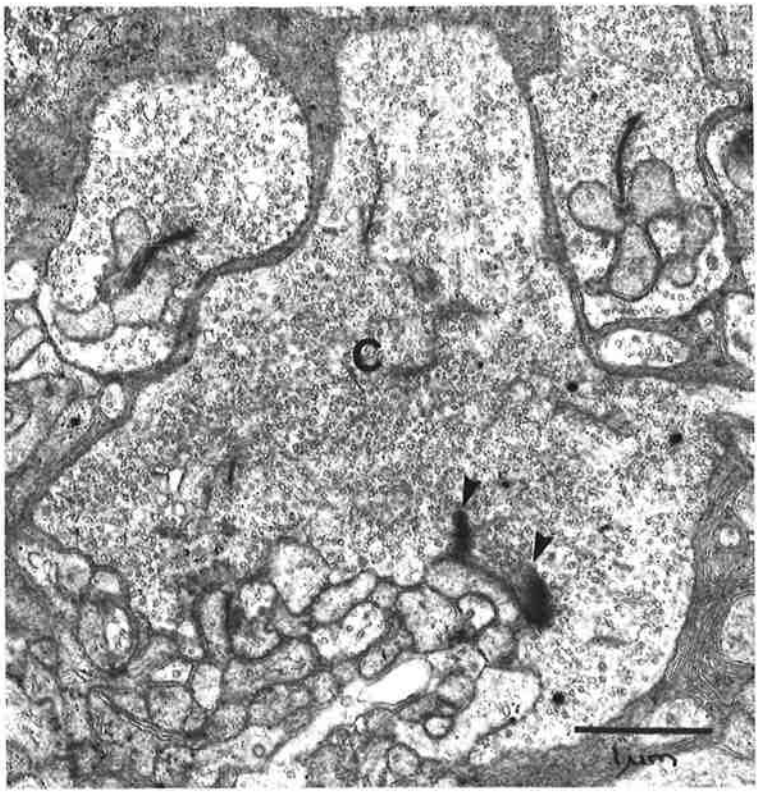

Figure 4.12.3 Outer plexiform layer, possum. Electron micrograph showing a cone pedicle (c) in radial section. Note the small synaptic ribbons (arrows) and the numerous post-synaptic processes.

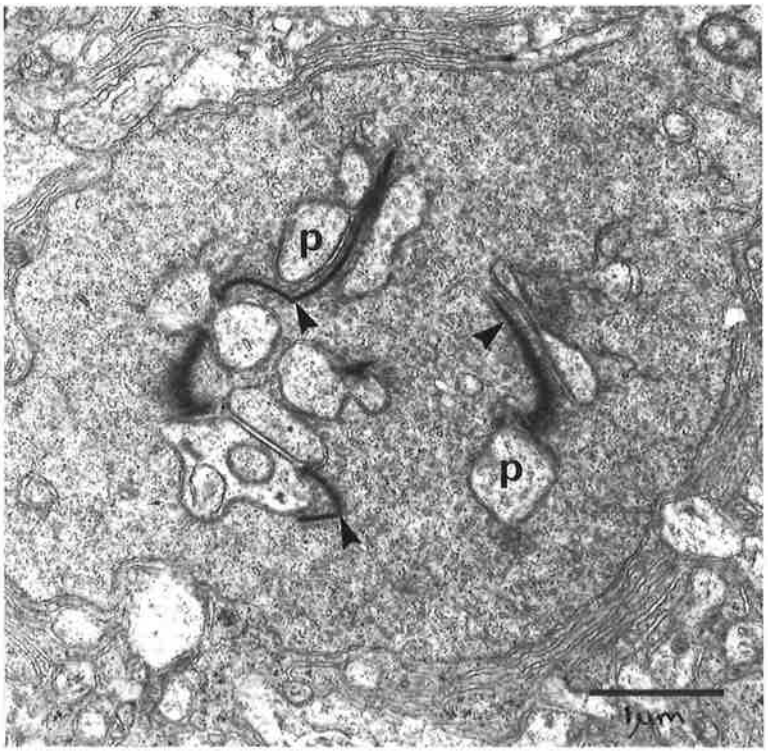

Figure 4.12.4 Outer plexiform layer, possum. Electron micrograph showing a tangential section of a cone pedicle with multiple synaptic ribbons (arrows) and post-synaptic processes (p).

4.13 Inner Nuclear Layer

The INL lies vitread to the OPL and is approximately 25.0 µm thick in the retina of the Brush-tailed possum. The cell bodies are arranged in 2 layers peripherally and 3 or 4 layers centrally,

It is generally accepted that the cells whose cell bodies lie within the INL are both neuronal and non-neuronal. The neurons are bipolar (BC), horizontal (HC) and amacrine cells (AC), while the MC constitute the non-neuronal cell population (RODIECK, 1973). Despite the use of serial light and electron micrographs wherever possible and the different morphologies evident (see Figure 4.13.1) identification of these cell types has proven difficult and at best is only tentative.

The presumed HC appear to be sparse; their cell bodies being found along the sclerad edge of the INL. Both their light and electron microscopic appearances are very similar to that of a second cell type, probably AC, found in the INL.

Their large, rounded nuclei measure several µm in diameter, exhibit slight basophilia and contain a large prominent nucleolus. In electron micrographs they show moderate electron density, and coarse granular chromatin without clumping. There is usually a narrow rim of pale-staining cytoplasm that contains small, rounded mitochondria, minimal RER, a few polyribosomes and neurfilaments. Some of these cells apparently give rise to long thin processes that extend toward the OPL. Since it has not been possible to trace these processes back to synapses it has not been possible to positively identify them.

The presumed BC have small, rounded nuclei of

approximately 6.0 µm in diameter, exhibit moderate basophilia and granular chromatin. Many nuclei matching this descrption contain a large prominent nucleolus. Electron microscopic examination has shown that the nuclear chromatin of these neurons is moderately electron dense.

The cytoplasm of these presumptive BC is more electron dense than that of the presumed HC and contains a small number of polyribosomes and mitochondria which aggregate immediately sclerad to the nucleus.

The cell bodies of the neurons thought to be AC lie along the vitread edge of the INL. Their large nuclei are circular or elliptical. The moderately electron dense chromatin is granular but slightly less so than the chromatin in the HC nuclei.

Moderate numbers of small, rounded mitochondria, numerous polyribosomes and abundant perinuclear RER are evident in the cytoplasm of these presumed AC. Circular membrane-bound inclusions of moderate electron density and no obvious internal structure occur in the cytoplasm of these cells. The cytoplasm of these amacrine-type neurons is slightly more electron dense than that of the presumed HC.

The cytoplasm of some of these presumed AC contains orderly arrays of tubular cristae and polyribosomes (see Figure 4.13.2) typical of Nissl substance (RODIECK,1973). This may suggest that they are displaced retinal ganglion cells (RGCs).

The elongate cell bodies of the MC are easily distinguished from the other cells of the INL. Their nuclei measure approximately 10.0 to 16.0 µm in length and only 3.0

to 4.0 μm in diameter, and contain finely granular chromatin more electron dense than that of other INL nuclei. Numerous microtubules and free polyribosomes fill the moderately electron dense cytoplasmic matrix.

Extending sclerally from each cell body is the outer process which gives rise to fine lateral branches that occupy much of the extracellular space of the OPL and ONL. Near the OLM these processes expand to form mitochondria-filled outer terminals which are triangular in radial section (see Figure 4.7.1) and are rounded with short, thick lateral processes in tangential section (see Figure 4.10.1). Numerous microvilli extend from these outer terminals beyond the OLM into the ventricular space as described in Section 4.7 and seen in Figures 4.7.1 and 4.7.2.

A corresponding inner process extends toward the ILM from each MC cell body. These processes cross the inner plexiform layer (IPL), RGC layer and optic nerve fibre layer (NFL) where their lateral proceeses fill the intercellular spaces before expanding to form the inner terminals along the vitread surface of the possum retina. Numerous microtubules and few mitochondria fill the cytoplasm of the inner (vitread) terminals which are more prominent in the peripheral retina than centrally.

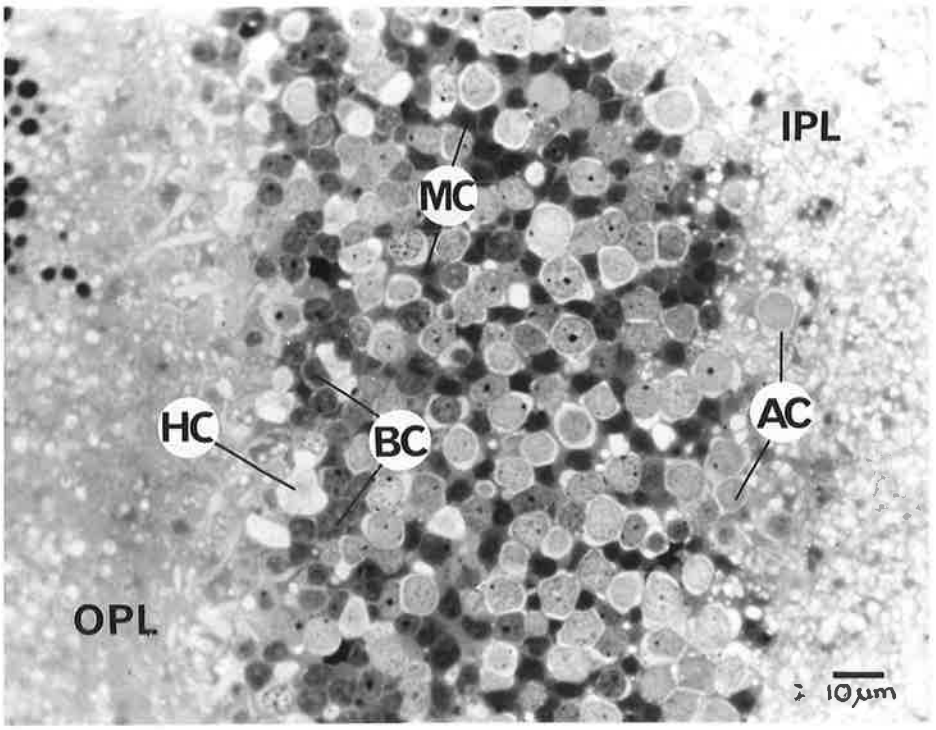

Figure 4.13.1 Inner nuclear layer, possum.
Light micrograph showing a tangential section through the inner nuclear layer (INL) which is sandwiched between the inner (IPL) and outer plexiform (OPL) layers. The horizontal cells (HC) and smaller bipolar cells (BC) generally lie sclerally within the inner nuclear layer while the amacrine cells (AC) lie vitreally. Small, dense cross-sections of Müller cells (MC) are seen throughout the INL.

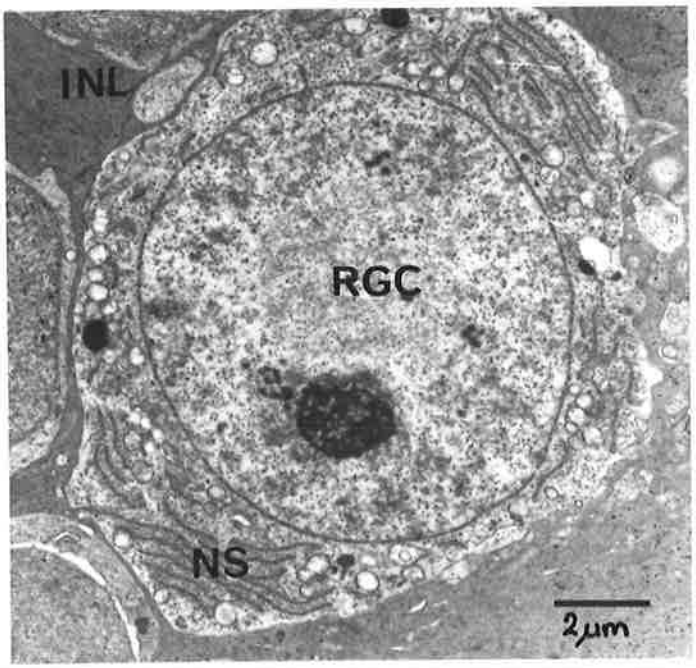

Figure 4.13.2 Inner nuclear layer, possum.
Radial electron micrograph showing a possible displaced retinal ganglion cell (RGC) lying within the inner nuclear layer adjacent the inner plexiform layer (IPL). Note the abundant Nissl substance (NS) in the cytoplasm which consists of membranous cristae and polyribosomes.

4.14 Inner Plexiform Layer

The IPL is a broad layer approximately 30.0 μm thick that lies immediately vitread to the INL. By light microscopy the IPL is slightly basophilic and foamy in appearance. Electron microscopy shows that this layer consists entirely of cell processes. The neuronal processes appear to be randomly arranged and are generally considered to be axons of BC, AC processes and RGC dendrites (RODIECK, 1973). These processes exhibit low electron density and are difficult to distinguish from one another. The MC processes are easily recognisable as broad radially directed processes of greater electron density which give rise to fine lateral branches or lamellae that run between the neuronal processes.

A variety of cell contacts have been found within this complex fibrous layer. Numerous conventional synapses occur between neuronal processes throughout the IPL (see Figure 4.14.1). While ribbon synapses, such as those shown in Figure 4.14.2 and similar to those in the OPL, appear to be confined to the more sclerad third of the IPL. Non-synaptic intercellular junctions have also been observed between the neuronal processes.

Several examples of ribbon synapses with a characteristic form were found lying close to the INL. The pre-synaptic terminal shows light to moderate electron density, a few small mitochondria and contains large numbers of synaptic vesicles with a diameter of 30 to 50 nm. Only one synaptic complex has been sectioned in each of the pre-synaptic terminals examined. However, large terminals of similar structure have been seen in a post-synaptic relationship to several conventional synapses, possibly

reciprocal in nature, which suggests that these pre-synaptic terminals may possess multiple ribbon complexes. Each synaptic complex has a small, electron dense ribbon, surrounded by a halo of synaptic vesicles, lying close to and at right angles to the ridge of the V-shaped pre-synaptic membrane. A small, dense structure similar to the arciform density is positioned between the ribbon and the pre-synaptic membrane. Thickening of the post-synaptic membranes is more marked than that of the pre-synaptic membrane, and there is a V-shaped synaptic cleft (see Figure 4.14.2).

Generally there are 2 post-synaptic processes that contain fewer vesicles than the pre-synaptic terminal but are of similar electron density and may also contain mitochondria. One of these post-synaptic processes has a reciprocal conventional synapse with the pre-synaptic terminal as seen in Figure 4.14.3. There is a wide synaptic cleft with thickening of both the pre- and post-synaptic membranes, and an aggregate of synaptic vesicles adjacent the pre-synaptic membrane of the post-synaptic process as seen in Figure 4.14.3.

This arrangement of a single pre-synaptic ribbon complex with 2 post-synaptic processes conforms with that given by DOWLING and BOYCOTT (1966) for the bipolar axodendritic junctions in primate retina. They have called these dual synapses 'dyads' and have shown that the pre-synaptic terminal is from a bipolar axon and that the post-synaptic processes belong to AC and RGCs. The post-synaptic process that makes the reciprocal synapse is considered to be the AC process.

Numerous conventional synapses, such as that seen in

Figure 4.14.1, occur throughout the IPL of the possum retina. The size of these interneuronal contacts appears to vary considerably, although this may be an artifact of sectioning. Pre-synaptic processes contain moderate numbers of synaptic vesicles and have dense aggregates of these vesicles adjacent the pre-synaptic membrane. Fusion of synaptic vesicles with the pre-synaptic membrane is sometimes apparent. Both the pre- and post-synaptic membranes are thickened and are separated by a 20 nm wide cleft. The post-synaptic region may occur anywhere along the length of a neuronal process and contains a small number of synaptic vesicles.

Non-synaptic contacts have also been observed between the neuronal processes of the IPL but not between MC processes and neuronal processes. These small intercellular contacts appear to be tight junctions.

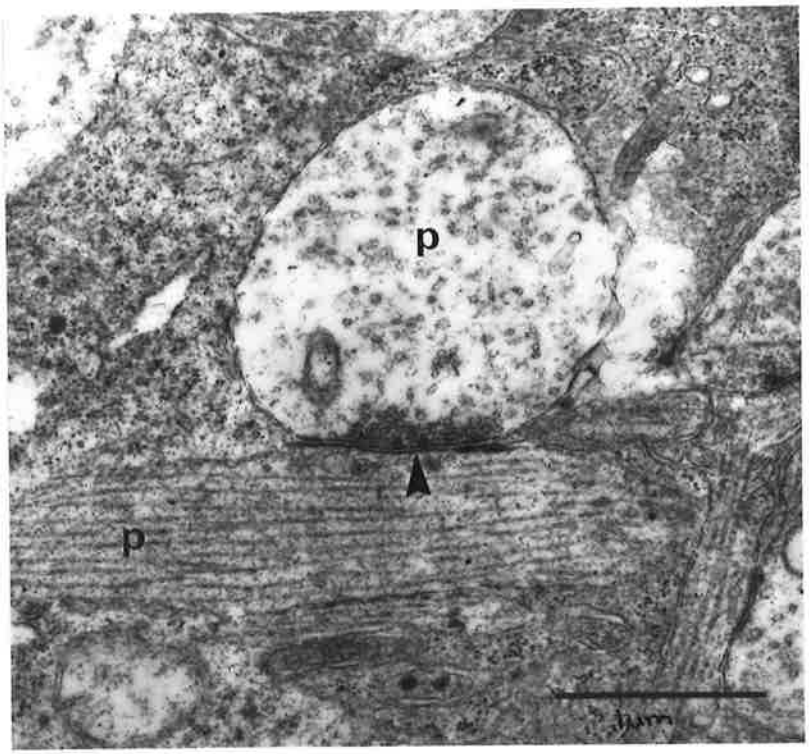

Figure 4.14.1 Inner plexiform layer, possum. Electron micrograph of a conventional synapse (arrow) between 2 neuronal processes (p) within the inner plexiform layer.

Figure 4.14.2 Inner plexiform layer, possum. An electron micrograph of a 'dyad'-type bipolar ribbon synapse. Note the array of vesicles around the small synaptic ribbon (r) and thickening of the post-synaptic membrane (arrows).

4.15 Retinal Ganglion Cell Layer

The ganglion cell layer contains the cell bodies of the RGCs. Their cell bodies occur along the vitread adge of the retina and are larger than the other retinal neurons.

At the light microscopic level these cells stain lightly with the polychrome stain used. The moderately basophilic nuclei are round to elliptical in shape and often have a single dense nucleolus. In large RGCs the nuclei are positioned eccentrically when seen in tangential section and in the smaller cells, where they constitute a greater volume of the cell body, they are positioned more centrally. The cytoplasm is slightly basophilic and granular.

Examination of these cells with the electron microscope has shown that the nuclear chromatin is rather coarse but without clumping (see Figure 4.15.1) and that a nucleolus is usually present. The RGC cytoplasm contains abundant polyribosomes and numerous mitochondria measuring 0.5 to 1.0 µm in diameter. A small number of moderately electron dense membrane-bound inclusions are also present. These inclusions, of unknown composition, appear slightly granular and they are elliptical (measuring approximately 0.25 µm across and 0.5 µm in length) or irregular in shape.

The most striking feature of the cytoplasm of the RGCs is the large amount of RER present in orderly arrays. As is evident in Figure 4.15.1 the cristae are arranged in whorls or concentric layers separated by intervals of 0.2 µm. They are also fenestrated and covered with numerous ribosomes. The cytoplasm that separates the cisternae contains numerous free polyribosomes. The intercisternal spaces are filled with a fine granular matrix that is less electron dense than

the cytoplasm. This arrangement of RER is typical of that described by FAWCETT (1981) for Nissl substance.

From sections prepared for routine light and electron microscopy it was difficult to determine whether the RGC population consists of different morphological types. However, using Nissl-stained wholemounted retinae it was possible to divide the population into 3 three groups corresponding to the α-, β- and γ-type RGCs described by HUGHES (1975a) for the cat. For the Brush-tailed possum RGCs measuring from 22.0 µm in diameter (α-type) make up approximately 1.0% of the total population. β-cells measure from 10.0 to 22.0 µm in diameter and comprise 53.0% of the population while the smallest α-cells measure from 4.0 to 10.0 µm and make up 46.0% of the population. The diameter of the RGCs measured ranges from 4.0 to 24.0 µm and their size distribution is shown in Figure 4.15.2.

Cells within the RGC layer measuring less than 4 µm in diameter were almost invariably found to have small darkly staining nuclei with no visible cytoplasm or Nissl substance. These cells were presumed to be glial in type and therefore were not included in the RGC counts. The remaining cells were considered to be presumptive RGCs and the counts were not corrected for the presence of displaced AC.

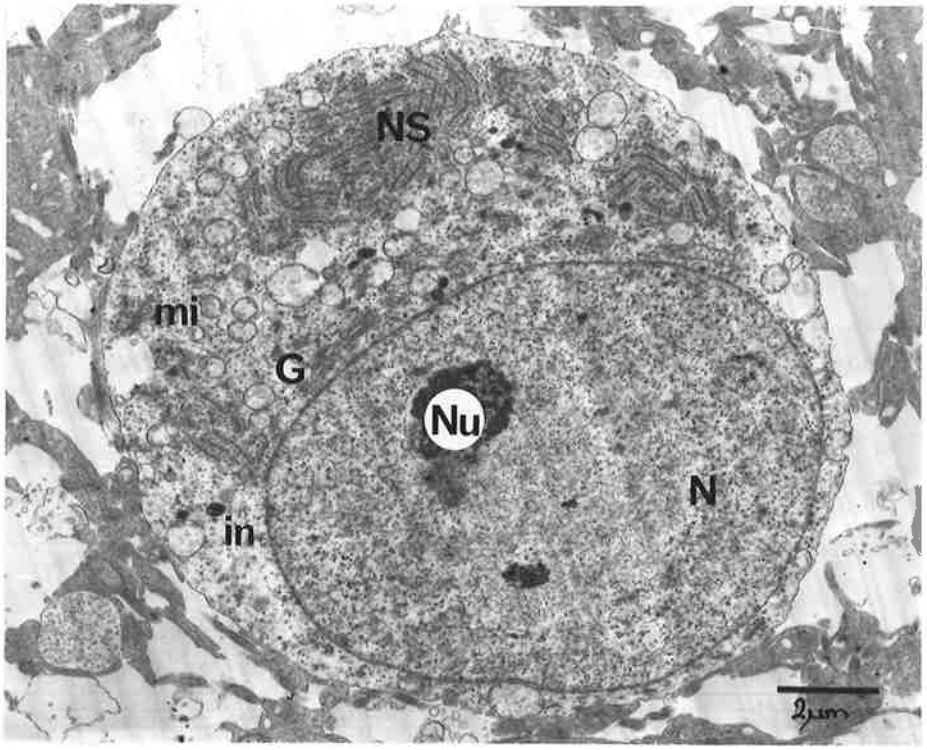

Figure 4.15.1 Retinal ganglion cell, possum. Electron micrograph of a large retinal ganglion cell with an eccentric nucleus (N) and single nucleolus (Nu). The cytoplasm contains abundant cisternae of Nissl substance (NS), mitochondria (mi), perinuclear Golgi complexes (G) and small dense inclusions (in).

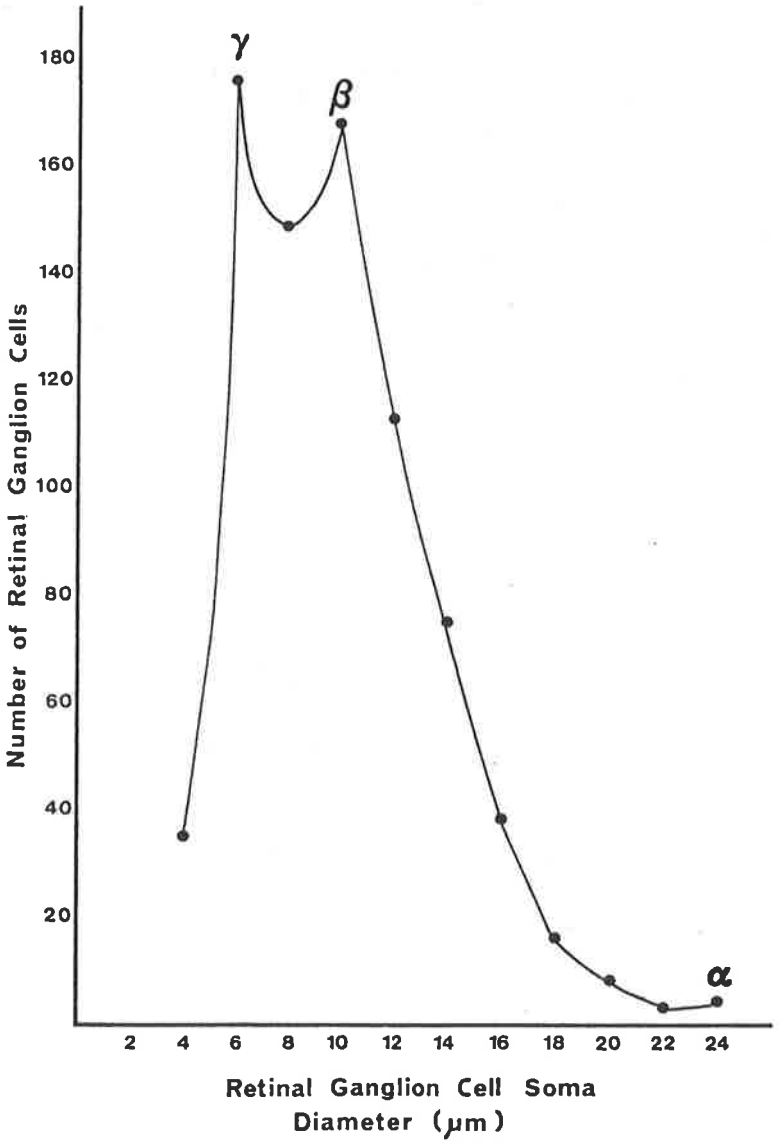

Figure 4.15.2 Retinal ganglion cell soma diameter distribution for wholemounted possum retina. The α, β and γ indicate the peaks within each of the 3 RGC groups. Sample size = 785 cells

4.16 Optic Nerve Fibre Layer

The NFL contains neuronal processes which are the axons of the RGCs but, unlike the IPL and OPL, does not contain any synapses. The axons arise from the vitread aspects of the RGCs and run beneath the inner limiting membrane (ILM) to converge at the optic disc.

In the peripheral retina of the possum these axons occur in small bundles that are completely surrounded and isolated from each other by the MC processes. Single axons also occur in this region of the retina.

As the axons approach the central retina the bundles merge to form a tightly packed layer; very few MC processes are seen running between the axons.

The diameter of the axons in the NFL, most readily established in sections that cut the axons in transverse section, varies from approximately 0.2 to 2.0 μm. The cytoplasm of these axons contains numerous neurotubules and neurofilaments, and a small number of rounded mitochondria,

The NFL is separated from the ILM by the terminals of the MC. This separation is more marked in the peripheral retina where the small fibre bundles are surrounded by a large amount of MC material.

4.17 Inner Limiting Membrane

The ILM is a continuous membrane that separates the vitread surface of the retina from the vitreous. It is generally considered to be the basement membrane of the MC (HOGAN, ALVARADO and WEDDELL, 1971), whose terminals form the vitread surface of the retina. In the possum this basement membrane measures approximately 25 nm in thickness.

The surface of the ILM that faces the MC terminals is fairly smooth, while the vitread surface is irregular. This irregular appearance results from the numerous short fibrils that insert into and contribute to the ILM. Such fibrils are referred to as vitreous fibrils (HOGAN, ALVARADO and WEDDELL, 1971).

This membrane is clearly separated from the vitread surface of the retina by a narrow gap that measures approximately 50 nm, and appears to be filled with fine granular material of low electron density.

5 RETINAL ANATOMY OF THE KOWARI

5.1 Fundus and Retinal Blood Supply

The fresh eyecup of the Kowari is divided into roughly equal superior and inferior portions (see Figure 5.1.1A) by an irregular horizon, represented in Figure 5.1.1B by a broken line, that curves to pass inferior to the optic disc. The superior fundus appears grey-brown and the inferior fundus is a darker brown colour. The retina in both superior and inferior fundi appears to be transluscent indicating that the colour seen may result from the pigmentation of the RPE and choroid. The optic disc is positioned just inferotemporal to the posterior pole.

Blood vessels can be seen on the vitread surface of the Kowari retina in both fresh and recently fixed eyecups, although they do not show up well in macrophotographs such as that seen in Figure 5.1.1A. There are 3 main arterial vessels that enter the eyecup through the optic disc,from which they radiate and divide to supply the entire retina.

A short thick superior vessel branches profusely to supply most of the upper fundus. There is also a short inferotemporal vessel which divides to send branches to the retina of the inferotemporal quadrant. Finally a short inferonasal vessel gives rise to several branches that supply the inferonasal quadrant. Variations occur in this pattern as the inferonasal vessel may run in a more nasal direction or be replaced by 2 vessels supplying the same quadrant.

These arterial vessels are accompanied by veins and run across the vitread surface of the retina just beneath the fibres of the NFL (see Figure 5.14.2), and give rise to numerous capillaries that penetrate the retina to reach

the OPL where they form capillary loops indicative of a plexus.

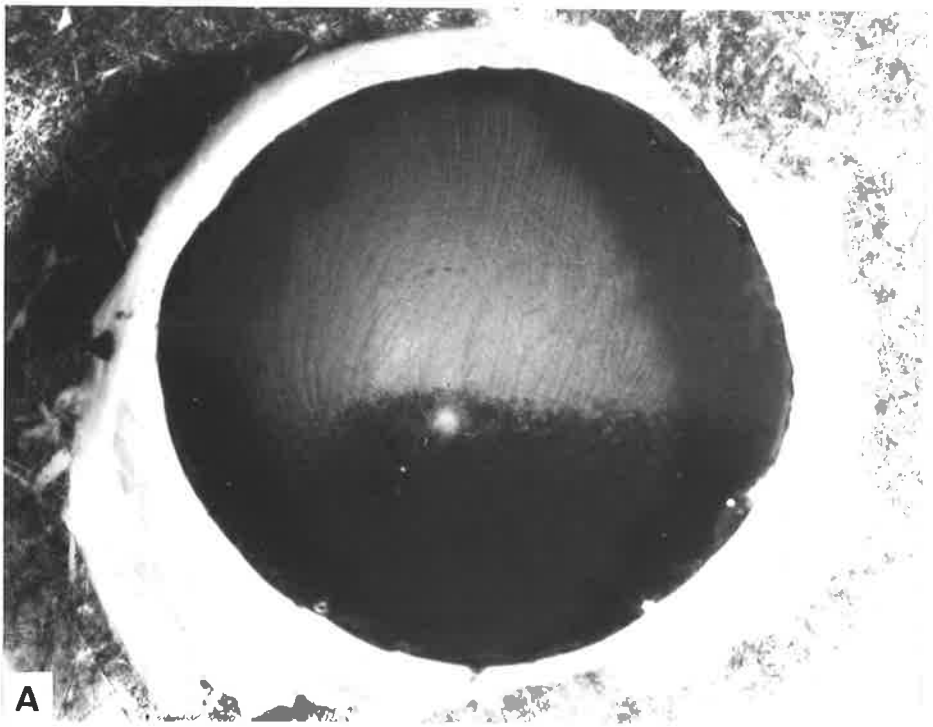

B

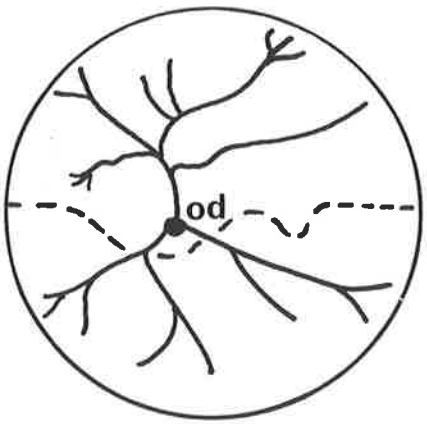

Figure 5.1.1 Eyecup, Kowari.
A. Macrophotograph of a fresh left eyecup of the Kowari showing the division into superior and inferior fundi.
B. Schematic diagram of the right eyecup of the Kowari showing the distribution of the retinal vessels radiating from the optic disc (od) and the horizon (----) separating the superior and inferior fundi.

5.2 Choroid

The choroid of the Kowari consists of several loosely arranged layers running parallel to the surface of the eyeball, and containing several cell types, extracellular fibres, numerous capillaries and nerve bundles (see Figure 5.2.1).

Melanocytes, such as those seen in Figure 5.2.1, were the most commonly found cells of the choroid. The cytoplasm of these large flattened cells contains numerous membrane-bound pigmented granules, measuring up to 1.0 μm in diameter, that are brown in unstained retina and fail to show any internal ultrastructure, indicating that they are melanin. Occasionally immature melanosomes were seen amongst the mature granules. Other cytoplasmic organelles include a few mitochondria, small perinuclear Golgi complexes and small membrane-bound inclusions of moderate electron density and unknown type. The coarse granular chromatin of the melanocyte nuclei exhibits moderate clumping; single nucleoli are usually present.

The cells of the choroid are supported by an extensive network of randomly orientated fibres which stain deeply with basic fuchsin in polychrome-stained sections. These fibres were found to have the 64 nm periodicity typical of collagen and also stain grey-purple with Gomori's reticulin method. The finer fibres of the supportive network stain black with Gomori's method showing them to be reticulin.

Capillaries of the choriocapillaris occur in the most vitread part of the choroid adjacent the RPE. The intensely basophilic nuclei of the endothelial cells are prominent and also exhibit marked electron density. Evenly distributed

fenestrations,of approximately 80 nm diameter and containing central densities, are present in the endothelial wall of capillaries adjacent BM (see Figure 5.2.2).

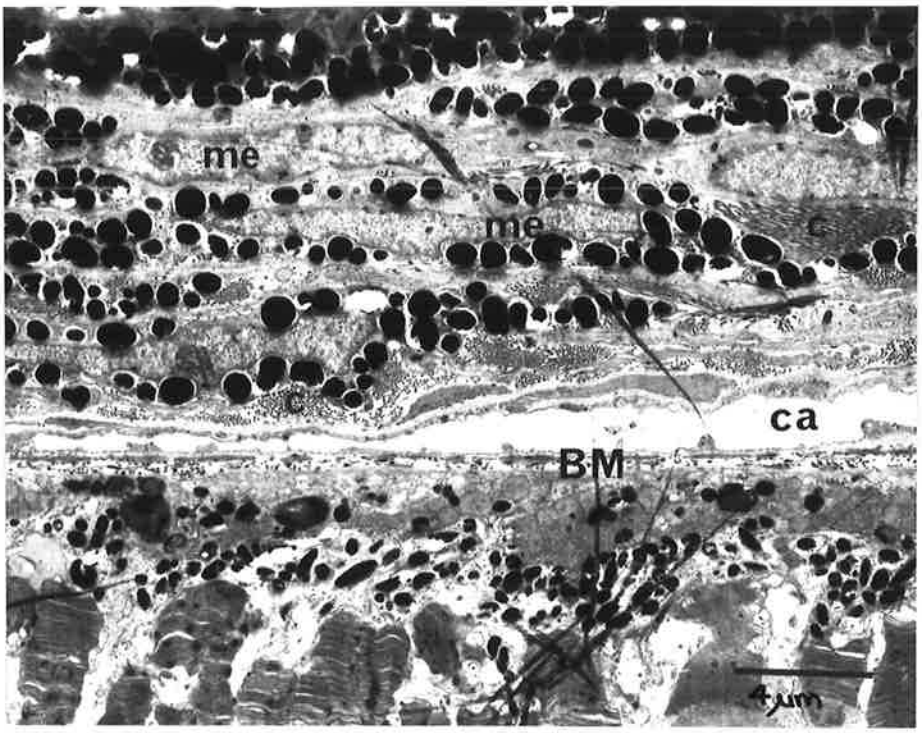

Figure 5.2.1 Choroid, Kowari.
Electron micrograph of a radial section showing the layered arrangement of the choroid. Note the capillary (ca) of the choriocapillaris adjacent Bruch's membrane (BM). The pigment granules are prominent in the melanocytes (me) which are separated by layers of collagen fibres (c).

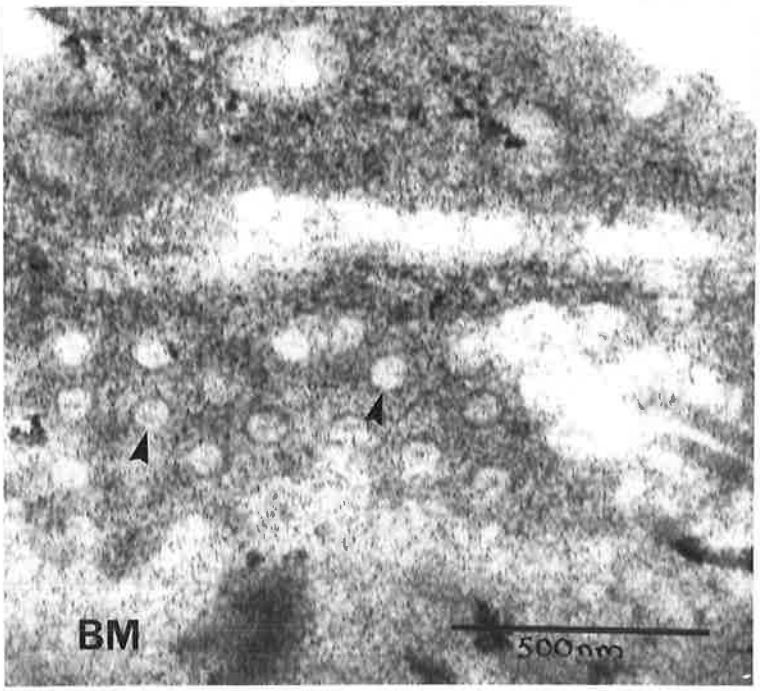

Figure 5.2.2 Choroid, Kowari.
Electron micrograph showing a tangential section through the endothelial wall of the capillary adjacent Bruch's membrane (BM). The fenestrations (arrows) in the endothelial cells are clearly evident.

5.3 Bruch's Membrane

With well preserved material it was possible, even at the light microscopic level, to see the layered arrangement of BM which separates the choroid from the retina.

As seen in Figure 5.3.1 BM is a laminated structure consisting of 5 layers. The most vitread layer is the basement membrane of the RPE seen as a thin line of amorphous PAS-positive material that follows the curvature of the eyeball. It is separated from the basal cell membrane of the RPE by a gap of approximately 60 nm but does not follow the infoldings of these basal membranes. This basement membrane is firmly adherent to the RPE; should the choroid tear away from the retina the RPE remains attached to it, and not to the neuroretina, opening up the ventricular space.

The second layer stains deeply with basic fuchsin, is approximately 0.17 µm wide and consists of randomly arranged collagen fibres with the usual 64 nm periodicity. As expected its fibres stain grey-purple with Gomori's reticulin method.

The most electron dense layer in BM is the middle elastic layer. This layer, approximately 0.11 µm thick, is made of orcein-positive elastic fibres and is interrupted by pores through which collagen fibres sometimes pass.

Sclerad to the middle elastic layer is the outer collagen layer which is structurally similar to the inner collagen layer.

The fifth and most sclerad layer of BM is the basement membrane of the choroid which is best seen adjacent the endothelial cells of the choriocapillaris where it is separated from them by approximately 30 nm.

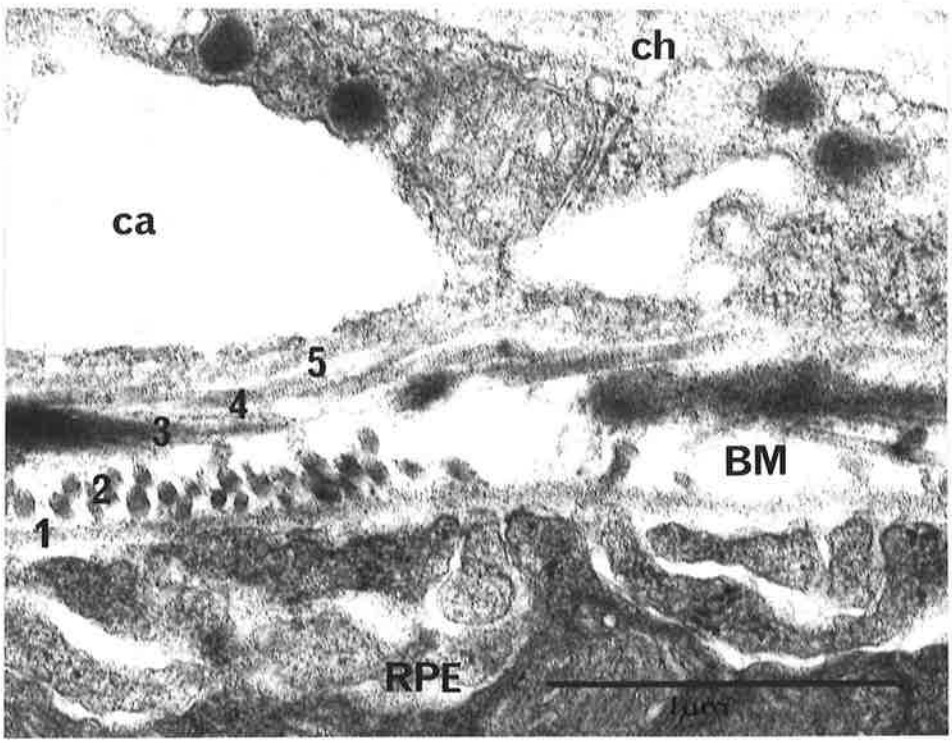

Figure 5.3.1 Bruch's membrane, Kowari.
Electron micrograph showing a radial section through Bruch's membrane (BM). Note the five layers of Bruch's membrane (1-5). Retinal pigmented epithelium (RPE); capillary of the choriocapillaris (ca); choroid (ch).

5.4 Retinal Pigmented Epithelium

The RPE is the only non-neuronal layer of the retina and in the Kowari is a thin (8.0 μm) single layer of cells lying immediately vitread to BM (see Figure 5.4.1).

In radial section the cells of the RPE are oblong in shape with a microvillous apical border. Tangential sections show them to be polygonal, mostly hexagonal, in cross-section (see Figure 5.4.2). The basally positioned nuclei are disc-shaped, elliptical in radial section and circular in tangential section. They are basophilic, contain a single nucleolus and show clumping of the nuclear chromatin.

The cytoplasm of these cells contains numerous basal mitochondria with transverse cristae, perinuclear Golgi complexes, abundant SER, numerous pigment granules and droplets. The membrane-bound pigment granules lack any internal ultrastructure, and are seen as highly electron dense circular or elongate profiles measuring 0.5 μm in diameter and up to 2.0 μm in length. They are generally confined to the apical cytoplasm and, like the larger choroidal pigment granules, appear brown in unstained retina. These granules are presumed to be melanin. The droplets, however, remain unstained in polychrome-stained retina, are refractile in fresh tissue, and occur in the basal cytoplasm. They exhibit electron density as a result of their affinity for osmium tetroxide, do not appear to be membrane-bound, lack any internal ultrastructure and are probably lipid in nature. Occasionally phagosomes containing irregular photoreceptor outer segment discs were seen in the basal cytoplasm of the cells of the RPE.

The lateral cell membranes of the RPE cells are

modified to form cell junctions (see Figure 5.4.3). Apically there are 2 bands of junctional complexes that encircle each cell. A tight junction, or zonula occludens (FAWCETT, 1981), characterised by fusion of the adjacent cell membranes, occurs nearest the apex. Immediately beneath this is a zonula adherens-type junction, where the intercellular space is wider and the adjacent cytoplasm is more dense than usual. These cells also have localised lateral cell contacts of a desmosomal type in a more basal position. No attachment of these cells to their basement membrane via cell junctions was seen in the material examined.

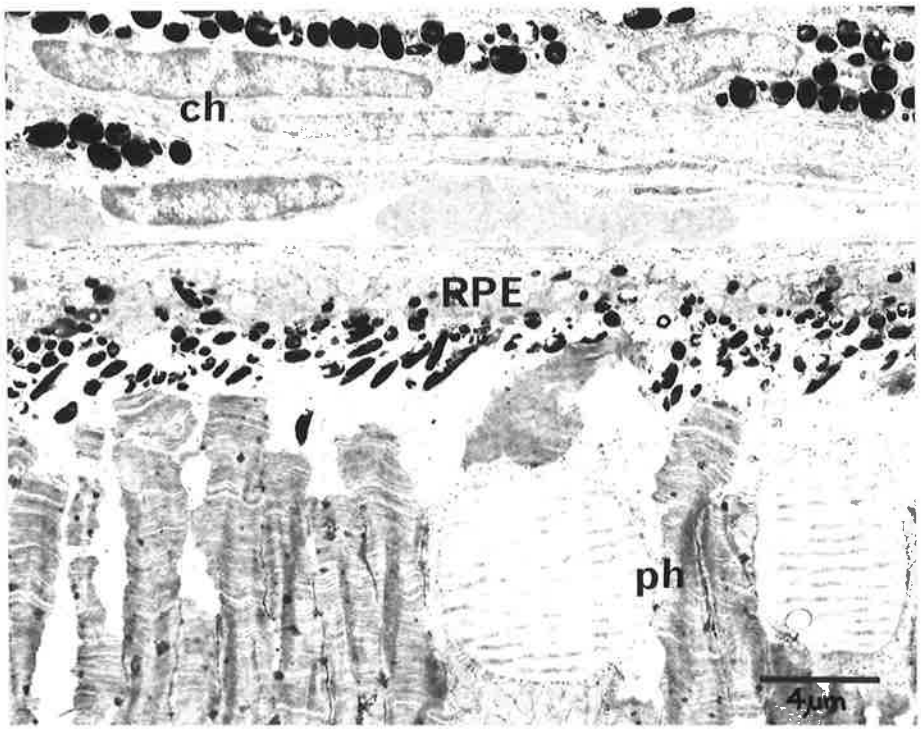

Figure 5.4.1 Retinal pigmented epithelium, Kowari.
Electron micrograph showing a radial section through the retinal pigmented epithelium (RPE). Choroid (ch); Photoreceptor outer segments (ph).

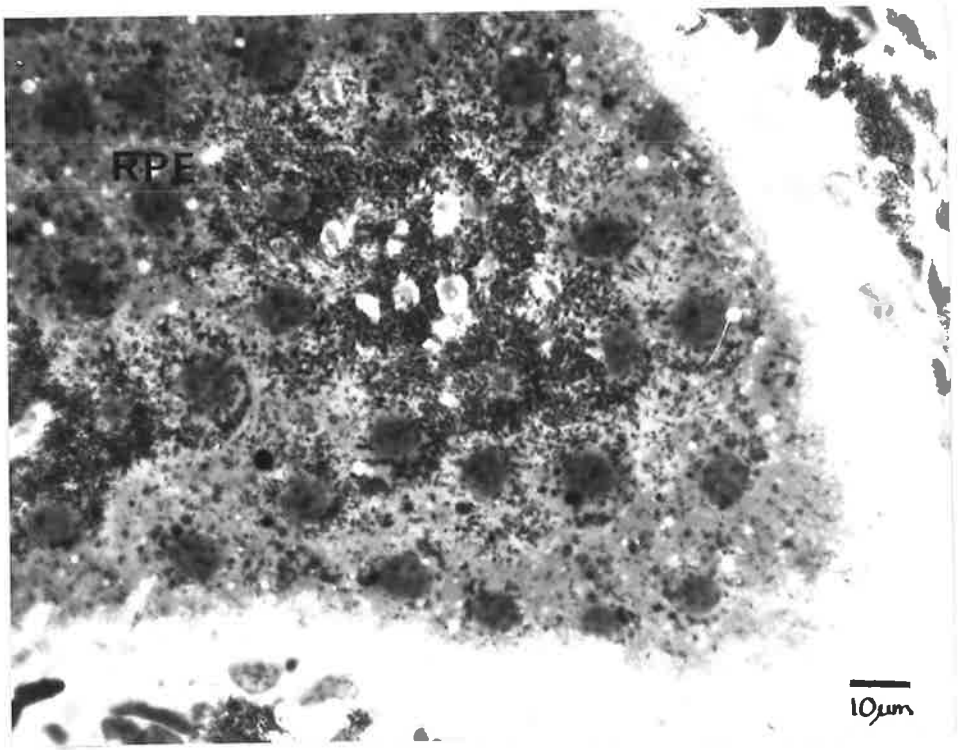

Figure 5.4.2 Retinal pigmented epithelium, Kowari.
Light micrograph of tangentially sectioned retinal pigmented epithelium (RPE) showing the polygonal profiles of the cells.

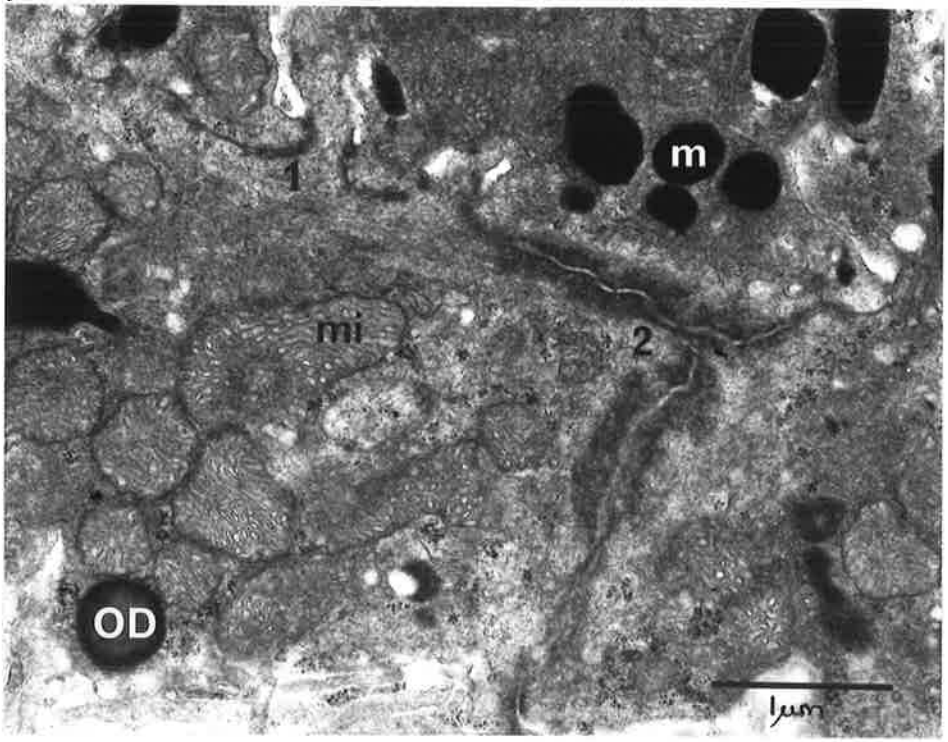

Figure 5.4.3 Retinal pigmented epithelium, Kowari.
A tangential electron micrograph of the retinal pigmented epithelium showing the apical zonula occludens tight junction (1) and a more basally positioned zonula adherens (2). Large melanin granules (m), mitochondria (mi) and an oil droplet (OD) are also seen.

5.5 Rod Outer Segments

The cylindrical ROS of the Kowari measure approximately 2.0 μm in diameter and vary in length from around 21.0 μm in central retina to 16.0 μm in the periphery. They extend from their connections with the inner segments to the microvillous border of the RPE. Electron microscopy shows that they only make loose contact with the epithelial microvilli.

In light microscopic preparations the ROS stain lightly with methylene blue-azure II and appear finely cross-striated (see Figure 5.5.1). This striation results from the presence of flattened membranous discs resolved only by electron microscopy. The discs are stacked at right angles to the longitudinal axis of the ROS and are completely enclosed by the cell membrane. Structurally each disc is a flattened sac consisting of 2 parallel membranes that are continuous with each other at a circumferential dilatation. The narrow space within each disc is more electron dense than the wider inter-disc space. All the discs in any one ROS are of similar diameter, and none appear to make any connection with the surrounding cell membrane nor with any other disc.

Examination of thin tangential sections, such as that seen in Figure 5.5.2, has shown that the disc margins have a smooth outline. A narrow space of low electron density exists between the periphery of each disc and the cell membrane. At the site corresponding to the position of the connective cilium the discs occupying the vitread portion of the ROS possess a single deep incisure (see Figure 5.5.2). Peripherally the incisure is quite broad but narrows considerably as it extends into the centre of the disc. Near the base of many ROS sections of single microtubules, not

arranged in the '9+0' pattern typical of sensory cilia,were found in the incisure. While a little further sclerad, groups of small granules are often present. These apparent granules may in fact be cross-sections of filaments extending sclerad from the microtubules. Occasionally one of the incisures divides, and rarely there are 2 incisures per disc. There was no evidence to suggest that double cilia exist.

As seen in Figure 5.5.3 some ROS have an irregular arrangement of tubules at their base adjacent the connective cilium. The significance of such tubules is not known. However, they may take part in disc formation.

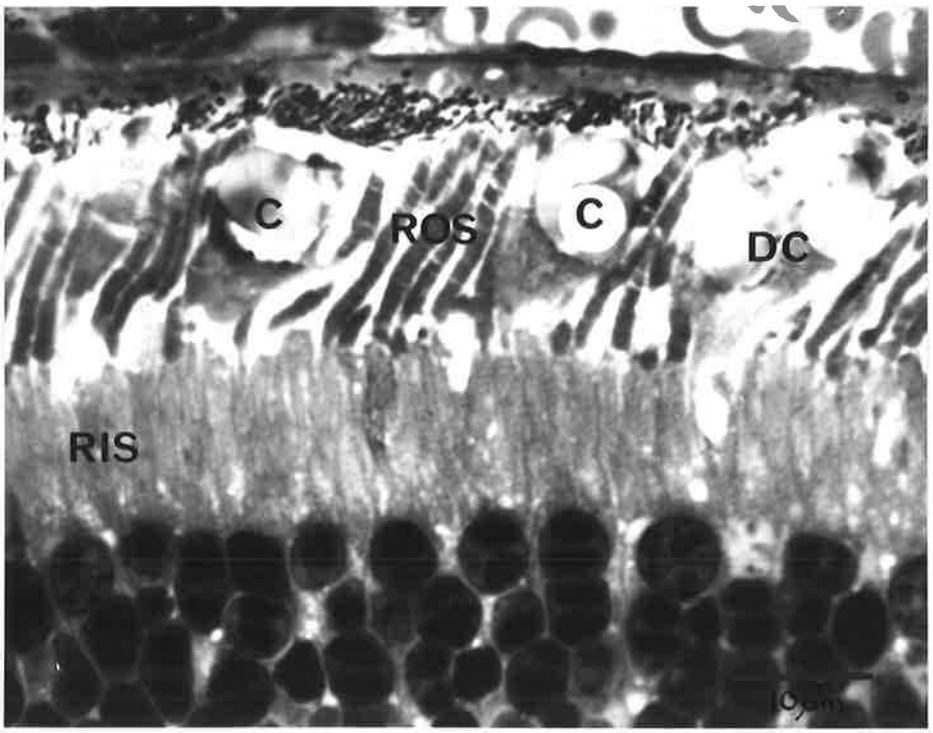

Figure 5.5.1 Photoreceptor layer, Kowari.
Light micrograph showing a radial section through the photoreceptor layer. Note the long, slender rod outer segments (ROS) and inner segments (RIS). Several single cones (C) with oil droplets and a double cone (DC) with an oil droplet in each member is also present.

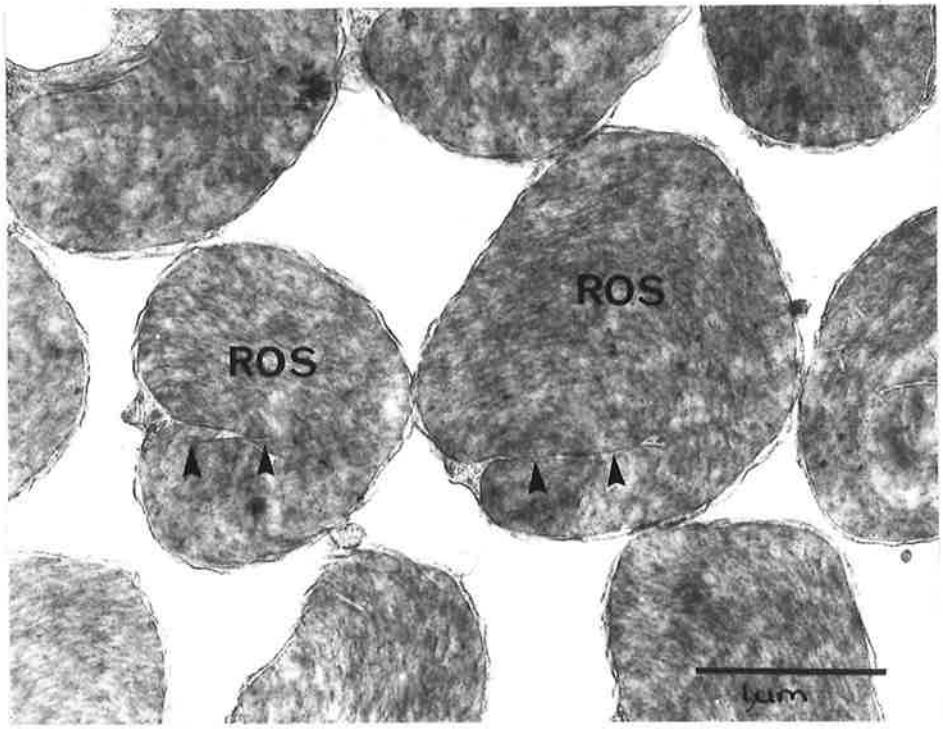

Figure 5.5.2 Rod outer segments, Kowari.
Electron micrograph of tangentially sectioned rod outer segments (ROS) showing the membranous discs with their incisures (arrows).

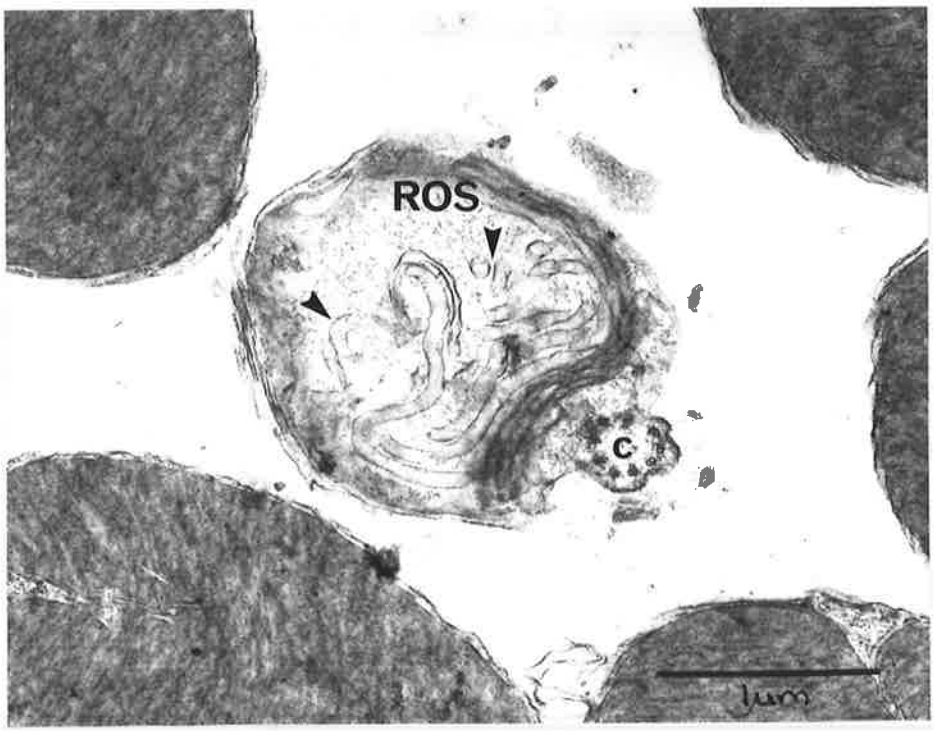

Figure 5.5.3 Rod outer segments, Kowari.
Electron micrograph of a tangential section through the base of a rod outer segment (ROS) showing the cilium (c) and an irregular arrangement of tubules (arrows).

5.6 Rod Ciliary Region

In the retina of the Kowari the majority of ROS are connected to their inner segments via a modified ciliary stalk.

This connective stalk measures approximately 1.0 μm in length and 0.3 μm in diameter and arises from a basal body, or primary centriole, embedded in the apical cytoplasm of the inner segment (see Figure 5.6.1) The basal body is the anchor for the connective stalk and consists of 9 microtubular elements arranged to form a short cylinder. Each of the peripheral elements, or triplets, comprises 1 complete and 2 incomplete microtubules. Short filamentous tufts, which vary in number and position, extend radially from the basal body as seen in Figure 5.6.2. In a few instances the position of these tufts has been suggestive of connectivity between the basal body and the cell membrane. There are a small number of basal bodies that show fine filaments extending vitread from the bases of the triplets. Despite careful sectioning, no secondary centrioles were found in the RIS in Kowari retina.

As the connective stalk leaves the inner segment the microtubular triplets become doublets giving the connective stalk 9 peripheral doublets. No centrally positioned microtubular elements are present, and the stalk has the '9+0' structure typical of non-motile sensory cilia. The cytoplasmic matrix within the ring of doublets is less electron dense than the more peripheral matrix in which the microtubules are embedded.

It is interesting to note that the cross-sectional outline of the connective stalk is irregular due to the

presence of membrane thickenings adjacent the doublets. These thickenings (see Figure 5.6.3) are present at all levels of the cilium suggesting that the external surface of the connective stalk has longitudinal ridges. Currently it is not known whether there is any relationship between these ridges and the doublets; no physical connection was found between them.

The number of component microtubules in each of the axial elements is once again reduced as the connective stalk joins the outer segment. This leaves just 9 single microtubules, of variable length, which may anchor the stalk to the ROS.

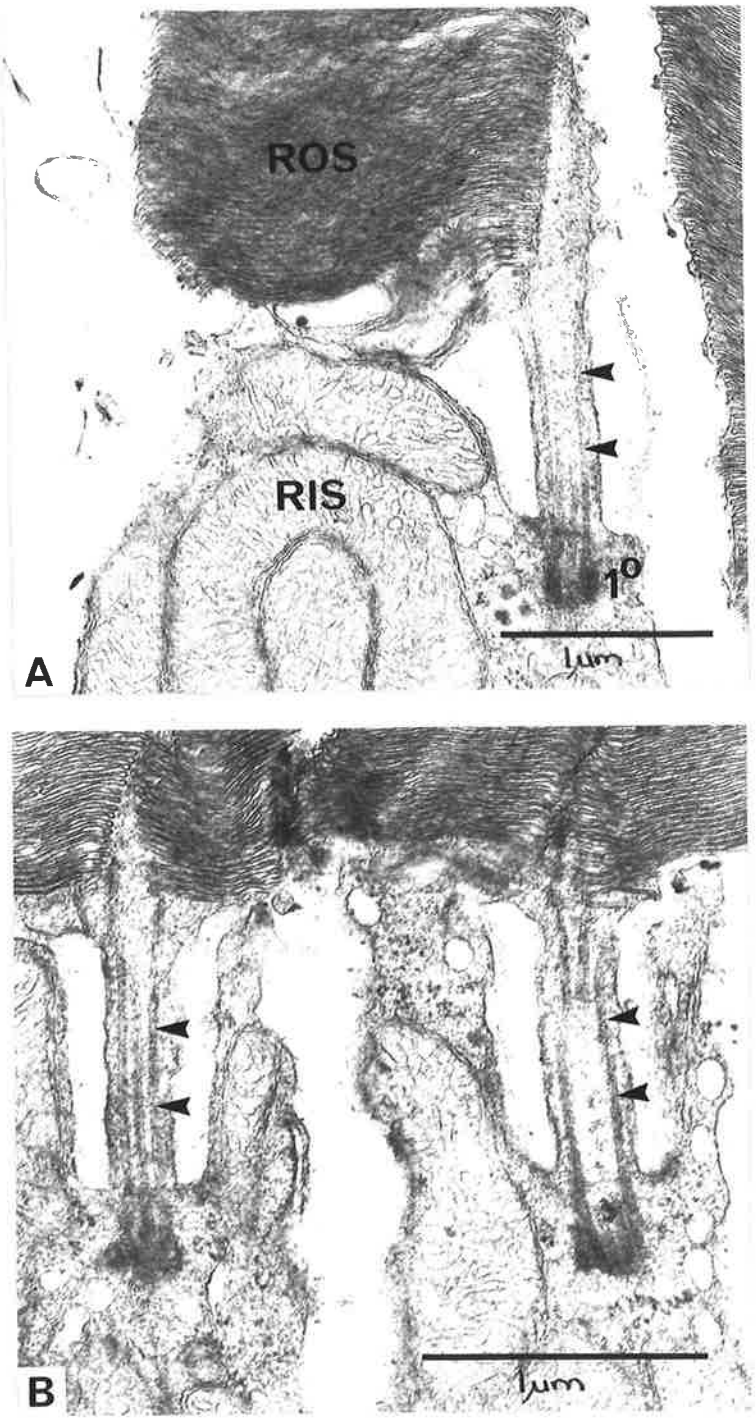

Figure 5.6.1 Rod ciliary region, Kowari.
Both electron micrographs, A and B, show radial sections through the ciliary region connecting the rod inner segments (RIS) to their outer segments (ROS).Note the presence of the primary centriole (1^{o}) and microtubules (arrows) in the modified ciliary stalk.

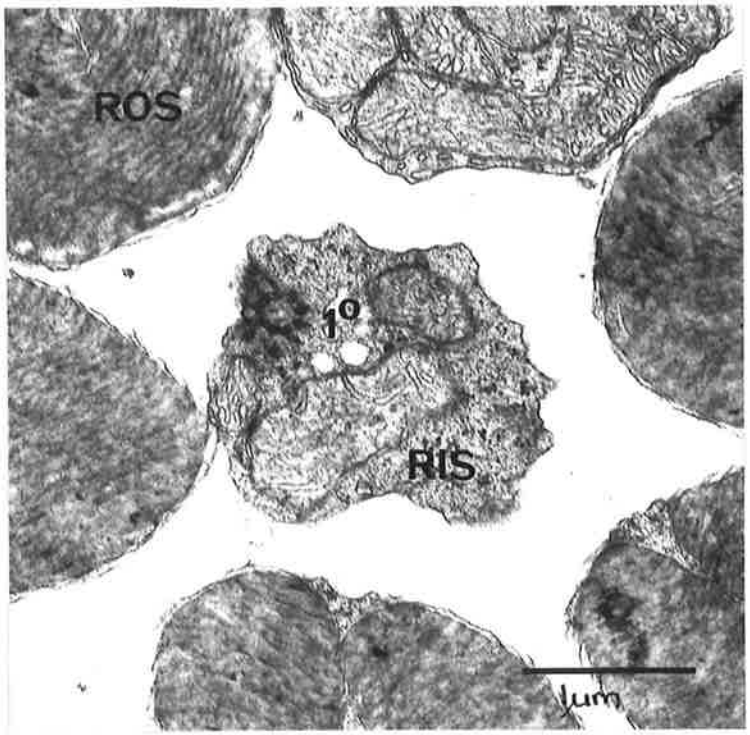

Figure 5.6.2 Rod inner segments, Kowari.
Electron micrograph showing cross-sections of both rod inner (RIS) and outer (ROS) segments. A primary centriole (1^{o}) with radial tufts is evident in the central rod inner segment.

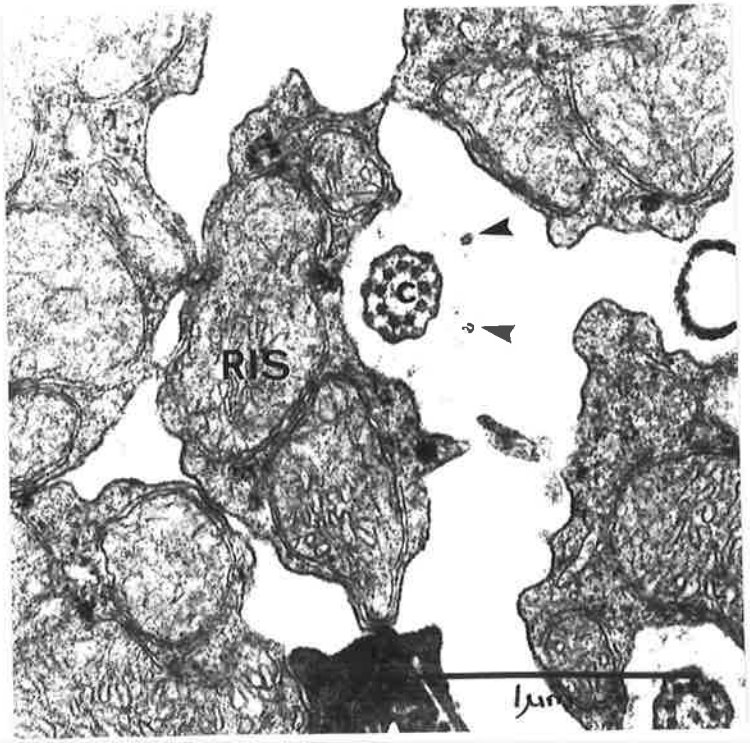

Figure 5.6.3 Rod ciliary region, Kowari.
Electron micrograph of a tangential section through the ciliary region of a rod inner segment (RIS) showing the connective cilium (c) and adjacent calycal processes (arrows) lying in a niche.

5.7 Rod Inner Segments

The RIS extend from the level of the OLM, just sclerad to the visual cell nuclei, to their connections with the outer segments. They measure approximately 20.0 μm in length and 2.0 μm in diameter. In polychrome-stained 1 μm sections the RIS appear to stain uniformly throughout. However, electron microscopic examination of these structures reveals that each comprises an inner and outer portion.

The inner, more vitread portion of each RIS is similar in structure to the myoids seen in the rod cells of other mammalian retinae. This moderately electron dense structure is continuous with the outer conducting fibre in most rods. Less frequently the cell body of the rod lies very close to the OLM and there is no intervening conducting fibre. The cytoplasm of the myoids contains moderate amounts of RER, abundant free polyribosomes, rather large Golgi complexes and occasional mitochondria.

The more sclerad portion of the inner segment, the ellipsoid, measures 2.0 to 3.0 μm across; wider than its outer segment. Generally the ellipsoids are so tightly packed with mitochondria that there is little room for other organelles; free polyribosomes were often seen. In radial sections the mitochondria are seen to run for several μm along the length of the ellipsoids. Frequently small vacuoles or vesicles and electron dense granules, probably glycogen, occur in the apical portion of the ellipsoids (see Figure 5.6.1A). The ellipsoids give rise to 2 fine calycal processes that run for several um along the length of the ROS adjacent the connecting cilium.

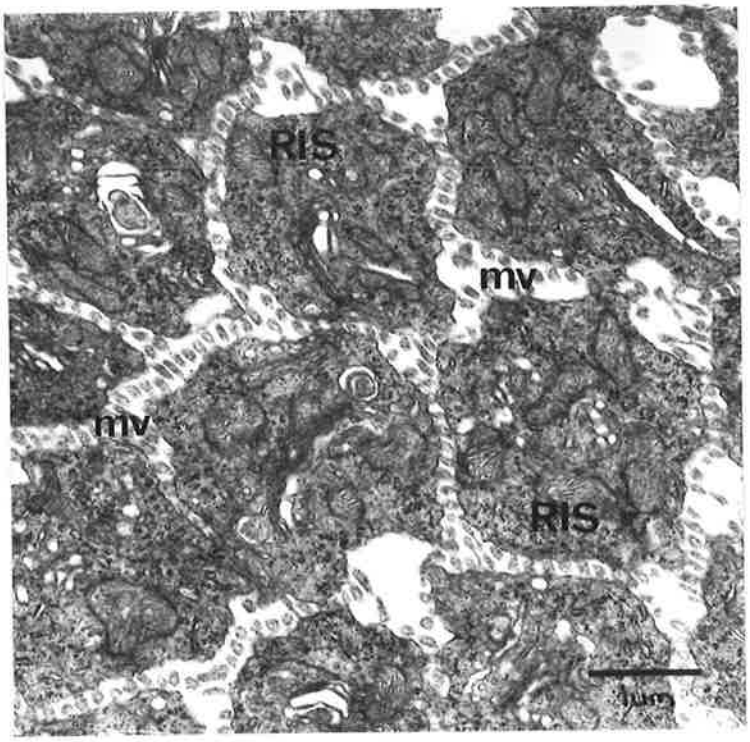

Figure 5.7.1 Rod inner segments, Kowari.
Electron micrograph showing cross-sections of the rod myoids just sclerad to the outer limiting membrane. Note the Müller cell microvilli (mv) separating the rod inner segments (RIS).

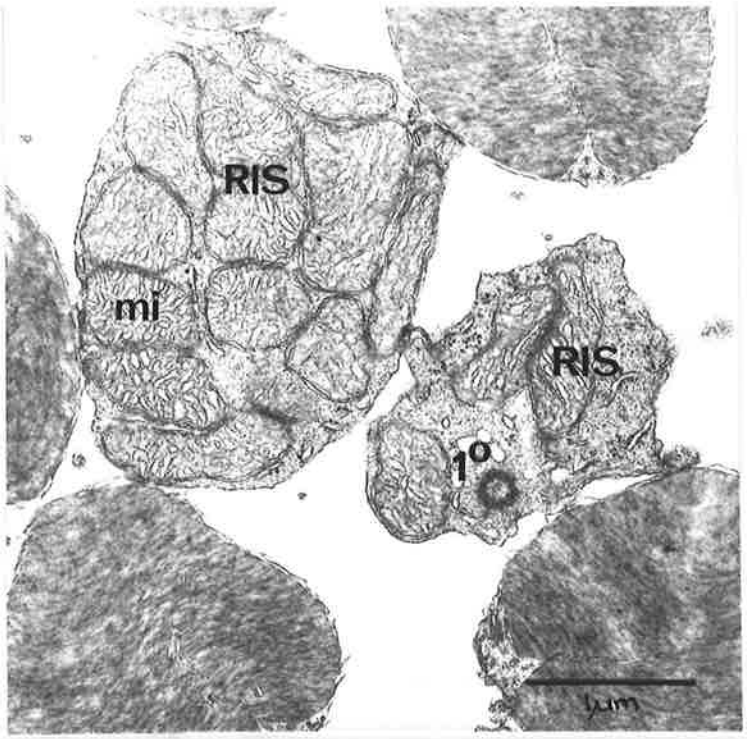

Figure 5.7.2 Rod inner segments, Kowari.
Rod inner segment ellipsoids (RIS) are seen in cross-section in this tangential electron micrograph. Note the closely packed mitochondria (mi) and primary centriole (1^{o}).

5.8 Cone Outer Segments

In the Kowari the COS are small and conical; their broad bases lie over the sclerad aspect of their inner segment while the narrower apex contacts the RPE as seen in Figures 5.8.1 and 5.8.2. The COS measure 3.0 to 5.0 μm in length and have a diameter of 4.0 to 5.0 μm at the base.

In radial sections, such as that shown in Figure 5.8.1, it is evident that the COS lie sclerad to the ROS and are surrounded by the apical microvilli of the RPE. In addition to lateral contacts made with the microvilli, the COS often make contact with the cell bodies of the RPE cells.

While the COS have the same staining properties as ROS in light microscopic preparations, some variation between their structure can be resolved using electron microscopy. As in rods the membranous discs are stacked at right angles to the long axis of the outer segment. They are, however, fewer in number and their diameter gradually decreases from the base to the apex of the COS. Furthermore, the COS discs are not completely surrounded by the cell membrane in the basal part of the COS. They are a series of invaginations of the cell membrane and the spaces between the discs are continuous with the extracellular (ventricular) space. The discs in the apical part of the COS are similar to those described for the ROS.

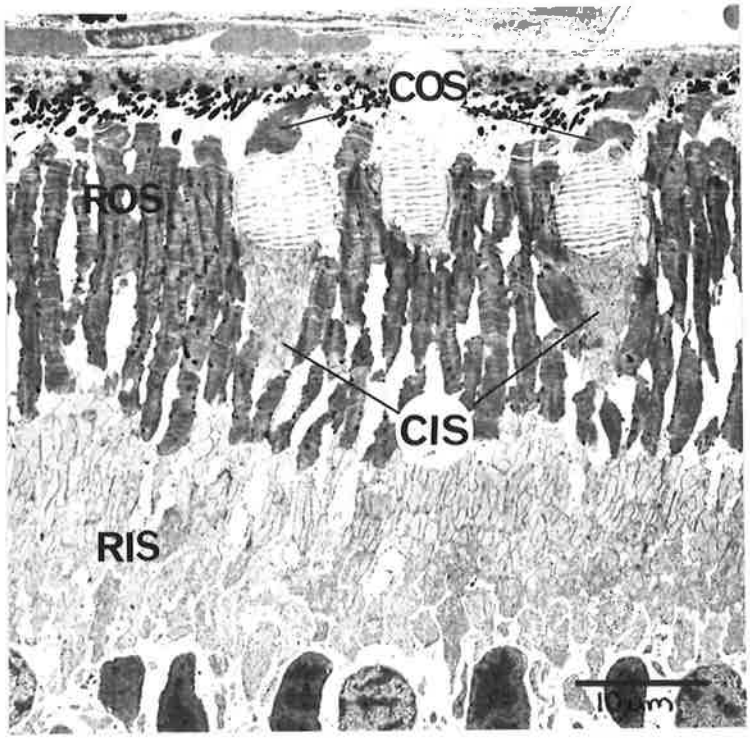

Figure 5.8.1 Photoreceptor layer, Kowari.
A low power electron micrograph showing the arrangement of cone inner (CIS) and outer (COS) segments in relation to the more numerous rod inner (RIS) and outer (ROS) segments.

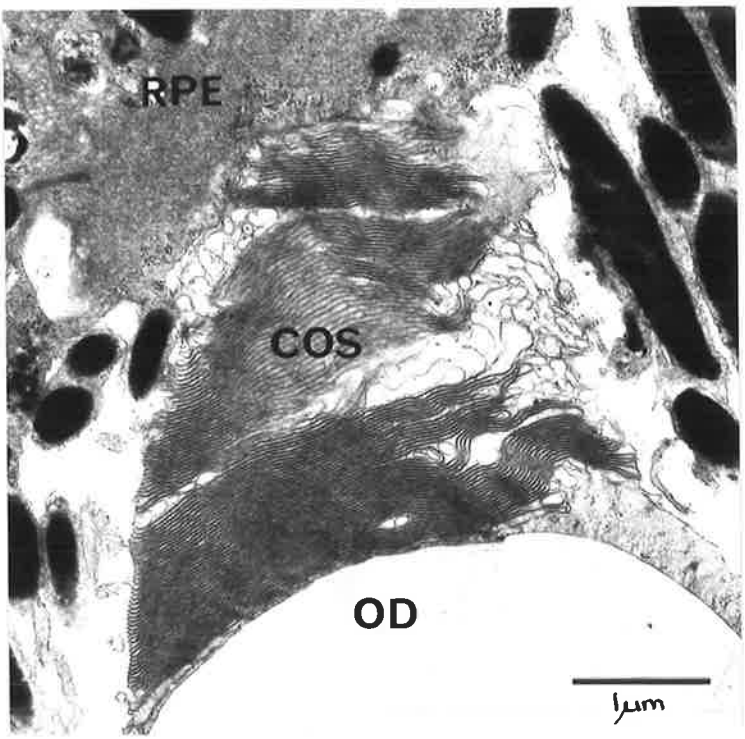

Figure 5.8.2 Cone outer segment, Kowari.
Electron micrograph showing a cone outer segment (COS) in radial section contacting the cell body of a retinal pigmented epithelial cell (RPE). Note the large space (OD) that remains in the inner segment from an oil droplet lost during processing.

5.9 Cone Inner Segment

Even at the light microscopic level it is apparent that the inner segments of the cones differ from those of the rods (see Figure 5.5.1). In the sclerad portion of the CIS there is a large unstained droplet not present in the RIS. These droplets are refractile in fresh tissue and blacken in osmium tetroxide, they are electron dense, membrane-bound and lack any internal ultrastructure.

The COS extend along the combined length of the RIS and ROS beginning at the level of the OLM as narrow cylinders that extend beyond the ciliary stalks of the rods and then gradually expand to accommodate the droplet sclerad to the ellipsoid. The cylindrical myoids are slightly electron dense, contain a moderate number of polyribosomes and a few elongate mitochondria as seen in Figure 5.9.2. The ellipsoids measure 4.0 to 5.0 μm in diameter and contain numerous small elongate mitochondria (0.5 μm in diameter and up to 3.0 μm long). The mitochondria extend further sclerad to surround the oil droplet.

Three types of cones are recognisable in the retina of the Kowari. Single cones with one oil droplet as seen in Figure 5.5.1 predominate: single cones without an oil droplet are the exception. The cone population also contains a few paired cones with an oil droplet in each member. The members are dissimilar in shape with the oil droplet of the principal cone lying closer to the OLM than the oil droplet of the accessory cone (see Figure 5.5.1). These cones are therefore double cones.

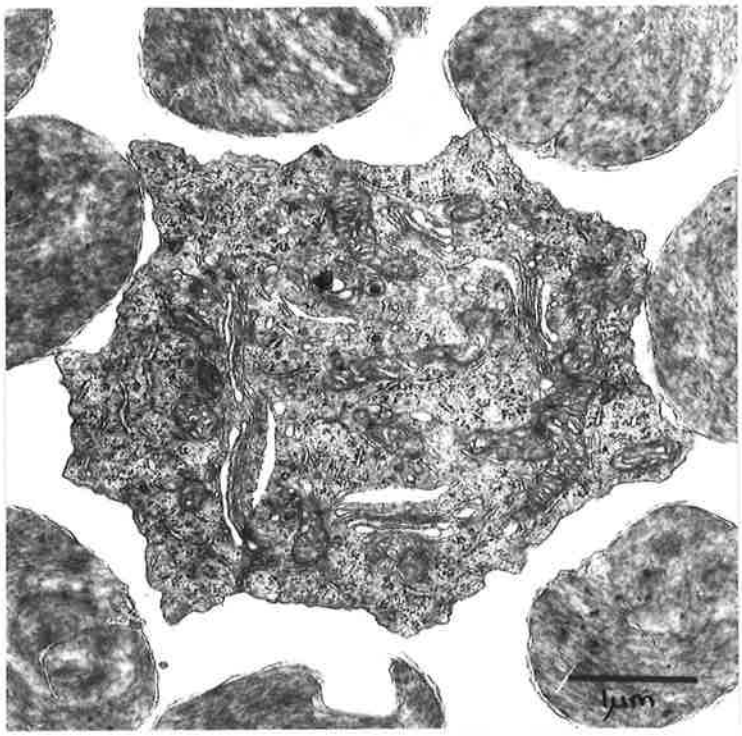

Figure 5.9.1 Cone inner segment, Kowari.
The central profile in this electron micrograph is a cross-section of a single cone inner segment.

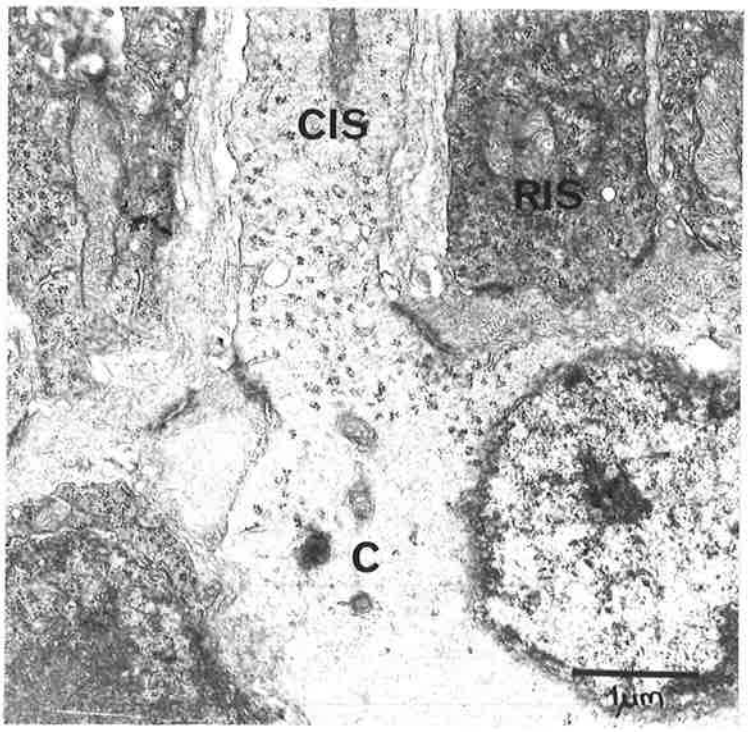

Figure 5.9.2 Cone inner segment, Kowari.
A radial electron micrograph showing a cone inner segment (CIS) extending sclerally from its cell body (C) in the outer nuclear layer. The CIS is surrounded by rod inner segments (RIS).

5.10 Outer Limiting Membrane

By light microscopy the OLM appears as a distinct but discontinuous line just sclerad to the ONL running parallel to the vitread surface of the retina.

This 'membrane' is in fact a continuous junctional band 0.4 µm wide just sclerad to the ONL. The most common cell junctions are those between photoreceptors and MC, and those between adjacent MC (see Figures 5.10.1 and 5.10.2).

These cell junctions appear to be zonulae adherentes, as is generally true of junctions between epithelial cells just beneath their free border (FAWCETT, 1981). Such contacts are also referred to as terminal bars: the cell membranes are thickened on either side of the 27 nm wide intercellular space (see Figure 5.10.2). Although the cytoplasm adjacent the thickened membranes is dense no tonofibrils were seen.

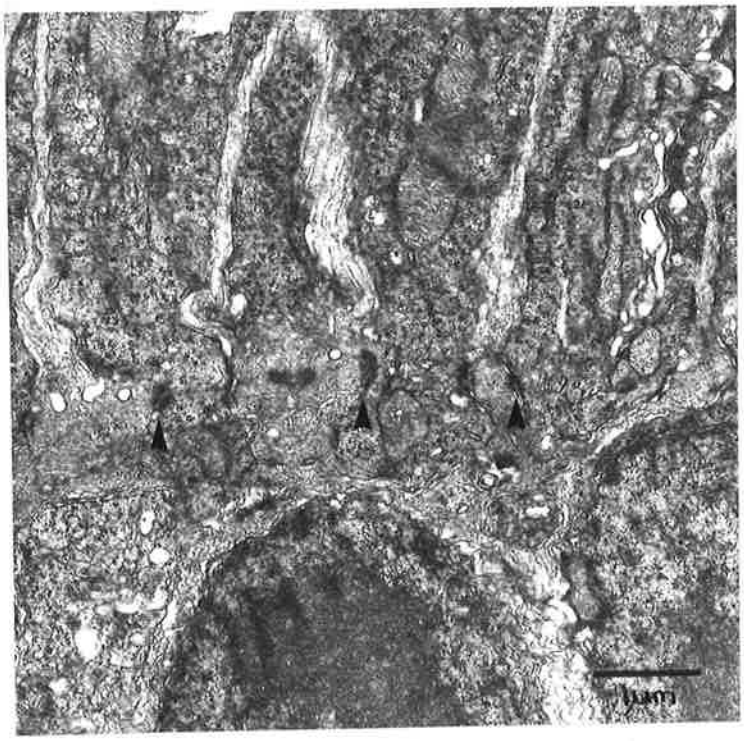

Figure 5.10.1 Outer limiting membrane, Kowari. In this radial electron micrograph the intercellular junctions (arrows) of the outer limiting membrane are seen as short complexes.

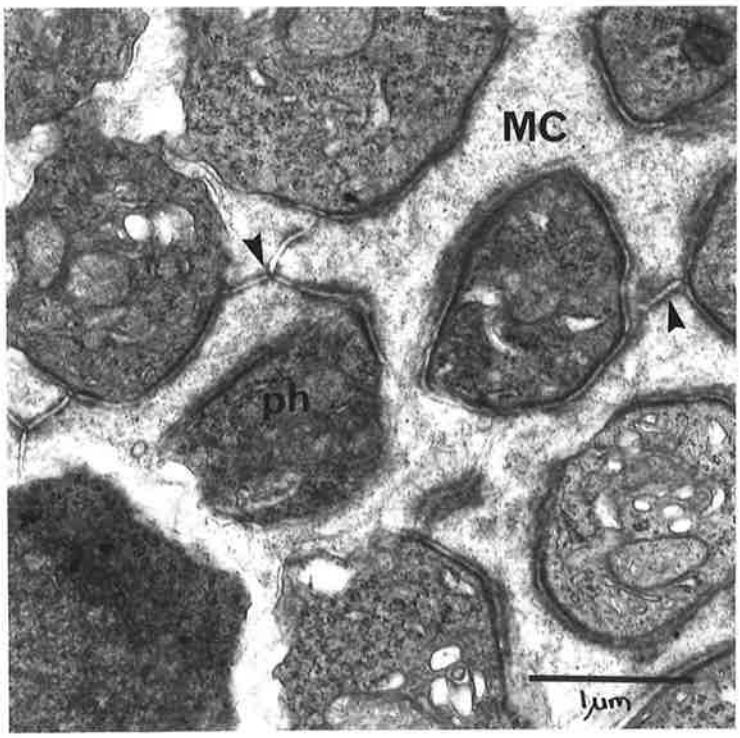

Figure 5.10.2 Outer limiting membrane, Kowari. When seen in tangential section the extensive intercellular junction (arrows) that comprise the outer limiting membrane are more apparent. Here junctions are seen between Müller cell processes (MC) and between photoreceptors (ph) and Müller cell processes.

5.11 Outer Nuclear Layer

As seen in Figure 5.11.1 the cell bodies of the rods and cones are closely packed together in radially orientated columns in the ONL (see Figure 5.11.1). In the peripheral retina each column contains between 5 and 7 cell bodies while centrally there are 7 or 8.

From examination of both radial and tangential sections it is evident that the rod nuclei outnumber the cone nuclei. Most of the cone nuclei lie along the sclerad edge of the ONL; though occasionally a cone nucleus was seen to occupy a more vitread position.

The more intensely staining rod nuclei are elliptical and measure 5.0 μm long and 4.0 μm in diameter. Typically they have 2 large, densely staining masses of chromatin as shown in Figure 5.11.2; although nuclei containing 1 or 3 chromatin masses are occasionally seen. Surrounding each nucleus is a thin, moderately electron dense rim of cytoplasm which is apparently devoid of organelles.

The slightly larger cone nuclei are roughly spherical with a diameter of 6.0 μm, stain less intensely and have a rather granular appearance (see Figure 5.11.3). The chromatin is scattered in small electron dense masses, often seen just beneath the nuclear envelope. Each cone nucleus is bounded by a rim of cytoplasm of low electron density which contains polyribosomes.

The cell body of each photoreceptor gives rise to 2 radially directed cytoplasmic processes. That process which extends sclerally to join the inner segment is the outer conducting fibre. While the narrower inner conducting fibre is directed vitreally to end in a synaptic

swelling in the OPL.

The length of these processes is variable and dependent upon the position of the cell body within the ONL. For instance, the outer conducting fibres of the cone cells are short because the nuclei lie adjacent the OLM. Moderate electron density is shown by the neurofilament-containing cytoplasm of these processes.

Filling the vertical spaces between the columns of visual cell somata are the long outer processes of the MC. Finer lateral processes branch from these to cover much of the surface of the ONL cell bodies.

The proportion of rods and cones in the total photoreceptor population was determined by counts made from tangentially cut 1 µm sections taken at the level of the ROS and CIS. In both the peripheral and central retina the ratio of rods to cones was found to be approximately 25:1.

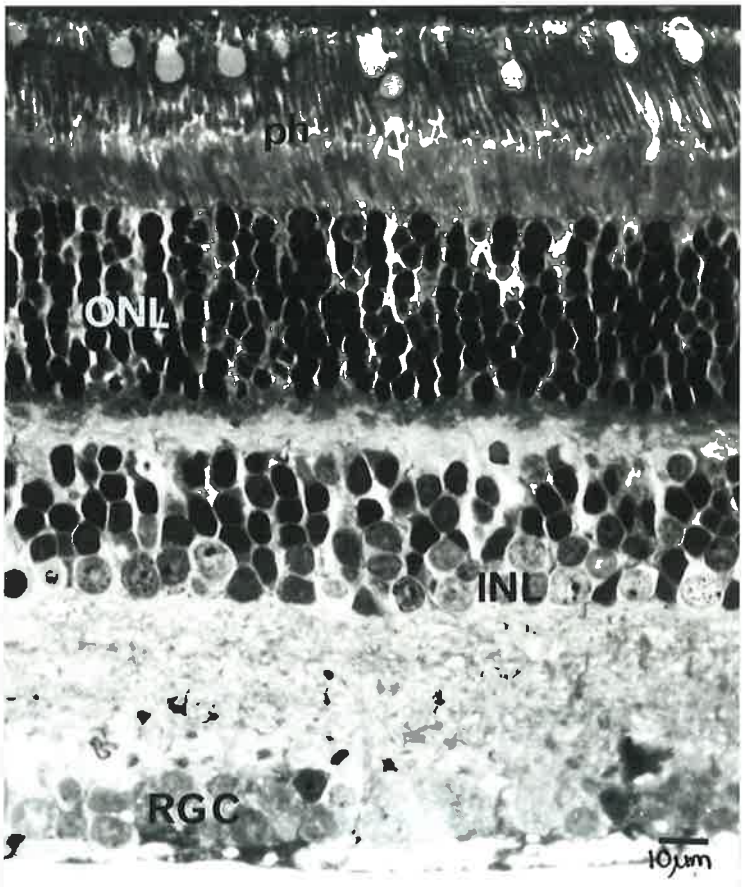

Figure 5.11.1 Outer nuclear layer, Kowari.
Light micrograph of a radial section of central retina showing the columns of photoreceptor cell bodies in the outer nuclear layer (ONL). Photoreceptor layer (ph); inner nuclear layer (INL); retinal ganglion cell layer (RGC),

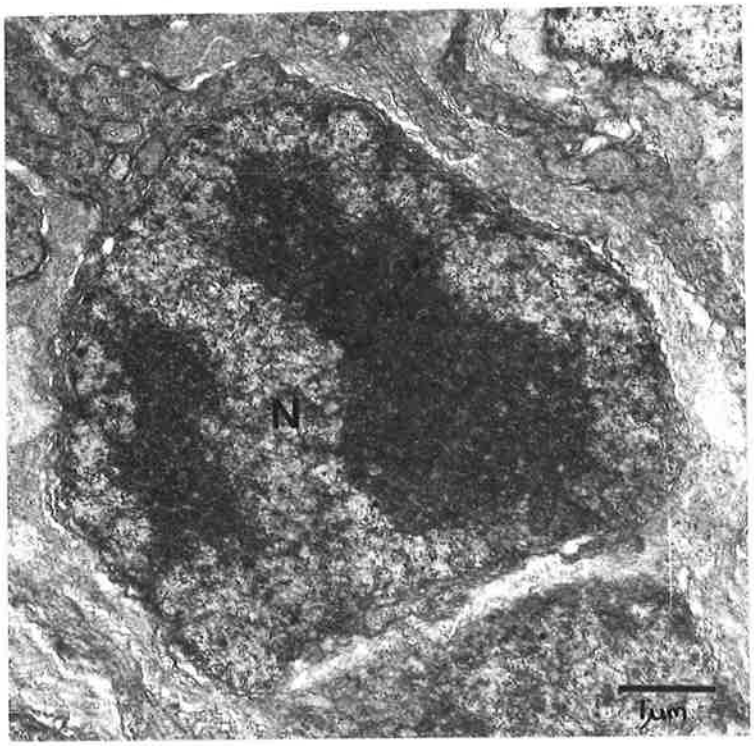

Figure 5.11.2 Outer nuclear layer, Kowari. Electron micrograph of a radial section showing the nucleus (N) of a rod with 2 masses of electron dense chromatin.

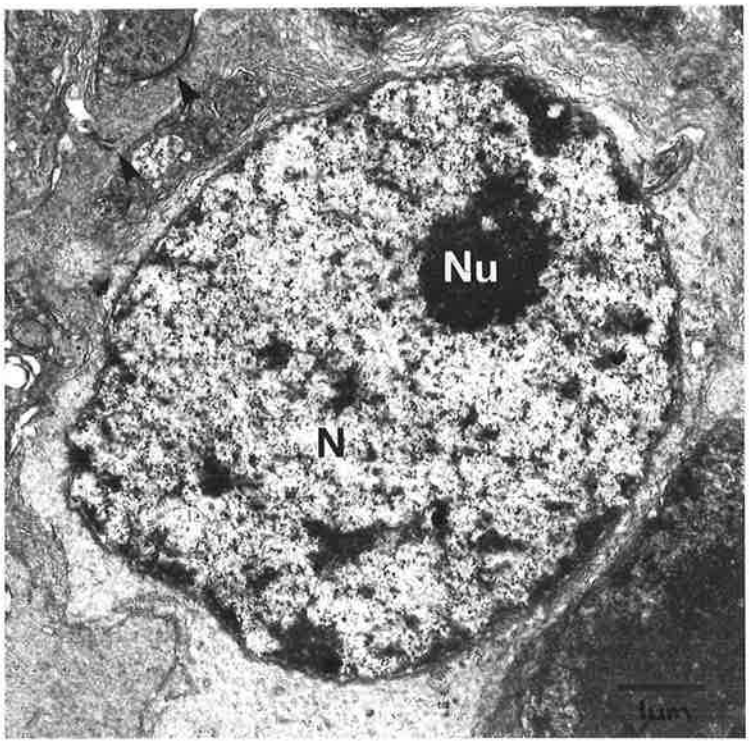

Figure 5.11.3 Outer nuclear layer, Kowari. Electron micrograph showing the nucleus (N) of a cone adjacent the outer limiting membrane (arrows). The nucleus contains a single nucleolus (Nu) and is surrounded by a rim of cytoplasm.

5.12 Outer Plexiform Layer

In the Kowari retina it was possible to see 2 layers within the OPL. Adjacent the photoreceptor cell bodies lies the narrow and denser staining synaptic layer which contains the synaptic portions of the rods and cones. Between this and the INL is the fibrous layer; a wide, pale-staining band containing the dendrites of BC and the processes of HC and MC.

The most numerous synaptic structures of the OPL are the synaptic spherules of the rods. In general, these pre-synaptic terminals are small bulbous dilatations of the inner conducting fibres. However, when the rod nuclei lie along the vitread edge of the ONL no conducting fibres are present and the spherules are directly attached to the cell bodies as sessile synapses. The cytoplasmic matrix of the spherules exhibits moderate electron density, and contains abundant synaptic vesicles measuring 40 nm in diameter. Most of the rod spherules appear to contain 2 closely apposed mitochondria such as those seen in Figure 5.12.1, while the remaining spherules appear to contain only 1 mitochondrion sclerad to the synaptic ribbon. Each spherule contains only 1 synaptic complex, but makes contact with multiple processes which arise from cells of the INL. Characteristic of each spherule is the presence of a single synaptic ribbon located just beneath the pre-synaptic membrane. The ribbon is a flat pentalaminate electron dense structure that is orientated at right angles to the pre-synaptic membrane and is convex toward the cell body as described for the possum and illustrated in Figure 4.12.2. The ribbon is usually surrounded by an aggregate of synaptic vesicles; a narrow

space of cytoplasm intervenes. Lying between the synaptic ribbon and the pre-synaptic membrane is a semitubular, electron dense structure called the arciform density.

The cytoplasmic cleft appears to be wider than the unspecialised intercellular space seen in non-synaptic areas, and associated with the cleft is a thickening of the pre-synaptic membrane. Sometimes the post-synaptic membrane exhibits similar thickening.

The post-synaptic elements of each spherule are probably dendrites from bipolar neurons and HC processes as seen in the primate retina (DOWLING and BOYCOTT, 1966).

Many of the synapses occuring between rods and INL cells have 3 post-synaptic processes, in an arrangement similar to the 'triads' of cone pedicles described in human retina by MISSOTTEN (1965). When this is the case there is 1 central and 2 lateral invaginating processes. The central process ends short of the ribbon and the lateral processes penetrate further into the spherule to end in irregular-shaped dilatations. Occasionally there appears to be 4 invaginating post-synaptic processes.

The synaptic terminals of cone cells are broad conical expansions called pedicles that measure approximately 5.0 μm in diameter and make multiple synapses (see Figures 5.12.4 and 5.12.5). Each pedicle contains about 12 synaptic ribbons, each of which appears to synapse with 3 post-synaptic elements. As in the case of rods these post-synaptic elements belong to HC and BC (see RODIECK, 1973) and appear to synapse in the 'triad' configuration (MISSOTTEN, 1965).

In addition to ribbon synapses cone pedicles make

conventional synapses with cells of both the INL and ONL. Firstly, surface contacts occur between the base of the pedicles and numerous post-synaptic processes. The second group of conventional surface contacts is afforded by the basal filaments, several of which extend from each pedicle at the level of the synaptic ribbons to reach neighbouring rod spherules.

The cytoplasm of the pedicles appears to be less electron dense than that of the spherules because of a lower concentration of synaptic vesicles. Each pedicle contains at least 2 mitochondria lying just sclerad to the synaptic ribbons. These large mitochondria contain closely packed tubular cristae, and usually lie in such close proximity that they appear to be in pairs. Occasionally 1 of these mitochondria contains a membrane-bound packet of 40 to 50 nm granules of variable electron density (see Figure 5.12.6). This may be an enlarged cisterna and the granules resemble β-glycogen (DROCHMANS, 1960).

The fibrous layer of the OPL contains neuronal processes that cross the layer directly or course along it for some distance before synapsing. In vertebrates these processes usually belong to BC and HC (RODIECK, 1973) while the intervening non-neuronal processes belong to MC.

In the Kowari the largest neuronal processes of the OPL lie close to the INL and are distinguished by their low electron density, abundant neurofilaments and few long, thin mitochondria. Where these processes leave the HC somata they contain polyribosomes, RER, and small, non-membrane-bound electron dense inclusions in addition to neurofilaments and mitochondria.

BC dendrites are more difficult to identify but are generally smaller and more electron dense. Furthermore, it has not been possible to distinguish between the dendrites from the 2 types of BC present in the INL (see Section 5.13).

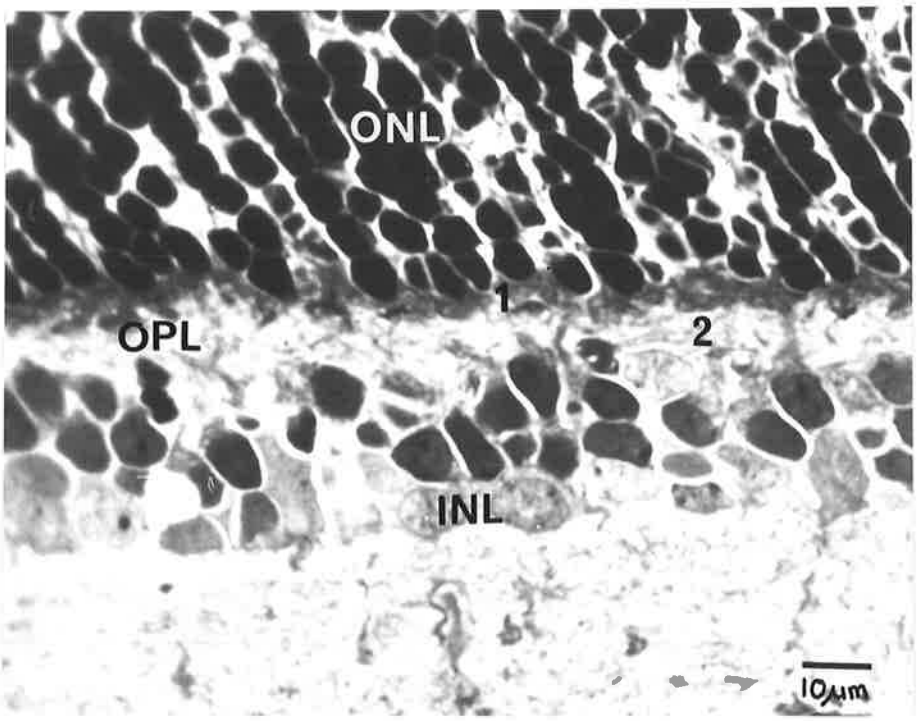

Figure 5.12.1 Outer plexiform layer, Kowari.
A light micrograph of a radial section of Kowari retina showing the synaptic (1) and fibrous (2) layers of the outer plexiform layer (OPL). The outer nuclear layer (ONL) and the inner nuclear layer (INL) are also seen.

Figure 5.12.2 Outer plexiform layer, Kowari.
A radial electron micrograph of a rod synaptic spherule. The large synaptic ribbon and associated arciform density and vesicles (arrows) are seen adjacent 3 post-synaptic processes (1-3).

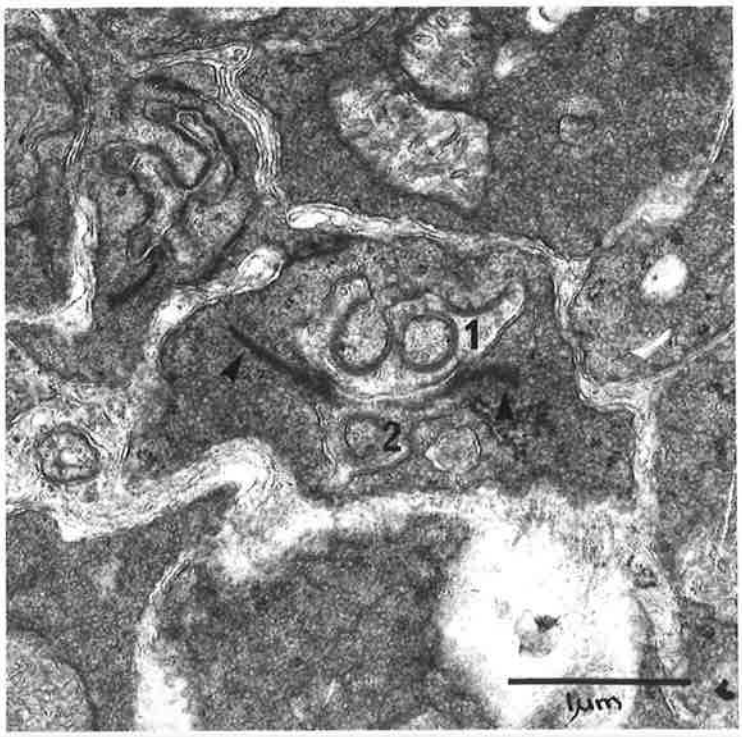

Figure 5.12.3 Outer plexiform layer, Kowari
A tangential electron micrograph of a rod synaptic spherule. Note the large synaptic ribbon (arrows) and irregularly-shaped post-synaptic processes (1 and 2).

Figure 5.12.4 Outer plexiform layer, Kowari. Radial electron micrograph of a cone synaptic pedicle showing numerous ribbons (arrows) and post-synaptic processes. Note the pair of large mitochondria (mi) sclerad to the ribbon complexes.

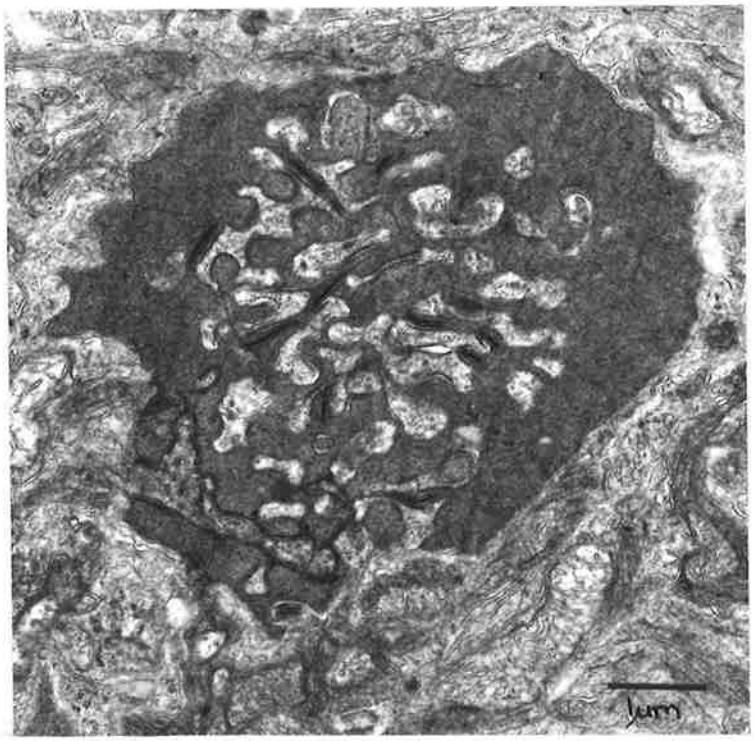

Figure 5.12.5 Outer plexiform layer, Kowari. Tangential electron micrograph of a cone pedicle at the level of the synaptic complexes.

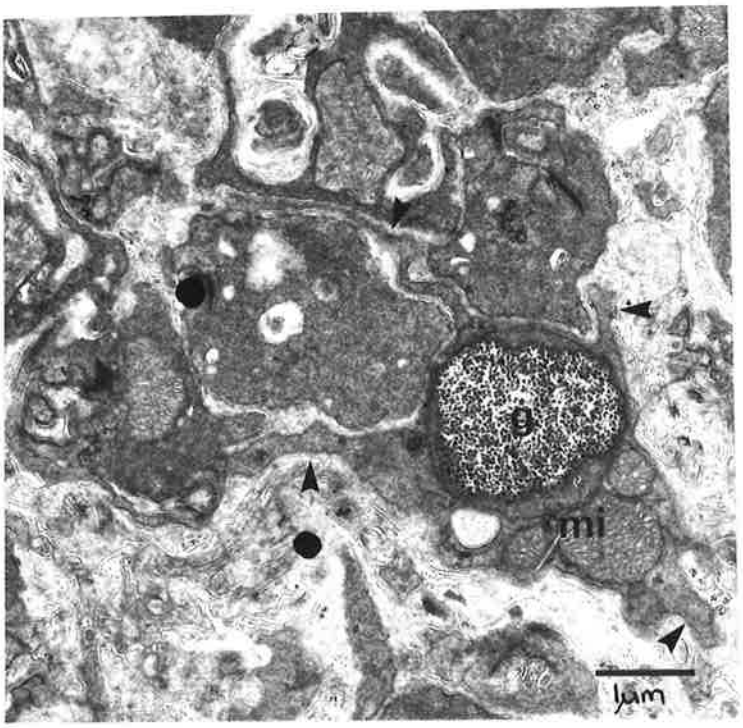

Figure 5.12.5 Outer plexiform layer, Kowari. Electron micrograph of a tangential section showing a cone synaptic pedicle which contains several mitochondria (mi) and has a number of basal filaments (arrows). The most striking feature is the granule-filled enlarged cisternae (g) of a mitochondrion.

5.13 Inner Nuclear Layer

The INL of the Kowari retina contains cell bodies of both neuronal and non-neuronal cells. The neuronal elements are presumably involved in relaying and monitoring information from the photoreceptors. Peripherally the INL comprises 2 to 3 layers of nuclei while centrally it contains 4 to 5 layers (see Figure 5.12.1).

The nuclei of the BC lie in the sclerad half of the INL. This is most clearly evident in tangential 1 µm sections, where the BC are seen as a band of small, round basophilic nuclei of 2 types. The first type, here designated B1, are smaller, stain very densely and appear to have a centrally positioned nucleolus. The second nuclear type (B2) are larger, pale-stainig and show little chromatin clumping, but also appear to have a single nucleolus.

The existence of 2 BC types in the retina of the Kowari was confirmed by electron microscopy where 2 nuclear morphologies are evident (see Figure 5.13.1).

It was difficult to make an association between the light and electron microscopic appearances of these 2 BC types. This was achieved, however, by cutting serial thick and thin sections. By choosing a landmark, such as a capillary, it was possible to compare the appearance of the same cells by light and electron microscopy.

The BC have the most dense nuclei of the INL. The B1 type nuclei possess single, centrally located nucleoli and the chromatin appears as small evenly distributed masses. Whereas the B2 nuclei have a coarse granular appearance, show no clumping of chromatin and often have a single nucleolus. In both cell types the nuclei lie in the vitread part of the

cell body. The sclerad cytoplasm is filled with small round mitochondria but the cytoplasm lateral and vitread to the nucleus contains few.

Despite the occurence of 2 BC nuclear morphologies no difference was found between the cytoplasmic contents. In addition to the numerous mitochondria, the cytoplasm contains Golgi complexes, and a small amount of RER and free polyribosomes.

As the dendritic processes leave the cell body they gradually lose many of the organelles found in the perinuclear cytoplasm and neurofilaments and neurotubules become increasingly abundant.

The presumed HC lie along the sclerad edge of the INL, and can be readily recognised in 1 µm sections by their large granular nuclei of moderate density and their pale-staining cytoplasm. Their large cytoplasmic processes often run through the OPL. The nuclei are roughly elliptical and often show deep invaginations.

The finely granular HC cytoplasm of low electron density contains elongate mitochondria with irregular cristae, scattered polyribosomes, a small amount of RER and abundant neurotubules running along the cytoplasmic processes. There are also small perinuclear Golgi complexes, and the occasional small deposit of moderately electron dense material.

Using the light microscope the AC were identified as the large, rounded, slightly basophilic nuclei that occupy the vitread part of the INL. They have a small, eccentrically placed nucleolus and a rim of pale-staining cytoplasm. Occasionally cells resembling the AC were seen

displaced in the IPL.

Electron microscopy has shown that the nuclei of these presumptive AC are unremarkable. They are moderately electron dense, and contain evenly distributed granular chromatin with some clumping beneath the nuclear envelope. The perinuclear cytoplasm is densely packed with organelles including abundant small mitochondria, a moderate amount of RER, and Golgi complexes. In addition there are numerous free polyribosomes and a few membrane-bound inclusions of moderate electron density and slightly granular appearance. In some examples a few neurofilaments were present.

MC are the non-neuronal supportive elements of the retina; their nuclei generally lie in the vitread half of the INL. In radial sections their cell bodies have an irregular, elongate profile, while in tangential sections they present a roughly circular cross-section. Clearly their shape is determined by the packing of the other cell bodies in the INL; MC fill the spaces left by the other cells.

Within the INL the MC may be identified by the presence of thin, laterally projecting cytoplasmic processes which run for several um between neighbouring cell bodies.

The cytoplasm of the MC somata appears moderately electron dense and contains few organelles. The long processes extending through the IPL also has moderately dense cytoplasm, granular in appearance. They are more electron dense than the surrounding processes and contain abundant microtubules running parallel to the longitudinal axis of the cell. Occasionally elongate mitochondria with tubular cristae occur within the MC proceeses.

Finer processes branch from these radial processes and

run between the neuronal processes of the IPL. These processes have the same cytoplasmic structure but lack mitochondria.

MC extend sclerally through the OPL and ONL to reach the OLM. These outer processes are narrow and difficult to identify in radial sections. They have a granular cytoplasm similar to that of the inner processes. When these processes reach the OLM they form conical dilatations containing mitochondria. Beyond the OLM the MC give rise to numerous microvilli thatextend into the ventricular space and run between the photoreceptor inner segments.

At the vitread border of the retina the MC processes expand to form terminal dilatations that surround the RGCs and NFL, and contribute to the ILM. The cytoplasm of these terminals resembles that of the large inner processes. No specialised cell contacts were seen between the MC along the vitread border of the retina.

The nuclei of the MC take the shape of the cell bodies, although they often have a long, narrow invagination. By electron microscopy these nuclei appear less dense than those of the INL neurons. The finely granular chromatin is evenly distributed and a single nucleolus is usually present.

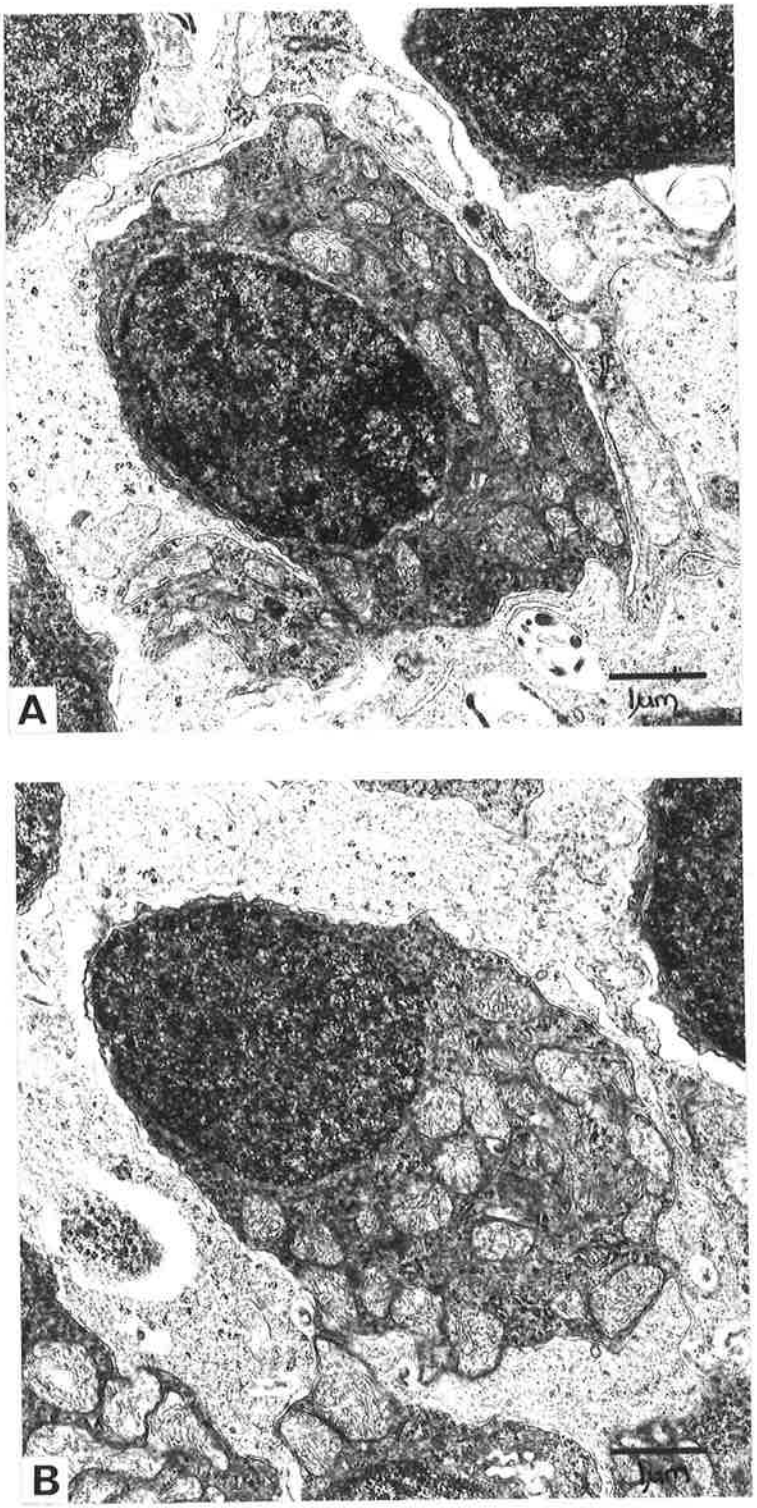

Figure 5.13.1 Inner nuclear layer, Kowari.
Electron micrographs showing the 2 types of bipolar neurons in the retina.
A. A B1 bipolar cell showing moderate clumping of chromatin.
B. A B2 bipolar cell with evenly distributed chromatin

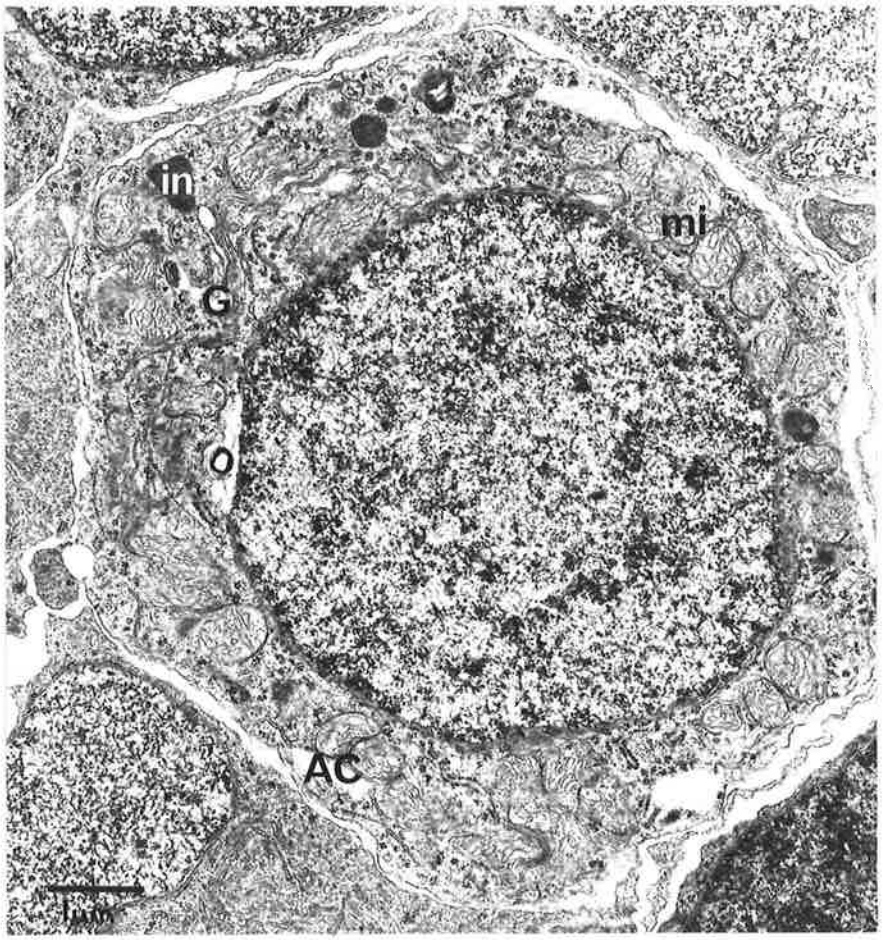

Figure 5.13.2 Inner nuclear layer, Kowari. Electron micrograph of a presumptive amacrine cell (AC). The cytoplasm contains moderately electron dense inclusions (in), mitochondria (mi), small Golgi complexes (G) and abundant polyribosomes.

5.14 Inner Plexiform Layer

The IPL is a wide band of low electron density consisting of various neuronal processes and the inner processes of MC. This layer is not well resolved at the light microscopic level, and its ultrastructure is difficult to interpret.

The BC and AC of the INL contribute axons and processes respectively, while the RGCs contribute dendrites to this layer (RODIECK,1973). It was not possible to distinguish between these 3 types of processes using the electron microscope because of the difficulty of tracing processes back to their cell bodies. However, it seems reasonable to assume that the large processes seen adjacent the RGCs arise from these cells, and that the smaller processes adjacent the INL are mainly BC and AC processes. On the other hand, MC processes were easily identified by virtue of their greater electron density and microtubule-filled cytoplasm.

As in other vertebrates such as the monkey (DOWLING and BOYCOTT, 1966) the structures most readily identified in the IPL are the bipolar synapses. These large structures, such as that seen in Figure 5.14.1, appear to occur more frequently in the outer 2 thirds of the IPL. They contain large numbers of evenly distributed vesicles of 40 to 50 nm diameter, a few mitochondria and small synaptic ribbons lying close to and at right angles to the pre-synaptic membrane. Positioned between the ribbon and the cell membrane there is a small semi-tubular structure of high electron density like the arciform density of the visual cell synapses. An elliptical array of synaptic vesicles surrounds each ribbon.

The synaptic cleft is V-shaped, with its point toward

the post-synaptic elements, and measures approximately 25 nm across. Small aggregations of electron dense cytoplasmic material lie adjacent the thickened post-synaptic membranes.

Each of the 2 post-synaptic elements contains fewer vesicles than the bipolar terminal (see Figure 5.14.1). Some planes of section show 1 of these post-synaptic processes making a reciprocal synapse, of a conventional nature, with the bipolar terminal. DOWLING and BOYCOTT (1966) refer to this axodendritic arrangement as a 'dyad'. They identify the 2 post-synaptic elements as being a RGC dendrite and an AC process. The AC process is thought to make the reciprocal synapse.

Several other types of synapses are known to occur in the mammalian IPL (DOWLING and BOYCOTT, 1966). In the Kowari retina conventional synapses occur throughout the IPL, but it was not possible to identify the processes involved. The pre-synaptic processes which presumably belong to BC and AC contain numerous synaptic vesicles, some of which fuse with the pre-synaptic membrane. Thickening of the pre- and post-synaptic membranes is usually evident, and the synaptic cleft measures 25 nm wide.

Intercellular contacts without evidence of synaptic specialisation were often seen between the processes of this complex layer.

That portion of the IPL immediately adjacent the INL appears to be free of synapses and at the light microscopic level level appears pale-staining and amorphous (see Figure 5.14.2).

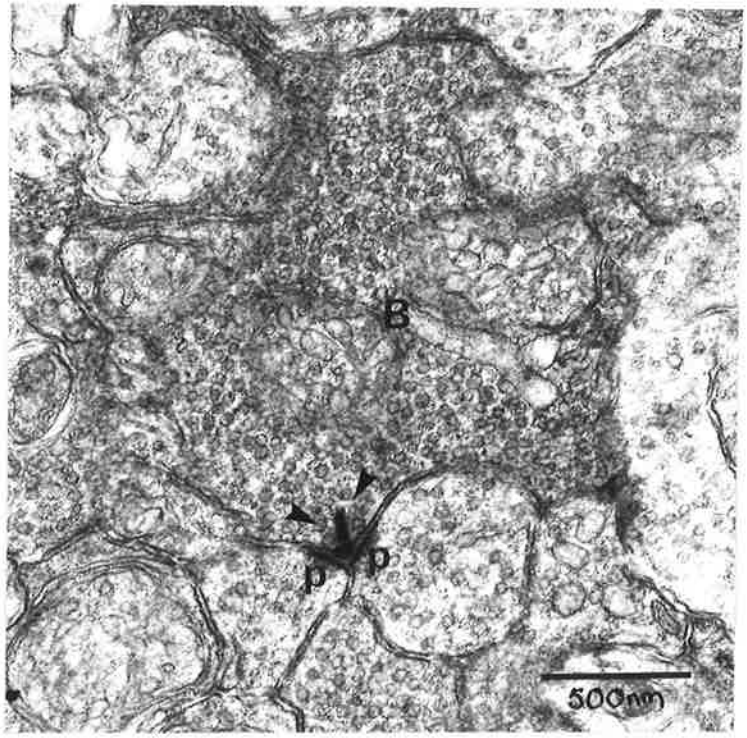

Figure 5.14.1 Inner plexiform layer, Kowari. Electron micrograph of a bipolar synapse (B). Note the small electron dense ribbon and arciform density (arrows) and thickening of the post-synaptic membranes (p).

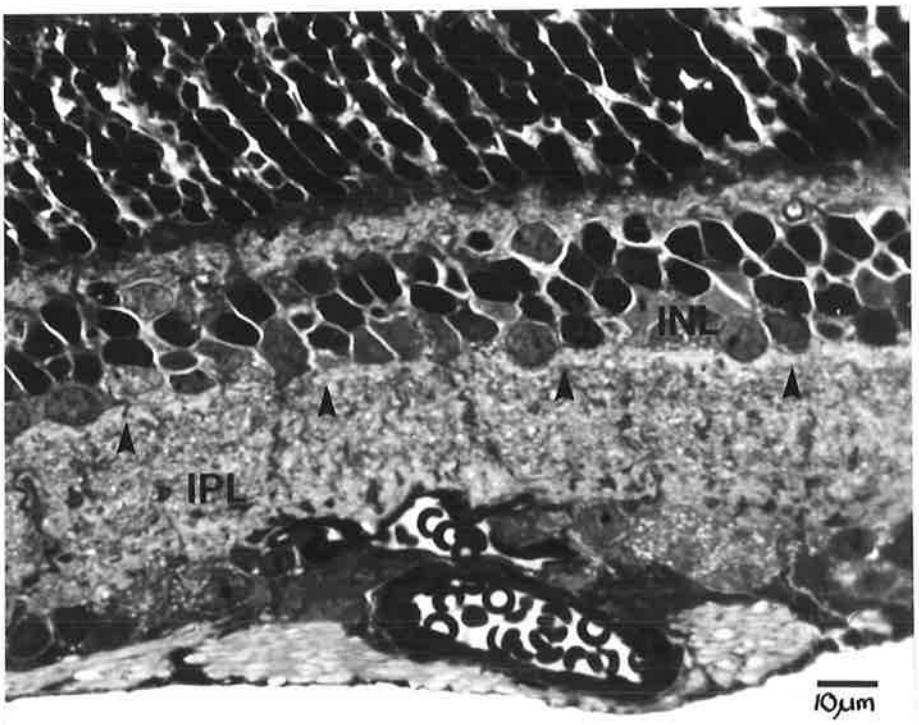

Figure 5.14.2 Inner plexiform layer, Kowari. Light micrograph of a polychrome-stained section showing the pale-staining band (arrows) of the inner plexiform layer (IPL) lying adjacent the inner nuclear layer (INL).

5.15 Retinal Ganglion Cell Layer

In the Kowari retina the RGCs form the most vitread layer of neuronal cell bodies; being separated from the ILM by only the optic nerve fibres.

Using electron microscopy the pale-staining cytoplasm of the RGCs was found to contain numerous small, round mitochondria approximately 1.0 µm in diameter, abundant polyribosomes and RER, and a few moderately electron dense membrane-bound inclusions.

At both the light and electron microscopic levels 2 distinct nuclear morphologies are evident within the RGC population of the Kowari. In general the nuclei of the larger RGCs are eccentric and occupy approximately half of the cell's cross-sectional area and possess coarse, granular chromatin showing minimal clumping and a pale central region. These nuclei, which are often invaginated, each possess a large dense nucleolus. The nuclei of the smaller RGCs are usually invaginated and possess evenly distributed, fine granular chromatin. In cells exhibiting this second nuclear morphology the nucleus occupies more than half of the cell's cross-sectional area.

Using HUGHES' (1975a) criteria the RGC population of the Kowari was found to consist of RGC whose diameter ranges from 4.0 to 26.0 µm (see Figure 5.15.1). The largest α-cells measure from 20.0 to 26.0 um and constitute 3.0% of the total population. β-cells measure from 12.0 to 20.0 µm and make up 20.0% of the population. While the smallest cells, γ-cells, range in diameter from 4.0 to 12.0 µm and make up 77.0% of the population. The larger and more irregularly shaped cells of each group were found in the periphery while the central

retina contains smaller, more rounded cells.

A preliminary study was carried out on the distribution of RGCs in the Kowari using 4 Nissl-stained wholemounts. Counts (cells/mm^2) were made on the central retina around the optic disc and the peripheral retina, and along the horizon as shown in Figure 5.15.2. In general the peripheral counts are lower than the central counts and the central counts slightly lower than those along the horizon (see Figure 5.15.2) and counts above the horizon are higher than counts below the horizon suggesting the presence of a visual streak lying superior to the optic disc. The high RGC counts superior to the horizon suggest a greater visual acuity which may be relevant to the prey-catching activity ot the Kowari as this part of the retina receives an image of the area immediately below the animal's visual horizon.

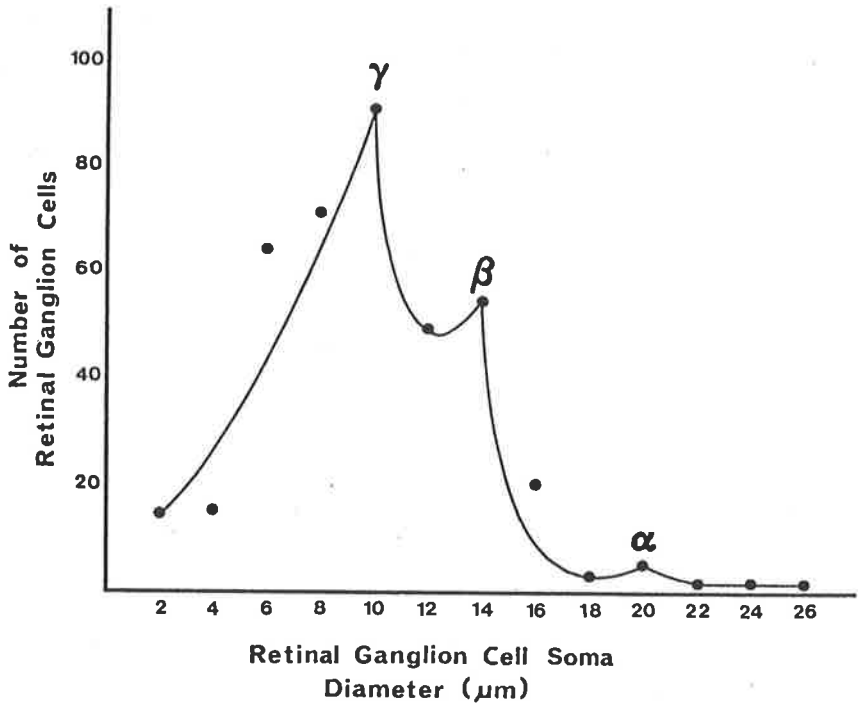

Figure 5.15.1 Retinal ganglion cell soma diameter, Kowari. Graph showing the spread of soma diameter among the population of retinal ganglion cells. The α, β and γ indicate the peaks within each of the 3 cell types. Sample size = 377 cells.

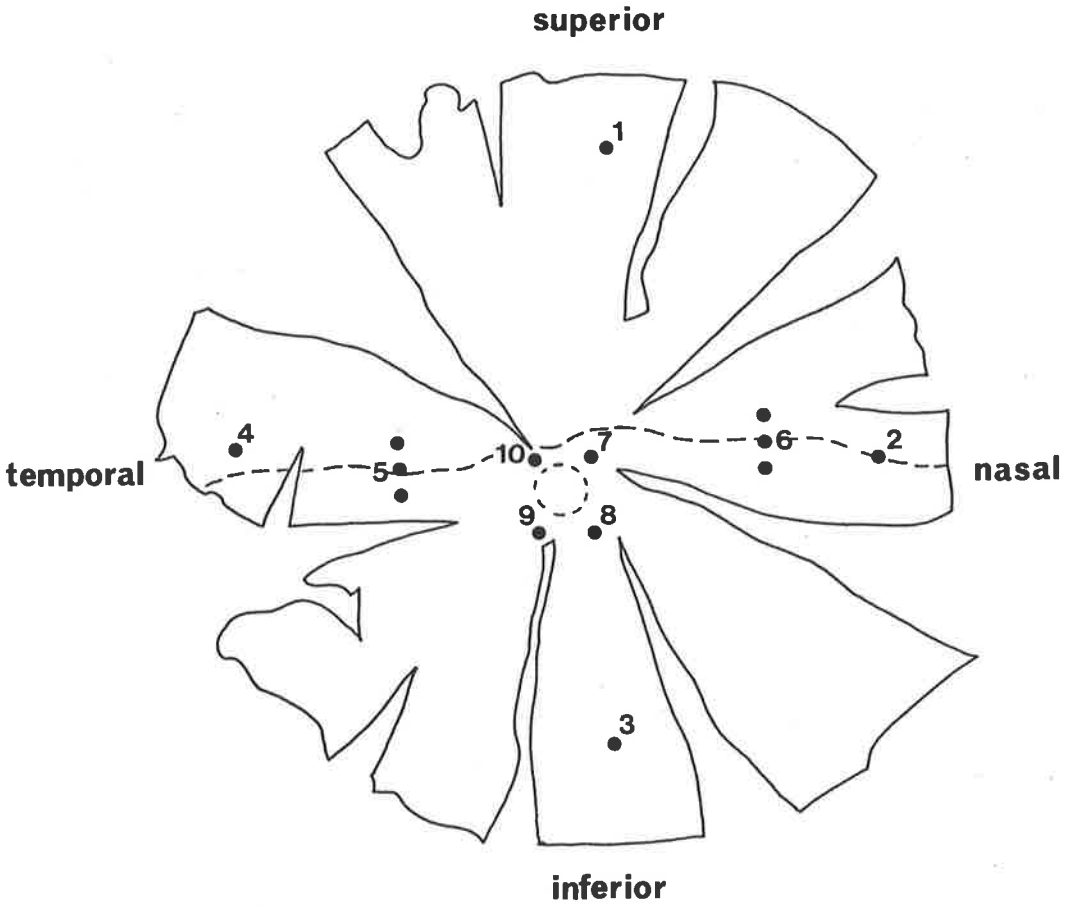

Figure 5.15.2 Retinal wholemount, Kowari.
Map of a retinal wholemount prepared using a camera lucida showing the positions (1-10) in which the density of retinal ganglion cells was counted.

5.16 Optic Nerve Fibre Layer

The NFL consists of axons that arise from the RGCs and run radially along the vitread edge of the retina to converge at the optic disc where they leave the eye to contribute to the optic nerve.

The size of the fibres varies between 0.2 and 2.5 μm in diameter. All the fibres exhibit the same structural characteristics despite the variation in size. They generally contain a large number of neurotubules running along the fibre, fewer neurofilaments, and a few small mitochondria with tubular cristae. The axoplasm itself shows low electron density.

In sections cut such that the nerve fibres appear in cross-section it is possible to see that they occur in bundles surrounded by MC processes.

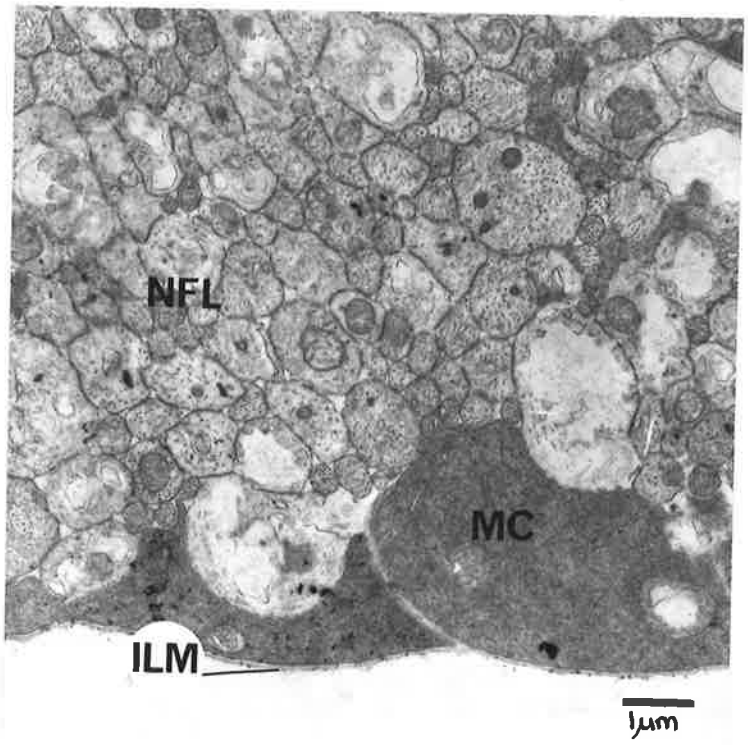

Figure 5.16.1 Optic nerve fibre layer, Kowari. Electron micrograph of a section showing the variation in axon diameter within the nerve fibre layer (NFL). The inner terminal expansions of Müller cells (MC) can be seen adjacent the inner limiting membrane (ILM).

5.17 Inner Limiting Membrane

The ILM separates the retina from the vitreous. In the Kowari the ILM comprises a 50 nm thick basement membrane belonging to the MC. This basement membrane is not seen with the light microscope as it is below the level of resolution. Vitreous fibrils also contribute to the ILM by inserting into the vitread surface of the basement membrane (see Figure 5.17.1).

The vitread surface of the ILM is smooth while the sclerad surface follows the contours of the apposing MC terminals. The MC terminals which form the inner surface of the retina proper, are separated from their basement membrane by a narrow space of 25 nm which is evident in Figure 5.17.1.

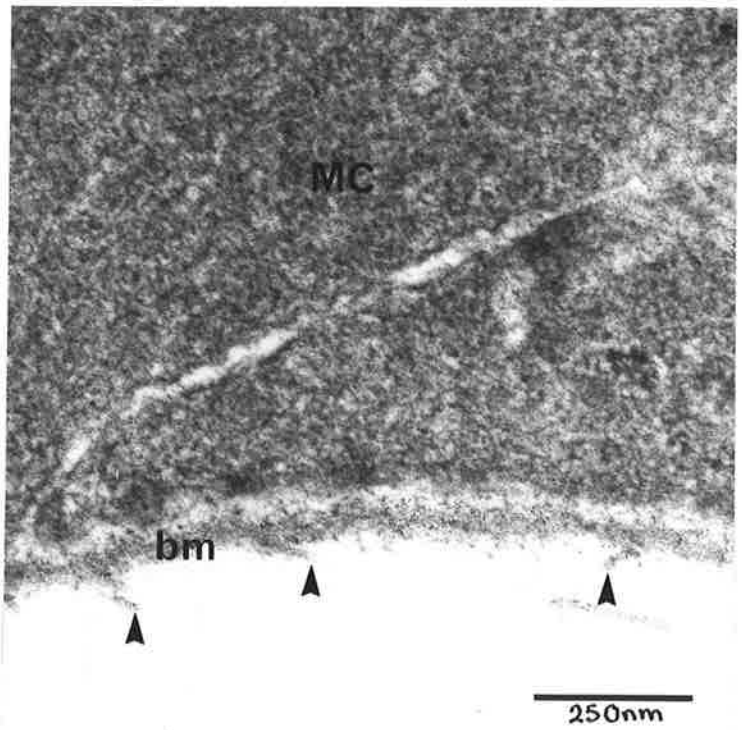

Figure 5.17.1 Inner limiting membrane, Kowari.
A high power electron micrograph showing the 25 nm separation of the basement membrane (bm) from the Müller cell terminals (MC). Vitreous fibrils (arrows) can be seen inserting into the basement membrane.

6 RETINAL ANATOMY OF THE KANGATOO ISLAND KANGAROO

6.1 Eyecup

The formalin-fixed eyecup of the Kangaroo Island kangaroo is grey in both the superior and inferior fundus with a more dense white line that demarcates an horizon superior to the optic disc (see Fig. 6.1.1). The retina is transluscent allowing the pigmentation of the choroid to be seen clearly. No tapetum lucidum was seen in the superior fundus. Fibres of the NFL converge toward the optic disc which lies in the inferotemporal quadrant of the eyecup.

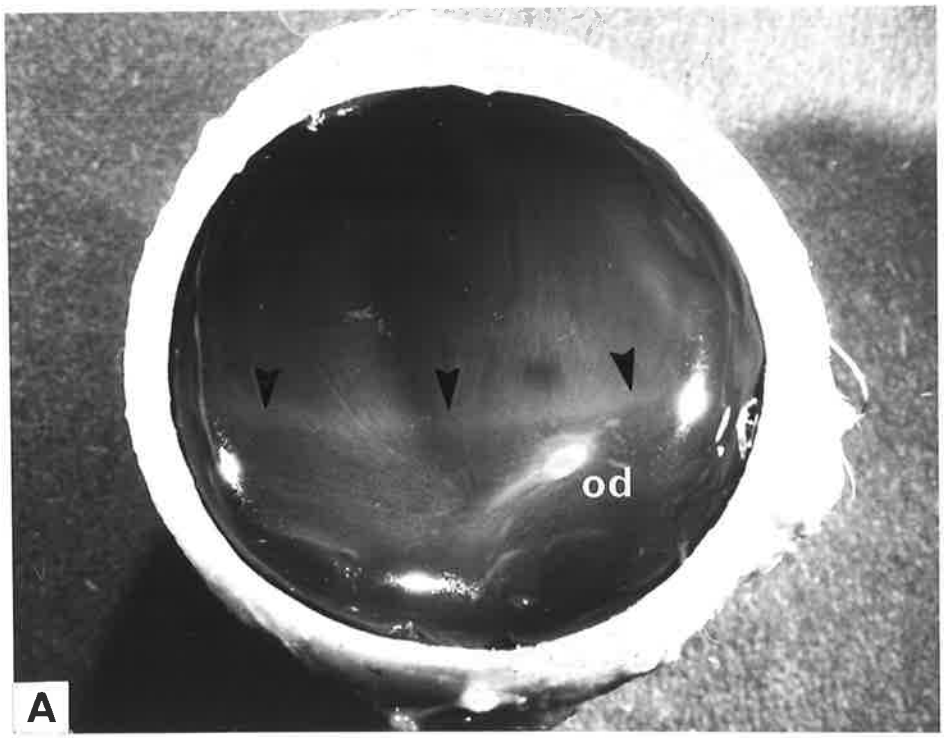

B

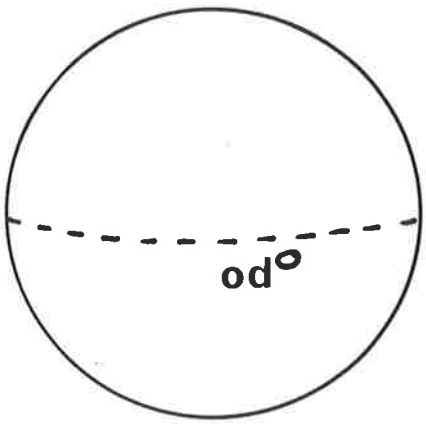

Figure 6.1.1. Eyecup, kangaroo.
A. Macro-photograph of a formalin-fixed left eyecup showing the optic disc (od) lying in the inferior-temporal quadrant, horizon (arrows) and the evenly transluscent retina of the fundus.
B. Schematic diagram of the kangaroo fundus.

6.2 Choroid

The choroid of the Kangaroo Island kangaroo contains large flattened melanocytes which contain electron dense pigment granules. These granules are membrane-bound, lack any internal ultrastructure and are usually seen as round to elliptical cross-sections that measure from 0.17 to 0.88 µm. Moderate numbers of small, round profiles of mitochondria, approximately 0.5 µm in diameter, are also present.

The layers of melanocytes are separated by dense layers of randomly arranged fibres which exhibit the 64 nm periodicity typical of collagen and stain intensely pink in 1.0 µm polychrome-stained orientation sections.

The layered arrangement of the melanocytes and fibres of the choroid is evident in Figure 6.2.1.

Occasionally cross-sections of small nerves surrounded by collagen fibres are seen. These bundles contain myelinated nerve fibres measuring from 0.6 to 2.0 µm in diameter. The axoplasm is of low electron density, contains numerous microtubules and small (0.1 µm diameter), electron dense granules.

The capillaries of the choriocapillaris lie vitread within the choroid immediately adjacent BM. The structure of the endothelial cells of these capillaries is typical with the exception of pores adjacent BM (see Section 6.3).

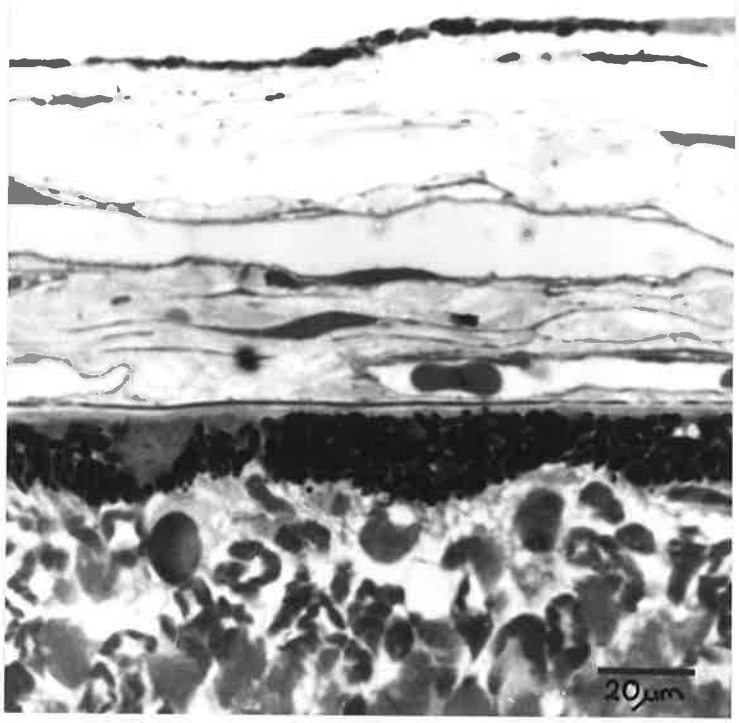

Figure 6.2.1. Choroid, kangaroo.
Light micrograph of a polychrome-stained radial section showing the layered arrangement of the choroid.

6.3 Bruch's Membrane

In the kangaroo, as in other vertebrates, BM lies sclerad to the retina and separates the RPE from the choriocapillaris of the choroid (see Figure 6.3.1).

The most vitread layer of this pentalaminate structure is the basement membrane of the RPE which follows the curvature of the eyeball but not the contours of the basal folding of the RPE cell membranes. This typical basement membrane measures 50 nm in thickness and is separated from the RPE cells by a narrow (25 nm) space of low electron density.

Immediately sclerad to this basement membrane is the inner collagen layer which measures 0.3 μm across and contains randomly orientated fibres, with the same 64 nm periodicity as collagen, scattered throughout a matrix of low electron density. These fibres stain deeply with basic fuchsin in polychrome-stained sections.

The middle elastic layer of BM measures approximately 0.25 μm in thickness and by electron microscopy appears as an electron dense layer which is interrupted at irregular intervals by pores through which collagen fibres pass. The fibres of this layer are arranged randomly, stain deeply blue with the polychrome stain and black with orcein in paraffin sections.

Lying immediately sclerad to the middle elastic layer is a 0.3 μm thick layer, called the outer collagen layer.

The most sclerad layer of BM is the basement membrane of the endothelial cells of the choriocapillaris, which measures 70 nm in thickness and is separated from the endothelial cells by a 25 nm space of low electron density.

The endothelial cell wall adjacent BM shows numerous pores, each of which measures 80 nm in diameter and has a central electron density (see Figure 6.3.2).

Where there are no capillaries adjacent BM the outer collagen layer appears to merge with the collagen of the choroid, as shown in Figure 6.4.1.

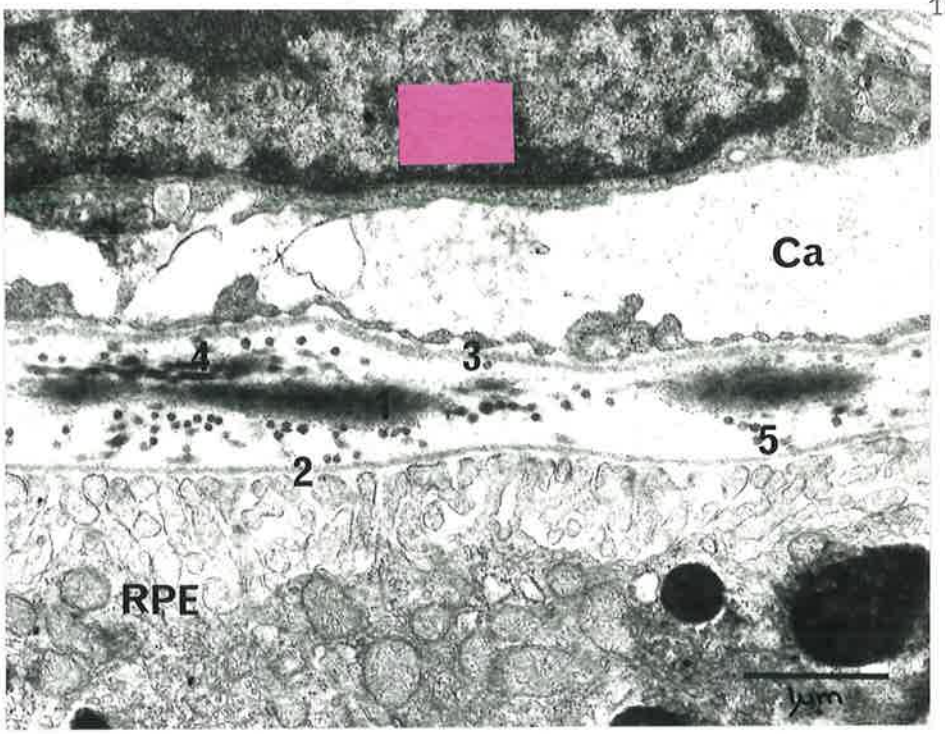

Figure 6.3.1. Bruch's membrane, kangaroo.
Bruch's membrane contains a central layer of elastic fibres (1) separated from basement membranes of RPE (2) and choriocapillaris (3) by a space containing collagen fibres (4 and 5). Retinal pigmented epithelium (RPE); capillary of the choriocapillaris (Ca).

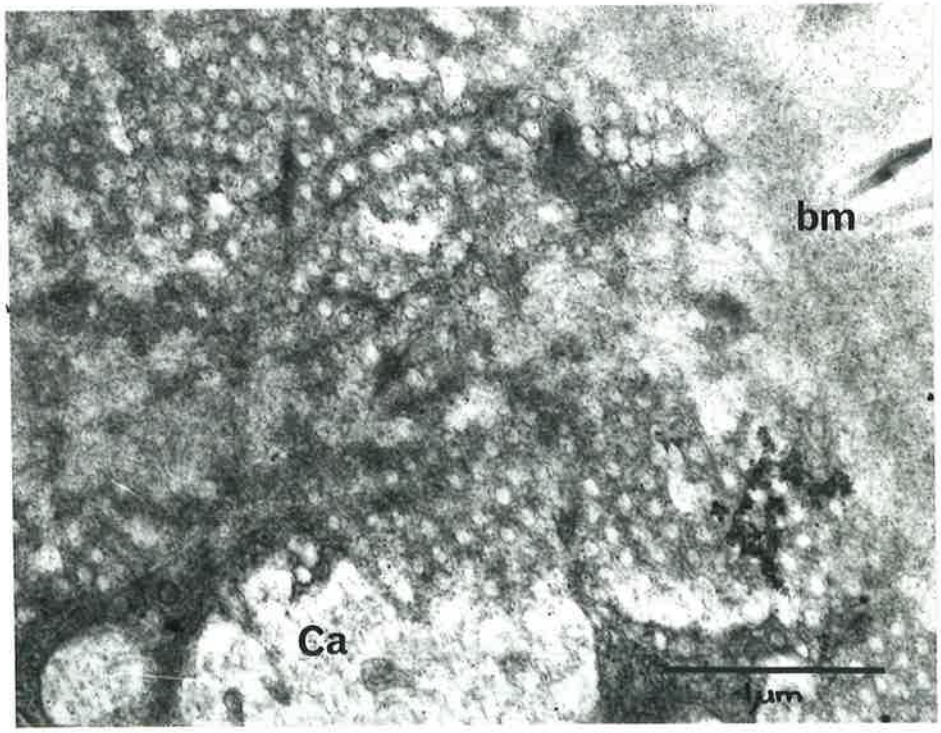

Figure 6.3.2. Bruch's membrane, kangaroo.
Tangential electron micrograph showing the circular pores with central densities in the endothelial cells of the choriocapillaris adjacent Bruch's membrane. The lumen of the capillary (Ca) lies sclerad to the fenestrated endothelial cell. The basement membrane (bm) of the endothelial cell forms part of Bruch's membrane.

6.4 Retinal Pigmented Epithelium

The RPE of the kangaroo consists of a single layer of epithelial cells lying immediately sclerad to the neuroretina, and separated from the choroid by BM, as shown in Figure 6.4.1.

In radially cut sections the cells of the RPE appear oblong measuring only 4.0 to 5.0 μm in height. While in tangential sections they appear polygonal, mostly hexagonal, and have an average diameter of 30.0 μm (see Figure 6.4.2). The basal cell membrane of these cells shows extensive infolding, as seen in Figure 6.4.1, which extends 0.5 μm into the cytoplasm. The basal cytoplasm adjacent the membranous infolding contains numerous mitochondria measuring 0.2 μm in diameter and up to 2.0 μm in length. Membrane-bound droplets, such as those seen in Figure 6.4.3, which measure from 1.3 to 1.6 μm in diameter and stain with osmium tetroxide in fresh tissue but remain unstained in polychrome-stained 1 μm sections are also present.

Moderate numbers of large elliptical or spindle-shaped granules, measuring approximately 0.6 μm in diameter and up to 2.0 μm in length, generally occur in the apical cytoplasm of the RPE cells but may also be found basally. These highly electron dense granules are bound by a single membrane, show no internal ultrastructure, appear brown in unstained sections and are regarded as melanin. Arising from the apical portion of the RPE cells are numerous microvillous processes which extend for several um into the ventricular space where they surround the photoreceptor outer segments (see Figure 6.4.4).

Large disc-shaped nuclei, such as those seen in Figure

6.4.2, are typical of the RPE cells of the Kangaroo Island kangaroo. They appear oval in radial sections, measuring approximately 5.0 µm across and up to 8.0 µm in length, and circular in tangential sections with a diameter of about 8.0 µm. They are moderately electron dense, have vesicular chromatin and usually possess a single nucleolus. In no instances were any RPE cells seen to contain more than one nucleus.

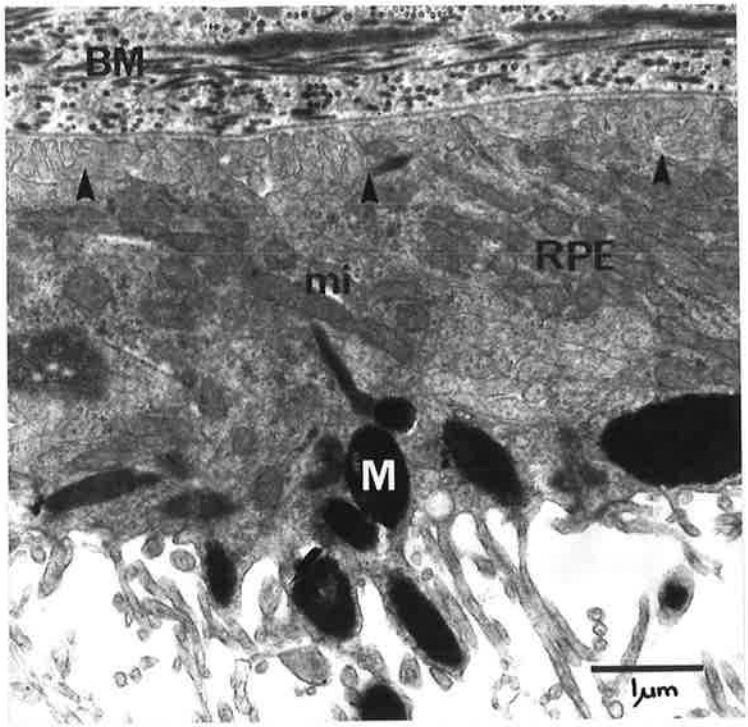

Figure 6.4.1. Retinal pigmented epithelium, kangaroo.
The retinal pigmented epithelium (RPE) lies immediately sclerad to Bruch's membrane (BM). The RPE cells contain numerous mitochondria (mi) and large melanin granules (M). Infolding of the basal cell membrane (arrows) and apical microvilli are also evident.

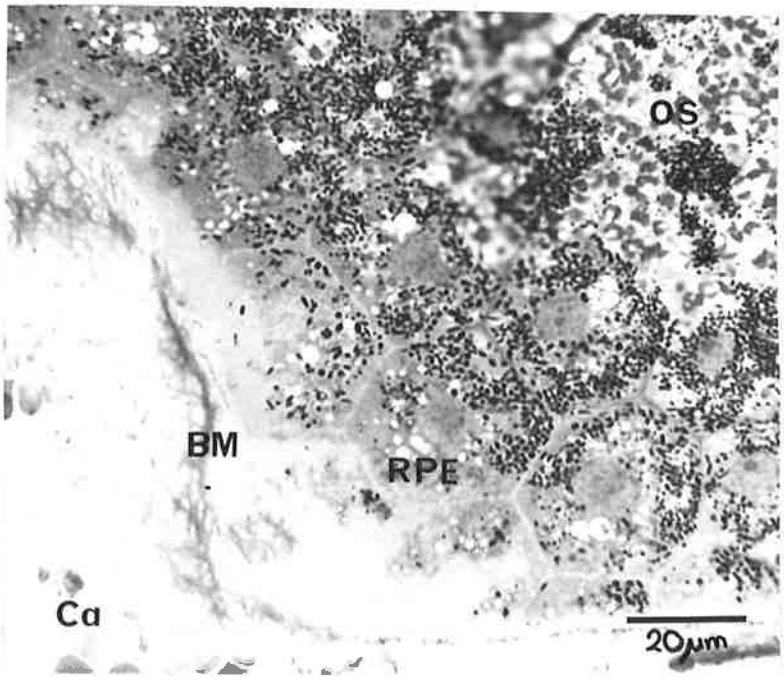

Figure 6.4.2. Retinal pigmented epithelium, kangaroo.
In tangentially orientated sections the cells of the retinal pigmented epithelium (RPE) are polygonal in outline as seen in this light micrograph. Capillary of the choriocapillaris (Ca); Bruch's memhbrane (BM); photoreceptor outer segments (OS).

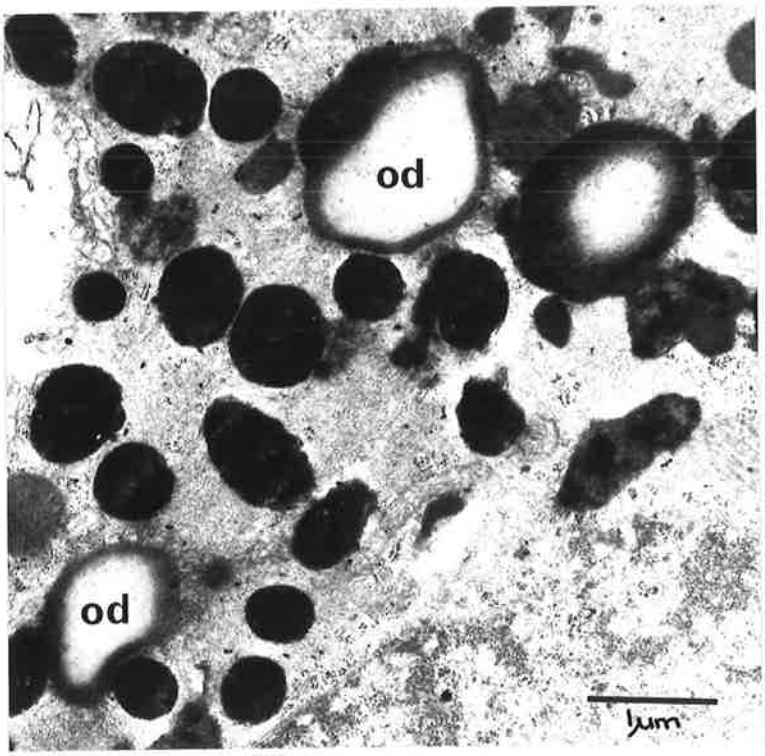

Figure 6.4.3. Retinal pigmented epithelium, kangaroo.
Electron micrograph showing the membrane-bound droplets (od) of the retinal pigmented epithelium.

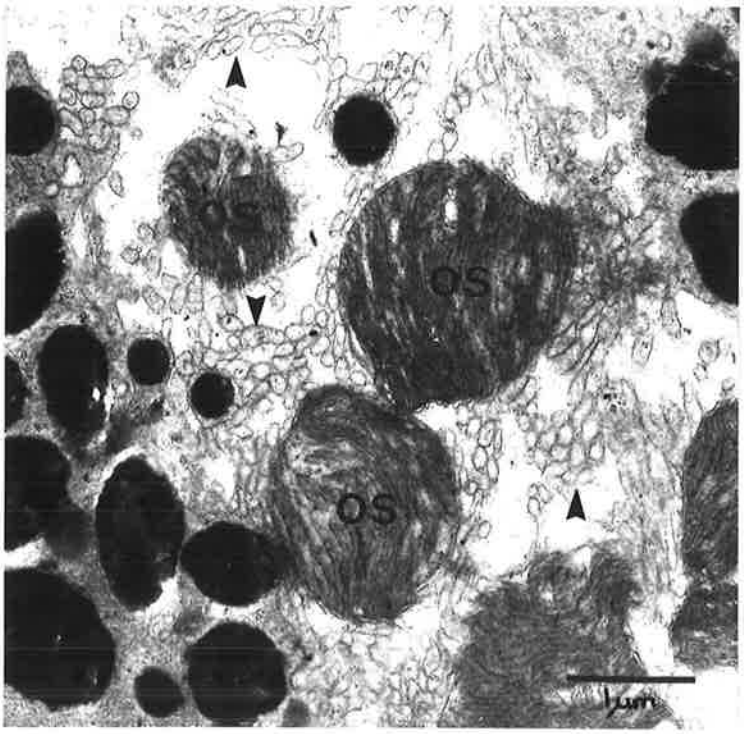

Figure 6.4.4. Retinal pigmented epithelium, kangaroo.
As seen in this tangential electron micrograph the apical microvilli (arrows) of the retinal pigmented epithelial cells surround the photoreceptor outer segments (OS),

6.5 Rod Outer Segments

The ROS, which are cylindrical in shape, extend from their connections with the inner segments to the apical microvillous processes of the RPE with which they make contact. They measure approximately 13.0 μm in length, and 2.0 μm in diameter, and contain large numbers of membranous discs stacked at right angles to the longitudinal axis.

The ROS discs are flattened sacs, the two parallel membranes of which are continuous with one another at a circumferential dilatation. In radially sectioned material these discs are separated by an interdisc space which is wider and less electron dense than the intradisc space. These discs are roughly circular in cross-section, have a smooth outline and do not appear to contact the surrounding cell membrane. In cross-sections, such as shown in Figure 6.5.1, a single incisure is usually seen extending into the disc and it corresponds to the position of the connective ciliary stalk.

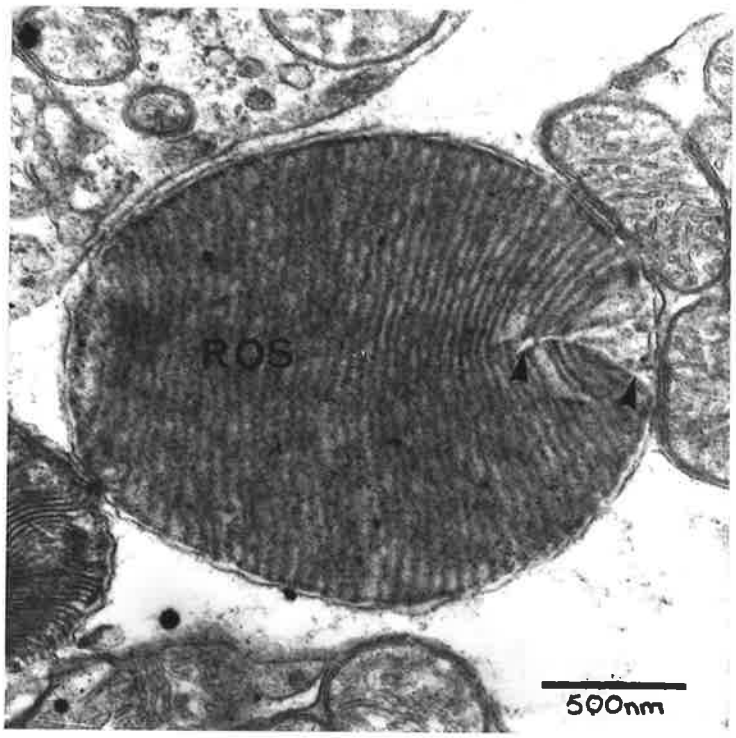

Figure 6.5.1. Rod outer segments, kangaroo.
The central figure in this tangential electron micrograph is a cross-section through a rod outer segment (ROS) showing the disc with its single incisure (arrow).

6.6 Rod Ciliary Stalk

Attaching each ROS to its inner segment is a modified ciliary stalk. This connective structure, which measures approximately 2.0 μm in length and 0.3 μm in diameter, arises from a basal body, or primary centriole, in the apical region of the RIS as seen in Figure 6.6.1.

The primary centriole is a short cylindrical structure made from 9 peripheral microtubular triplets each of which comprises 1 complete and 2 incomplete microtubules. Extending from the centriole in radial fashion are short electron dense tufts. The variation in the number of these tufts may be due to the obliquity of the plane of section. In none of the sections examined, radial or tangential, were any secondary centrioles associated with the ciliary stalks seen.

Each ciliary stalk lies in a niche at the apical end of the RIS and has the '9+0' structure typical of sensory cilia. The cylindrical framework consists of 9 microtubular doublets (see Figure 6.6.2) each of which is made of 1 complete and 1 incomplete microtubule. No central pair of microtubules is present. The cytoplasm within the cylinder of doublets is less electron dense than that peripheral to them.

Electron microscopy of tangential sections showed that the ciliary stalk is not simply circular in cross-section. As seen in Figure 6.6.2 there is an outward notch or thickening of the cell membrane adjacent each microtubular doublet indicating the presence of longitudinal ridges.

Typically 2 calycal processes lie adjacent and peripheral to each stalk (see Figure 6.6.2). However, up to

5 calycal processes have been found peripheral to the apical portion of the RIS. These narrow finger-like processes extend from the apical region of the RIS along the stalk and approximately half of the ROS.

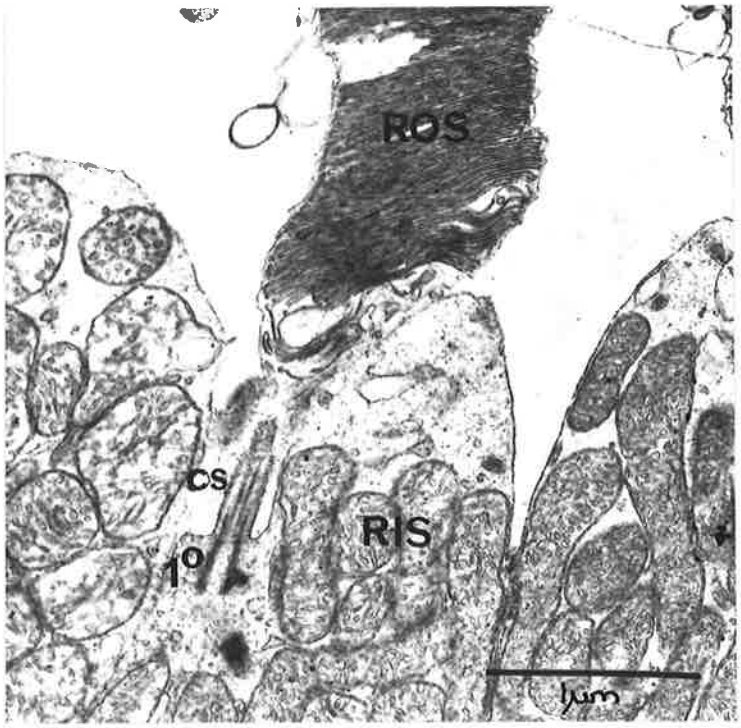

Figure 6.6.1. Rod ciliary region, kangaroo.
A radial electron micrograph showing the ciliary stalk (cs) that connects the rod inner segment (RIS) to its outer segment (ROS). The primary centriole (1^{o}) can be seen in the inner segment.

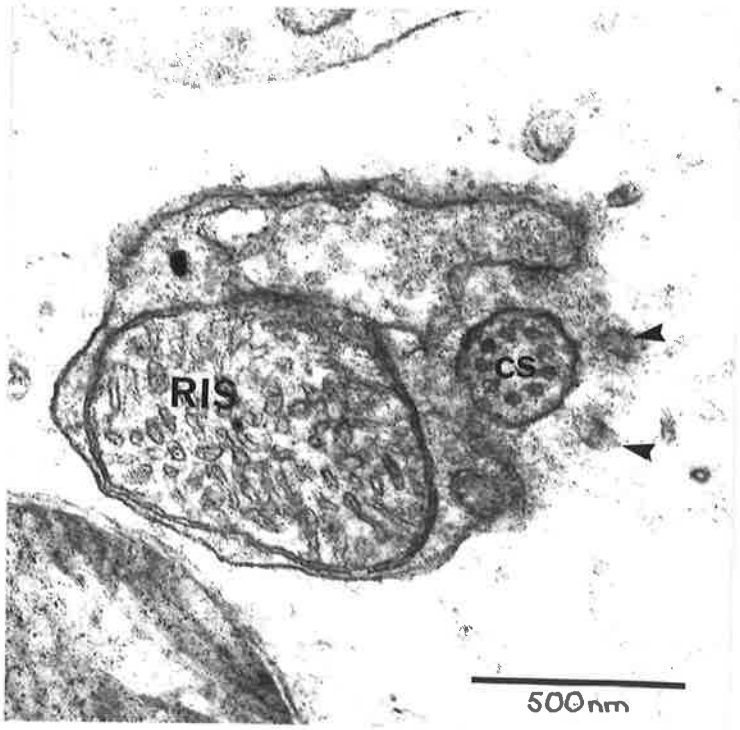

Figure 6.6.2. Rod ciliary region, kangaroo.
Electron micrograph showing a tangential section through a rod inner segment (RIS) at the level of the ciliary stalk (cs). Two calycal processes (arrows) are present peripheral to the ciliary stalk (cs) and the microtubular doublets of the stalk can be seen.

6.7 Rod Inner Segments

The RIS of the Kangaroo Island kangaroo are differentiated into myoids and ellipsoids as in other vertebrates (RODIECK, 1973). The myoids lie immediately sclerad to the OLM and exhibit low electron density. Cytoplasmic organelles typically observed include abundant free polyribosomes, SER and a few moderately electron dense, membrane-bound inclusions measuring from 0.5 to 0.7 µm in diameter (see Figure 6.7.1).

Lying further sclerad, and occupying approximately 1/2 to 2/3 of the RIS are the ellipsoids. The degree of electron density is similar to that of the myoids but the cytoplasm contains numerous elongate mitochondria. These mitochondria are closely packed, as seen in Figure 6.7.2, appear to have have tubular cristae and measure up to 3.0 µm in length and from 0.2 to 0.5 µm in diameter.

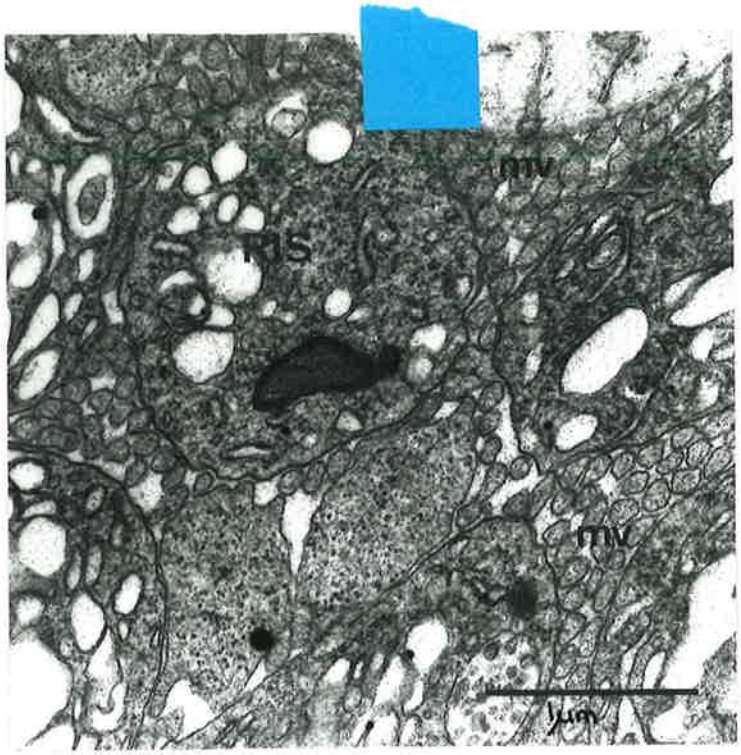

Figure 6.7.1. Rod inner segments, kangaroo. Electron micrograph showing the organelles of the myoids of the rod inner segments (RIS). Müller cell microvilli (mv) are seen between the rods.

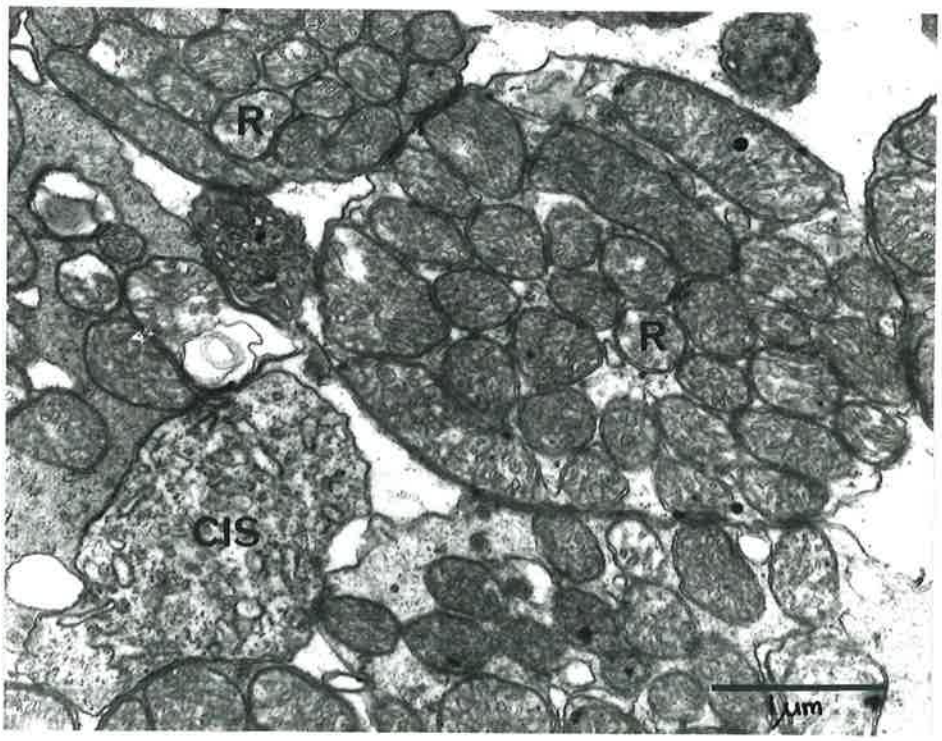

Figure 6.7.2. Rod inner segments, kangaroo. This tangential electron micrograph shows cross-sections of rod ellipsoids (R) packed with numerous mitochondria. This micrograph also shows the myoid of a cone inner segment (CIS).

6.8 Cone Outer Segments

The COS lie along the sclerad edge of the photoreceptor layer of the kangaroo retina adjacent the RPE (see Figure 6.8.1). They appear to be triangular or elongate in radial sections and stain lightly blue in polychrome-stained 1 µm sections.

The COS are shorter (approximately 4.5 to 5.0 µm) than the ROS and contain fewer membranous discs stacked at right angles to the longitudinal axis. The discs appear to be flattened sacs that consist of 2 parallel electron dense membranes that are continuous with each other at a peripheral dilatation. At the base of the COS these discs sometimes appear continuous with one another but are separate further apically, and in neither of these sites do the discs appear to contact the cell membrane. As in the ROS the discs are separated by interdisc spaces that are wider and less electron dense than the intradisc spaces. Unlike the COS discs of the possum and Kowari those of the Kangaroo Island kangaroo are of roughly equal diameter resulting in more elongate COS.

These relatively ordered stacks of discs often lie adjacent irregular membrane formations (see Figure 6.8.2). This unusual arrangement may be indicative of poor fixation of the COS in which case the irregular membranes observed may in fact be distorted COS discs. The adjacent ROS, however, show relatively good fixation of the discs which may suggest that irregular membranes are a normal feature of the kangaroo COS rather than an artifact of preparation.

As a result of the plane of section and the small number of cones relative to rods, no ciliary stalks were seen

in either radial or tangential thin sections. A primary centriole consisting of 9 peripheral microtubular triplets was seen in a single cone containing an oil droplet. A single thick calycal process, such as that seen in Figure 6.8.2, was usually present along the length of the COS.

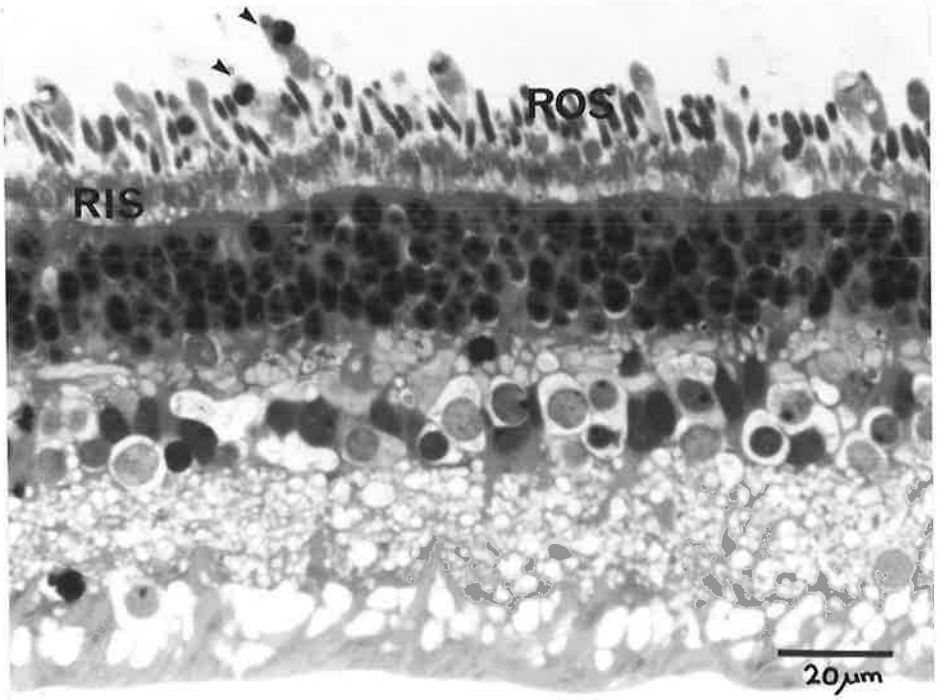

Figure 6.8.1 Photoreceptor layer, kangaroo. Light micrograph of a radial polychrome-stained section of neuroretina showing that the cone myoids generally extend along the combined length of the rod inner segments (RIS) and outer (ROS) segments. The cone outer segments (arrows) lie along the sclerad edge of the photoreceptor layer.

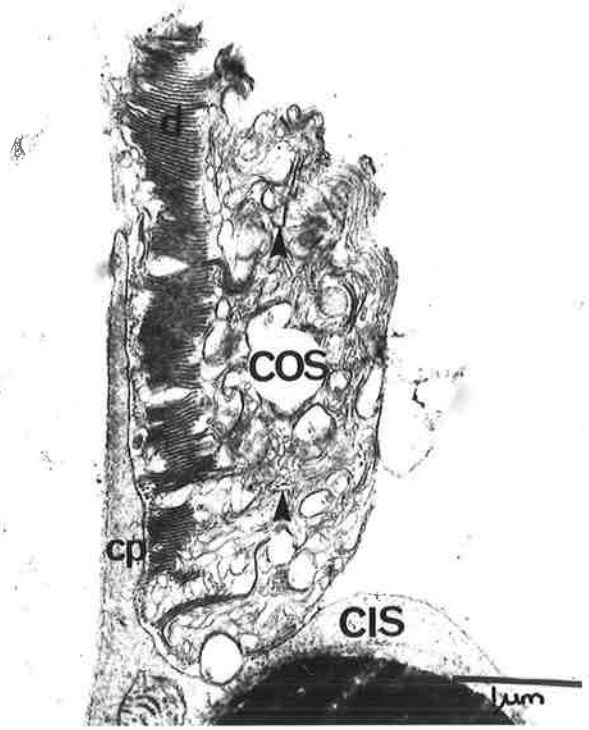

Figure 6.8.2 Cone outer segment, kangaroo. Electron micrograph of a radially sectioned cone outer segment (COS) showing the apparently small discs (d) and adjacent irregular membranes (arrows). A large calycal process (cp) can be seen extending sclerally from the inner segment (CIS).

6.9 Cone Inner Segments

The CIS of the Kangaroo Island kangaroo run radially from the level of the OLM to their outer segments in the sclerad portion of the photoreceptor layer (see Figure 6.8.1). They measure approximately 2.0 μm in diameter as they pass through the OLM and generally increase in diameter to reach a maximum near their attachment to the COS. In those cones containing a droplet, such as seen in Figure 6.9.1, the maximum diameter corresponds to the position of that droplet.

As with the RIS the CIS are differentiated into myoids and ellipsoids. The cytoplasmic matrix of the ellipsoids typically shows low electron density and contains numerous elongate mitochondria with tubular cristae (see Figure 6.9.1) and few free polyribosomes. The ellipsoids often contain a single, membrane-bound droplet measuring approximately 4.0 μm in diameter. These droplets remain unstained in polychrome-stained sections, are osmiophilic and lack any internal ultrastructure. They are refractile in fresh tissue and probably lipid in nature.

The myoid of each CIS lies vitread to the ellipsoid and contains free polyribosomes and SER within its cytoplasm of low electron density.

Three types of cones were seen to occur in radial sections of kangaroo retina: single cones both with and without oil droplets and double cones with a droplet in both the principal and accessory members.

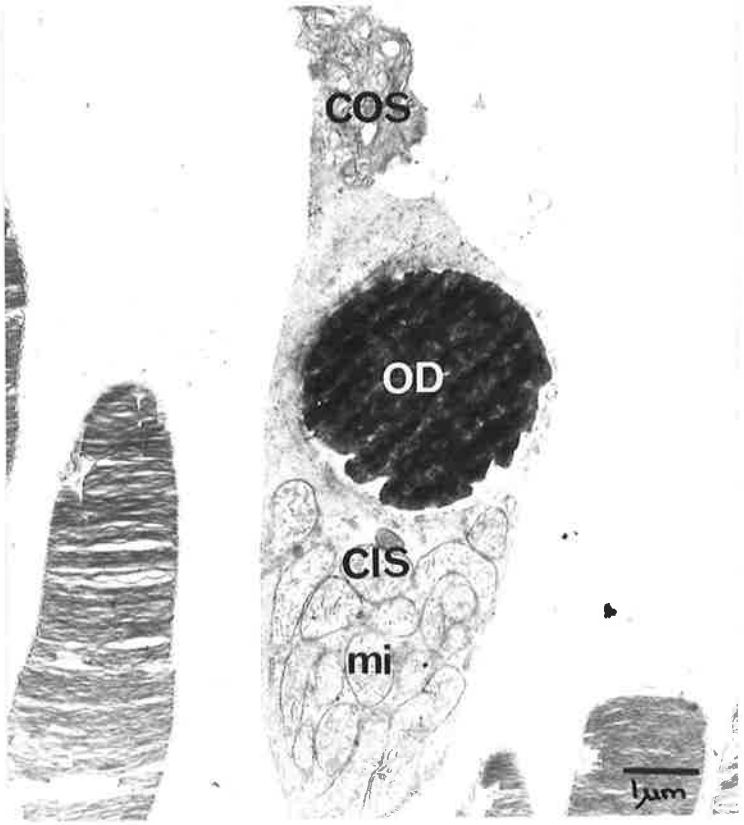

Figure 6.9.1 Cone inner segment, kangaroo. Radial electron micrograph showing a cone outer segment (COS) attached to the ellipsoid of its inner segment (CIS). The ellipsoid contains an oil droplet (OD) lying sclerad to an aggregation of mitochondria (mi).

6.10 Outer Limiting Membrane

In 1 um sections of Kangaroo Island kangaroo retina the OLM is seen as a densely staining, discontinuous line running parallel to the vitread surface of the retina immediately sclerad to the ONL. Electron microscopy has shown that the OLM is actually a continuous band of intercellular junctions. These junctions occur between thhe processes of MC outer terminals and between these same MC processes and photoreceptors. No photoreceptor-to-photoreceptor contacts were seen.

The intercellular junctions that form the OLM show thickening of the cell membrane and increased electron density of the adjacent cytoplasm which indicates that they are zonulae adherentes junctions.

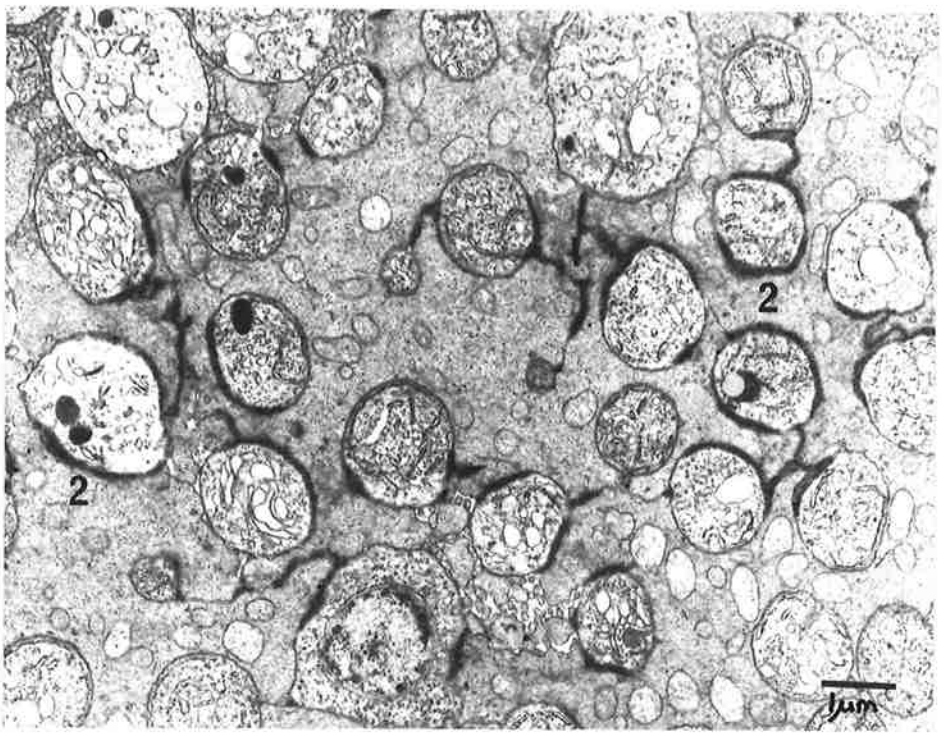

Figure 6.10.1 Outer limiting membrane, kangaroo. Tangential electron micrograph showing the intercellular junctions between the Müller cells (1) and between the Müller cells and photoreceptors (2) that form the outer limiting membrane.

6.11 Outer Nuclear Layer

The most sclerad layer of nuclei in the vertebrate retina is the ONL which contains the photoreceptor cell bodies (RODIECK, 1973). In the retina of the kangaroo the ONL is 4 to 5 nuclei thick. These nuclei are arranged in closely packed, radially directed columns separated by conducting fibres and outer Muller cell processes.

The more numerous rod nuclei are elliptical in radial sections and measure approximately 8.0 µm in height and 5.0 µm in diameter. These nuclei are intensely basophilic in polychrome-stained sections and typically contain centrally located masses of chromatin. Occasionally 1 or 3 such masses are seen. A narrow rim of pale-staining cytoplasm of low electron density surrounds each nucleus and contains free polyribosomes.

The larger, spherical cone nuclei are scattered along the sclerad edge of the ONL. They measure approximately 6.0 µm in diameter, are moderately electron dense and have granular chromatin which show little clumping. The narrow rim of cytoplasm surrounding each cone nucleus is slightly electron dense and contains free polyribosomes.

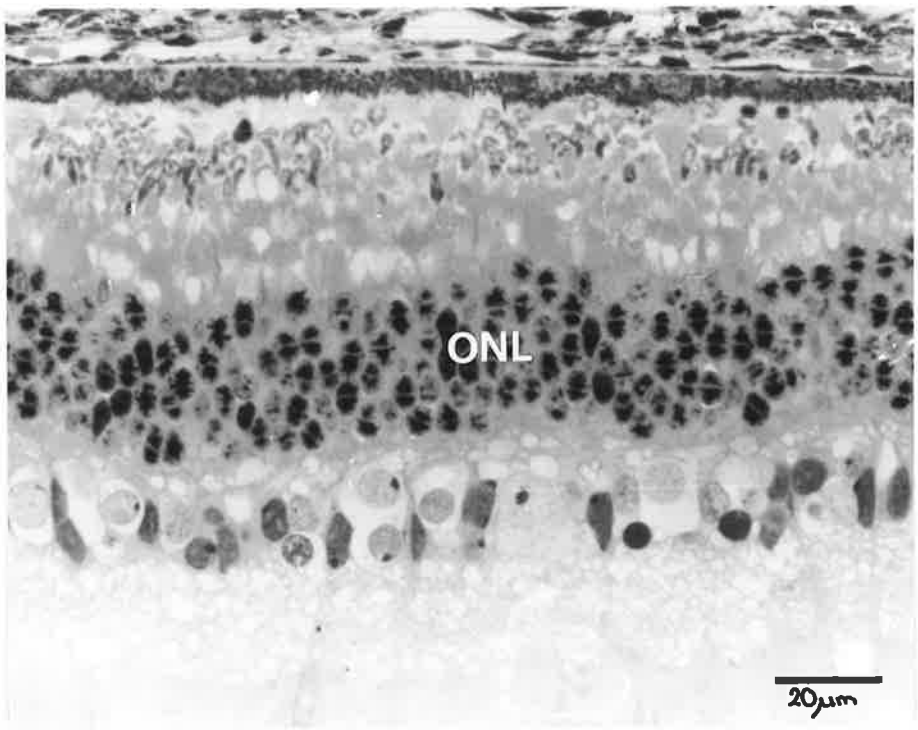

figure 6.11.1 Outer nuclear layer, kangaroo
Radial light micrograph showing the columnar arrangement of the photoreceptor nuclei in the outer nuclear layer (ONL).

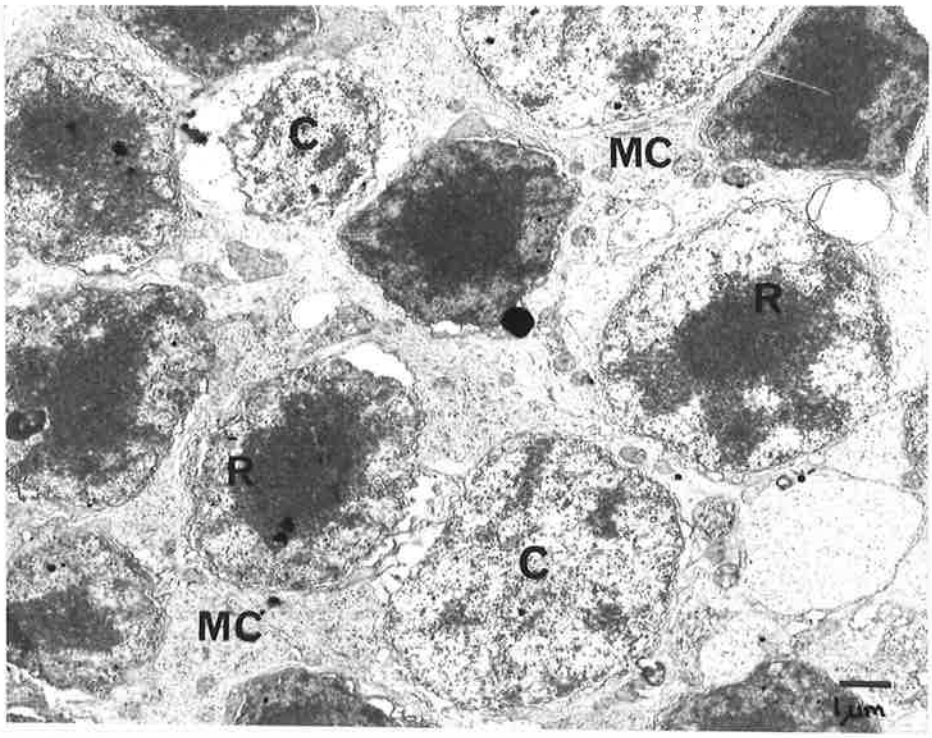

Figure 6.11.2 Outer nuclear layer, kangaroo.
Electron micrograph of a tangential section through the sclerad portion of the outer nuclear layer showing both rod (R) and cone (C) nuclei separated by Müller cell cytoplasm (MC).

6.12 Outer Plexiform Layer

The OPL of the Kangaroo Island kangaroo retina appears to be bilaminar: the synaptic layer lies adjacent the ONL while the fibrous layer occupies the more vitread position adjacent the INL.

The synaptic layer contains the synaptic terminals of the inner conducting fibres of both the rods and cones. Cone pedicles are larger and less numerous than the more sclerally positioned rod spherules. The pedicles are large conical structures, appearing triangular in radial sections and rounded when sectioned tangentially, that measure approximately 8.0 μm in diameter. The degree of electron density of the cone pedicles is similar to or lower than that of the rod spherules; yet they appear to have a considerably lower density density of synaptic vesicles. As seen in Figure 6.12.1 there are several synaptic pits in each pedicle; the maximim counted was 11. Each pit contains 3 post-synaptic processes, 2 lateral and 1 shallower penetrating central process (see Figure 6.12.2), in the "triad" arrangement described by MISSOTTEN (1965) for human retina. There also appear to be numerous less deeply invaginating processes which may correspond to the flat and flat midget bipolar processes identified contacting the cone pedicles in primate retina (see RODIECK, 1973). Each "triad" of post-synaptic processes is associated with a single pre-synaptic ribbon, similar to but smaller than those seen in the rod spherules. Each synaptic complex, which consists of a ribbon and its associated arciform density and post-synaptic processes, exhibits the same ultrastructure and arrangement as those previously described for both the possum

and Kowari. Numerous neuronal processes make contact with the base of each cone pedicle without invaginating. These contacts are conventional interneuronal synapses and as such are not associated with ribbons in the pre-synaptic terminal.

Tangentailly cut thin sections, such as that seen in Figure 6.12.1C, show that the cone pedicles of the kangaroo retina usually have 4 or 5 basal filaments that radiate through the OPL.

The rod spherules are small rounded terminal dilatations of the rod inner conducting fibres measuring 2.0 to 2.5 μm in diameter. Typically they contain numerous 20 to 30 nm synaptic vesicles and a single synaptic complex (see Figure 6.12.3) consisting of a synaptic ribbon and 3 associated post-synaptic processes. The synaptic ribbon, which is surrounded by a layer of vesicles separated from it by a narrow organelle-free space, lies at right angles to the pre-synaptic membrane and exhibits considerable electron density and the pentalaminate structure typical of other vertebrates (RODIECK, 1973). Between the ribbon and pre-synaptic membrane is the semi-tubular arciform density. Again these structures have the same arrangement as that described for the possum and Kowari.

The fibrous layer of the OPL presumably contains processes of INL neurons as in other vertebrate retinae (RODIECK, 1973). Most of these neuronal processes have a large diameter, low electron density, and probably belong to horizontal cells. They contain small, rounded mitochondria, numerous neurofilaments and ribosomes. Less frequent are smaller processes containing numerous neurofilaments and the occasional mitochondrion. In both large and small OPL

processes the neurofilaments generally run parallel to the long axis.

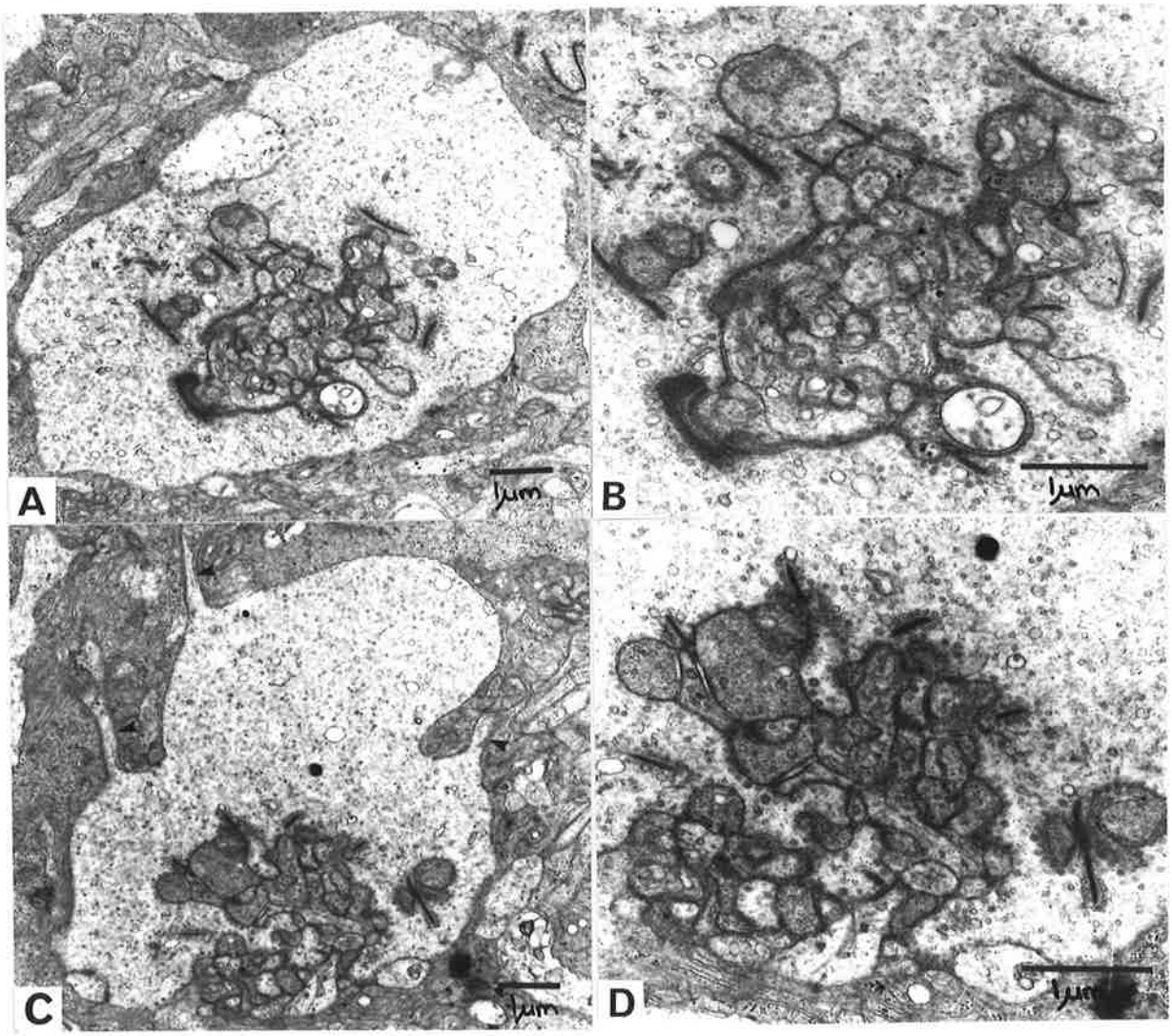

Figure 6.12.1 Outer plexiform layer, kangaroo. Electron micrographs of cone synaptic pedicles. Figure A shows a pedicle sectioned tangentially at the level of the ribbon synapses. Laterally extending processes (arrows) can be seen in the obliquely sectioned pedicle in Figure C. Figures B and D are higher power micrographs showing the multiple synaptic complexes belonging to the pedicles seen in Figures A and B respectively.

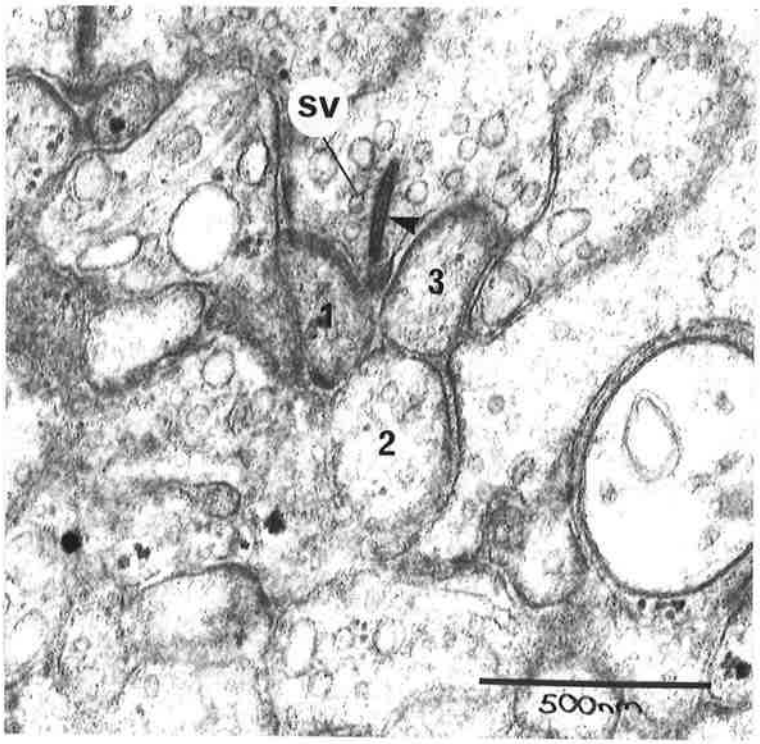

Figure 6.12.2 Outer plexiform layer, kangaroo. Electron micrograph showing a synaptic complex from a cone pedicle. A small array of synaptic vesicles (sv) is present around the pentalaminate synaptic ribbon (arrow). There are 3 post-synaptic processes seen (1-3); the 2 closest to the ribbon show thickening of their cell membranes adjacent the synaptic cleft.

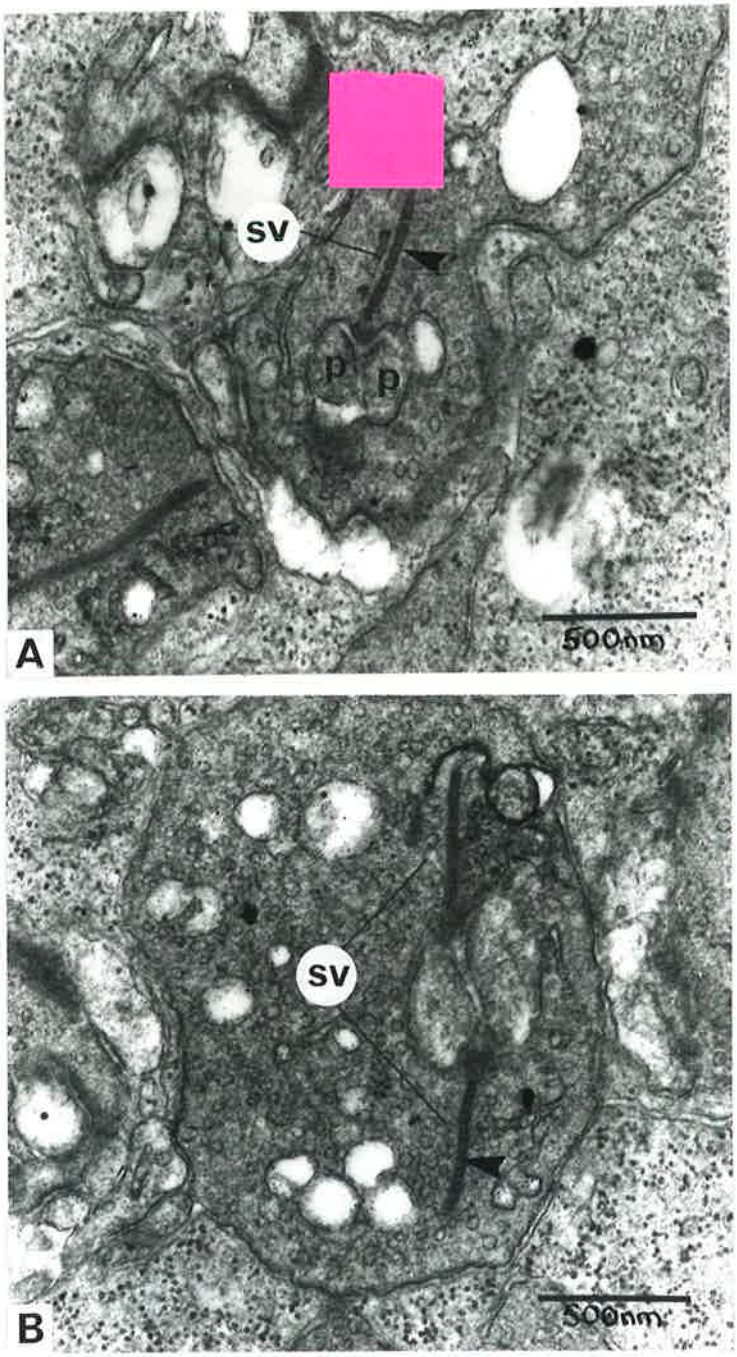

Figure 6.12.3 Outer plexiform layer, kangaroo. Electron micrographs of rod synaptic spherules; one seen in radial section (A) and the other in tangential section (B). Each spherule has a single synaptic ribbon (arrow) at right angles and concave toward the pre-synaptic membrane. An array of synaptic vesicles (sv) surrounds each ribbon and the arciform density lies between the ribbon and pre-synaptic membrane. The post-synaptic processes (p) show thickening of their cell membrane adjacent the synaptic cleft.

6.13 Inner Nuclear Layer

As seen in Figure 6.13.1 several nuclear types are apparent in the INL of the kangaroo retina. Despite the use of serial thick and thin sections for light and electron microscopy it has not been possible to positively identify the nuclei of horizontal, bipolar and amacrine cells. A tentative identification, however, has been made of some INL nuclei.

The presumptive HC were identified by their large diameter, close proximity to the OPL and large processes that radiate through the OPL. The nuclei contain coarse chromatin showing a small amount of clumping and an eccentric nucleolus as seen in Figure 6.13.2. Few free polyribosomes, small mitochondria and a small amount of RER occur in the somatic cytoplasm which is of low electron density.

The nuclei of the presumptive BC are more dense than those of the HC. They contain evenly distributed, fine granular chromatin which exhibits a small degree of clumping beneath the nuclear envelope. Electron density of the bipolar cytoplasm is greater than that of the HC examined. Small mitochondria of variable shape, a small amount of SER and numerous profiles of microtubules are usually present. Large mitochondria have also been seen within the cytoplasmic processes which extend sclerally and vitreally from the cell body.

The cell bodies of the non-neuronal MC lie within the INL of the retina of the kangaroo and were more readily identified than those cell bodies belonging to neurons. The shape of the MC is apparently determined by the packing of the other INL cells, being elongate in radial section

(see Figure 6.13.1) and irregular or polygonal in tangential section. Nuclear shape generally conforms to that of the cell body although an invagination is sometimes present. The nuclear chromatin is finely granular, does not exhibit clumping and is moderately electron dense. Occasionally these nuclei have an eccentric nucleolus in the plane of section. A thin rim of cytoplasm containing a small amount of RER surrounds each MC nucleus.

Two large processes with moderately electron dense cytoplasm containing abundant free polyribosomes and longitudinally orientated microtubules arise from the cell body of each MC. The outer process extends sclerally through the retina from the INL to the OLM in radial fashion and gives rise to smaller lateral processes that surround the processes and synapses of the OPL. Adjacent the OLM the outer processes expand to form pyramidal dilatations, rounded in tangential section and triangular in radial section, of moderate electron density and containing numerous ovoid mitochondria measuring approximately 1.0 μm in length (see Figure 6.13.4).

Occasionally large processes with cytoplasm like that found in MC were seen to extend for several um beyond the OLM into the ventricular space. These large processes which appear to arise from the outer MC terminals are narrow (0.5 μm in diameter) as they pass through the OLM and expand to a width of approximately 7.0 μm. They are less numerous than the microvilli, rounded or irregular in cross-section (see Figure 6.13.5). Together the microvilli and the rod-like processes extend from the MC into the ventricular space and separate the photoreceptor inner segments for most of their

length.

Tangential sections cut close to the ILM show irregularly arranged, closely packed, rounded cross-sections of the inner terminals of the MC. The cytoplasm of these terminals is similar to that found in the outer and inner processes. These terminals, however, often have several cisternae of endoplasmic reticulum (ER) lying parallel to each other and the adjacent cell membrane and separated by approximately 3.0 μm as seen in Figure 6.13.6. Free polyribosomes occur in the intercisternal cytoplasm but do not appear to be adherent to the surface of the cisternae. The significance of these ER figures is not known although they resemble the single cisterna of ER found in Sertoli cells which form part of the intercellular "Sertoli" occluding junction (FAWCETT, 1981). Given the close proximity of the inner MC terminals to the free vitread surface of the retina it is conceivable that the ER figures observed take part in or indicate the presence of intercellular junctions that isolate the retinal neurons from the vitreous.

Smaller cross-sectional profiles are also seen in these tangential, and radial (see Figure 6.17.1) sections, and may be the lateral processes of the inner MC terminals.

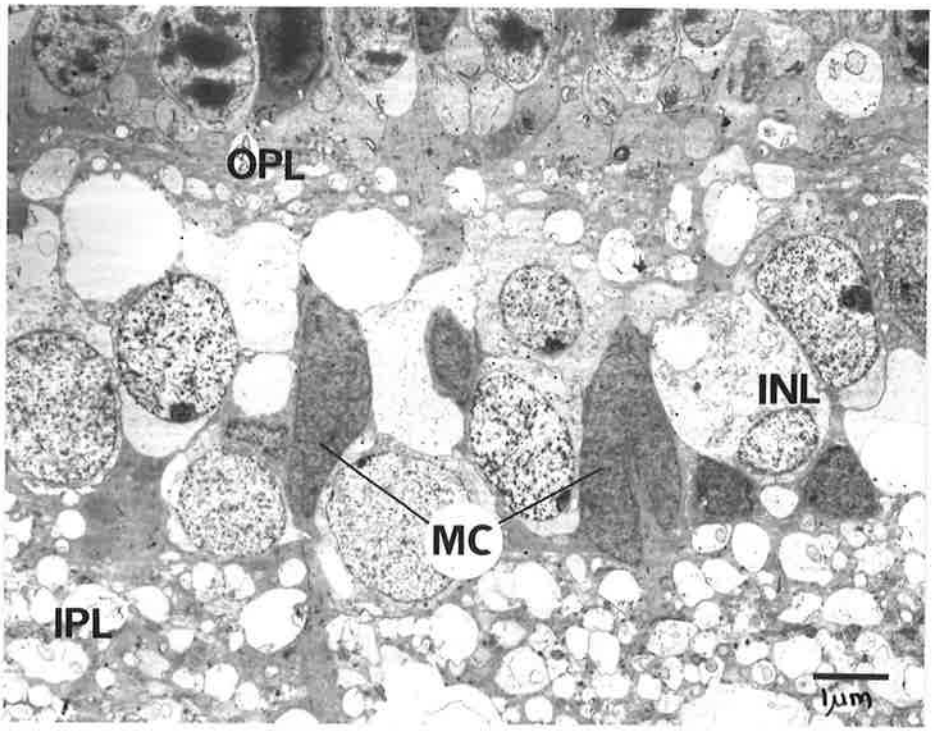

Figure 6.13.1 Inner nuclear layer, kangaroo. Low power electron micrograph showing a radial section of the inner nuclear layer (INL) sandwiched by the outer (OPL) and inner (IPL) plexiform layers. The elongate Müller cell nuclei (MC) are readily seen.

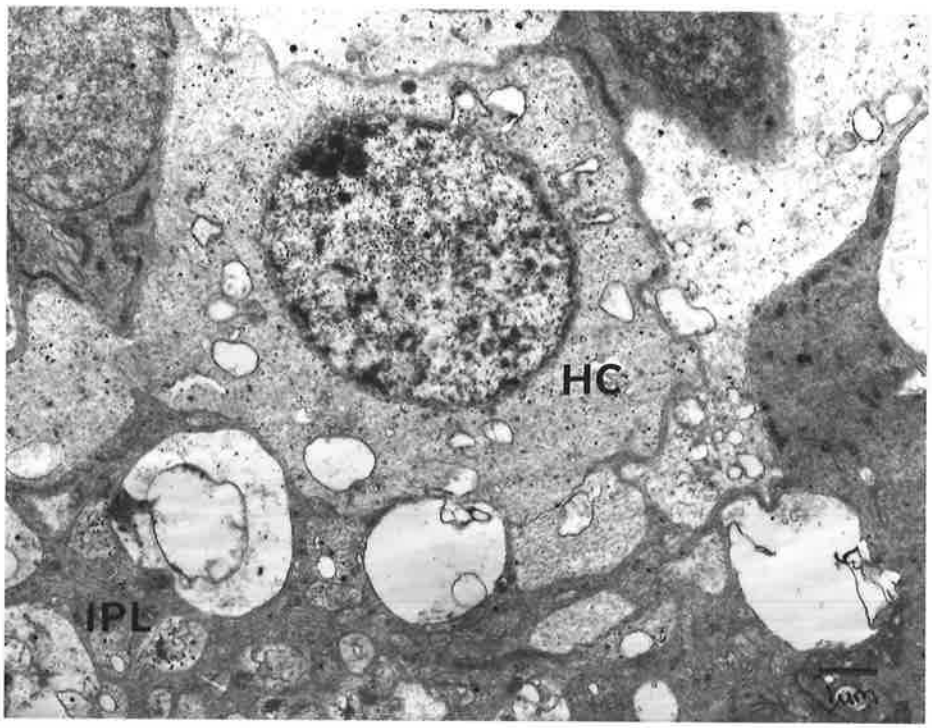

Figure 6.13.2 Inner nuclear layer, kangaroo. Radial electron micrograph showing a presumptive horizontal cell (HC) adjacent the outer plexiform layer (IPL).

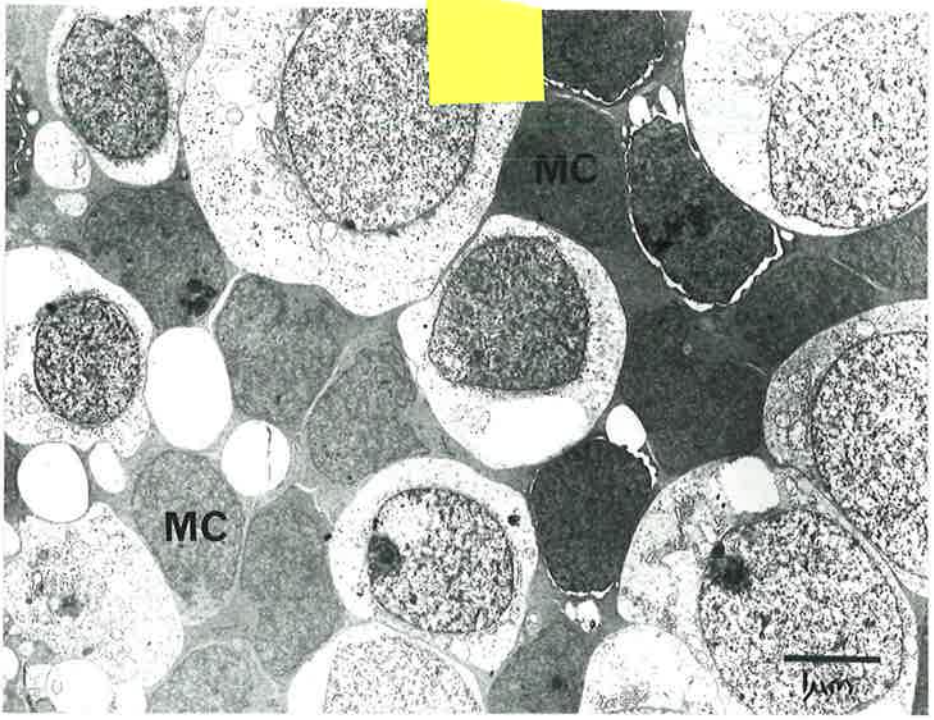

Figure 6.13.3 Inner nuclear layer, kangaroo. The Müller cell nuclei (MC) are easily identified among other inner nuclear layer cells in this tangential electron micrograph.

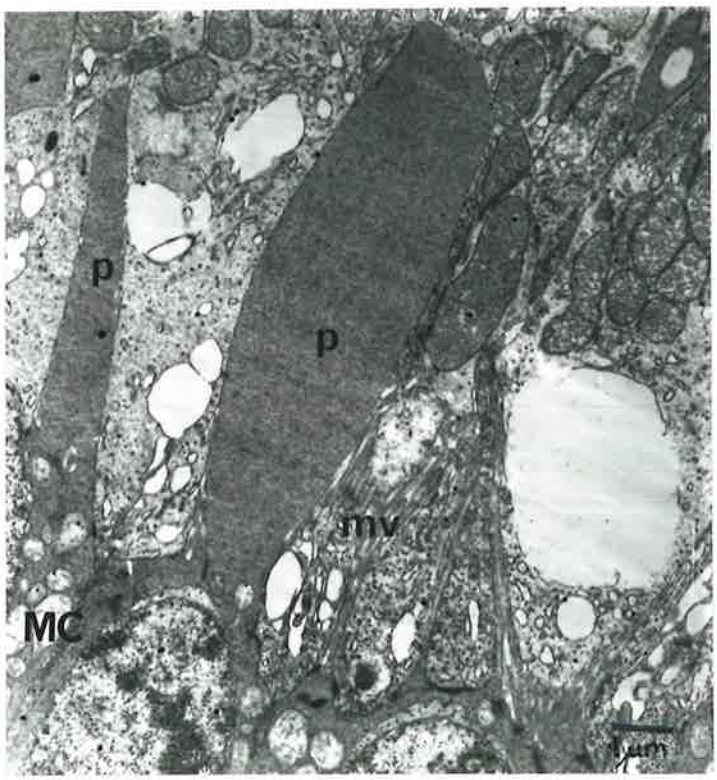

Figure 6.13.4 Müller cells, kangaroo. Microvilli (mv) extend sclerally from the Müller cell terminals (MC) at the level of the outer limiting membrane. Occasionally the Müller cells appear to give rise to a rod-shaped process (p) rather than microvilli.

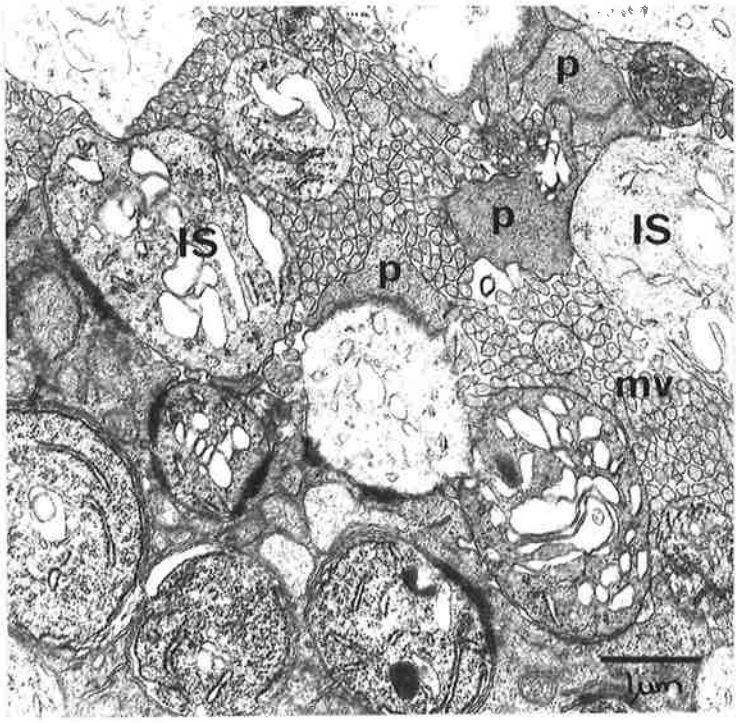

Figure 6.13.5 Müller cells, kangaroo.
Tangential electron micrograph showing transverse sections of the microvilli (mv) and rod-shaped processes (p) lying between photoreceptor inner segments (IS).

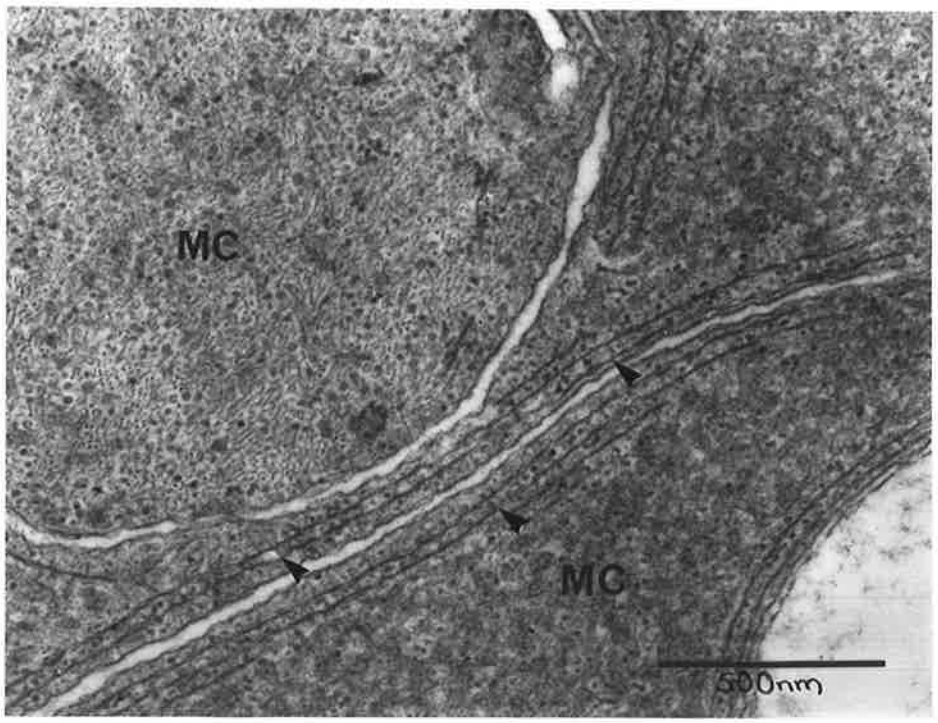

Figure 6.13.6 Müller cells, kangaroo.
Electron micrograph showing the cisternae (arrows) that lie adjacent and parallel to the cell membrane of the inner terminals of the Müller cells (MC).

6.14 Inner Plexiform Layer

In polychrome-stained radial sections the IPL of the Kangaroo Island kangaroo is seen as a lightly stained band measuring approximately 30.0 μm thick, extending from the INL to the RGC layer. The IPL contains neuronal processes which presumably belong to the amacrine and bipolar neurons of the INL and the cells of the RGC layer as in the retinae of other mammals (RODIECK, 1973). In the kangaroo retina these neuronal processes are packed closely together being separated by very thin MC lateral processes as seen in Figure 6.14.1.

Two types of synapses are evident in the IPL of the kangaroo. The ribbon synapses, which appear to outnumber the conventional synapses, are more numerous in the middle and vitread third of the IPL than the sclerad third where very few were found. Whereas most conventional synapses occur in the sclerad and middle third of the IPL. These observations have not been confirmed quantitatively.

The arrangement of the ribbon synapses is much the same as that described for the possum and Kowari, and conforms to that of other vertebrates (RODIECK, 1973). The pre-synaptic terminals are of moderate electron density, contain numerous synaptic vesicles measuring from 25 to 60 nm in diameter, a few mitochondria, free polyribosomes and 1 or more synaptic ribbons as seen in Figure 6.14.1. Typically the ribbons, which are thought to indicate the site of synaptic contact (see DOWLING and BOYCOTT, 1966), are smaller than those in the photoreceptor terminals and highly electron dense. Each ribbon issurrounded by an elliptical array of synaptic vesicles which are separated from it by a narrow organelle-

free space (see Figure 6.14.1). The electron dense, semi-tubular structure corresponding to the arciform density of the photoreceptor terminals does not appear to be present between each ribbon and the pre-synaptic membrane.

The 25 nm wide synaptic cleft is V-shaped with the point of the V directed toward the post-synaptic processes. As shown in Figure 6.14.1 both the pre- and post-synaptic membranes are thickened. Small, rounded electron dense granules measuring approximately 10 to 20 nm in diameter may be seen in some pre-synaptic terminals. These granules may be scattered throughout the terminal as seen in Figure 6.14.1 or clustered together (see Figure 6.14.2), and resemble the β-glycogen granules reported by FAWCETT (1981) in the cat myocardium.

Usually the ribbons are associated with 2 post-synaptic processes of low electron density which may contain mitochondria and a few vesicles (as seen in Figure 6.14.1). This arrangement is similar to that described by DOWLING and BOYCOTT (1966) for bipolar synapses which they referred to as "dyads". In the kangaroo retina 1 of these post-synaptic processes often makes reciprocal contact with the bipolar terminal (see Figures 6.14.1 and 6.14.2). This reciprocal synapse, which is of a conventional type, is 1 of the criteria by which DOWLING and BOYCOTT (1966) identified AC processes in primate retina. These authors considered the second post-synaptic process to be a RGC dendrite.

Besides the reciprocal synapses associated with the presumed BC terminals numerous other conventional synapses occur in the IPL of the kangaroo retina. Typically these synapses show an aggregation of synaptic vesicles adjacent

the pre-synaptic membrane with which some of them make contact. Across the 25 nm wide synaptic cleft the post-synaptic membrane exhibits moderate thickening. As shown in Figure 6.14.3 neuronal processes of the kangaroo IPL may be involved in numerous synapses of this type. A small number of IPL processes were seen to contact RGC by means of conventional synapses (see Figure 6.14.4). These synapses show thickening of the post-synaptic (RGC) membrane adjacent a 25 nm wide synaptic cleft. These contacts resemble the amacrine axosomatic synapses described by DOWLING and BOYCOTT (1966) in primate retina.

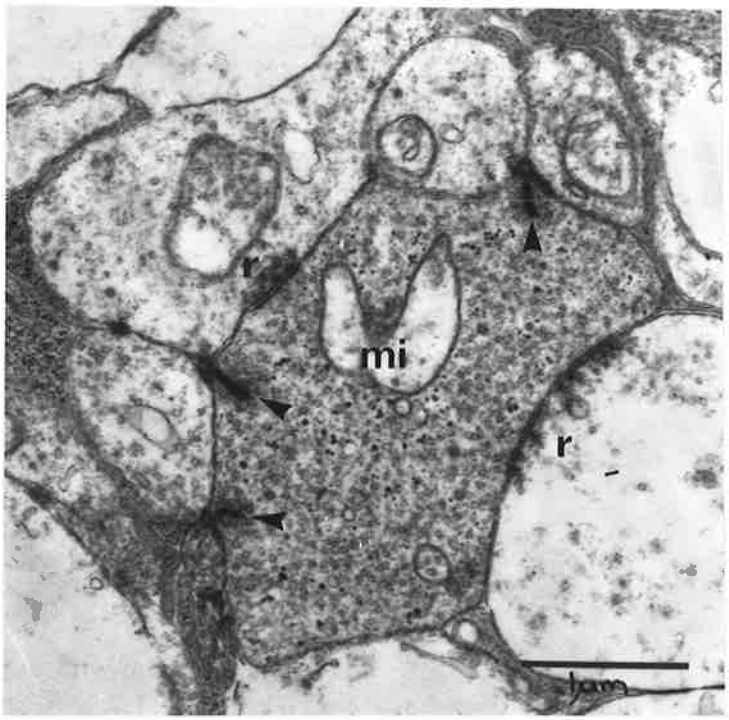

Figure 6.14.1 Inner plexiform layer, kangaroo. Electron micrograph of a presumed bipolar synapse showing multiple ribbon synapses (arrows) and 2 reciprocal conventional synapses (r). The bipolar synaptic terminals typically contain abundant vesicles and few mitochondria (mi).

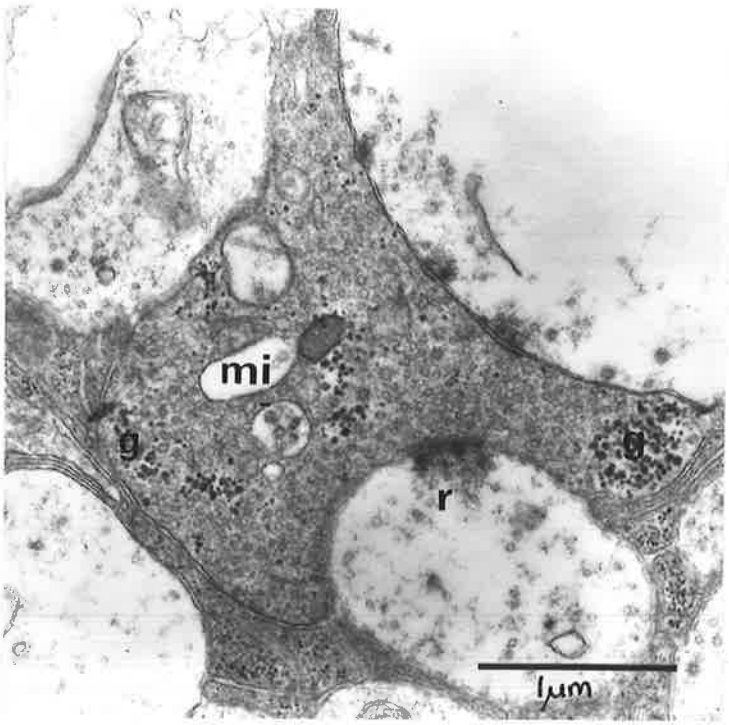

Figure 6.14.2 Inner plexiform layer, kangaroo. Electron micrograph of a presumed bipolar synapse showing mitochondria (mi), reciprocal conventional synapses (r) and aggregates of 20 to 30 nm granules (g) of variable electron density.

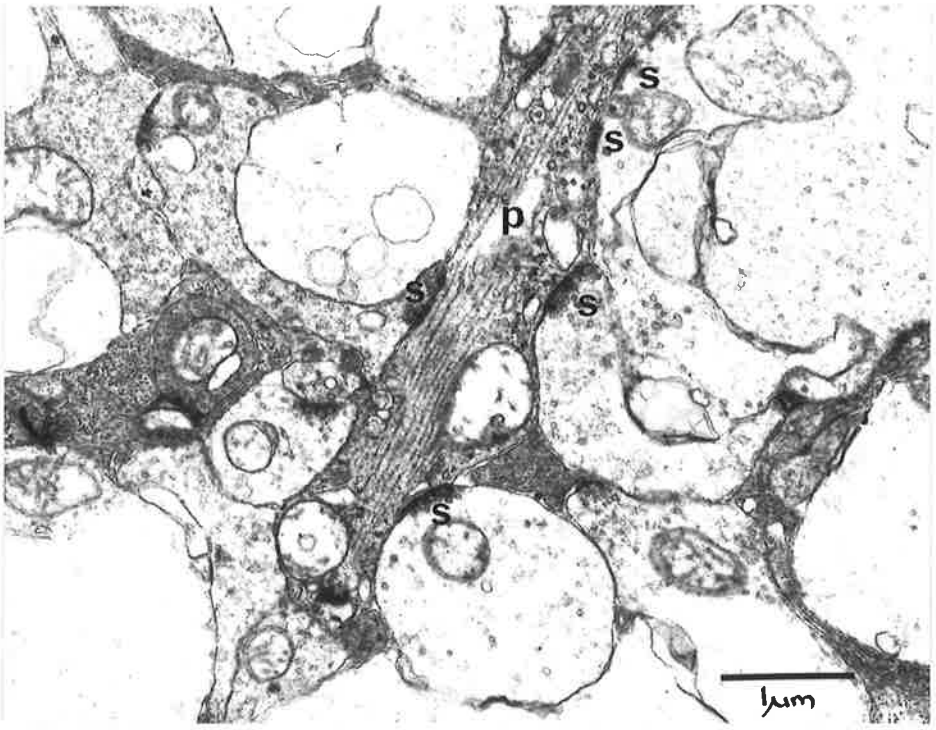

Figure 6.14.3 Inner plexiform layer, kangaroo. Electron micrograph of the inner plexiform layer showing a neuronal process (p) making multiple synaptic contacts (s).

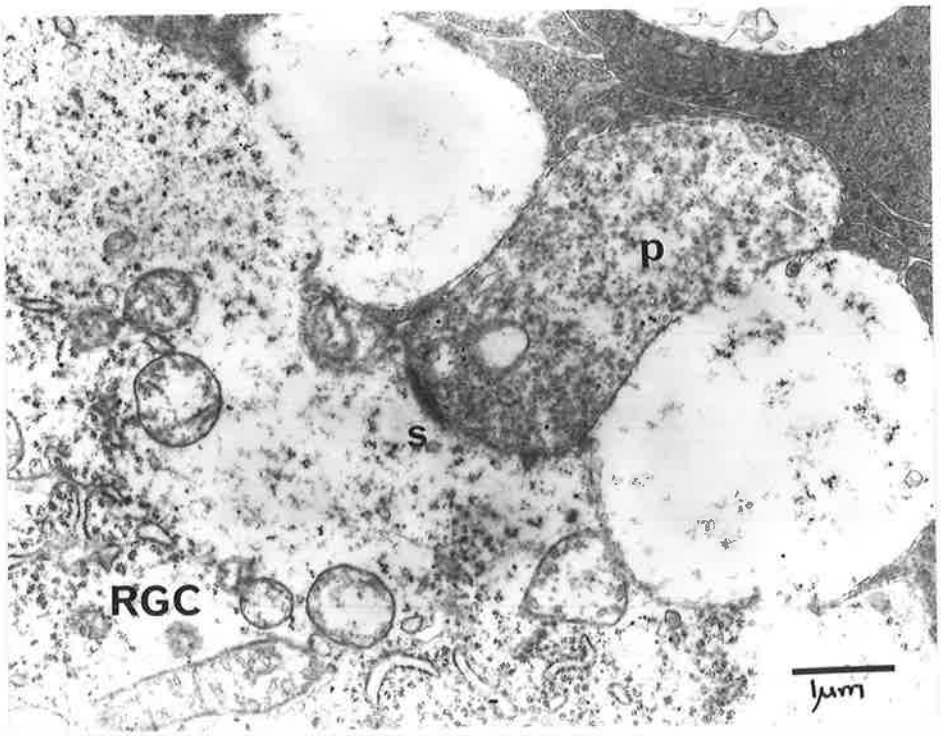

Figure 6.14.4 Inner plexiform layer, kangaroo. Electron micrograph showing a possible axosomatic synapse (s) between a neuronal process (p) of the inner plexiform layer with a retinal ganglion cell (RGC).

6.15 Retinal Ganglion Cell Layer

Scattered throughout the most vitread layer of the Kangaroo Island kangaroo retina are the cell bodies of the RGCs. They are rounded or elliptical in outline (see Figure 6.15.1) and their diameter ranges from 4.0 to 32.0 μm.

The cytoplasm is of low electron density and contains abundant organelles including numerous free polyribosomes, perinuclear RER and small Golgi complexes. Small, round mitochondria measuring from 0.3 to 1.0 μm in diameter are abundant their fixation, however, was not adequate to allow the arrangement of the cristae to be determined.

Electron microscopy has also shown the presence of orderly arrays of cisternae (see Figure 6.15.2) which usually lie parallel to one another being separated by 0.2 to 0.4 μm. Abundant free polyribosomes occur between these membranous cisternae resulting in an arrangement typical of Nissl substance (FAWCETT, 1981). When sectioned transversely the 60 nm cisternae are seen in clusters.

The RGC cytoplasm also contains a moderate number of highly electron dense granules measuring approximately 0.5 μm in diameter. These rounded granules do not exhibit any internal ultrastructure and do not appear to be membrane-bound (see Figure 6.15.3). These granules, which may be related to the ingestion of a neurotoxic grass (see Section 3.3), were more numerous in retina of some individuals than in others.

The RGC nuclei are positioned eccentrically in tangential sections, rounded, of low electron density and have coarse vesicular chromatin. Single nucleoli of high electron density occur in some RGCs.

While it was not possible to identify different RGC types on a morphological basis using light and electron microscopy it was possible to divide the population into groups by cell soma diameter and Nissl-staining properties using wholemount preparations. Three groups corresponding to the α, β and γ type RGCs reported by HUGHES (1975a) in the cat retina were found. In the 3 kangaroo retinae sampled (2 peripheral and 2 central samples from each) 41.0% of the total population constitutes γ cells with diameters of 4.0 to 10.0 um, 51.0% are β cells measuring from 10.0 to 20.0 um, and 7.1% are α cells measuring between 20.0 and 32.0 um across (see Figure 6.15.4). In the peripheral retina 61.0% of the RGCs belong to the smallest or γ cell type. While in the central retina 62.6% of the RGCs measured are of the β type.

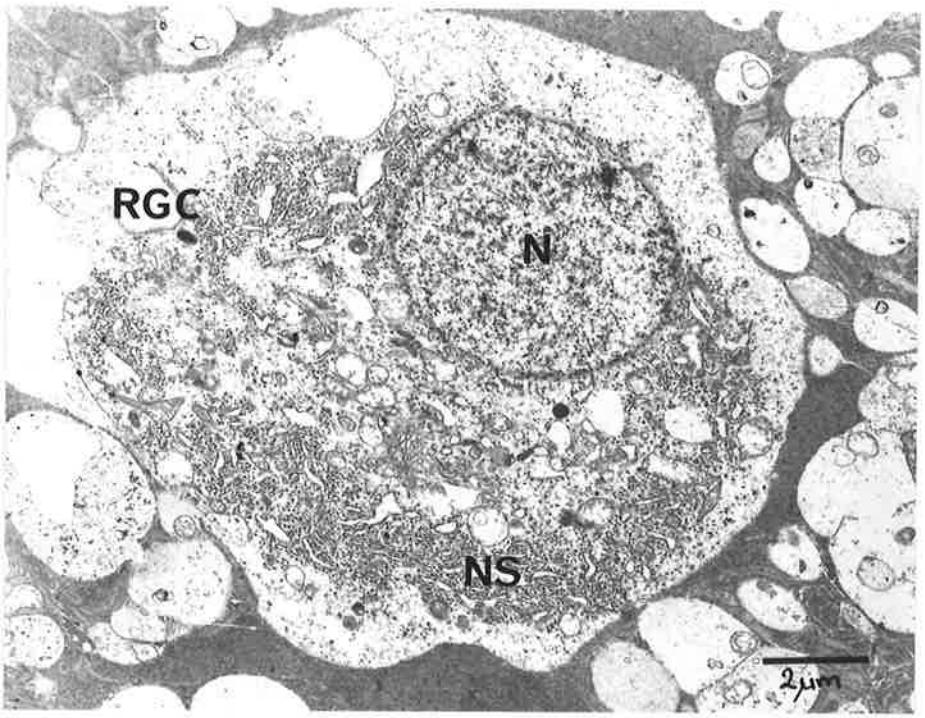

Figure 6.15.1 Retinal ganglion cell, kangaroo. Electron micrograph of a retinal ganglion cell (RGC) with an eccentric nucleus (N) and abundant Nissl substance (NS) in the cytoplasm.

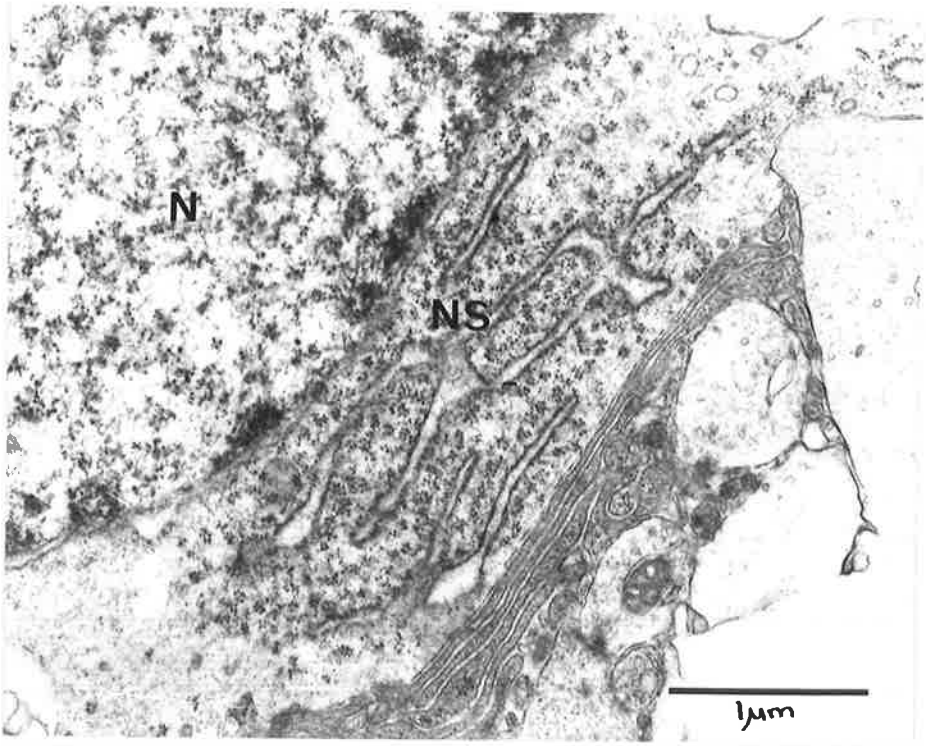

Figure 6.15.2 Retinal ganglion cell, kangaroo. Electron micrograph showing the cisternae and polyribosomes of the Nissl substance (NS) adjacent the nucleus (N).

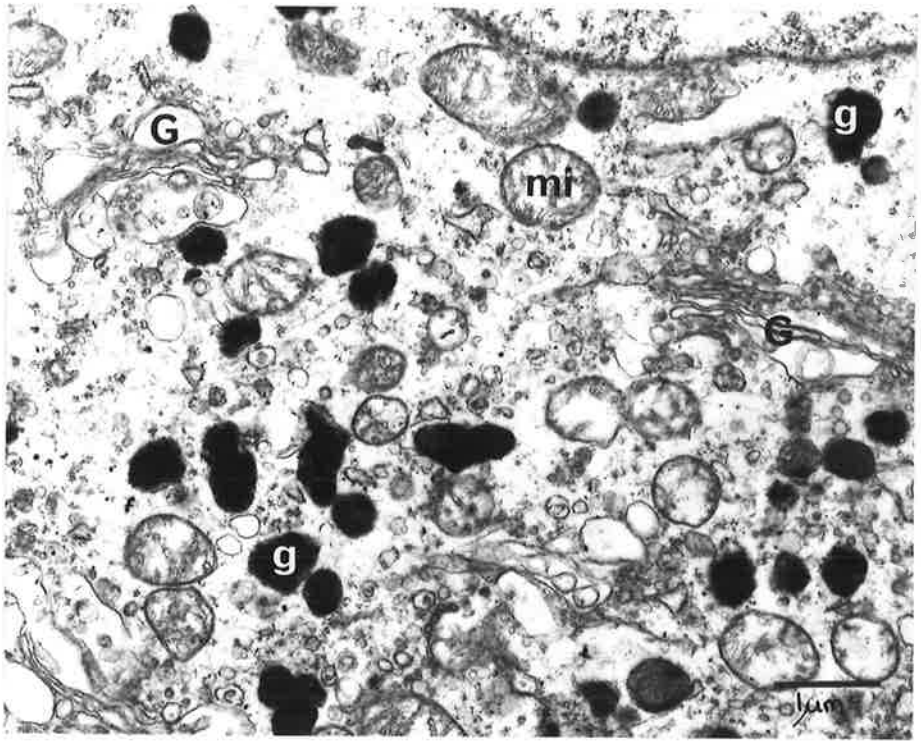

Figure 6.15.3 Retinal ganglion cell, kangaroo. Electron micrograph showing the cytoplasmic organelles of the retinal ganglion cell. Electron dense granules (g), mitochondria (mi), and profiles of Golgi complexes (G) are evident.

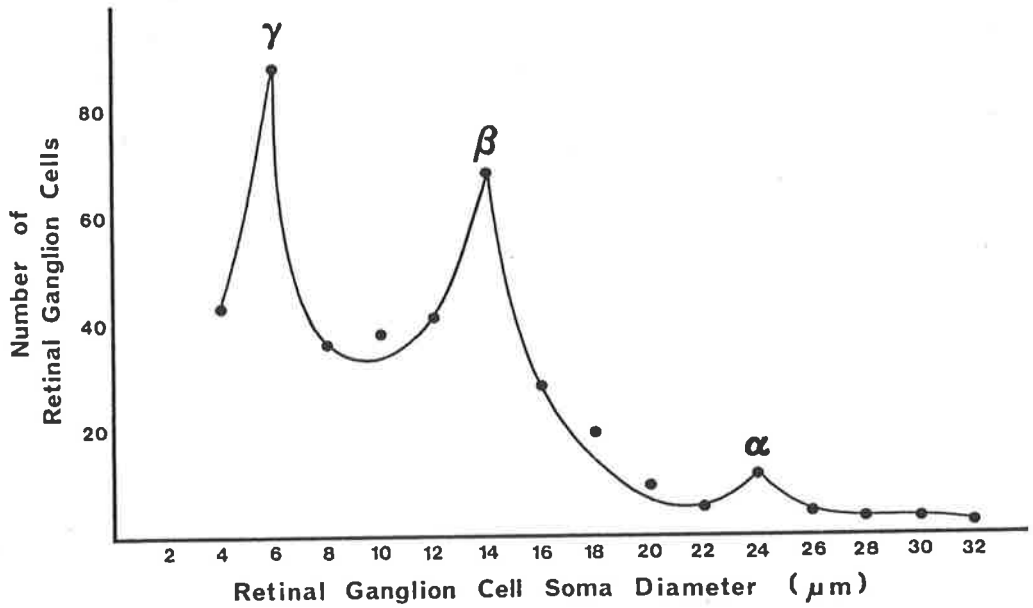

Figure 6.15.4 Retinal ganglion cell soma diameter distribution of the kangaroo. The α, β, and γ indicate the peaks within each range of diameter. Sample size = 405 cells.

6.16 Optic Nerve Fibre Layer

Tangentially cut sections of the NFL of the kangaroo retina show large numbers of longitudinally sectioned neuronal processes and a few in cross-section. These processes, presumably the axons of the RGCs, are orientated in a radial manner, follow a slightly irregular path and converge toward the optic disc. They exhibit low electron density, are arranged in bundles beneath the ILM in the peripheral retina. These bundles are separated by Müller cell processes peripherally, but as they near the optic disc in the central retina they tend to merge. Abundant neurofilaments run parallel to the longitudinal axis of the axons and small, round mitochondria were occasionally seen (see Figure 6.16.1).

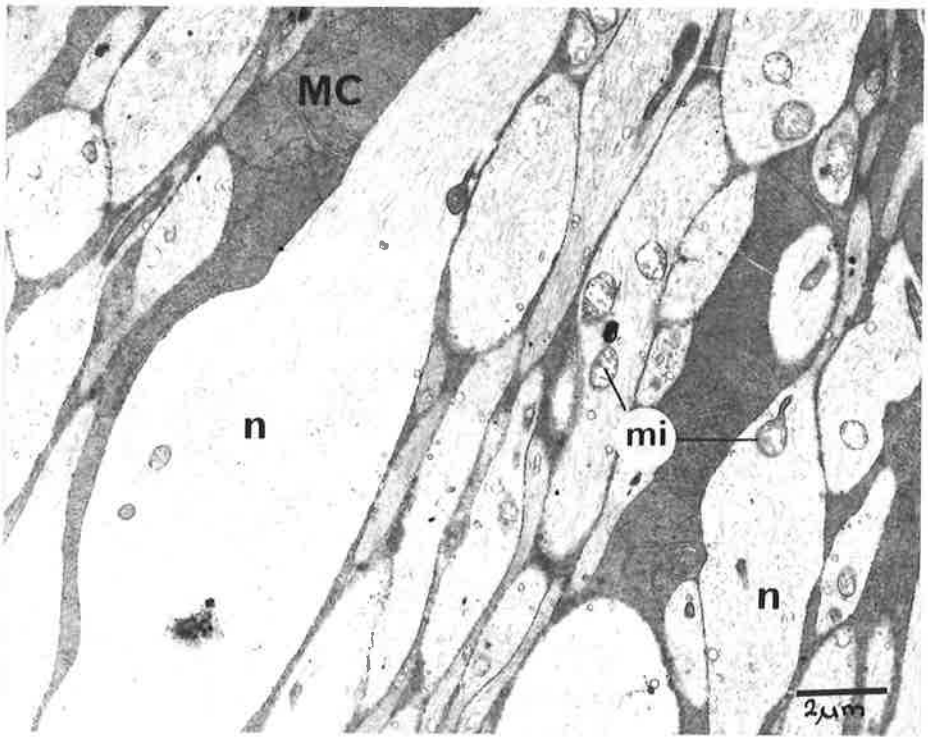

Figure 6.16.1 Optic nerve fibre layer, kangaroo. Tangential electron micrograph of the optic nerve fibre layer. Note the variation in fibre size, abundant neurofilaments (n), occasional mitochondria (mi) and the intervening Müller cell processes (MC).

6.17 Inner Limiting Membrane

The ILM separates the inner, or vitread, surface of the retina from the vitreous and comprises a basement membrane and vitreous fibrils as shown in Figure 6.17.1. The basement membrane belongs to the inner terminals of the MC, measures approximately 30 nm thick and is separated from the MC by a 50 nm wide space of low electron density. Numerous vitreous fibrils measuring at least 0.2 μm long insert into but do not penetrate through the basement membrane.

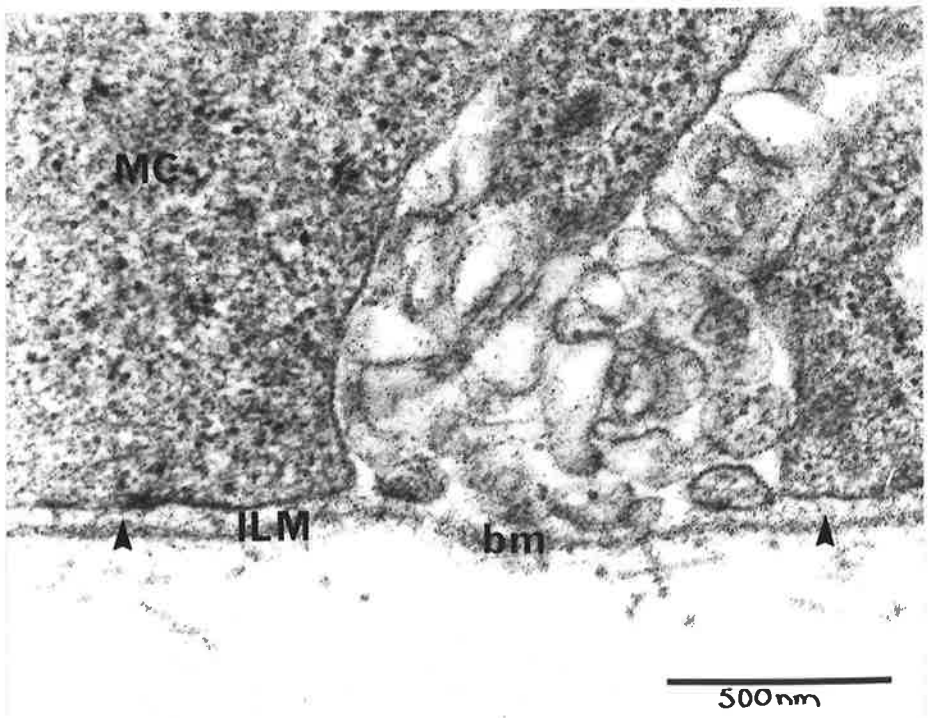

Figure 6.17.1 Inner limiting membrane, kangaroo. A high power electron micrograph showing the inner limiting membrane (ILM) adjacent the inner Müller cell terminals (MC). The basement membrane (bm) is separated from the Müller cells by a narrow space (arrows) of low electron density.

7 GOLGI SILVER STAINING

7.1 Brush-tailed Possum

Several rod photorecptors were identified in radial section of Golgi silver-stained retina from the possum (see Figure 7.1.1A). Only 1 complete profile was obtained.

Lying sclerad to the OLM are the radially directed RIS and ROS. The rod-shaped ROS measure approximately 2.0 µm in diameter and 12.0 µm in length. They are connected to their similarly shaped RIS by a short narrow process, identified as the ciliary stalk using electron microscopy, and extend from it to the RPE. The RIS measure approximately 2.0 µm in diameter and 16.0 µm in length. At the OLM each RIS stained narrows to become continuous with its outer conducting fibre which attaches to the sclerad aspect of the cell body. The elliptical cell bodies lie at any level within the ONL, and measure 4.0 to 5.0 µm in diameter and from 7.0 to 8.7 µm long. A single narrow process, the inner conducting fibre, was seen to arise from the vitread aspect of each rod cell body. The inner conducting fibres terminate in the fibrous lamina of the OPL as small rounded dilatations called spherules. These spherules were shown to be synaptic by electron microscopy although no connections were seen between these and other neuronal cells in the Golgi material. No sessile synapses were seen in the Golgi material examined.

Only 2 poorly impregnated cone cells were identified in the Golgi-stained possum retina (see Figure 7.1.1B). Unfortunately neither of these cells showed the CIS or COS. They did, however, clearly show a large terminal expansion in the OPL. These terminals measure approximately 9.0 µm at their widest point and are triangular in radial

section. Extending laterally from the base of each pedicle are a few incomplete processes. Their irregular outline, however, suggests that several such processes are present but were not stained or included in the section. The shape of the cone terminals and their lateral processes corresponds to the ultrastructural description of the pedicles presented in Section 4.12. The discrepancy in diameter probably arose from the small amount of tissue included in the thin sections necessary for electron microscopy.

The cone cell bodies are rounded, lie along the sclerad edge of the ONL and measure approximately 7.0 µm in diameter.

Running through the ONL to the OPL and connecting the cell body to the synaptic pedicle is a narrow, radially directed process measuring approximately 1.5 µm in diameter.

Along the vitread edge of the possum retina several RGCs were found to have silver impregnation adequate for much of the morphology to be seen (see Figure 7.1.2A).

The large, rounded cell bodies stained measure from 12.8 to 20.0 µm in diameter in radial sections and most showed extensive branching of the dendrites within the vitread half of the IPL. The dendritic trees were seen to arise from either 1 main trunk which quickly divides in 2 or from 2 separate trunks on the sclerad aspect of the cell body. Staining of some of these dendritic trees appeared incomplete. However, those trees exhibiting more complete filling show radiating, dividing branches with a spread of up to 25 µm. All of these dendritic trees show circular terminal dilatations. In no cases was it possible to see an axon arising from the vitread aspect of the cell body and

running along the NFL toward the optic disc as they were seen to do using electron microscopy.

Several cells with extensively branched radially directed processes were seen in the IPL and considered to be MC. Although these cells were mostly incomplete (see 7.1.2B) some description is possible.

The elongate cell bodies of the MC lie within the INL; they are approximately 7.0 µm in diameter and may extend through the INL. Extending toward the OLM from the sclerad aspect of the cell body is a thick process, approximately 3.0 µm in diameter, that crosses the OPL and enters the ONL where it gives rise to lateral processes that run between the photoreceptor cell bodies and give it the appearance of honeycomb. A more slender vitreally directed process measuring from 1.5 to 2.0 µm in diameter leaves the vitread surface of the MC cell body and extends to the ILM where it has a dilated terminal which is triangular in radial section as seen in thin sections for electron microscopy. As this process passes through the IPL it gives rise to multiple lateral branches that give it a bottlebrush appearance.

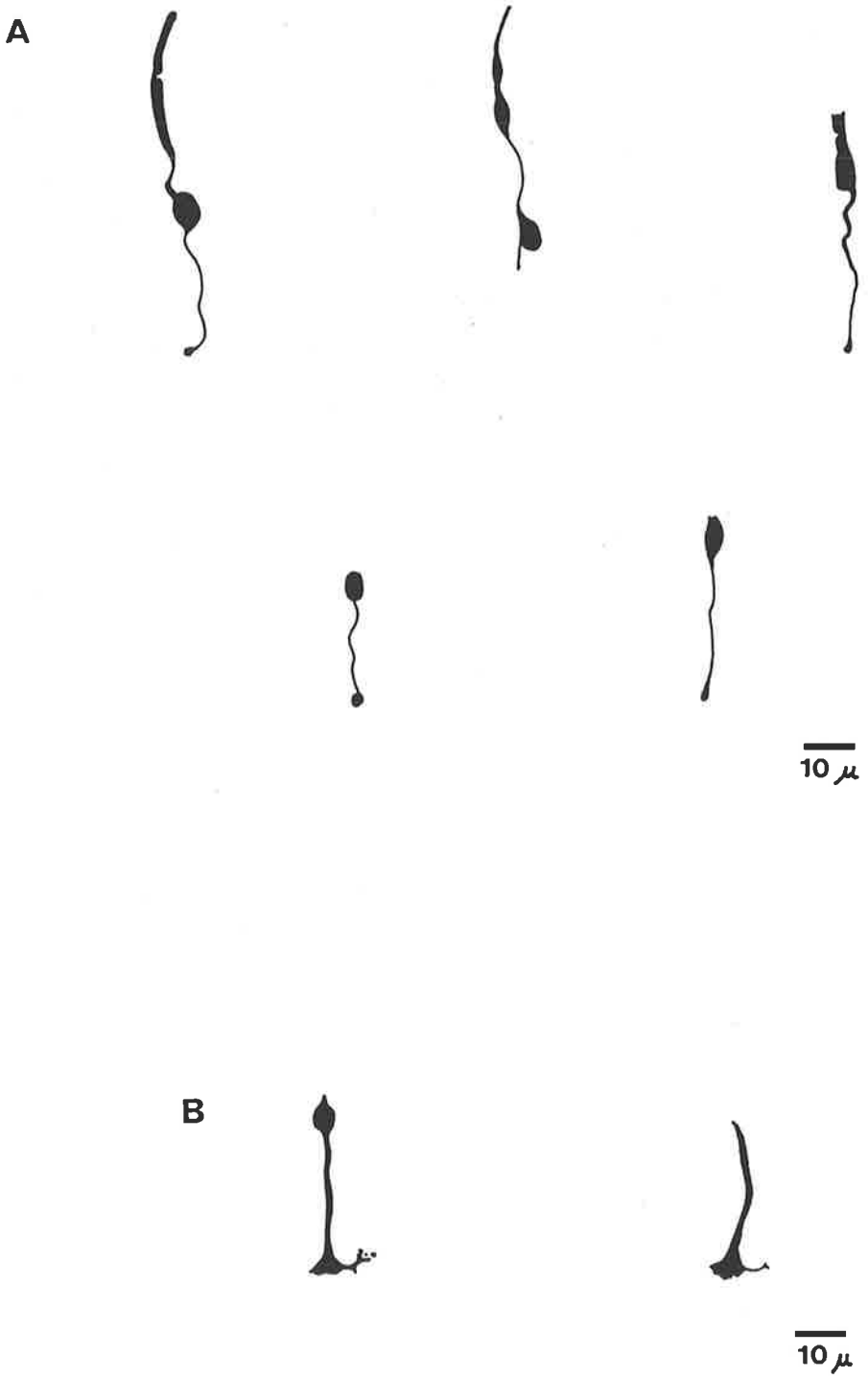

Figure 7.1.1 Golgi-stained photoreceptors, possum.
A. Rod cell radial profiles.
B. Cone cell radial profiles.

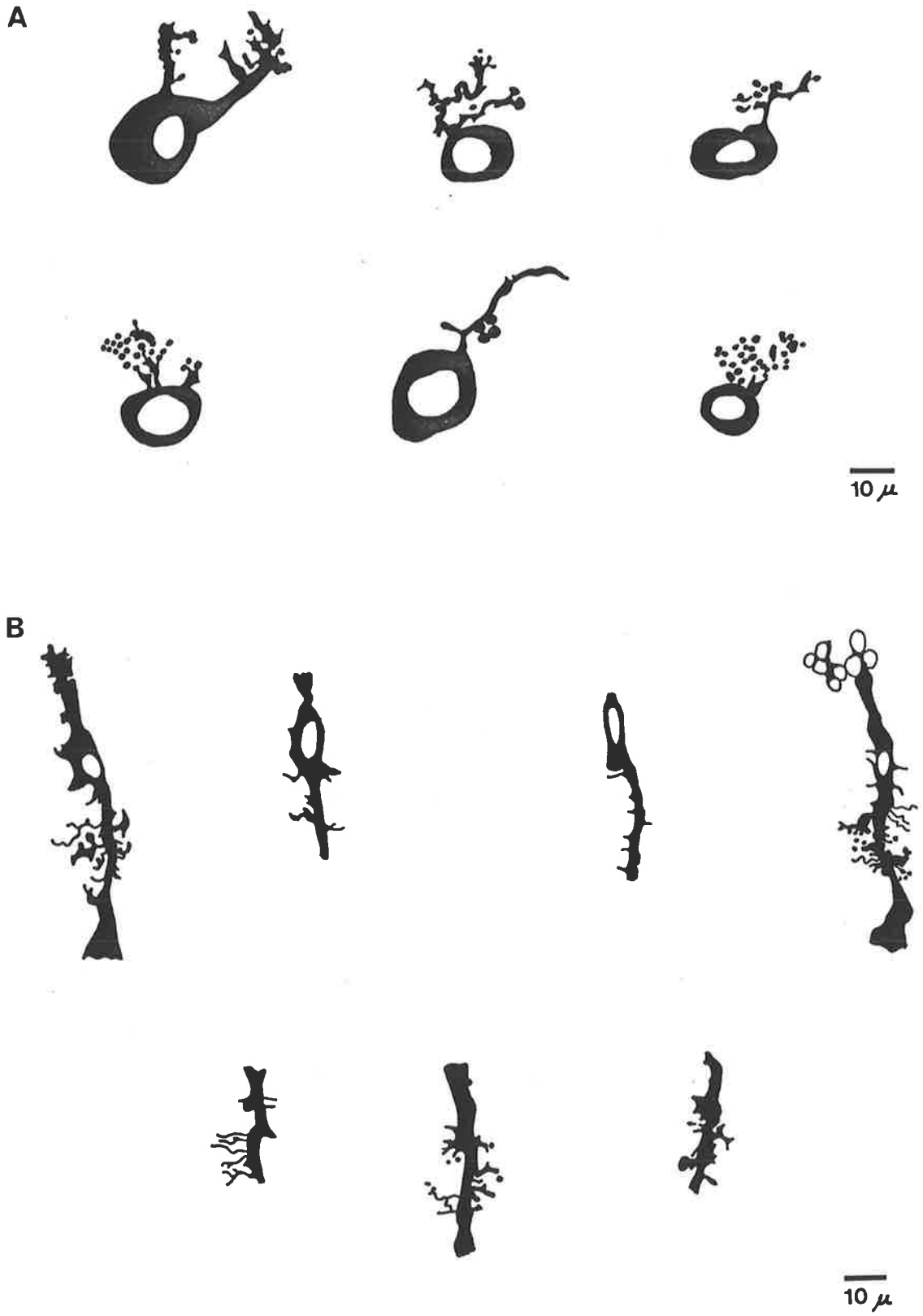

Figure 7.1.2 Golgi-stained retinal cells, possum.
A. Retinal ganglion cells seen in radial section
B. Muller cell radial profiles.

7.2 Kowari

Only a small number of rods showed filling adequate to allow their identification in Kowari retina. As no ROS were seen (either not included in the section or not impregnated) identification was made on the basis of the arrangement of the cell body, conducting fibres and the presence of spherules in the synaptic lamina of the OPL.

The rod cell bodies are elliptical with a diameter of approximately 5.0 μm and a length of approximately 9.0 μm. Arising from the sclerad aspect of each rod cell body the outer conducting fibres, which have a diameterof approximately 1.5 μm as do the inner conducting fibres, extend toward the OLM. Each inner conducting fibre was seen to swell at its vitread end to form a spherule approximately 3.0 μm in diameter.

RIS were evident sclerad to the OLM in only half of the impregnated rods examined; they measure approximately 2.0 μm in diameter.

Several cone cells were identified despite poor filling of their inner and outer segments (see Figure 7.2.1B).

As in routine microscopy the cone cell bodies were seen to lie along the sclerad edge of the ONL; they are rounded and measure approximately 10.0 μm in diameter. Smaller diameters of the profiles seen are probably due to the plane of section.

The length of the inner conducting fibres ranged from 16.5 to 28.0 μm while the diameter was measured at 1.4 μm Each conducting fibre was found to end in the synaptic lamina of the OPL as a large dilatation seen as triangular in radial section. This confirms the information obtained by electron

microscopy. These pedicles range from 3.5 to 6.0 μm in height and have a diameter of approximately 6.0 μm. Up to 4 basal filaments were seen to arise from the most vitread part of each cone pedicle in radially sectioned cells. The spread of these basal filaments ranges from 11.0 to 17.0 μm.

HC were readily identified among the cells of the INL of the Kowari. Their cell bodies generally lie along the sclerad edge of the INL and give rise to numerous processes that enter the OPL (see Figure 7.2.2A). In no case did any cell identified as a HC have any vitreally directed processes.

The cell bodies were found to be slightly ovoid with the diameter (5.7 to 8.5 μm) being slightly greater than the height (6.4 to 7.1 μm).

Each stained HC was found to possess approximately 10 processes radiating from the sclerad aspect of the cell body. In most cells these processes were seen to arise, either individually or in groups, from a short, thick trunk.

Despite incomplete filling of the dendritic processes it was possible to determine that they have rounded terminal dilatations. These HC were found to have a dendritic spread of up to 63.0 μm (measured from radially section retina).

BC were well represented in Golgi-stained Kowari retina; 11 of these had a considerable degree of filling (see Figure 7.2.2B) allowing measurements to be taken.

The cell bodies of all the BC examined were found to lie along the sclerad edge of the INL. They are elliptical in shape and most measure between 6.0 and 8.5 μm in diameter and from 7.0 to 14.0 μm in length. Smaller values were recorded but are thought to be a sectioning artifact (i.e.

only a small portion of the cell body being included in the section).

Dendrites were seen to arise from the sclerad aspect of the cell body in many of the BC examined. In 2 cells the dendrites arise from a single trunk and 1 cell body gives rise to 2 separate trunks. The spread of the dendritic trees was found to range from 14.0 to 28.0 µm. The dendrites of at least 5 BC end in small circular dilatations.

Most of the BC examined possess a single axon that arises from the vitread aspect of the cell body and follows a fairly straight course through the IPL to its small rounded terminal dilatation. Approximately half of these simple axonal processes divide in 2 as they near the RGC layer. They were seen to extend from 17.0 to 34.0 µm into the IPL and in 1 instance reach the RGC layer (it was not apparent whether this axon made contact with a RGC dendrite or cell body).

Two BC were seen to possess a single axon which quickly gives rise to numerous processes that extend laterally for several um and end in spherical dilatations. These highly branched axons have the appearance of a bottle-brush and probably represent stratified BC.

In only 1 instance was a cell whose cell body lies along the vitread edge of the INL filled well enough to allow its identification as an AC (see Figure 7.2.3A).

The small rounded cell body measures approximately 3.0 um in diameter and has a short, thick trunk arising from its vitread aspect. The trunk measures 1.3 µm in diameter, large in relation to the cell body, and gives rise to a large number of long, slender processes some of which branch twice

and radiate into the IPL. The spread of these processes is approximately 17.0 µm which may be artificially low as no terminal swellings were seen.

Where there had been adequate staining of the RGCs in the Kowari retina these cells were recognisable by their large, rounded cell bodies lying adjacent the ILM. Cell soma diameter was found to range from 7.3 to 26.0 µm in the cells examined; these diameters are similar to those recorded from wholemounts (see Section 5.15).

These large neurons were usually seen to possess highly branched dendritic trees consisting of up to 20 processes with marked rounded terminal dilatations (see Figure 7.2.3B). The spread of these dendritic trees was found to be as much as 73.0 µm. Much smaller measurements were obtained but are probably due to incomplete filling of dendrites or their exclusion from the section.

RGC dendrites were found to arise from the sclerad aspect of their cell body via a short, thick trunk. In most of the RGCs examined dendrites arise from a single trunk while in others this trunk divides in 2 before giving rise to the dendrites. In only 1 instance were 2 trunks seen to arise from the cell body of a RGC.

Only a few MC were impregnated in the Kowari retina examined in this Golgi study. Rather unexpectedly the cell bodies, which lie in the INL, appeared to be rounded with a diameter of about 5.7 µm (see Figure 7.2.3C).

Arising from the sclerad aspect of the cell body is a slender process that crosses the OPL before entering the ONL where it gives rise to branches that divide and surround the photoreceptor cell bodies. At this level of the retina the

MC have the appearance of honeycomb.

The inner process, which arises from the cell body to enter the INL, gives rise to numerous fine, wavy lateral processes which give it the appearance of a bottlebrush.

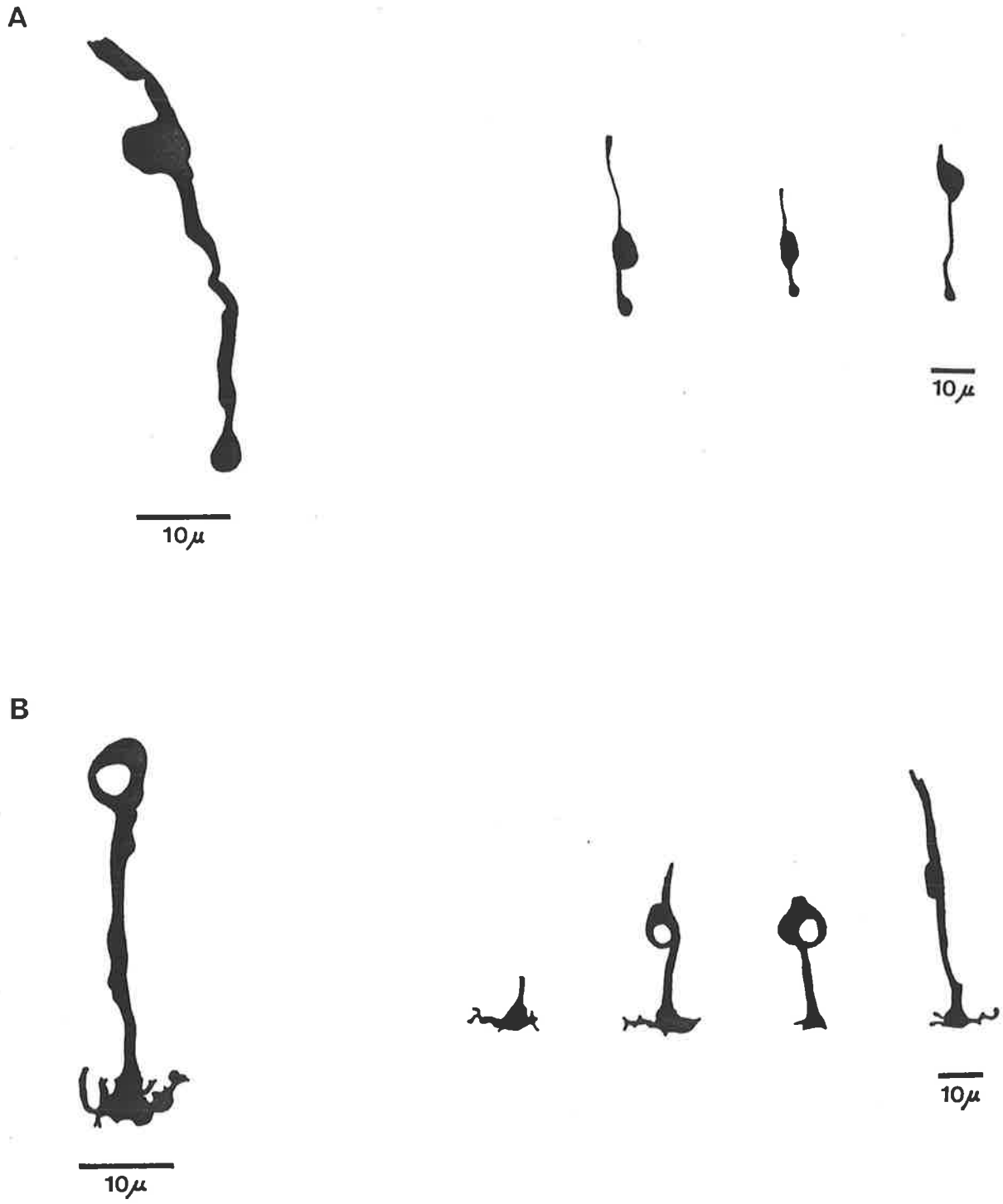

Figure 7.2.1 Golgi-stained photoreceptors, Kowari.
A. Rod cell radial profiles.
B. Cone cell radial profiles.

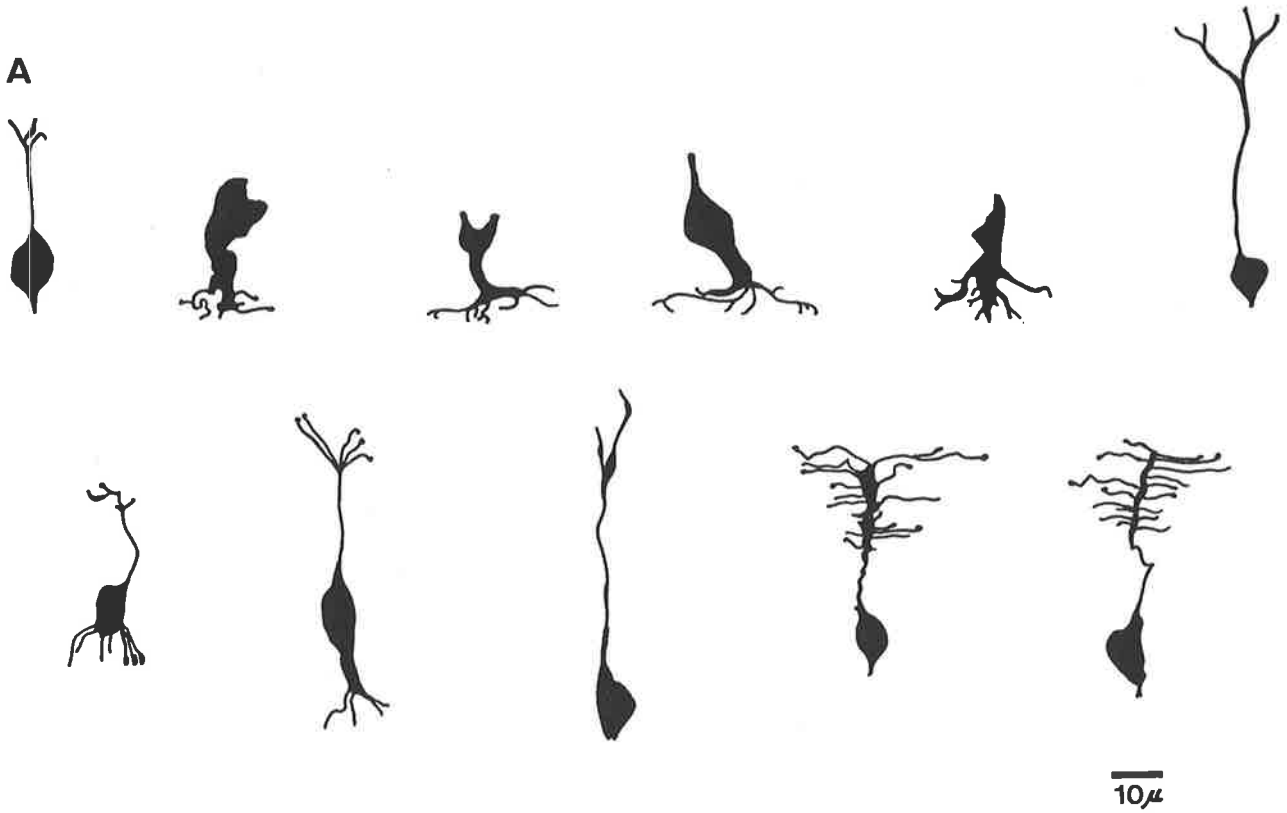

Figure 7.2.2 Golgi-stained retinal cells, Kowari.
A. Horizontal cells.
B. Bipolar cells.

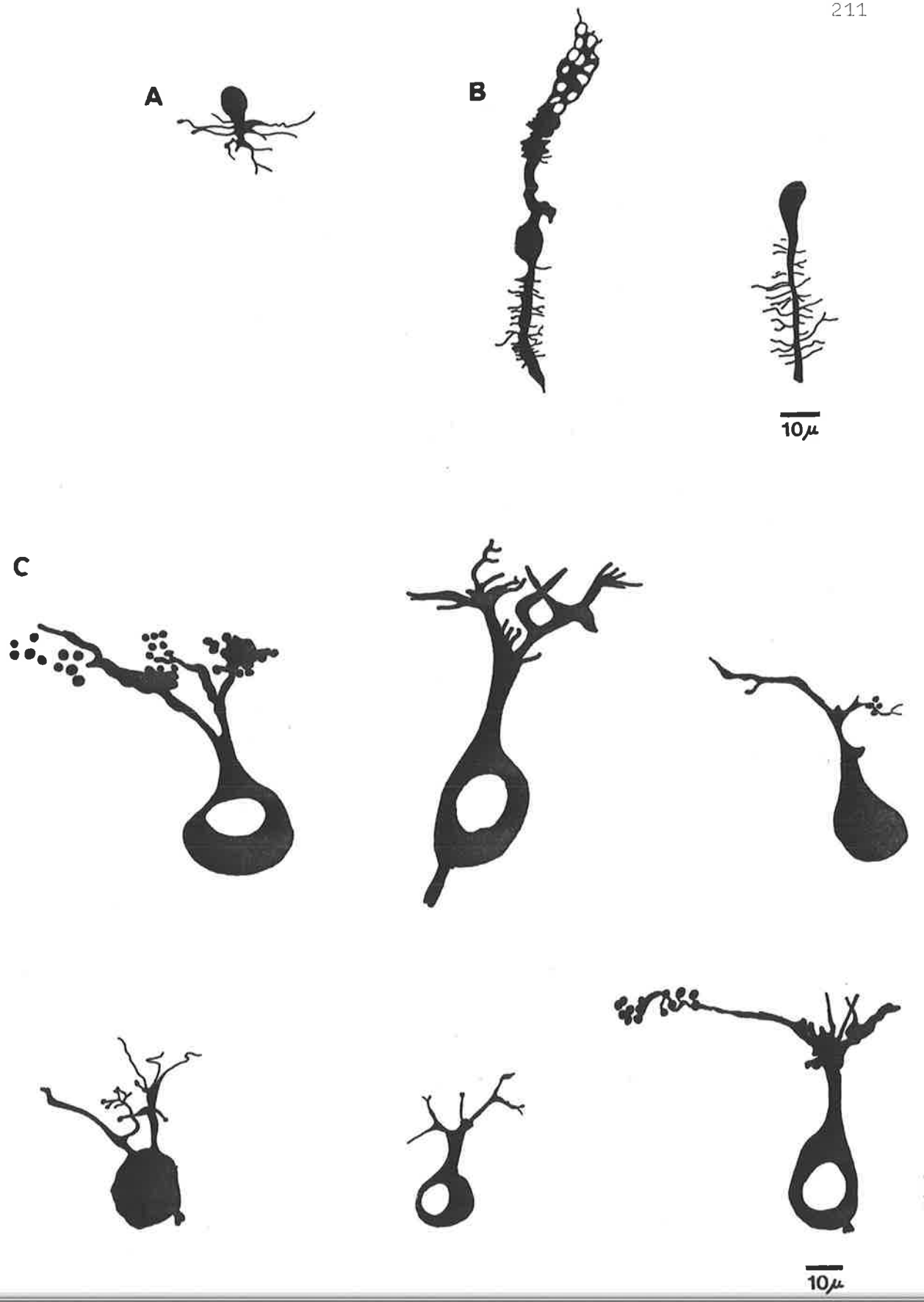

Figure 7.2.3 Golgi-stained retinal cells, Kowari.
A. Amacrine cell.
B. Retinal ganglion cells.
C. Muller cells.

7.3 Kangaroo Island Kangaroo

Most of the cells showing adequate filling in the Golgi-stained Kangaroo retina were photoreceptors (see Figure 7.3.1A). Filling of ROS was generally incomplete. While RIS measuring 2.0 µm wide and approximately 7.0 µm long were found attached to their cell bodies by narrow outer conducting fibres. Cell bodies measuring approximately 4.5 µm across and 7.0 to 8.5 µm long were found at various levels within the ONL. In 3 instances narrow inner conducting fibres were seen arising from the vitread aspect of the rod cell body, and terminating in 2.0 µm diameter rounded dilatations in the OPL. The diameter of the spherules, shown to be synaptic by electron microscopy, correlate with that of the RIS.

Cone cells were less well impregnated than rods and none showed CIS or COS (see Figure 7.3.1B). The rounded cell bodies were found along the sclerad edge of the ONL and have a diameter of approximately 7.0 µm. Narrow tortuous conducting fibres arise from the cell bodies and end in the OPL as large swellings seen to be triangular in radial section. The basal filaments which extend laterally from these terminals were poorly filled and only appear as very short processes in the cells examined.

One cell whose cell body lies within the INL was seen to make contact with a cone pedicle in the synaptic lamina of the OPL. This interneuronal contact appeared to be made by a single dendrite arising from the sclerad aspect of a presumptive BC cell body (see Figure 7.3.1C). A single axon arises from the vitread pole of the cell body and crosses the IPL for approximately 4.5 µm before dividing into several

branches with a spread of only 8.0 µm. This small spread is probably the result of incomplete filling and/or the plane of section not including the entire processes. The elongate cell body of the BC was found to measure approximately 4.5 µm across and 8.5 µm in length.

In the kangaroo retina the outer processes of the MC were found to form a honeycomb meshwork around the cell bodies in the ONL. Whereas the inner processes give rise to single lateral processes that extend between the processes of the IPL giving it the appearance of a bottlebrush. The thick inner processes terminate in large dilatations at the ILM such as that seen in Figure 7.3.1D. These inner terminals are triangular in radial section, measure approximately 8.0 µm wide at the base and give rise to numerous short processes basally. These short processes extend to the ILM and may correspond to the small profiles seen in the thin sections such as that in Figure 6.7.1.

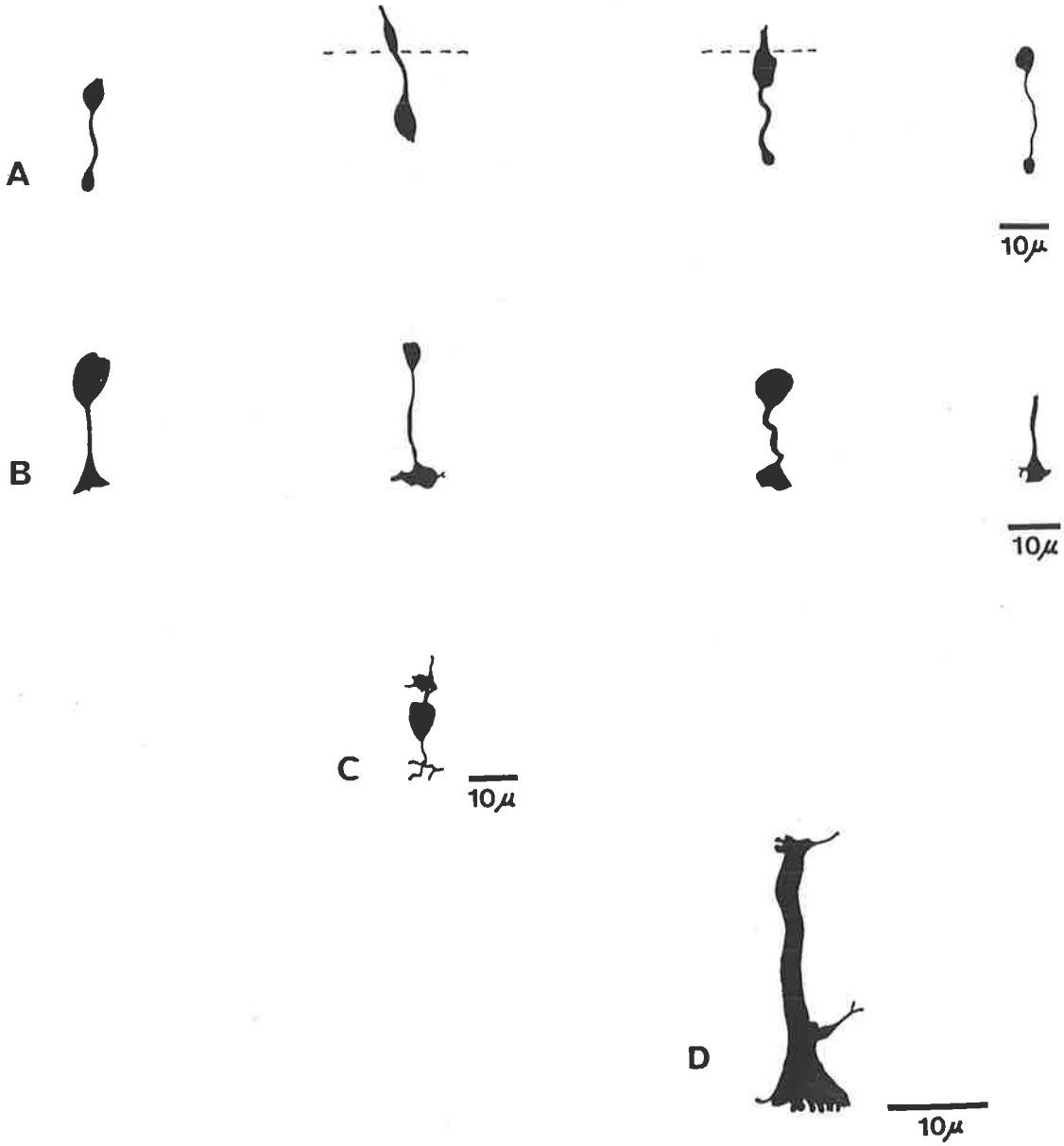

Figure 7.3.1 Golgi-stained retinal cells, kangaroo.
A. Rod cell profiles.
B. Cone cell profiles.
C. Bipolar cell.
D. Muller cells.

8 DISCUSSION

The difference observed between the fundi of the 3 marsupials studied may be related to their belonging to different phylogenetic groups and/or their differing lifestyles. The features of the eyecup of the Brush-tailed possum conform to those reported for other phalangers (JOHNSON, 1901): the fundus is devoid of retinal vessels and the choroidal vessels are prominent. JOHNSON (1901) described the fundus of macropods as grey-brown in colour, free of retinal vessels but with prominenent choroidal vessels. The fundus of the Kangaroo Island kangaroo fits this general description. While the Kowari differs only slightly from JOHNSON'S description of the fundus of another daryurid, the Tasmanian devil. Both have brown fundi with retinal vessels branching out from the optic disc but the Tasmanian devil, unlike the Kowari, does not reportedly have visible choroidal vessels.

The Kowari eyecup was seen to have retinal vessel radiating from the optic disc. Microscopy showed that these paired arteries and veins run along the retinal surface just sclerad to the ILM (see Figure 5.14.2) giving rise to capillaries that penetrate to the OPL where they apparently form a plexus.

D. virginiana, like the Kowari and Tasmanian devil, has retinal vessels which radiate from the optic disc in pairs (JOHNSON, 1901; WALLS, 1942). WALLS also reported that the retina of M. mexicana is highly vascular.

These species appear to be unusual as most marsupials, unlike placental mammals, lack retinal vessels. Retinal vessels with capillary branches penetrating to the OPL, as

in the Kowari, are numerous in primates, artiodactyls, sciurids and carnivores (WALLS, 1942) all of which are diurnal or arhythmic.

Tapeta are typically found in the eyes of nocturnal animals as it is important that their retinal photoreceptors capture as much light as possible (see Section 2.5).

An orange-coloured tapetum was found in the superior fundus of the Brush-tailed possum thus confirming an earlier report by FREEMAN and TANCRED (1978). The presence of a tapetum in this tree-dwelling marsupial was expected as it is nocturnal in habit. The North American counterpart of the Brush-tailed possum, D. virginiana, is also a nocturnal tree-dweller and has a tapetum. Despite the similar lifestyle the type of tapetum in these 2 species apparently differs. While the North American opossum has a retinal tapetum in which the reflective material is lipoidal spheres (BRAEKEVELT, 1976; HAZLETT, 1976) there are too few oil droplets in the RPE of the possum (see Section 4.4) to constitute a retinal tapetum. Polarising microscopy of the choroidal material from the possum failed to demonstrate the presence of any reflective particles. Therefore it seems reasonable to suggest that the abundant choroidal collagen constitutes a fibrous choroidal tapetum. The distribution of pigment within the RPE (see Section 4.1) also suggests a choroidal tapetum.

In light of field observations that the Kowari is nocturnal (WOOLLEY, 1971; ASLIN, 1974) it is perhaps surprising that no tapetum was found as the lack of a tapetum is contradictory to a nocturnal lifestyle. There has been a report, however, of captive animals being active during

daylight (ASLIN, 1974). The lack of a tapetum and the fact that the Kowari has capillaries penetrating the retina as do diurnal placental mammals (WALLS, 1942) point to an eye more suited to a diurnal life style. Perhaps the Kowari's nocturnal habit is consequent to the hot, arid environment it occupies.

The structure of both the choroid and BM are unremarkable in the 3 species of marsupials examined and conforms to the general vertebrate pattern (RODIECK, 1973).

No major differences were found between the morphology of the RPE of possum, Kowari and kangaroo. The features observed are similar to those reported by BRAEKEVELT (1973) for the Quokka and are typical of many vertebrates. The RPE of these 4 Australian marsupials are made of low oblong or cuboidal cells that measure only 3.0 to 11.0 um in height and do not show any apparent variation related to their differing lifestyles and habitats.

The North American opossum, however, has a retinal tapetum; a specialisation of its RPE related to its nocturnal habit. The cells of its tapetal RPE measure approximately 90.0 to 100.0 μm in height, considerably higher than the RPE of the 4 marsupials just discussed, and have abundant oil droplets in their basal cytoplasm (BRAEKEVELT, 1976; HAZLETT, 1976).

The RPE of the possum, Kowari and kangaroo all show apical microvillous processes that extend into the ventricular space to surround the photoreceptor outer segments. This arrangement is not shared by all vertebrates. Some of the apical processes of the human RPE, for example, form sheaths around the outer segments (HOGAN, ALVARADO and

WEDDELL, 1971).

The layered arrangement of the neuroretina of each of the 3 marsupial species examined conforms to the general pattern for other vertebrates as described by DOWLING (1970). The cell bodies of the retinal neurons and glial MC are arranged in 3 defined layers; ONL,INL and RGC layer. While the interneuronal synapses are confined to the 2 plexiform layers which separate the nuclear layers.

Each of the marsupials examined in this study has a duplex retina, with both rods and cones, in which the rods outnumber the cones. The Kangaroo Island kangaroo has a rod to cone ratio of approximately 40:1. This relatively high proportion of cones suggests that the kangaroo retina is well adapted for the animal's crepuscular lifestyle. A ratio of 50:1 was reported by BRAEKEVELT (1973) for the Quokka, also a crepuscular macropod. HOFFMAN (1876), however, reported a rod to cone ratio of 3-4:1 for the 2 macropod retinae he examined (see Section 2.3). This discrepancy may be due to problems with fixation and staining. If this figure is accurate, however, it indicates a considerable variation in the duplicity of the retinae of macropods which is unexpected considering that they belong to the same family and have similar lifestyles.

The Brush-tailed possum was found to have a rod to cone ratio of about 130:1 in both the central and peripheral retina. The predominance of rods over cones is consistent with the nocturnal habit of this phalanger.

The relatively high proportion of cones found in both the central and peripheral retina of the Kowari (25:1) and this species' apparent lack ofa tapetum (see earlier

discussion) are consistent with an eye adapted for photopic rather than scotopic vision.

Light and electron microscopy of the retinae of the 3 marsupials examined has shown that the photoreceptor cell bodies occupy the ONL. This was also apparent in the Golgi-stained retinae examined. They are arranged in radially directed columns packed closely together, with the less frequent cone cell bodies lying along the sclerad edge of the ONL. There are 8 to 10 layers of nuclei in the ONL of the Kowari, as in the Native cat (O'DAY, 1936). The observation of 5 layers in the ONL of the Kangaroo Island kangaroo is also in agreement with HOFFMAN'S (1876) report of 5 rows of ONL nuclei in M. giganteus and W. bennetti*.

Differentiation of the rod and cone nuclei is evident in the Brush-tailed possum, Kowari and Kangaroo Island kangaroo. This is true of other marsupials (O'DAY, 1936; WALLS, 1938; BRAEKEVELT, 1973) and placental mammals (WALLS, 1942) but not in lower vertebrates (WALLS, 1942). Nor is it evident from O'DAY's (1938) description of monotreme photoreceptors. According to WALLS (1942) the increased differentiation of marsupial cone nuclei over monotremes and the persistence of oil droplets in cones suggests that the ancestral marsupials were diurnal. Cone nuclei have coarse granular chromatin with little clumping while the rod nuclei typically have 2 densely staining masses of chromatin.

As reported by WALLS (1942) both the single and double cones of marsupials have the same elements as reptilian cones: outer segments, inner segments with ellipsoids and myoids, outer and inner conducting fibres arising from the cell body, and a footpiece or synaptic pedicle. Marsupial

ellipsoids often lie vitread to an oil droplet but, as in placental mammals, paraboloids are absent. WALLS' observation is consistent with BRAEKEVELT's (1973) description of cones in the Quokka and the elements seen in the species examined in this study.

The COS of the Quokka (BRAEKEVELT, 1973), Kowari and kangaroo are shorter than the RIS; this is usual for vertebrate photoreceptors. The double membrane discs are flattened sacs not normally enclosed by the cell membrane of the tapering COS of the Quokka (BRAEKEVELT, 1973) and Kowari. This was not readily apparent in the kangaroo COS in which discs were found adjacent irregular profiles of membranes (see Section 6.8). This unusual arrangement may be indicative of poor fixation of the COS in which case the irregular membranes observed may in fact be distorted COS discs. The adjacent ROS, however, showed relatively good fixation of the discs. This suggests that either the cone discs are more susceptible to poor fixation or that the irregular membranes are a normal feature of the kangaroo COS. This is supported by the presence of incomplete discs arranged in relative disorder in the COS of the gecko, the alligator and the pigeon (see PEDLER, 1965).

Vertebrate photoreceptor inner segments may consist of an oil droplet, an ellipsoid containing mitochodria, a paraboloid, and a myoid (PEDLER, 1969). The presence of these components varies between species. In the possum, Kowari and kangaroo the CIS are differentiated into ellipsoid and myoids; oil droplets are generally present sclerad to the ellipsoid (see later discussion). O'DAY's (1936) description of differentially staining ellipsoid (with oil droplets) and

myoids is consistent with this finding, as is BRAEKEVELT's (1973) description of the CIS of the Quokka which have ellipsoids and myoids with the ellpsoids lying vitread to the oil droplet.

The Golgi investigation carried out during this study confirms WALLS' (1942) observation that the rods of marsupials are filamentous. Like the Quokka, the possum, Kowari and kangaroo all have long cylindrical ROS with double membranous discs stacked at right angles to the longitudinal axis. In the Quokka these discs have multiple incisures giving them a scalloped outline (BRAEKEVELT, 1973) similar to that seen in human rods (COHEN, 1965). The possum, Kowari and kangaroo, however, have ROS discs with a circular outline that is interrupted by only a single incisure. Irregular membranous tubules were found at the base of some of the ROS in the Kowari retina (see Section 5.5). This may be an artifact of fixation or, in light of the irregularity of COS membrane discussed earlier and PEDLER and TILLY's (1964) report of irregular ROS membranes, it may be normal. The significance of such irregular ROS membranes near the ciliary stalk is not known although it is possible that they are involved in disc formation.

The RIS and ROS of these 4 marsupials are connected by a modified ciliary stalk with a framework of 9 microtubular doublets. Such a ciliary stalk is a consistent feature of vertebrate photoreceptors (COHEN, 1965). In these marsupials the ciliary stalk arises from a basal body, or primary centriole, made of microtubular triplets. In the possum the primary centriole appears to be connected to a secondary centriole by filaments. It would appear from BRAEKEVELT's

(1973) text, but not from his micrographs, that the ciliary stalk of the Quokka photoreceptors have both primary and secondary centrioles. As in human rods (COHEN, 1965) the primary centriole in the marsupial rods examined in this study have short filamentous radial tufts. It seems likely that the variation in the number and position of these tufts is an artifact resulting from the obliquity of the thin sections.

Marsupials have simple rods in which the inner segments are differentiated into ellipsoids and myoids but lack oil droplets and paraboloids as do placental mammals.

In the retinae of most marsupial species examined prior to this study there is more than one type of cone cell. The 3 species examined here conform to this pattern.

In his study of the Quokka BRAEKEVELT (1973) found that single cones with oil droplets predominate and that 'twin' (double) cones with an oil droplet in each member occur occasionally. The retina of the Kangaroo Island kangaroo displays a similar cone population in which most of the cones are single with an oil droplet and the remainder are double with an oil droplet in each member. This macropod does, however, have a few single cones that lack oil droplets. In contrast to these findings are the result of HOFFMAN's study conducted in the 19th. century. He only described the presence of single cones with oil droplets in the retinae of both M. giganteus and W. bennetti*. If correct, HOFFMAN's obervations are indicative of interspecific variation in the cone types in the retinae of macropods. This variation can not be accounted for in terms of lifestyle and habitat as all 4 species are crepuscular animals that graze on open plains.

The Kowari was also found to have both single and double cones. Single cones with 1 oil droplet predominate while only a few double cones with 2 oil droplets, 1 in each member, are present. Single cones without any droplet were found to be the exception. It appears that this type of data is available for only 1 other dasyurid, D. viverrinus. O'DAY (1936) reported that the retina of this Australian marsupial contains both single cones with 1 oil droplet and double cones with 2 oil droplets. O'DAY did not find any single cones lacking an oil droplet as seen in the Kowari.

The present study showed that the Brush-tailed possum has both single and double cones in its retina. The single cones possess a single oil droplet while the double cones have an oil droplet in both the principal and accessory members. This phalanger is a nocturnal tree-dweller as are D. virginiana and M. mexicana, 2 closely related opossums from North and Central America respectively. The cone types of these 2 marsupials differ, however, from those seen in the Brush-tailed possum. Both opossums reportedly have single cones with and without oil droplets and double cones with 1 oil droplet in the principal member (WALLS, 1938). In addition Marmosa has the occasional double cone with 2 oil droplets, 1 in each member. WALLS also reported that the single cones lacking oil droplets are most abundant in the superior retina. As these marsupials share similar habitats, although on different continents, it seems reasonable to suggest that the different cone types may correlate with their phylogeny. The presence of oil droplets is often considered a primitive feature and is common in the cones of lower vertebrates.

Placental mammals , and teleosts which have twin cones, appear to be the only vertebrates in which double cones are not present. Marsupials join many fish, amphibians, reptiles, birds and monotremes in having double cones.

Oil droplets, in all cases colourless, were found in the cones of the species of marsupial examined thus confirming earlier reports of colourless oil droplets in marsupial photoreceptors (O'DAY, 1936; WALLS, 1938; BRAEKEVELT, 1973). HOFFMAN's (1876) report of coloured oil droplets in the cones of M. giganteus and M. mexicana* is inconsistent with these findings. Considering the lack of pigment in the oil droplets of all other marsupial cones examined it seems unlikely that HOFFMAN's report is correct.

Oil droplets occur in the photoreceptors of a variety of vertebrates (RODIECK, 1973). They usually occur as single droplets positioned at the sclerad extremity of the inner segment. WALLS (1942) reported the presence of oil droplets in the rods of the Sphenodon, lungfish and some geckos. It is more usual, however, for oil droplets to occur in cones as is the case in certain primitive fish (see MUNK, 1968), most amphibians, reptiles, birds, monotremes and marsupials (RODIECK, 1973); no oil droplets have been reported in the photoreceptors of placental mammals to date.

Coloured oil droplets, containing carotenoid pigment, have been reported in the photoreceptors of amphibians, reptiles and birds (WALLS, 1942). Light must pass through these coloured oil droplets before reaching the visual pigment in the photoreceptor outer segment and may function as simple filters that absorb short-wavelength scattered light thus improving the visibility of distant objects

through atmospheric haze (WALLS, 1942). Coloured oil droplets function as cut off filters and restrict the range of wavelengths to which cones are sensitive (BOWMAKER and KNOWLES, 1977).

WALLS (1942) suggested that when animals change from a diurnal to a nocturnal lifestyle the coloured filters are lost to increase photoreceptor sensitivity. It is more likely, however, that any increase in photoreceptor sensitivity is a result rather than a cause of the loss of oil droplet pigments. WALLS further proposed that once lost the pigments are never regained although the colourless oil droplets may remain throughout further evolutionary change. This may help to explain why marsupials, such as those examined, possess colourless oil droplets in their cones despite some of them being crepuscular rather than nocturnal.

Colourless oil droplets occur in some photoreceptors of fish (only few teleosts), amphibians, reptiles, birds, monotremes and marsupials (WALLS, 1942). The function of such colourless oil droplets is not known although it has been suggested by RODIECK (1973) that they may absorb ultraviolet light. RODIECK (1973) has also suggested that should the refractive index of these oil droplets be higher than that of the surrounding medium, as was seen to be the case in fresh retina examined in this study, they will cause incident rays of light to converge on the outer segments. A model for the light collecting function of avian oil droplets has been proposed by YOUNG and MARTIN (1984). Such a light-focusing system would be useful to animals active during periods of darkness or poor illumination, as they need to make the most of the limited available light, and may help to

account for the phylogenetic retention of oil droplets in the cones of marsupials.

It appears that little is known of the composition of such oil droplets in these and other vertebrate retinae. Currently, the only histochemical investigation into the nature of the lipid is that of KUNZ and REGAN (1973) in which they studied the oil droplets of twin cones in the guppy.

An earlier study of the CIS of the guppy conducted by BERGER (1966) showed that mitochondria in the ellipsoids differentiate into oil droplets. This was confirmed by ANCTIL and ALI (1976) in their study of teleost oil droplets. In both instances the transformation of the mitochondria was found to occur in a vitreal-scleral direction.

Studies conducted by YOUNG and BOK (1969) showed that continual growth of the ROS in the chick does not result in increased outer segment length because packets of membranous discs are shed intermittently from their tips and subsequently phagocytosed and digested by the RPE. It was later found that this process is cyclic and initiated by the onset of light in both rats (LA VAIL, 1976) and frogs (BASINGER, HOFFMAN and MATTHES, 1976).

In this study the possums and Kowaris were killed mid-morning and the kangaroos killed late in the afternoon. Phagosomes remain in the the apical cytoplasm of the RPE of the North American opossum for only 1 or 2 hours after the onset of light and are degraded in the basal cytoplasm (HERMAN and STEINBERG, 1982a and b). Therefore it was expected that partially degraded phagosomes would be found in the basal cytoplasm of the RPE in both the possum and Kowari retinae. In the kangaroo it was thought that more completely

degraded phagosomes would lie in the basal cytoplasm of the RPE.

In both the possum and Kowari findings were much as expected; phagosomes containing disc-like membranes were found in the basal cytoplasm of the RPE. In general the membranes were either parallel or curled into whorls indicating partial degradation (see MARSHALL and ANSELL, 1971). Some of these membranes lacked definition in the possum. No phagosomes were present in the apical cytoplasm of the RPE in either species and in the possum a few phagosomes were seen in the middle third of the cytoplasm. Since it is generally believed that packets of photoreceptor outer segments are phagocytosed by the apical cytoplasm of the RPE the presence of phagosomes further basally indicates that they migrate in an apical-basal direction. More simply, the presence of such phagosomes suggests that outer segment disc turnover occurs in these 2 marsupials as it does in the North American opossum (HERMAN and STEINBERG, 1982a). The basally-positioned phagosomes in this opossum mostly appear as dense whorls in which the structure of the membranes is not often apparent (HERMAN and STEINBERG, 1982b). This is comparable to the phagosomes seen in the possum and Kowari.

Rather unexpectedly no phagosomes were found in the RPE of the kangaroo. As these animals were killed late in the afternoon it is possible that all evidence of phagocytosis of ROS has been destroyed. This would be comparable to the situation with COS membranes in other vertebrates (see YOUNG, 1978) in which all evidence of the phagocytic process has been destroyed by the end of the night.

Originally it was thought that cones neither make new

outer segment discs nor shed old discs and that only the molecular components are replaced (YOUNG, 1971). Further investigation, however, showed that the process of disc shedding and phagocytosis in vertebrates does not differ significantly between rods and cones (YOUNG, 1978).

In the vertebrate retina the photoreceptor layer is separated from the ONL by the OLM, a band of intercellular junctions. The photoreceptors are joined laterally to MC by zonulae adherentes junctions. MC also frequently contact MC.

Contacts were frequently seen between photoreceptors and MC, and between adjacent MC in the possum, Kowari and kangaroo. In the tissue examined during this study there was no evidence of photoreceptor-to-photoreceptor contacts at the level of the OLM. With the exception of the principal and accessory members of the double cones the photoreceptors are isolated from other photoreceptors by MC processes at this level. BRAEKEVELT (1973) described the cones of the Quokka retina as being joined to neighbouring cells by lateral intercellular junctions and 'usually separated from other photoreceptors by the intervening Muller cells'. It is not clear whether he is suggesting the occasional contact of otherwise separate photoreceptors or the apposition of the members of the so-called 'twin' cones.

The OPL in each of the 3 marsupial retinae examined in this study is bilaminar. There is a sclerad synaptic layer and a vitread fibrous layer adjacent the INL. This arrangement corresponds to the middle and internal zones described in the OPL of the human retina (HOGAN et al., 1971), and has not been previously described for marsupials.

The cone pedicles of the possum, Kowari and kangaroo

are larger and more complex than the rod spherules thus conforming to the general vertebrate pattern. Vertebrate cone pedicles generally have numerous synaptic pits (KOLB, 1970; RODIECK, 1973) and are thus referred to as polysynaptic (UNDERWOOD, 1968). These large conical structures were found to have at least 11 synaptic pits in the kangaroo, 12 in the Kowari and 5 in the possum compared with 20 to 25 in the Quokka (BRAEKEVELT, 1973). Overall these figures compare closely with data available on placental cones. For example, the number of invaginations per pedicle varies from 12 to 25 in primate cones and is dependant on retinal position (see KOLB, 1970).

Typically the synaptic pits in vertebrate cone pedicles consist of 2 lateral and 1 less deeply invaginating central process in association with a synaptic ribbon (MISSOTTEN, 1965; DOWLING and BOYCOTT, 1966; DOWLING, 1970). The ribbon is thought to indicate the site of synaptic contact (see DOWLING and BOYCOTT, 1966). It is generally considered that the 2 lateral processes belong to HC while the central process is a BC dendrite. MISSOTTEN (1965) described this arrangement in human cone pedicles and termed it a 'triad'.

The invaginated synaptic contacts seen in the cone pedicles of the possum, Kowari and kangaroo all appear to have 2 lateral and 1 central invaginating process in the 'triad' arrangement. Likewise, BRAEKEVELT (1973) reported that the cone pedicles of the Quokka conform to this pattern.

Superficial contacts in the form of slight indentations of the base of the cone pedicles are common in vertebrates (DOWLING and BOYCOTT, 1966; RODIECK, 1973). This type of synapse was also found in the Kowari, kangaroo and possum

cone pedicles. Supportive of this is BRAEKEVELT's report of such contacts in the Quokka (1973).

The rod spherules in vertebrate retinae typically have only 1 synaptic pit which results in a small number of synaptic contacts. UNDERWOOD (1968) classified these synaptic terminals as oligosynaptic. According to MISSOTTEN (1965) mammalian rod spherules possess from 3 to 7 invaginating processes in the synaptic pit. There are 2 or 3 centrally positioned processes surrounded by 1 to 5 lateral processes that penetrate further into the spherule.

The rod spherules of the possum, Kowari and kangaroo were found to contain 1 synaptic pit and thus conform to the usual vertebrate pattern (DOWLING, 1970). BRAEKEVELT (1973) described the rod spherules of the Quokka as having 1 or perhaps 2 synaptic pits. In the kangaroo and Kowari each synaptic pit appears to have one central and 2 lateral processes. While this is true of most rod spherules in the possum there are occasionally 3 lateral processes.

The arrangement of post-synaptic processes in both rod and cone synaptic terminals of marsupial retina appears to fit the mammalian pattern as described by MISSOTTEN (1965).

In both the rod and cone synaptic terminals of the possum, Kowari and kangaroo the invaginated post-synaptic processes were found to be associated with synaptic ribbons and synaptic vesicles. The arrangement of these presumably related structures (see Sections 4.12, 5.12 and 6.12) is similar to that seen in other vertebrates such as the Rhesus monkey (KOLB, 1970).

Some of the photoreceptor terminals examined by electron microscopy in the present study were found to

contain large mitochondria, usually paired. The cone pedicles in the OPL of the kangaroo retina possess 1 or 2 mitochondria. While in the Kowari most of the rod spherules have a single pair of mitochondria and cone pedicles may have up to 3 pairs.

Paired mitochondria are often indicative of division or fusion of mitochondria (see FAWCETT, 1981). Careful examination of the outer mitochondrial membranes of the paired mitochondria did not reveal any evidence suggestive of either division or fusion. This suggests that pairing is the normal arrangement of these mitochondria.

Neither rod nor cone terminals in the Brush-tailed possum nor rod spherules in the kangaroo, however, were found to possess such mitochondria. The significance of this apparent variation in the components of the photoreceptor terminals between both rods and cones and between species is not clear.

Of further interest is the presence of inclusion granules within enlarged cisternae of the mitochondria of some of the cone pedicles in the OPL of the Kowari (see Figure 5.12). Structurally these inclusions resemble β-glycogen granules as described in rat liver cells by DROCHMANS (1960), and the intracisternal location is similar to that in the Purkinje fibres of the rat myocardium (FAWCETT, 1981). The significance of these presumed glycogen granules is not known. It seems reasonable to suggest, however, that they may play a role in supplying energy used during synaptic transmission between the photoreceptors and the second order neurons.

It was only possible to make tentative identification

of the cells whose cell bodies occupy the INL in the 3 marsupial retinae examined.

In all 3 species studied the large, lightly staining cells lying along the sclerad edge of the INL are thought to be AC because of their size, position and large cytoplasmic processes extending into the OPL.

The smaller, more numerous cell bodies with the denser nuclei are considered to be the BC in each of the species studied. It was apparent from routine light and electron microscopy of the Kowari retina that 2 types of BC with differing nuclear morphologies are present (see Section 5.13). The presence of 2 BC types was confirmed by examination of Golgi stained retina in which 2 different axonal arrangements were apparent (see Section 7.2). As the cell soma diameters of the 2 BC are similar it has not been possible to correlate the nuclear and axonal morphologies.

The simple BC axons in the Kowari are comparable to the axons of BC in placental mammals which are smooth and only rarely have the collateral branches common to lower vertebrates (RODIECK, 1973).

In vertebrates the axons of cone BC terminate in numerous small swellings that form stratified arborisations within the IPL (RODIECK, 1973). From this it may be implied that the stratified BC type cells seen in Golgi stained Kowari retina are cone BC.

There was no evidence from either routine microscopy or Golgi investigation to suggest that 2 types of BC occur in the retinae of the possum and kangaroo. In view of the numerous BC types found in other vertebrate retina examined (POLYAK, 1957; KOLB, BOYCOTT and DOWLING, 1969; KOLB, 1970)

it seems probable that several BC types existin marsupial retina.

The presumptive AC of the Brush-tailed possum, Kowari and Kangaroo Island kangaroo have similar cytoplasmic contents, are large and lie along the vitread edge of the INL adjacent the IPL.

The MC of vertebrate retina perform a space-filling function (HOGAN et al., 1971). The cytoplasmic extensions of the MC occupy the retinal areas not filled by neurons. MC are also thought to perform metabolic functions such as synthesis and storage of glycogen (COGAN and KUWABARA, 1967). It is also thought that MC move potassium to and from the vitreous via their inner terminals and function as a 'spatial-buffer' system (GARDNER-MEDWIN, 1984).

In Golgi stained material from the possum and Kowari the MC have a bottlebrush appearance due tothe numerous lateral horizontal processes that arise from the thick radially directed process as it crosses the IPL. While they have a honeycomb-like meshwork of processes around the cell bodies of the ONL.

The MC of the Brush-tailed possum and Kowari were found to be very similar in form. In both species the elongate nuclei lie in cell bodies that cross the INL and give rise to thick outer and inner processes whose cytoplasm contains numerous ribosomes and microtubules. Thin lateral processes arise from the outer processes, which end in large conical terminals beneath the OLM. Similarly the inner processes have collaterals and terminate in conical swellings adjacent the ILM. In both species the outer and inner terminals contain numerous oval mitochondria.

In both the possum and Kowari numerous microvillous processes arising from the outer terminals extend beyond the OLM into the ventricular space where they separate the photoreceptor inner segments.

With the exception of 2 features the MC of the Kangaroo Island kangaroo are similar to those of the possum and Kowari. Firstly, the inner terminals possess Sertoli-type junctions (see FAWCETT, 1981). Second and more interesting is the presence of large diameter processes seen extending beyond the OLM in addition to the microvilli. These processes appear to arise directly from the outer terminals of the MC and so are not Landolt's clubs which are processes of BC found in some lower vertebrates (see LOCKET, 1970).

The IPL of the vertebrate retina is the second synaptic region: it is here that the second order neurons synapse with the RGCs. Both light and electron microscopic examination of the marsupial retinae used in this study show that the IPL is thicker than the synaptic lamina of the OPL; this is the usual arrangement in vertebrate retina (RODIECK, 1973).

It is generally considered that the vertebrate IPL consists of RGC dendrites, BC axons and their terminals (telodendrons), MC and blood vessels plus associated glia in some species (RODIECK, 1973).

No description of the marsupial IPL processes or synapses has been published to date. Both conventional and ribbon synapses were found amongst the closely packed neuronal processes of the IPL of the 3 species used in this study.

In the Brush-tailed possum conventional-type synapses

were found to be evenly distributed throughout the IPL. While in the Kangaroo Island kangaroo they were mostly seen in the outer two thirds of the OPL.

The only synapses in the primate retina to contain syanptic ribbons are the bipolar axodendritic synapses (DOWLING and BOYCOTT, 1966). On the basis of this, presumptive presynaptic BC terminals were identified in the possum, Kowari and kangaroo retina examined. They were seen more frequently in the outer third of the IPL of the possum, outer two thirds in the Kowari and inner two thirds in the kangaroo. As in other vertebrates the synaptic ribbons in these BC terminals lie close to and at right angles to the pre-synaptic membrane. The ribbons are associated with a halo of synaptic vesicles in all 3 species while only the possum and Kowari were found to have an arciform density between the ribbon and its adjacent pre-synaptic membrane. DOWLING and BOYCOTT (1966) suggested that the presence of 2 processes post-synaptic to each ribbon in primate bipolar synapses indicates a dual contact. Dual contacts similar to those described by DOWLING and BOYCOTT (1966) were seen adjacent the ribbons of the presumptive BC terminals in the marsupial retinae examined.

In the possum, Kowari and kangaroo 1 of these 2 processes may be involved in a second interneuronal junction with the BC terminal. As seen in Figures 4.14.3 and 6.14.1 the relationship is reversed as it is the BC terminal that is postsynaptic to its own post-synaptic process. These contacts resemble the reciprocal conventional chemical synapses described by DOWLING and BOYCOTT (1966) in primate retina in which the post-synaptic process involved in the

reciprocal synapse is an AC process and the other belongs to a RGC.

The IPL of the kangaroo retina examined in this study was found to contain synapses, resembling conventional chemical synapses, between smooth neuronal processes and RGC soma. This type of interneuronal contact may be an amacrine axosomatic junction such as that described by DOWLING and BOYCOTT (1966) in primate retina.

In all 3 marsupials studied the RGCs were similar to those of other vertebrates (RODIECK, 1973) and were found to occupy the most vitread cell layer of the retina. The pale-staining cytoplasm was found to contain numerous polyribosomes, small rounded mitochondria and, in the case of the possum and Kowari, small, membrane-bound inclusions of moderate density. Nissl substance was seen in thin sections of possum and kangaroo RGCs.

The nuclei are larger and more eccentric in the larger RGC and have coarse granular chromatin that exhibits little or no clumping. Two distinct morphological types of nuclei were found in the RGCs of the Kowari but it was difficult to correlate these with the α-, β- and γ-RGC types described by HUGHES (1975a).

The Golgi-stained RGCs of both the possum and Kowari showed similar morphology. The highly branched dendritic trees were found to arise from the sclerad pole of the cell bodies from either a single trunk which bifurcates orfrom 2 separate trunks. The terminal branches of the dendritic trees show rounded dilatation. No axons were seen in either species.

The ranges of RGC soma diameter for the marsupials

examined in this study were as follows: 4.0 to 24.0 μm in the possum, 4.0 to 26.0 um in the Kowari and 4.0 to 32.0 μm in the kangaroo. These ranges are well within the limits found by other authors working with marsupials (see Figure 2.4.1).

The range of diameters found for the Brush-tailed possum is similar to that reported by FREEMAN and TANCRED (1978) for the same species (5.0 to 26.0 μm). These authors found an increase in the average RGC soma diameter from the central to the peripheral retina. This was not evident from the wholemounted possum retinae examined during this study in which most of the cells measured in the periphery belong to the smallest γ- group.

As in the possum most of the RGCs in the peripheral retina of the kangaroo belong to the γ-group and most belong to the β-group in the central retina. This may be indicative of a decrease in RGC soma size from central to peripheral retina: a situation not consistent with the data already available on marsupial RGCs. It seems likely, therefore, that this gradient is due to shrinkage of the periphery of the wholemounts.

The gradient of RGC soma diameter in the Kowari is consistent with that in other Australian marsupials (FREEMAN and TANCRED, 1978; TANCRED, 1981).

Preliminary counts carried out on the RGC population of the Kowari were indicative of the presence of a horizontally orientated band of increased RGC density. The presence of such a band, or visual streak, is not uniquely associated with the retinae of predatory animals (HUGHES, 1977) although the Kowari is a carnivorous predator. Further, the Kowari occupies sparcely vegetated gibber plains and the

presence of a visual streak conforms to HUGHES' theory that terrestrial species whose field of view is not totally obscured by nearby vegetation possess a visual streak. On the other hand, the visual streak is common in ground-dwelling animals that are active in daylight and absent in small nocturnal species that occupy heavily vegetated areas (HUGHES, 1977). This may be further evidence that the eyes of the Kowari are adaptd for scotopic vision.

The structure and organisation of the RGC axons and MC processes in the optic NFL in the marsupial retinae studied is unremarkable and conforms to the description of the human optic NFL by HOGAN et al. (1971).

Similarly, the marsupial ILM conforms to the structure of the ILM in other vertebrates (RODIECK, 1973) in comprising the basement membrane of the MC inner teminals and vitreous fibrils.

9 CONCLUSION

While it was not possible to examine all features of the 3 marsupial retinae used in this study, the information obtained conforms to that presented in the small number of reports published on marsupial retinal structure (see Section 2.3). It is also apparent that the structure of the marsupial retina conforms to the general vertebrate pattern; the marsupial photoreceptor nuclei show differentiation similar to that in mammals. The cones resemble those of reptiles while the filamentous rods are more like those of placental mammals than lower vertebrates.

The structure of the photoreceptor synapses in the OPL of the 3 marsupials studied and in the Quokka conform to the general vertebrate arrangement of ribbon synapses.

Many aspects of the marsupial retina deserve further investigation; particularly the OPL, IPL and the distribution of the RGC population. The detailed arrangement of the processes involvedin the photoreceptor synapses in the OPL might be characterised in much the same way as DOWLING and BOYCOTT (1966) studied the primate plexiform layers using combined Golgi staining and electron microscopy. The connectivity of neurons that synapse within the IPL might also be studied in this manner. The data published to date on the marsupial RGC populations has proven to be interesting in terms of HUGHES' theory relating habitat and lifestyle to specialisations of the RGC layer. Further study of this type on marsupials may be interesting because of the unique phylogenetic position they occupy.

The presence of oil droplets in the cone cells of all marsupials examined to date is also of interest from a

phylogenetic viewpoint and deserves further investigation in terms of their evolutionary retention and functional significance.

The marsupial retinal structure has been all but neglected in the past and opportunities remain for considerable future research.

APPENDIX I

Current genus and species names for original names used in the text

Author	Binomial in original article	Common name in original article	Current binomial
JOHNSON (1901)	Dasyurus ursinus	Tasmanian Devil	Sarcophilus harissi
	Halmaturus brachyurus	Short-tailed Wallaby	?
	Dendrolagus inustus	Bennett's Tree-Wallaby	Dendrolagus bennettianus
	Hypsiprimnus rufescens	Rufous Rat-Kangaroo	Aepyprymnus rufescens
	Belideus sciureus	Squirrel-like phalanger	?
	Perameles obesula	Bandicoot	Isodon obesulus
	Perameles lagotis	Rabbit-eared Bandicoot	Marcotis lagotis
	Phalangista vulgaris	Black Phalanger	?
FRANZ (1934)	Sarcophilus ursinus	-	Sarcophilus harissi
HOFFMANN (1876)	fWallabia bennetti	Bennett's Wallaby	Macropus rufogriseus
O'DAY (1936)	Pseudocheirus laniginosus	Ring-tailed Possum	Pseudocheirus laniginosus

APPENDIX II

Phosphate-buffered glutaraldehyde-paraformaldehyde fixative (Glauert, 1974).

10.0 ml 25% glutaraldehyde

20.0 ml 10% paraformaldehyde

50.0 ml 0.2M phosphate buffer, pH 7.2

30.0 ml double distilled water

0.2M phosphate buffer

Solution A 0.2M dibasic sodium phosphate

$Na_2HPO_4.2H_2O$ 35.61 g/litre

Solution B 0.2M monobasic sodium phosphate

$NaH_2PO_4.H_2O$ 27.60 g/litre

Add 38.0 ml solution A to 12.0 ml solution B to obtain 50.0 ml 0.2M phosphate buffer at pH 7.2 at 20°C.

APPENDIX III

Combined glutaraldehyde-paraformaldehyde fixative

(FORSSMAN, 1981)

Rinse

9.0 g	sodium chloride
25.0 g	polyvinylpyrrolidone (MW=40,000)
0.25 g	heparin
5.0 g	procaine-HCl

Dissolve in double distilled water to obtain a final volume of 1.0 litre.

Fixative

45 ml	0.2M NaH_2PO_4
405 ml	0.2M Na_2HPO_4
60 ml	25% glutaraldehyde
60ml	25% formaldehyde (madefrom para-formaldehyde powder)
25 g	polyvinylpyrrolidone (MW=40,000)
15 ml	100mM magnesium chloride

Make the buffer, add the polyvinylpyrrolidone and dissolve, add both aldehydes and make up to 1.0 litre with double distilled water.

(Final concentrations: 1.5% glutaraldehyde
1.5% paraformaldehyde
1.5mM magnesium chloride).

0.2M phosphate buffer

Solution A	0.2M dibasic sodium phosphate
	$Na_2HPO_4.2H_2O$ 35.61 g/litre
Solution B	0.2M monobasic sodium phosphate
	$NaH_2PO_4.H_2O$ 27.60 g/litre

APPENDIX IV

Dehydration of Tissue for Plastic Sections

70% ethanol	15 minutes
80% ethanol	15 minutes
90% ethanol	15 minutes
95% ethanol	15 minutes
100% ethanol	15 minutes
100% ethanol over anhydrous copper sulphate	2x15 minutes
100% ethanol over anhydrous copper sulphate with propylene oxide in the ratio of	
2 : 1	15 minutes
1 : 1	15 minutes
1 : 2	15 minutes
100% propylene oxide	3x15 minutes

APPENDIX V

Araldite Embedding Resin (Polaron Euqipment Ltd., England)

10.0 ml	Araldite MY753 resin
10.0 ml	Dodecenyl succinic anhydride (DDSA)
0.15 ml	Dibutyl phthalate (DBP)
0.2 ml	Benzyl dimethylamine (BDMA)

APPENDIX VI

Polychrome Stain for Thick Plastic Sections

(HUMPHREY and PITTMAN, 1974 modified by LOCKET, personal communication)

Methylene blue-Azure II

0.13 g	methylene blue
0.02 g	azure II
10.0 ml	glycerol
10.0 ml	methanol
30.0 ml	phosphate buffer, pH 6.9
50.0 ml	double ditilled water

Basic fuchsin-Borax

Solution A	0.125 g	basic fuchsin
	50.0 ml	double ditilled water
Solution B	0.125 g	sodium tetraborate
	50.0 ml	double distilled water

Mix solutions A and B in equal volumes to make the working solution. Use fresh.

Method

1. Dry down 1.0 um sections on a drop of double distilled water on a hotplate at 60°C.

2. Place a drop of methylene blue-azure II on the slide and stain for 2 minutes on a hotplate at 60°C.

3. Rinse off stain with double distilled water and dry the slide.

4. Place a drop of basic fuchsin-borax on the slide and stain for 1 minute on a hotplate at 60°C.

5. Rinse off stain with double distilled water and dry the slide.

APPENDIX VII

Staining of Thin Plastic Sections

Uranyl acetate

Prepare approximately 5.0 ml of saturated uranyl acetate in 50% ethanol.

Lead citrate (REYNOLDS, 1963).

1. Mix 1.33 g of lead nitrate with 1.76 g of sodium citrate and 30.0 ml of double distilled water in a 50.0 ml volumetric flask. Shake thoroughly for 1 minute and intermittently for 30 minutes to assure complete conversion of lead nitrate to lead citrate.

2. Add 8.0 ml of 1N sodium hydroxide and dilute the suspension to 50.0 ml with double distilled water. Mix by inversion.

This stain has a shelf life of 6 months if stored in a sealed container and should be centrifuged before use.

Staining procedure

1. Place drops of freshly prepared and millipored uranyl acetate into a wax-lined glass petri dish. Also place a snall piece of filter paper soaked in 50% ethanol into the petri dish and cover.

2. Place each grid, sections down, on a drop of uranyl acetate and stain covered for 10 minutes at room temperature in the dark.

3. Rinse grids briefly in 70% ethanol and immediately wash in a beaker of double distilled water.

4. Dry grids.

5. Pipette drops of lead citrate into a wax-lined glass petri dish. Also place a few pellets of sodium hydroxide into the dish and wet with double distilled water to achieve

a carbon dioxide-free environment.

6. Place each grid, sections down, on a drop of lead citrate and stain covered for 10 minutes at room remperature.

7. Wash grids in a weak solution of sodium hydroxide and wash thoroughly in double distilled water.

8. Dry grids.

APPENDIX VIII

Periodic Acid-Schiff's Reaction

Schiff's reagent

600.0 ml double distilled water

3.0 g basic fuchsin

60.0 ml 1N HCl

6-8 g sodium metabisulphite

2.0 g charcoal

Bring water to the boil and very slowly add the basic fuchsin. Shake for 5 minutes. Cool to 50°C, filter and add HCl. Cool to 25°C and add sodium metabisulphite. Leave overnight on a magnetic stirrer. Add charcoal, shake and filter.

Bisulphite solutions

10.0 ml 1N HCl

10.0 ml 10% $NaHSO_4$, $K_2S_2O_3$ or $Na_2S_2O_3$

200.0 ml double distilled water

Method

1. Bring sections to water.

2. Oxidise in 1.0% aqueous solution of periodic acid for 10 minutes,

3. Wash in tap water for 5 to 10 minutes.

4. Place in Schiff's reagent for 5 to 15 minutes.

5. Rinse in 3 changes of freshly prepared bisulphite solution for 2 minutes each.

6. Dehydrate sections and mount.

Gomori's Reticulin Method

Ammoniacal silver solution

1. Add 4.0 ml 10% potassium hydroxide to 20.0 ml

10% silver nitrate. Dissolve the resulting precipitate by adding strong ammonia dropwise.

2. Add more 10% silver nitrate dropwise until the resulting precipitate dissolves on shaking.

3. Dilute with an equal volume of double distilled water.

4. Use fresh.

Method

1. Bring sections to water.

2. Oxidise with 1% potassium permanganate for 1 to 2 minutes.

3. Rinse in tap water.

4. Bleach with 3% potassium metabisulphite.

5. Wash thoroughly in tap water.

6. Treat with 2% ferric ammonium sulphate for 1 minute.

7. Wash thoroughly in tap water and rinse twice in double distilled water.

8. Treat with ammoniacal silver solution for 1 minute.

9. Rinse briefly in double distilled water.

10. Reduce with 10% neutral formalin for 3 minutes.

11. Wash in tap water.

12. Tone with 0.2% gold chloride for up to 10 minutes.

13. Rinse with double distilled water.

14. Treat with 3% potassium bisulphite for 1 minute.

15. Rinse withn double distilled water.

16. Fix with 2.5% sodium thiosulphate (hypo') for 1

to 2 minutes.

17. Wash in tap water.

18. Dehydrate, clear and mount.

Result - reticulin fibres stain black

- background stains grey or according to the counterstain.

Orcein (Modified Taenzer-Unna orcein method (Unna, 1891) from DRURY andWALLINGTON, 1980).

Fixation - not critical.

Sections - thin paraffin.

Staining solution

1.0 g orcein (synthetic)

100.0 ml 80% ethanol

1.0 ml concentated HCl

Method

1. Partially hydrate sections by taking to 70% ethanol.

2 Place in a closed jar of orcein for 30 minutes to 2 hours at room temperature (or for a shorter time at 37°C).

3. Wash thoroughly in 70% ethanol. Staining of collagen may be removed by treatment with 1% acid-alcohol at this stage.

4. Wash in tap water.

5. Counterstain nuclei lightly with methylene blue or alum haematoxylin.

6. Dehydrate, mount and clear.

Result - elastic fibres stain dark brown

- nuclei stain blue

APPENDIX IX

Golgi-Colonnier Method (modified from NASSEL and SEYAN (1979); cited by STRAUSFELD (1982)).

Low-molarity buffered glutaraldehyde-paraformaldehyde

Stock buffer

Solution A 0.2M dibasic sodium phosphate

$Na_2HPO_4.2H_2O$ 35.61g/liter

Solution B 0.2M monobasic sodium phosphate

$NaH_2PO_4.H_2O$ 27.60g/litre

Add 40.5 ml solution A to 9.5 ml solution B to obtain a pH 7.4 at 25°C.

Stock sucrose solution

0.14 g $MgCl_2$ in 50.0 ml distilled water

17.0 g sucrose in 50.0 ml distilled water

Add equal volumes to make solution C.

Stock paraformaldehyde

Add 10.0 g paraformaldehyde powder to 100.0 ml double distilled water and heat to 60°C. Then add 1N NaOH dropwise until the solution clears (about 6.0 ml), then add an extra 0.5 ml NaOH. Cool and filter.

Fixative

40.5 ml solution A

9.5 ml solution B

20.0 ml solution C

20.0 ml 10% paraformaldehyde

10.0 ml 25% glutaraldehyde

(Final concentrations - 3mM $MgCl_2$

- 0.1M sucrose)

Stock solutions

1. Holmes' borax-borate buffer

Solution A 0.2M boric acid

H_3BO_4 12.4 g/litre

Solution B 0.05M borax

$Na_2B_4O_7.10H_2O$ 19.0 g/litre

Add 90.0 ml solution A to 10.0 ml solution B to obtain pH 7.4 at 20°C.

2. Buffered potassium dichromate

Dissolve 2.5 g potassium dichromate in 100.0 ml Holme's buffer (pH7.4). This will have a final pH of 5.4 to 5.6 at 20°C.

3. Buffered dichromate glutaraldehyde

Add 1 volume of 25% glutaraldehyde to 4 volumes of buffered potassium dichromate. This gives a pH of 5.3 to 5.4, which rises to pH 5.5 after 2 days.

4. Buffered silver nitrate

Dissolve 0.75 g silver nitrate in 100.0 ml of Holme's buffer at pH 7.0 to 7.4.

Method

1. Fix tissue in low-molarity phosphate buffered glutaraldehyde-paraformaldehyde at room temperature for 2 to 6 hours.

2. Wash out excess aldehydes in several changes of phosphate buffer with 0.1M sucrose and 3 mM magnesium chloride.

3. Wash out phosphate buffer in several changes of Holme's buffered potassium dichromate over 2 hours.

4. Chromate in Holme's buffered dichromate-glutaraldehyde for 24 to 72 hours in the dark at room temperature.

5. Rinse several times in Holme's buffered silver

nitrate. When red precipitate is no longer evolved, immerse in fresh buffered silver nitrate for 24 to 72 hours in the dark at room temperature.

6. Check impregnation and repeat steps 4 and 5 if necessary.

7. Dehydrate through ethanol and embed in Araldite.

Rapid Golgi-Aldehyde Method (MOREST 1981 after KOPSCH 1896; COLONNIER, 1964; BLACKSTAD, 1965)

1. Perfusion and immersion fixation overnight at 4°C with phosphate-buffered glutaraldehyde-formaldehyde [see Appendix II]. Eyes were dissected after 1 hour in fixative.

2. Impregnate with dichromate solution

A. 3% $K_2Cr_2O_7$ and 5% glutaraldehyde in double distilled water or B. 3% $K_2Cr_2O_7$ and 0.25% OsO_4 in double distilled water for 5 to 7 days at room temperature in the dark.

3. Rinse in distilled water.

4. Rinse in several changes of 0.75% silver nitrate until no red precipitate appears.

5. Immerse in 0.75% silver nitrate for 5 to 7 days at room temperature in the dark.

6. Dehydrate through a graded series of ethanol.

7. Embed in Araldite (Polaron Equipment Ltd., England).

8. Cut thick (50.0 to 200.0 µm) sections by hand using a sharp razor blade.

This method was also tried with recycling (i.e. repeating steps 2 to 5).

Rapid Golgi Method (modified from KEMALI, 1976)

Stock solutions

A. 3.0 g $K_2Cr_2O_7$

100.0 ml double distilled water

B. 1.0% OsO_4 in sodium barbital buffer

Sodium barbital buffer, pH 7.2

0.61 g sodium barbital

0.29 g sodium chloride

0.22 g calcium chloride

100.0 ml double distilled water

pH adjusted to 7.2 with HCl

Working solutions

C. 85.0 ml A

15.0 ml B

D. 70.0 ml A

30.0 ml B

Method

1. Place fresh tissue in working solution C or D for 6 hours at room temperature in the dark.

2. Wash in several changes of 0.75% silver nitrate until no more red precipitate forms.

3. Place tissue in 0.75% silver nitrate for 6 hours at room temperature in the dark.

4. Wash in double distilled water.

5. Dehydrate through a graded series of ethanol.

6. Embed in Araldite (Polaron Equipment Ltd., England).

7. Cut thick sections by hand using a sharp razor blade.

Glutaraldehyde modification of the Golgi-Kopsch Method (Colonnier, 1964).

Dichromate-Glutaraldehyde solution

2.5% $K_2Cr_2O_7$ 80.0 ml

25.0% glutaraldehyde 20.0 ml

Final concentrations - 2.0% $K_2Cr_2O_7$

- 5.0% glutaraldehyde

Method

1. Perfusion and fixation overnight at 4°C with phosphate-buffered glutaraldehyde-formaldehyde [see Appendix II]. Eyes were dissected after 1 hour in fixative.

2. Wash in saline for 30 minutes.

3. Transfer to dichromate-glutaraldehyde solution for 3, 4, 5 and 6 days.

4. Rinse in double distilled water.

5. Rinse in several changes of 0.75% silver nitrate until no more red precipitate appears.

6. Transfer to 0.75% silver nitrate for 2 to 4 days.

7. Rinse in several changes of double distilled water and remove any crystals from the tissue with a brush.

8. Dehydrate through a graded series of ethanol.

9. Embed in Araldite (Polaron Equipment Ltd., England).

10. Cut thick sections by hand using a sharp razor blade.

COLONNIER's Golgi method was then repeated for possum retina using a variety of dichromate solutions.

A. 2.0% $K_2Cr_2O_7$

B 2.5% $K_2Cr_2O_7$ in double distilled water, pH adjusted to 7.2 with concentrated KOH 80.0 ml

25% glutaraldehyde 20.0 ml

C. 2.5% $K_2Cr_2O_7$ in double distilled water 80.0 ml

25% glutaraldehyde 20.0 ml

for 1, 3, 5 and 7 days. Tissue was subsequently placed in 0.75% silver nitrate for 1 to 5 days.

APPENDIX X

Nissl-staining of Retinal Wholemounts (after STONE, 1976)

1. Wash briefly in distilled water.

2. Stain for 6 minutes in hot (approximately 60°C) 0.05% cresyl violet.

3. Dehydrate 70% ethanol 30 seconds
90% ethanol 30 seconds
100% ethanol 1 minute

4. Clear for 2 minutes in a 1:6:1 mixture of ether, chloroform and ethanol.

5. Dehydrate 95% ethanol 15 seconds
100% ethanol 3 minutes
100% ethanol 3 minutes
100% butanol 3 minutes

6. Clear in 2 x 3 minute changes of xylol.

7. Coverslip with Gurr's Neutral Mounting Medium.

8. Allow to dry under weights for at least 24 hours.

11 BIBLIOGRAPHY

Anctil, M. and Ali, M.A. (1976) Cone droplets of mitochondrialorigin in the retina of Fundulus heteroclitus (Pisces: Cyprinodontidae). Zoomorphol. **84**: 103-111.

Aslin, H. (1974) The behaviour of Dasyuroides byrnei (Marsupialia) in captivity. Z. Tierpsychol. **35**: 187-208.

Basinger, S., Hoffman, R. and Matthes, M. (1976) Photoreceptor shedding is initiated by light in the frog retina. Science **194**: 1074-1076.

Beazley, L.D. and Dunlop, S.A. (1983) The evolution of an area centralis and visual streak in the marsupial Setonix brachyurus. J. Comp. Neurol. 216: 211-231.

Benevento, L.A. (1968) Organization of visual cortex in the opossum. Anat. Rec. **160**; 313. (abstract).

Benevento, L.A. and Ebner, F.F. (1969) Lateral geniculate nucleus projections to neocortex in the opossum. Anat. Rec. **163**: 294. (abstract).

Benevento, L.A. and Ebner, F.F. (1971) The contribution of the dorsal lateral geniculate nucleus to the total pattern of thalamic terminations in striate cortex of the Virginian opossum. J. Comp. Neurol. **143**: 243-260.

Berger, E.R. (1966) On the mitochondrial origin of oil drops in the retinal double cone inner segments. J. Ultrastruct. Res. **14**: 143-157.

Bowmaker, J.K. and Knowles, A. (1977) The visual pigments and oil droplets of the chicken retina. Vision Res. **17**: 755-764.

Braekevelt, C.R. (1973) Fine structure of the retinal pigmented epithelium and photoreceptor cells of an Australian marsupial Setonix brachyurus. Can. J. Zool. **51**: 1093-1100.

Braekevelt, C.R. (1976) Fine structure of the retinal epithelium and tapetum lucidum of the opossum (Didelphis virginiana). J. Morphol. **150**: 213-226.

Brucke, E. (1845) Anatomische Untersuchugen uber die sogenanten leuchtenden Augen bei den Wirbelthieren. Arch. f. Anat. Physiol., U. wiss. Med., S. 387-406.

Cavalcante, L.A., Rocha-Miranda, C.E. and Lent, R. (1975) Hypothalamic, tectal and accessory optic projections in the opossum. Brain Res. **84**: 302-307.

Cogan, D.G. and Kuwabara, T. (1967) The mural cell in perspective. Arch. Ophthalmol. **78**: 133-139.

Cohen, A.I. (1965) New details of the ultrastructure of the outer segments and ciliary connectives of the rods of human and macaque retinas. Anat. Rec. **152**: 68-80.

Colonnier, M. (1964) The tangential organisation of the visual cortex. J. Anat. **98**: 327-344.

Dowling, J.E. (1970) Organization of vertebrate retinas. Invest. Ophthalmol. **9**: 655-680.

Dowling, J.E. and Boycott, B.B. (1966) Organization of the primate retina: electron microscopy. Proc. Roy. Soc. Lond. B. **166**: 80-111.

Drochmans, P. (1960) Mise en evidence du glycogene dans la cellule hepatique par microscopie electronique. J. Cell Biol. **8**: 553-558.

Drury, R.A.B. and Wallington, E.A. (1980) Carleton's Histological Technique, 5th. edition. Oxford:Oxford University Press.

Duke-Elder, S. (1958) System of Ophthalmology, Vol. 1 The eye in evolution. London:Henry Kimpton.

Fawcett, D.W. (1981) The Cell, 2nd. edition. Philadelphia:W.B. Saunders Company.

Forssmann, W.-G. (1981) General methods in transmission electron microscopy of the nervous system. In: Techniques in Neuroanatomical Research (C.Heym and W.-G.Forssmann, eds.) Berlin:Springer-Verlag.

Freeman, B. (1978) The retinal origins of the optic nerve conduction latency groups in the brush-tailed possum, Trichosurus vulpecula. J. Comp. Neurol. **179**: 753-760.

Freeman, B. and Tancred, E. (1978) The number and distribution of ganglion cells in the retina of the brush-tailed possum, Trichosurus vulpecula. J. Comp. Neurol. **177**: 557-568.

Freeman, B. and Watson, C.R.R. (1978) The optic nerve of the brush-tailed possum, Trichosurus vulpecula: Fibre diameter spectrum and conduction latency groups. J. Comp. Neurol. **179**: 739-752.

Gardner-Medwin, A.R. (1984) A foot in the vitreous fluid. Nature **309**: 113.

Gawryszewski, L.G. and Hokoc, J.N. (1981) The nasotemporal division of the opossum's retina. An. Acad. Brasil Cienc. **53**: 632. (Abstract).

Gibson, J.J. (1950) The perception of the visual world. Boston:Houghton Muffin.

Giolli, R.A. (1965) An experimental study of the accessory optic system and of other fibers in the opossum, (Didelphis-virginiana). J. Comp. Neurol. **124**: 229-242.

Glauert, A.M. (1975) Practical methods in electron microscopy. Vol. 3, Part 1. Fixation, Dehydration and Embedding of Biological Specimens. Amsterdam:North-Holland.

Goldby, F. (1941) The normal histology of the thalamus in the phalanger, Trichosurus vulpecula. J. Anat. **7**: 197-224.

Goldman, K.L. and Steinberg, R.H. (1977) Ultrastructure of pigment epithelium and association with photoreceptors in the opossum retina. Invest. Ophthalmol. Visual Sci. (Suppl.): 113. (abstract).

Hayhow, W.R. (1966) The accessory optic system in the marsupial phalanger, Trichosurus vulpecula. J. Comp. Neurol. **126**: 653-672.

Hayhow, W.R. (1967) The lateral geniculate nucleus of the marsupial phalanger, Trichosurus vulpecula. J. Comp. Neurol. **131**: 571-604.

Hazlett, L.D. (1976) Fine structure of the opossum Didelphis virginiana retina. Anat. Rec. **184**: 587. (abstract).

Hazlett, L.D., Hazlett, J.C., Ireland, M. and Bradley, R.H. (1978) Microperoxisomes in retinal epithelium and tapetum lucidum of the American opossum. Exp.Eye Res. **27**: 343-348.

Herman, K.G. and Steinberg, R.H. (1982a) Phagosome movement and the diurnal pattern of phagocytosis in the tapetal retinal pigment epithelium of theopossum. Invest. Ophthalmol. Visual Sci. **23**: 277-290.

Herman, K.G. and Steinberg, R.H. (1982b) Phagosome degeneration in the tapetal retinal pigment epithelium of the opossum. Invest. Ophthalmol. Vis. Sci. **23**: 291-304.

Herman, K.G. and Steinberg, R.H. (1982c) Melanosome metabolism in the retinal pigment epithelium of the opossum. Cell Tissue Res. **227**: 485-507.

Hokoc, J.H. and Oswaldo-Cruz, E. (1978) Quantitative analysis of the opossum's optic nerve: An electron microscopy study. J. Comp. Neurol. **178**: 773-782.

Hoffmann, C.K. (1876) Zur anatomie der retina. II. Uber den bau der retina den beutelthieren. Niederl. Arch. Zool. **3**: 195-198.

Hogan, M.J., Alvarado, J.A. and Weddell, J.E. (1971) Histology of the human eye. Philadelphia:W.B. Saunders Company.

Hokoc, J.H. and Oswaldo-Cruz, E. (1979) A regional specialization in the opossm's retina: Quantitative analysis of the ganglion cell layer. J. Comp. Neurol. **183**: 385-396.

Hughes, A. (1975a) A quantitative analysis of the cat retinal ganglion cell topography. J. Comp. Neurol. **163**: 107-128.

Hughes, A. (1975b) A comparison of retinal ganglion cell topography in the plains and tree kangaroo. J. Physiol. (Lond.) **244**: 61-63P.

Hughes, A. (1977) The topography of vision in mammals of contrasting life style: Comparative optics and retinal organisation. In: Handbook of Sensory Physiology Vol. 7, Part 5. The Visual System in Vertebrates. pp. 613-756. (F. Crescitelli, ed.) Berlin:Springer-Verlag.

Humphrey, C.D. and Pittman, F. (1974) A simple methylene blue-azure II-basic fuchsin stain for epoxy-embedded tissue sections. Stain Technol. **49**: 9-14.

Johnson, G.L. (1901) Contributions to the comparative anatomy of vertebrates, chiefly based on ophthalmoscopic examination. Phil. Trans. Roy. Soc. Lond. **194**: 1-82.

Johnson, J.L. and Marsh, M.P. (1969) Laminated lateral geniculate in the nocturnal marsupial Petaurus breviceps (sugar glider). Brain Res. **15**: 250-254.

Kemali, M. (1976) A modification of the rapid golgi method. Stain Technol. **51**: 169-172.

Kolb, H. (1970) Organization of the outer plexiform layer of the primate retina: Electron microscopy of Golgi-impregnated cells. Phil. Trans. Roy. Soc. Lond. B **258**: 261-283.

Kolb, H., Boycott, B.B. and Dowling, J.E. (1969) A second type of midget bipolar cell in the primate retina. Phil. Trans. Roy. Soc. Lond. B **255**: 177-184.

Kunz, Y.W. and Regan, C. (1973) Histochemical investigations into the lipid nature of the oil droplet in the retinal twin-cones of Lebistes reticulatus (Peters). Rev. Suisse Zool. **80**: 699-703.

Kuwabara, T. (1975) Cytologic changes of the retina and pigment epithelium during hibernation. Invest. Ophthalmol. **14**: 457-467.

Land, M.F. (1972) The physics and biology of animal reflectors. Prog. Biophys. molec. Biol. **24**: 75-106.

La Vail, M.M. (1976) Rod outer segment disk shedding in rat retina: Relationship to cyclic lighting. Science **194**: 1071-1074.

Lent, R. and Rocha-Miranda, C.E. (1978) Aberrant retinofugal projections in the opossum after eye enucleation and tectal lesion. In:Opossum Neurobiology, (C.E. Rocha-Miranda and R. Lent, eds.), pp. 217-240. Rio de Janeiro:Academia Brasileira de Ciencias.

Lent, R., Cavalcante, L.A. and Rocha-Miranda, C.E. (1976) Retinofugal projections in the opossum. An anterograde degeneration and radioautographic study. Brain Res. **107**: 9-26.

Leure-du-Pree, A.E. (1975) Electron microscopic observations of the retina in the pouch young opossum Didelphis virginiana. Anat. Rec. **181**: 409-410. (abstract).

Locket, N.A. (1970) Landolt's club in the retina of the African lungfish, Protopterus aethiopicus, Heckel. Vision Res. **10**: 299-306.

Marshall, J. and Ansell, P.L. (1971) Membranous inclusions in the retinal pigment epithelium: Phagosomes and myeloid bodies. J. Anat. **110**: 91-104.

Missotten, L. (1965) L'ultrastructure des cones de la retine humaine. Bull. Soc. Belge Ophthalmol. **130**: 472-502.

Morest, D.K. (1981) The Golgi methods. In: Techniques in Neuroanatomical Research. (C. Heym and W.-G. Forssmann, eds.) pp. 124-138. Berlin:Springer-Verlag.

Munk, O. (1968) The eyes of Amia and Lepisosteus (Pisces, Holostei) compared with the brachiopterygian and teleostean eyes. Vidensk, Meddr. dansk naturh. Foren. **131**: 109-127.

Nicol, J.A.C., Arnott, H.J. and Best, A.C.G. (1973) Tapeta lucida in bony fishes (Actinopterygii): a survey. Can. J. Zool. **51**: 69-81.

Novikoff, A.B. and Novikoff, P.M. (1973) Microperoxisomes. J. Histochem. Cytochem. **21**: 963-966.

O'Day, K. (1936) A preliminary note on the presence of double cones and oil-droplets in the retina of marsupials. J. Anat. **70**: 465-467.

O'Day, K. (1938) The visual cells of the platypus (Ornithorhyncus). Brit. J. Ophthalmol. **22**: 321-328.

Oswaldo-Cruz, E. and Rocha-Miranda, C.E. (1967) The diencephalon of the opossum in stereotaxic coordinates. I. The epithalamus and dorsal thalamus. J. Comp. Neurol. **129**: 1-38.

Packer, A.D. (1941) An experimental investigation of the visual system in the phalanger, Trichosurus vulpecula. J. Anat. **75**: 309-329.

Pearson, L.J., Sanderson, K.J. and Wells, R.T. (1976) Retinal projections in the ringtailed possum Pseudochirus peregrinus. J. Comp. Neurol. **170**: 227-240.

Pedler, C. (1965) Rods and cones - a fresh approach. In: Colour Vision. (A.V.S. de Reuck and J. Knight, eds.), pp. 52-85. London:Churchill.

Pedler, C. (1969) Rods and cones - a new approach. Intl. Rev. Gen. Exp. Zool. **4**: 219-274.

Pedler, C. and Tilly, R. (1964) The nature of the gecko visual cell: A light and electron microscopic study. Vision Res. **4**: 499-510.

Pedler, C. and Tilly, R. (1967) The fine structure of photoreceptor discs. Vision Res. **7**: 829-836.

Pirie, A. (1959) Crystals of riboflavin making up the tapetum lucidum in the eye of a lemur. Nature **183**: 985-986.

Pirie, A. (1961) Cholesterol in the tapetum lucidum of the opossum Didelphis virginiana. Nature **191**: 708-709.

Polyak, S. (1957) The Vertebrate Visual System. Chicago:University of Chicago Press.

Rapaport, D.H., Rowe, M.H. and Wilson, P.D. (1978) The distribution of ganglion cells in the retina of the American opossum (Didelphis virginiana). Anat. Rec. **190**: 518.

Rapaport, D.H., Wilson, P.D. and Rowe, M.H. (1981) The distribution of ganglion cells in the retina of the American opossum Didelphis virginiana. J. Comp.Neurol. **199**: 465-480.

Reynolds, E.S. (1963) The use of lead citrate at high pH as an electron-opaque stain in electron microscopy. J. Cell Biol. **17**: 208.

Robison, W.G. and Kuwabara, T. (1975) Microperoxisomes in retinal pigment epithelium. Invest. Ophthalmol. **14**: 866-872.

Rodieck, R.W. (1973) The Vertebrate Retina: Principles of Structure and Function. San Francisco:W.W. Freeman and Company.

Rowe, M.H. and Stone, J. (1976) Properties of ganglion cells in the visual streak of the cat's retina. J. Comp. Neurol. **169**: 99-126.

Rowe, M.H., Wilson, P.D. and Rapaport, D.H. (1981) Conduction velocity groups in the optic nerve of the North American opossum (Didelphis-virginiana): Retinal origins and central projections. J. Comp. Neurol. **199**: 481-493.

Royce, G.J., Ward, J.P. and Harting, J.K. (1976) Retinofugal pathways in two marsupials. J. Comp. Neurol. **170**: 391-414.

Sanderson, K.J. and Pearson, L.J. (1977) Retinal projections in the native cat, Dasyurus viverrinus. J.Comp.Neurol. **174**: 347-358.

Sanderson, K.J. and Pearson, L.J. (1981) Retinal projections in the hairy-nosed wombat, Lasiorhinus latifrons. Aust. J. Zool. **29**: 473-482.

Sanderson, K.J., Pearson, L.J. and Dixon, P.G. (1978) Altered retinal projections in brushtailed possum, Trichosurus vulpecula following removal of one eye. J. Comp. Neurol. **180**: 841-868.

Sanderson, K.J., Pearson, L.J. and Haight, J.R. (1979) Retinal projections in the Tasmanian devil Sarcophilus harissi. J. Comp. Neurol. **188**: 335-345.

Stone, J. (1981) The wholemount handbook: A guide to the preparation and analysis of retinal wholemounts. Sydney:Maitland Publications.

Strausfeld, N.J. (1980) The Golgi method: Its application to the insect nervous system and the phenomenon of stochastic impregnation.In: Neuroanatomical Techniques-Insect Nervous System. (N.J. Strausfeld and T.A. Miller, eds.) pp. 132-203. New York:Springer-Verlag.

Sousa, A.P., Gattass, R., Hokoc, J.N. and Oswaldo-Cruz, E. (1978) The visual field of the opossum. In: Opossum Neurobiology (C.E. Rocha-Miranda and R.Lent, eds.) pp.51-66. Rio de Janeiro:Academia Brasiliera de Ciencias.

Sousa, A.P. and Oswaldo-Cruz, E. (1978) The striate area of the opossum: a morphological study. In: Opossum Neurobiology (C.E. Rocha-Miranda and R. Lent, eds.) pp.91-106. Rio de Janeiro:Academia Brasiliera de Ciencias.

Tancred, E. (1981) The distribution and sizes of ganglion cells in the retinas of five Australian marsupials. J. Comp. Neurol. **196**: 585-603.

Tancred, E., Freeman, B.W., Rowe, M.H. and Stone, J. (1977) Regional specialisation in the retinas of two Australian marsupials (brush-tailed possum and scrub-wallaby). Proc. Aust. Phys. Pharm. Soc. **8**: 124P.

Underwood, G. (1968) Some suggestions concerning vertebrate visual cells. Vision Res. **8**: 483-488.

Walls, G.L. (1938) Notes on the retinae of two Opossum genera. J. Morphol. **64**: 67-87.

Walls, G.L. (1942) The Vertebrate Eye and its Adaptive Radiation. Michigan:The Cranbrook Press.

Woolley, P. (1971) Maintenance and breeding of laboratory colonies of Dasyuroides byrnei and Dasycerus cristicauda. International Zoo Yearbook **11**: 351-354.

Young, R.W. (1971) An hypothesis to account for a basic distinction between rods and cones. Vision Res. **11**: 1-5.

Young, R.W. (1978) Visual cells, daily rhythms, and vision research. Vision Res. **18**: 573-578.

Young, R.W. and Bok, D. (1969) Participation of the retinal pigment epithelium in the rod outer segment renewal process. J. Cell Biol. **42**: 392-403.

Young, S.R. and Martin, G.R. (1984) Optics of retinal oil droplets: a model of light collection and polarization detection in the avian retina. Vision Res. **24**: 129-137.